The Use of Ion Pairs to Increase the Percutaneous Delivery of Diclofenac

Mignon Cristofoli

Submitted to the School of Human Sciences of London Metropolitan University in partial fulfilment of the requirements of a PhD degree

Month and Year of submission: November 2025

Supervised by:

Primary: Dr Bruno Sil Dos Santos

Second: Dr. Bhaven Patel

External: Dr. Majella E. Lane

Advisor: (Emeritus Professor Jonathan Hadgraft)

Plagiarism statement

This thesis describes research conducted at London Metropolitan University and UCL School of Pharmacy between February 2019 and November 2025 under the supervision Dr Bruno Sil Dos Santos. I certify that the research described is original. I also certify that I have written all the text contained herein and have clearly indicated, by suitable citation, any part of this dissertation that has already appeared in any publication.

Signature:  Date: 28 November 2025

Abstract

Like many topically applied formulations, diclofenac (DF) preparations face delivery challenges due to the highly effective skin barrier. This research explored a novel amino acid-based ion pairing strategy to enhance percutaneous DF delivery through rational counterion selection and solvent optimisation. The investigation progressed through three phases. First, potential amino acid counterions were identified based on size, toxicity and charge compatibility. Distribution coefficient studies evaluated their effectiveness in enhancing DF partitioning from aqueous to organic phases. L-histidine hydrochloride monohydrate (LHSS) was identified as optimal, a finding validated through porcine skin *in vitro* permeation testing (IVPT). Next, solubility challenges were addressed by assessing diclofenac sodium (DNa) solubility in various pharmaceutical solvents. Transcutol® (TC), propylene glycol (PG), and dipropylene glycol (DiPG) were selected for high DNa solubility and water miscibility. A model binary system of TC and water was developed to evaluate novel ion pair formulations. Finally, formulation optimisation investigated solvent substitution effects and developed ternary systems incorporating PG, TC and water.

Mechanistic insights revealed that individual solvent properties, rather than overall system solubility parameters, governed formulation performance. The optimal formulation (PG:TC:water; 10:40:50; v/v/v) containing 5 mg/mL DNa and 25 mg/mL LHSS achieved 145% greater delivery than a commercial 1% DNa product, despite containing only half the active ingredient concentration ($p < 0.05$).

This work establishes a framework for amino acid ion pairing to address fundamental skin penetration challenges in topical pharmaceutical formulations. The approach employs non-toxic, economical and sustainably produced counterions. The methodology has potential applications for other ionisable pharmaceutical compounds, particularly NSAIDs and pharmaceutical salts facing similar topical delivery challenges.

Acknowledgements

In a journey such as this, there are so many who have contributed, knowingly or unknowingly, to achieving this final goal. My thanks to all of you, for your words of encouragement, your assistance in debate and discussions, for answering my questions and for asking yours.

I would like to start with my main supervisor, Dr Bruno Sil Dos Santos. Thank you for supporting my unconventional ideas as far back as my BSc final year project. You allowed me a huge amount of freedom to try many of them, but still managed to keep me on track.

To Dr Majella Lane who allowed me to work in her Skin Research Lab 322, I will be forever grateful!

To my colleagues at London Met, I wish you well and thank you for your support. Congrats Dr Nada, thanks too, to the technicians at London Met. You have always been so helpful and supportive. John Morgan, I can't believe you're nor Dr John Morgan yet! Thanks too to Brunhilda, Saron, Haritha, Eric and Bilkis.

To the Chemical and Pharmaceutical Sciences Department at LMU - especially Dr Bhaven Patel, Dr Don Green, Dr Daniel Sykes and all those who helped guide the most inquisitive (and perhaps most annoying and demanding) undergraduate student through her degree, thank you for your patience, support, and encouragement.

To the "old guard" at Lab 322, Fotis, Dilek, Yanling, Ken, Miguel, Monjur and Lin thanks for all your support. To the current PhD cohort: Jingyi, Storay, Geoff, Shibo, Zihan, Chunrui and especially Annisa – thank you for everything. It's been great working with you.

To my friends, who have always been supportive (and perhaps grown a little tired of asking, *"How's the PhD going?"* only to hear my usual reply: *"Still working on it!"*) - thank you for your patience and encouragement all the same.

To my parents, Anita and Aldo, without your love, sacrifice, support and belief in me, I would never have got this far. The child always teaching her brothers and anyone who would listen… Mom you must be laughing.

To my brothers and sisters: although you haven't been directly involved in this PhD journey, I know you can all relate to the joy (and danger!) of going down a rabbit hole and becoming completely hyper-focused on a subject - a true family speciality.

To my children, Gianluca and Gabriella, I know that I have been studying for most of your lives, and it felt like it would never end. It has not always been easy for you; however, we must have done something right! I am incredibly proud to be your mum … and you were the most interesting scientific experiments I ever embarked on!

Finally, to my husband Niall, thank you for stepping up when I returned to university in 2014 and our children were turning 7 and 8 years old. It's 11 years later and I have completed a Foundation year, a BSc Honours in Pharmaceutical Sciences and hopefully my PhD. You've endured my ups and downs accompanied by plenty of stress. I'm told that PhDs are like childbirth, you forget the pain. Perhaps it wiIl work with the PhD…. Thank you for your love and unwavering support.

Table of contents

List of figures

List of tables

List of equations

Abbreviations

Abbreviations used in the document:

ACN	Acetonitrile
ADR	Adverse drug reactions
ANOVA	Analysis of variance
API	Active pharmaceutical ingredient
AUC	Area under the curve
CC	Commercial cream
CDER	Center for Drug Evaluation and Research
CG	Commercial gel
CHN	Choline
CNa	Sodium cholate
CP	Cetylpyridinium chloride
CRS	Confocal raman spectroscopy
DDAK	6-(dimethylamino)hexanoate
DEA	Diethylamine
DES	Deep eutectic solvents
DF	Diclofenac
DFA	Diclofenac free acid
DiPG	Dipropylene glycol
DL	Detection limit
DNa	Diclofenac sodium
DSC	Differential scanning calorimetry
DVS	Dynamic vapour sorption
FDA	Food and Drug Administration
FT-IR	Fourier-transform infrared spectroscopy

GN	Guidance Note
GRAS	Generally recognised as safe
HCl	Hydrochloride
HPLC	High-performance liquid chromatography
HSC	Hydrogenated soya phosphatidylcholine
IB-NA	Ibuprofen sodium
IB-PH	Ibuprofen-L-phenylalanine ethyl ester
IBU	Ibuprofen
IBU-G	Ibuprogen in gel formulation
ICH	International Conference on Harmonisation
IL	Ionic liquids
IND	Indomethacin
IPA	Isopropyl alcohol
IPM	Isopropyl myristate
IVPS	*In vitro* porcine skin permeation studies
IVPT	*In vitro* permeation testing
KC	6-ketocholestanol
KETO	Ketoprofen
L-Arg	L-Arginine
L-ASS	L-Arginine monohydrochloride
L-His	L-Histidine
L-HSS	L-Histidine hydrochloride monohydrate
L-Lys	L-Lysine
L-LSS	L-Lysine monohydrochloride
LHSS	L-histidine monochloride monohydrate
LOD	Limit of detection

LOQ	Limit of quantification
L-TC	Sucrose laureate
M	Matrine
MA	Mandelic acid
MB	Methylene blue
MDE	Maximum daily exposure
MO	Mineral oil
MPPUD	Maximum potency per unit dose
NAP	Naproxen
NICE	National Institute for Health and Care Excellence
NMR	Nuclear magnetic resonance
NSAIDs	Non-steroidal anti-inflammatory drugs
OA	Osteoarthritis; Oleic acid
OECD	Organisation for Economic Cooperation and Development
O-TC	Sucrose oleate
OTC	Over-the-counter
PBS	Phosphate buffered saline
PC	Partition coefficient
PG	Propylene glycol
PR	Propranolol
QSARs	Quantitative structure-activity relationships
QSPeRs	Quantitative structure-permeability relationships
RA	Retinoic acid
RSD	Relative standard deviation
SA	Salicylic acid

SC	*Stratum corneum*
SD	Standard deviation
SLP	Solid lipid nanoparticles
SP	Solubility parameters
SPE	Skin penetration enhancers
TC	Transcutol®
TEWL	Transepidermal water loss
TFA	Trifluoroacetic acid
TG	Test Guideline
TLC	Thin layer chromatography
TXA	Tranexamic acid
USP	United States Pharmacopeia
VC	Vasoconstrictors
VCRP	Voluntary Cosmetic Registration Program
VST	Valsartan
VST-CHN	Valsartan-choline
v/v	Volume/volume
v/v/v	Volume/volume/volume
w/v	Weight/volume

1 Introduction

1.1 Non-steroidal anti-inflammatory drugs (NSAIDs) and osteoarthritis: clinical context and challenges

NSAIDs are widely used for their analgesic, anti-inflammatory and anti-pyretic properties. Clinically they play a key role in the management of pain and fever, as well as in acute and chronic inflammatory disorders [1]. The global market for NSAIDs reflects their extensive use. In 2024 it was valued at USD 22.58 billion and projected to reach USD 31.29 Billion by 2030. Among therapeutic applications the arthritis segment dominated, accounting for 37.72% of the market. Growth in current and projected NSAID sales has been attributed to the increase in chronic pain-related conditions and the expanding geriatric population [2].

However, despite their widespread use, oral NSAID administration is associated with significant adverse effects that limit their clinical utility [3, 4]. Studies examining hospitalisation due to adverse drug reactions have demonstrated that NSAIDs account for 30% of hospital admissions from prescribed medications, with reactions including gastrointestinal bleeding, peptic ulceration, haemorrhagic cerebrovascular accidents and renal damage [5]. Similarly, 30% of adverse reactions requiring hospital admission from over-the-counter medications are gastrointestinal complaints caused by NSAIDs [6].

These safety concerns are particularly relevant in the treatment of osteoarthritis (OA), a painful and degenerative condition affecting the hips, knees, and hands. It affects approximately 7% of the global population, amounting to over 500 million people [7]. Beyond its clinical impact, OA imposes a substantial economic burden, with direct costs estimated at 1-2% of the Gross National Product in developed economies [8]. This burden is further compounded by indirect costs including loss of productivity and early retirement.

Given the substantial risks associated with oral NSAIDs, international treatment guidelines consistently recommend topical NSAIDs as a treatment for osteoarthritis. The UK's National Institute for Health and Care Excellence (NICE) recommends topical NSAIDs as a first-line pharmacological intervention, ahead of oral NSAIDs, COX-2 inhibitors or opioids [9]. Similarly, the European Society for Clinical and

Economic Aspects of Osteoporosis, Osteoarthritis and Musculoskeletal Diseases strongly recommend the use of NSAIDs, particularly where symptoms of OA have not been relieved by so-called symptomatic slow-acting drugs such as chondroitin sulfate and prescription crystalline glucosamine sulfate, in combination with paracetamol [10]. The American Academy of Orthopaedic Surgeons as well as the American College of Rheumatology in conjunction with the Arthritis Foundation, all endorse topical NSAIDS in the treatment of OA [11]. Such treatment has also been recommended by the global organisation, Osteoarthritis Research Society International, for the treatment of OA of the knee [12].

1.2 Topical drug delivery: advantages and limitations

The topical application of pharmaceuticals offers substantial therapeutic advantages over oral administration. These include the avoidance of first-pass metabolism [13], the potential for steady-state drug release [14], localised delivery at the target site [15], improved patient compliance and the capacity for rapid cessation in cases of adverse reactions [3]. Of particular clinical significance is the avoidance of gastrointestinal and renal complications [4] commonly associated with oral NSAID therapy.

Despite these advantages, topical drug delivery faces a fundamental limitation that affects many pharmaceutical compounds. The outermost layer of the skin, the *stratum corneum*, acts as a highly effective barrier, allowing only 1–2% of the applied drug to penetrate from topically applied formulations [16]. This barrier is particularly restrictive for ionised pharmaceutical compounds. As oral administration remains the most common drug delivery route [17], many drugs are developed as salts, to enhance both solubility and bioavailability [18]. However, their ionised state poses considerable challenges for transport across the lipid-rich *stratum corneum*.

This limited penetration means that even clinically effective topical formulations represent suboptimal utilisation of the active pharmaceutical ingredient (API). Where the majority of applied drug remains either on the skin surface or is removed without reaching the target site, this results in both economic inefficiency and unnecessary pharmaceutical waste. Enhanced formulation strategies that increase the proportion of applied drug reaching therapeutic targets could achieve equivalent clinical outcomes with reduced drug concentrations, offering significant economic and environmental advantages.

1.3 DF: Selection and clinical significance as a model drug

DF (IUPAC name: 2-[(2,6-dichlorophenyl)amino]benzeneacetic acid; CAS number 15307-86-5) is the most prescribed NSAID worldwide [19]. Synonyms include diclophenac and [o-(2,6-Dichloroanilino)phenyl]acetic acid [20]. First synthesised in the 1960s to provide both high activity and improved tolerability [21], DF has become a cornerstone therapy for pain and inflammation disorders, particularly OA. The main physicochemical properties of DF are summarised in Table 1.1.

Table 1. 1 Physicochemical properties of DF.

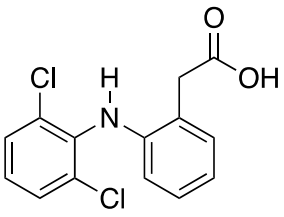 2D Structure of DF	Molecular weight	296.1 g/mol	[22]
	Molecular formula	$C_{14}H_{11}Cl_2NO_2$	[22]
	Melting point	156 – 158 °C	[20]
	Solubility in water at 25 °C	1.78 x 10^{-2} mg/mL	[23,227]
	pKa	4.2	[20]
	Log P	4.5	[20]
	CAS number	15307-86-5	[22]

Diclofenac sodium (DNa) represents one of the most common salt forms of DF, developed to overcome the low aqueous solubility of the free acid. It has extensive clinical application and is incorporated into numerous topical products including Diclofenac Dermapharm 3% Gel, Diclofenac Sodium Spray Gel 4% w/w Cutaneous Spray Solution, Solaraze® 3% gel, Spraymik 4% Cutaneous Spray, Pennsaid® 16 mg/mL Cutaneous solution, Diclo® Gel 1%, Voltaren 1%, Rofenac® 1% gel, Walgreens Diclofenac 1% gel, Diclofenac Sandoz® 10 mg/mL gel and Voltarol 140mg medicated plaster. The physicochemical properties of DNa are included in Table 1.2.

Table 1. 2 Physicochemical properties of DNa.

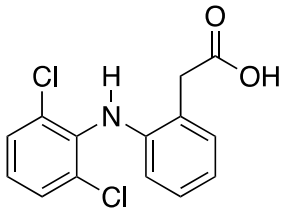 2D Structure of DNa	Na^+	Molecular weight	318.13 g/mol	[24]
		Molecular formula	$C_{14}H_{10}Cl_2NNaO_2$	[1]
		Melting point	283 – 285 °C	[20]
		Solubility in water at 32 ± 1°C	3.70 x 10^{-2} mg/mL	[25]
		CAS number	15307-79-6	[24]

Its widespread use in topical formulations, together with the substantial body of published research, establishes DNa as a well-characterised model permeant for investigating percutaneous drug delivery optimisation strategies. DNa exemplifies the class of ionisable drugs formulated as pharmaceutical salts for oral administration, which face similar delivery optimisation opportunities when applied topically. Success with DNa could provide a framework applicable to numerous other topically applied pharmaceutical compounds facing comparable delivery efficiency challenges.

1.4 Current approaches to enhancing percutaneous drug delivery

Strategies to overcome the skin barrier are typically categorised into active and passive methods [26, 27]. Active methods employ physical techniques such as iontophoresis [28-30], sonophoresis [31], magnetophoresis [32], electroporation [33], and microneedles [34-37] to physically disrupt or bypass the *stratum corneum*. While effective, these approaches require specialised equipment and may limit patient acceptability and clinical implementation.

In contrast, passive methods focus solely on formulation optimisation, without mechanical intervention or external devices. These include increasing the thermodynamic activity of drugs within formulations [38-40], incorporating skin penetration enhancers [38, 41-44] and employing ion pairing strategies [45]. Passive approaches are particularly attractive for clinical applications due to their simplicity and cost-effectiveness.

1.5 Ion pairing: a strategy for ionised drug delivery

Ion pairing is a passive enhancement strategy which can be used to address the challenges associated with ionised pharmaceutical compounds. The concept was established by Bjerrum [46] in the 1920s, who proposed that for ion pairs to form, the electrostatic energy of attraction between oppositely charged ions would need to exceed their mean thermal energy. Under these conditions, the ions may be drawn together and, if a critical distance is achieved, behave as a single, unionised species. Although such pairing is inherently fragile, relying solely on electrostatic attraction rather than covalent or ionic bonding, it can nonetheless facilitate partitioning into lipid environments such as the *stratum corneum* [23, 45, 47].

Ion pairing offers several potential advantages for topical applications including enhanced drug partitioning into the skin, improved permeation rates and the possibility of reducing required drug concentrations.

1.6 Counterion selection criteria and amino acid advantages

The selection of suitable counterion candidates for topical ion pair formulations requires the consideration of multiple factors. Charge compatibility and molecular size [23, 46] influence the formation of the ion pair, which in turn affects its ability to partition into lipid environments, while toxicity must be evaluated to ensure safe topical application [48].

Amino acids represent promising counterion candidates due to their established safety profiles. The basic amino acids L-arginine, L-histidine, and L-lysine, as well as their salts, are generally recognised as safe (GRAS) when used as food additives by the FDA [49]. Similarly, the Cosmetics Ingredients Review panel has concluded that amino acids are safe under current practices and concentrations in cosmetic formulations [50]. In addition to their safety profile, amino acids offer sustainability advantages as renewable, economical resources with low environmental impact.

1.7 Research rationale and innovation

Current diclofenac formulations, while clinically effective, represent suboptimal utilisation of the active pharmaceutical ingredient due to limited skin penetration. The inclusion of novel amino acid-based ion pairs as part of a rational formulation strategy could enhance the amount of the active both delivered to the membrane and permeating, while potentially reducing drug concentrations. Such an approach offers both economic and environmental benefits and aligns with major pharmaceutical companies' commitments to reducing the presence of pharmaceuticals in the environment [51-54].

The combination of DF’s clinical importance, its physicochemical challenges and the established safety and sustainability advantages of amino acids, presents a compelling opportunity for investigation. The aim of this research is to demonstrate the feasibility of amino acid-based ion pairing for diclofenac delivery, rather than to develop a complete market ready formulation. Success in this proof-of-concept study

would establish a framework applicable to other ionisable drugs facing similar topical delivery challenges.

2 Aims and objectives

2.1 Aims and objectives of the thesis

2.1.1 Aim

The aim of this work is to explore a novel ion pair strategy, using amino acids, to enhance the percutaneous delivery of diclofenac (DF).

The objectives of this thesis are detailed below, organised by chapter to reflect the structure of the work:

2.1.2 Objectives

Chapter 3

2.1.2.1 To consider the skin as a pathway and destination for drug delivery

This chapter is not intended as a comprehensive literature review, but rather as a concise overview of the skin as both a pathway and destination for drug delivery, providing essential context for the subsequent chapters.

Chapter 4

2.1.2.2 To review the literature relating to ion pairs for topical applications

The review paper titled *"Ion Pairs for Transdermal and Dermal Drug Delivery: A Review"* was originally published in 2019. Relevant updates and developments since its publication have been incorporated at the end of the chapter.

Chapter 5

2.1.2.3 To develop experimental protocols for demonstrating ion pair formation and evaluating formulation development, including distribution coefficient studies, *in vitro* permeation testing (IVPT), solubility and stability characteristics

Although the experimental methods are detailed in the published papers included in this thesis, this section provides an overview of the methodologies, with references to the relevant chapters for clarity and completeness.

Chapter 6

2.1.2.4 To characterise diclofenac free acid (DFA) and diclofenac sodium (DNa)

2.1.2.5 To identify potential amino acid counterion candidates based on size, toxicity and charge compatibility criteria

2.1.2.6 To assess, via distribution coefficient studies, the partitioning of DFA and DNa from an aqueous phase (pH 7.3 ± 0.2) into an organic phase, with and without the selected amino acids at different concentrations

2.1.2.7 To evaluate the combination of DNa and the amino acid counterion in simple aqueous formulations equivalent to both finite and infinite doses applied to porcine skin IVPT

This chapter is based on the work published in the paper titled *"A preliminary investigation into the use of amino acids as potential ion pairs for diclofenac transdermal delivery".* The overall aim was to explore the potential of amino acids to enhance the transdermal delivery of DF by forming ion pairs with either the free acid (DFA) or sodium salt (DNa) forms of the drug.

Chapter 7

2.1.2.8 To assess DNa solubility in various solvents and identify those miscible with water, the only solvent in which LHSS dissolves

2.1.2.9 To develop a model binary system for the evaluation of the ion pairs

The purpose of this chapter was to build on the findings presented in Chapter 6, addressing solubility challenges associated with DNa-amino acid ion pair formulations. The aim was to identify suitable solvent systems for DNa and the selected amino acid counterion, L-histidine hydrochloride monohydrate (LHSS) and to evaluate their potential for enhancing skin permeation under finite dose conditions.

Chapter 8

2.1.2.10 To consider the impact of solvent substitution

2.1.2.11 To develop a ternary system to enhance the delivery of DF

2.1.2.12 To compare the best novel system with a commercial DNa product using finite dose applications

2.1.2.13 To characterise the selected ion pairs using FT-IR

This chapter aimed to develop the work presented in the previous two chapters by investigating the impact of solvent substitution within the binary system described in Chapter 7. Subsequently, ternary systems were to be developed with the goal of further enhancing DF delivery using ion pair strategies.

3 The skin as a pathway and destination for drug delivery

The topical application of drugs provides a number of benefits including the avoidance of first pass metabolism, the potential for steady state release [14], localisation of application [15], patient compliance and, with particular reference to NSAIDs, the avoidance of gastrointestinal and renal problems [55]. However, as evidenced by the extensive body of literature focused on increasing topical, dermal or transdermal drug delivery, this area of research is not devoid of challenges. In order to understand this drug delivery route, an overview of the structure and physiology of the skin is essential.

3.1 The structure of the skin

Enveloping the surface of the body, the skin is a fundamental part of the integumentary system [56]. It is involved in a variety of functions including thermoregulation, detection of stimuli via sensory nerve receptors (mechanoreceptors, thermoreceptors, nociceptors and proprioceptors), prevention of excessive water loss and the production of vitamin D. It also protects against physical damage, UV rays and the ingress of xenobiotics and microorganisms [57].

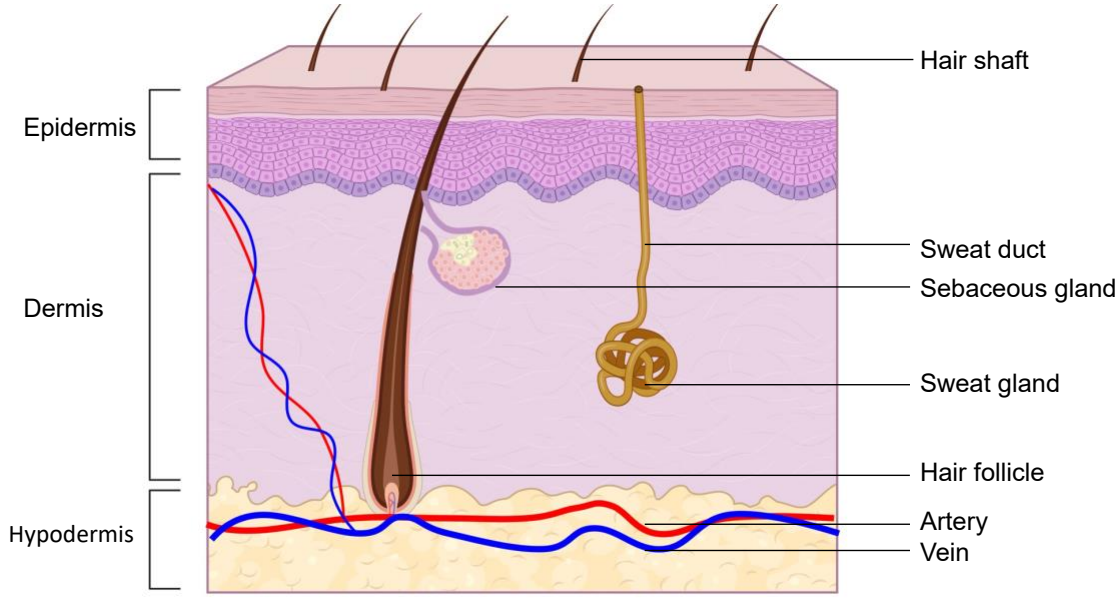

Figure 3. 1 The skin and its appendages (author's own illustration).

As shown in Figure 3.1, the skin comprises two main sections: the epidermis and the dermis, which rest upon an area of subcutaneous tissue known as the hypodermis or subcutis [58].

3.1.1 The hypodermis

The hypodermis is populated by mature adipose cells that are organised into lobules, separated by bands of collagen-based connective tissue or *septae*. This layer of fat cells provides insulation and protection from mechanical stress. It also serves as a source of energy and assists in thermoregulation [58]. As shown in Figure 3.1, a rich microvasculature runs through the *septae* supplying the dermis and facilitating the provision of oxygen and nutrients to the skin [59].

3.1.2 The dermis

The dermis, positioned directly above the hypodermis, plays a supporting role in relation to its elevated counterpart, the epidermis. It ranges in thickness from approximately 1 mm on the eyelids to over 5 mm on the back of the human body [60]. The principal cell type, fibroblasts, synthesise collagen and elastin that provide cushioning, support and elasticity [60]. The collagen fibres and elastic connective tissue exist in an aqueous gel-like matrix. Apart from housing appendages such as hair follicles, sebaceous glands and sweat glands, the dermis has a rich blood supply as well as lymph vessels. These enable the dermis to supply the epidermis, which lacks a blood supply, with oxygen and nutrients while also removing diffused waste products.

Drugs that reach the dermis are expected to be taken up by either the blood supply or, for larger molecules, the lymph vessels. This facilitates the concentration gradient required for the passive diffusion of any topically applied drugs. However, in cases of vasoconstriction, a lower systemic uptake of any permeant would be expected, leading to a greater accumulation of hydrophilic substances in the dermis [61-63].

3.1.3 The epidermis

Located above the dermis and linked by a cutaneous basement membrane zone [63], the epidermis provides the interface between the body and its external environment. It is therefore the epidermis which presents the principal area of concern in topical, dermal or transdermal drug delivery systems. Its thickness varies across different parts of the body, ranging from approximately 0.16 mm on the eyelids to 0.80 mm on the

soles of the feet of the human body [64]. However, literature in this area presents a diverse range of findings. When Mogensen *et al.* measured epidermal thickness at various anatomical locations including the forehead, ear, nose, cheek, chin, dorsum of hand, palm, palmar antebrachium, dorsal antebrachium, chest, back of the neck and calf, it was found that if the palms were excluded, the data across the rest of the areas followed a normal distribution [65].

In contrast, other investigations observed significant regional variations in individuals of both epidermal thickness and *stratum corneum* thickness [66]. Furthermore, whilst some publications attributed variations in epidermal thickness to gender and skin colour [66], Mogensen's group found no significant differences corresponding to these factors. There is much support for the concept that age does result in differences in epidermal thickness [65, 67, 68] though this is not confirmed by all studies [66].

The epidermis contains various cell types, as depicted in Figure 3.2. These include melanocytes, Langerhans and Merkel cells, but the most abundant cell type is the keratinocyte [61].

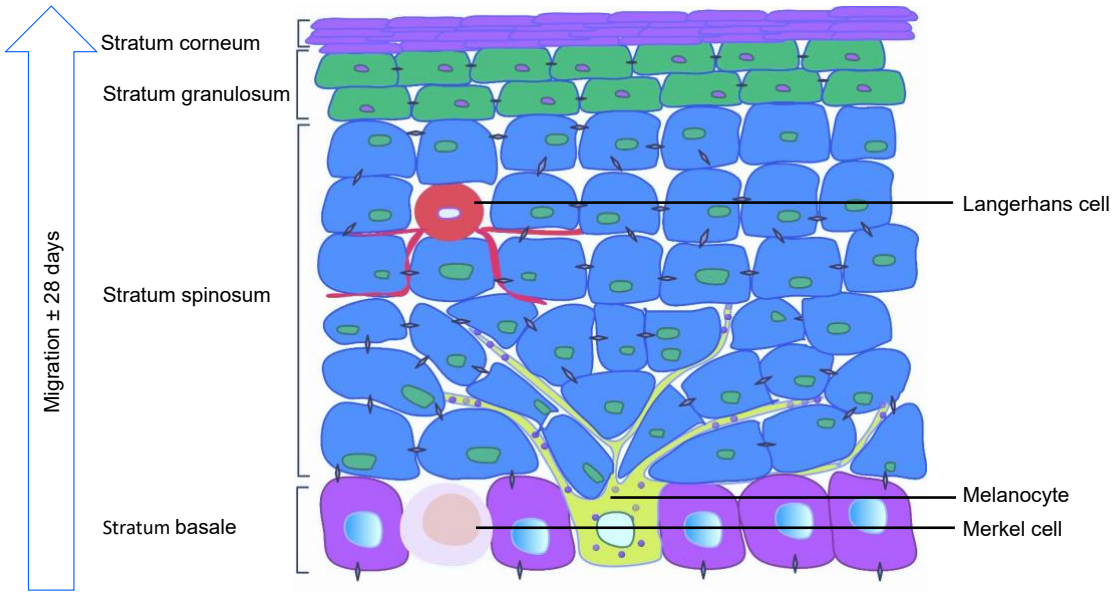

Figure 3. 2 The stratified layers of the epidermis (author's own illustration).

Melanocytes are dendritic cells that synthesise melanosomes within the Golgi apparatus. These pigment-producing granules are then transferred to the tips of their dendritic or cellular processes, which extend beyond their main cell bodies. This

facilitates interaction between a single melanocyte and multiple keratinocytes, whereby the endings of the dendritic processes are ingested by the keratinocytes via phagocytosis [59]. The melanin is then arranged to form caps over the nucleus of the keratinocyte protecting it from ultraviolet radiation. Persistent sun exposure stimulates the melanocytes to produce more melanosomes. Furthermore, it is the number, size and distribution of melanosomes that determine skin colour, rather than the number of melanocytes [59].

Langerhans cells, also dendritic cells, are involved in providing immune functions within the epidermis. They are able to extend and retract their dendrites through intercellular spaces of keratinocytes in surveillance activities termed “dendrite surveillance extension and retraction cycling habitude” [69]. In addition, they can enforce barrier integrity by creating tight junctions with keratinocytes [70].

It was previously thought that Langerhans cells, as the major antigen-presenting cells in the skin [71], operated by taking up any invaders, processing them, and then migrating to lymph nodes for presentation to and activation of T-cells [59]. It is now understood that these cells also play many roles in situ, including interacting with T-cells and clearing apoptotic keratinocytes [70].

Merkel cells are sensory receptors associated with the terminal filaments of cutaneous nerves [59].

The primary function of the epidermis is the construction of a thin, yet highly effective barrier, known as the *stratum corneum*. The production of this barrier occurs in stages, reflected by the stratified layers of the epidermis. As shown in Figure 3.2, there are generally four layers, the *stratum basale, stratum spinosum, stratum granulosum* and *stratum corneum*. On the palms of the hands and the soles of the feet, also known as glabrous or hairless skin, there is an additional layer called the *stratum lucidum*, located just below the *stratum corneum*.

The construction of the barrier commences in the *stratum basale*, also known as the *stratum germinativum* or basal layer. It is generally only one layer thick in non-glabrous skin and contains both Merkel cells and melanocytes. The latter represent 5 – 10% of the cells in this layer [60]. Division of the basal stem cells propels half of the cells into the next layer, the *stratum spinosum*. Here the shape of the keratinocyte transforms from columnar to polygonal. Desmosomes bind these keratinocytes together, and are

in turn bound together intracellularly by synthesised keratin [59]. As the differentiation process continues, cells move towards the *stratum granulosum.* These comprise keratohyalin granules which contain profilaggrin, the precursor of filaggrin [72]. Various enzymes cause the degradation of the nucleus and organelles within the cells. Profilaggrin is converted into filaggrin, and this transformation leads to the generation of several crucial structural proteins, including keratin and involucrin [59]. Lamellar bodies or granules fuse with the membrane of the flattening cells and secrete their contents into intercellular spaces [73]. The final stage of differentiation signals the end of what is often referred to as the viable epidermis and culminates in the formation of the *stratum corneum* [73]. Cells are now flattened and there is no longer a nucleus. The dead cells are encased in a cornified envelope made up of keratin, filaggrin and involucrin [59] and are known as corneocytes.

Epidermal turnover time from the basal layer to desquamation ranges from 40-56 days [74], with specific estimates of 45 days for volar forearm [75] and 47-48 days using refined kinetic models [76]. These values vary significantly with anatomical location [62, 77], age [78], and disease state [79]. Facial skin demonstrates faster turnover than unexposed regions [62, 80], while aging prolongs turnover [78]. Pathological conditions such as psoriasis dramatically reduce turnover to 6-8 days [76], whereas other dermatological disorders may exhibit either accelerated or delayed epidermal renewal [81].

3.1.3.1 The *stratum corneum* and routes of permeation

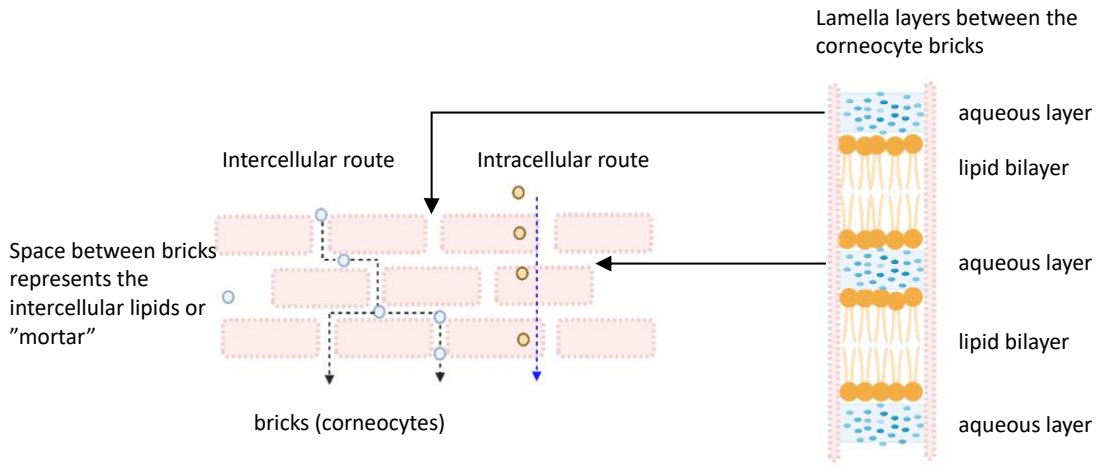

Figure 3. 3 The bricks and mortar structure of the stratum corneum. On the right is an enlargement of the lamellar structure of the intercellular lipids (author's own illustration).

The *stratum corneum* has long been acknowledged as the primary barrier to permeation [82], with its structure likened to a “brick and mortar” arrangement [83]. The “bricks” are composed of fully differentiated keratinocytes known as corneocytes, embedded in a lipid rich “mortar” containing a mixture of ceramides, free fatty acids and cholesterol. This “mortar” is organised into a lamellar structure comprising alternating lipid bilayers and aqueous layers, as illustrated by the magnification in Figure 3.3.

The *stratum corneum* is approximately 10 – 20 μm thick and comprises between 15 – 25 layers of cells. Each cell is in the region of 50 μm wide and circa 0.5 μm thick [77]. The permeation of any molecule across this barrier can occur via two potential pathways namely appendageal or shunt pathways, and the bulk diffusion pathways. The appendageal or shunt pathways refer to permeation via sweat glands, hair follicles, and associated sebaceous glands but are considered less significant due to the low surface area of these appendages [21]. It is important to note, as emphasised by Chilcott, that these pathways are not akin to "intergalactic wormholes" providing a paranormal route of entry into the skin [7]. They are still lined with the same barrier, requiring molecules to overcome the same obstacles.

The bulk diffusion pathways are indicated in Figure 3.3 and include the para- or intercellular route (as seen on the left-hand side of the figure) and the transcellular route (on the right-hand side of the figure). The intercellular route refers to the tortuous passage of a molecule between the cells, requiring the molecule to partition between the alternating lipid and aqueous layers, and making the pathlength significantly longer than the thickness of the *stratum corneum* [84]. The transcellular route requires a molecule to diffuse through the corneocytes or “bricks” as well as the intervening lipid or “mortar” layers. While there appears to be a great deal of evidence favouring the intercellular route [77, 84, 85], there are still proponents of the transcellular route [86].

3.2 Models used in permeation studies

The Organization for Economic Cooperation and Development (OECD) provide guidelines for the two categories of permeation studies, namely *in vivo* studies via Test Guideline 427 [87] and *in vitro* test methods in Test Guideline 428 (TG 428) [88].

Additionally the OECD published Guidance Document 28 for the conduct of skin absorption studies [89] in 2004 and Guidance Note 156 (GN 156) relating to Dermal Absorption [90] in 2011. Guidance Note 156 is currently under review [91].

3.2.1 *In vivo* studies

In vivo studies, using humans or animals, provide biochemically, immunologically and physiologically intact systems, which are critical to determining local or systemic toxicity. They are, however, subject to disadvantages. These may include the need for radiolabelled material to ensure reliable results, challenges in detecting early absorption data and differences in the permeability of the most frequently used rat models and human skin [87]. In addition, there are extensive legal and ethical constraints. For these reasons, as well as economic factors, *in vitro* studies are often employed as a useful alternative particularly in early stages of any study [62].

3.2.2 *In vitro* studies

In vitro experiments facilitate the measurement of the rate at which a permeant diffuses through a membrane. Moreover, the use of mass balance studies enables quantification of the amount of permeant in the receptor solution, the amount of permeant in the membrane and the amount of permeant remaining on the surface of the membrane [62].

The apparatus used to conduct *in vitro* studies are known as diffusion cells. The membrane is sandwiched between the two compartments of the diffusion cell, namely the donor and the receptor compartments. The membrane should be maintained at 32 ± 1°C to mimic normal skin temperatures. A quantity of the test substance that reflects its expected use, is applied via the donor compartment. TG 428 states that in normal circumstances this quantity, referred to as a finite dose, amounts to 1-5 mg/cm^2 of skin for a solid and up to 10 µL/cm^2 for liquids. The receptor compartment is filled with an appropriate solution to ensure solubility of the applied permeant so that sink conditions are maintained. The proposed amendment to GN 156 suggests that the solubility of the permeant in the receptor solution should amount to at least ten times the maximum concentration expected in the receptor solution at the end of an *in vitro* study [91]. If the permeant is water-soluble, a solution such as phosphate buffered saline (PBS) with a pH of 7.4 is normally chosen to reflect a physiological state. It is from this

receptor solution that samples are taken for quantitative analysis. Generally, 6 – 12 sampling points over a 24 h period are recommended. This is subject to the physicochemical properties of the compound, as more lipophilic drug compounds may accumulate in the skin and take considerably longer to diffuse into the receptor fluid, if at all, relative to more hydrophilic moeities [89, 90].

There are two main categories of diffusion cells, the first where the receptor solution is “static” i.e., it remains within the receptor compartment. In the second type the receptor solution flows through the receptor chamber [62, 77]. A Franz diffusion cell is an example of the static type and can be seen below in Figure 3.4.

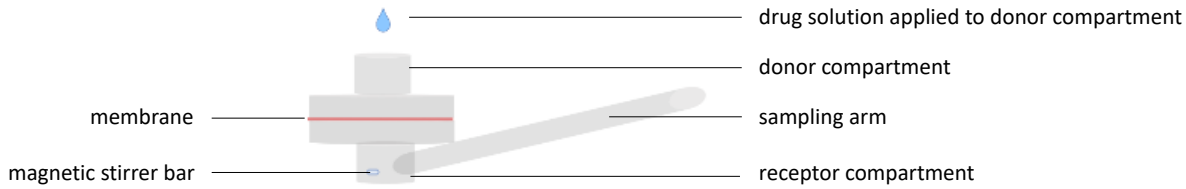

Figure 3. 4 Scheme of Franz diffusion cell. Drug formulation is applied to the membrane via the donor compartment. The membrane is sandwiched between the donor and receptor compartments. Clamps which hold these together are not shown. The receptor compartment contains a solution in which the drug will be soluble, often PBS at a pH of 7.4 to replicate the pH of plasma. The receptor fluid is stirred continuously using a magnetic stirrer bar. The Franz cell is warmed by keeping it in a water bath at a temperature sufficiently high to enable the membrane to attain the temperature of human skin 32 ± 1 ° C . Samples are taken from the sampling port, which is stoppered to prevent evaporation (author’s own illustration).

In vitro studies utilise a variety of different membranes including *ex vivo* human and animal skin, synthetic and three-dimensional (3D) human skin models.

3.2.2.1 Human and animal skin *ex vivo* models

Excised human skin is considered the gold standard for *in vitro* permeation studies when the primary aim is to determine permeation profiles of molecules in humans. Nonetheless, it is essential to consider inter- and intra-individual variability in the skin, when conducting permeation experiments.

Due to the limited availability of human skin, various animal skin models including rodent, snake and porcine models, have been investigated. Rigg and Barry [92] found

that hairless mouse and shed snake skin models were not suitable substitutes for human skin models. Mouse skin becomes increasingly permeable when exposed to hydration beyond 48 h [93]. The most favoured animal model membrane is porcine, in particular the skin obtained from the ear. It was found to have a similar permeability profile to human skin especially in relation to lipophilic compounds [94, 95]. Jacobi *et al.* found that the histological structure of porcine ear skin compared favourably with human skin [96]. This was supported by Starr et al who demonstrated comparable molecular composition and depth-dependent organisation of the *stratum corneum* in both species [95].

3.2.2.2 Synthetic *in vitro* studies

While human skin is the first choice for permeability studies, due to the constraints listed above it is often easier to begin with synthetic membranes. They are relatively easy to access and provide consistency in terms of the membrane structure. This consistency facilitates the assessment of the uniformity of different batches of a drug product [97]. Different types of synthetic membranes include silicone, polycarbonate and cellulose [97].

3.2.2.3 3D human skin models

The purpose of these models is to create human skin equivalents that will respond, and function, as human skin does. Some models are produced to represent the epidermis, such as EpiDermFT™, EpiSkin™ and SkinEthic™ RHE, while others also incorporate the dermis, for example Pheninon® FT. In general, these skin models are considered to overestimate flux [98]. Furthermore, the second draft of the amendment to GN 156 states that the use of cultured and reconstructed human skin models is not recommended for the determination of dermal penetration due to reports that their barrier function is not comparable to ordinary human skin [91].

3.2.2.4 Skin-on-a-chip microfluidic devices

Skin-on-a-chip is a type of microfluidic device generally referred to as organs-on-chips. These are cell culture devices that incorporate microchip manufacturing methods, enabling continuously perfused compartments containing living cells, to receive physical and chemical stimulation [99]. Skin-on-a-chip models can be divided into two categories: those using human skin, or an equivalent, that is transferred onto the chip; and the other where the skin is generated *in situ*. The *in situ* culturing of skin is however

subject to many limitations in terms of cell layers and differentiation, though improvements are continuous. Skin-on-a chip devices have also been used in multi-organ models [100], allowing researchers to study the response of several organs to drug compounds [101]. These devices present potential new technologies to evaluate not only drug permeation, but also drug efficacy and possible side effects [100] using high throughput methods [102].

3.2.3 *In silico* modelling

In silico modelling uses the physicochemical and structural properties of a molecule to predict the percutaneous absorption of the molecule via quantitative structure-activity relationships (QSARs) also known as quantitative structure-permeability relationships (QSPeRs). A well-known example of this is the “Potts and Guy equation”. The permeant’s size, in terms of molecular weight or molecular volume, together with its Log P value, was used to predict its percutaneous flux [103]. Unfortunately, the model has very limited applicability, as the data set on which it was based comprised mainly hydrophilic molecules and prediction was based on compounds applied in an aqueous solution to the skin. *In silico* modelling has subsequently developed from models based on linear regression only, to those incorporating machine learning schemes to predict permeation [104]. The field has continued to advance [105], with models now incorporating both techniques [106].

In silico models offer significant advantages in terms of economic efficiency and time savings. However, owing to the limitations associated with their application [105], guidance documents require a sound scientific basis for choosing these models as an alternative to experimental work [90]. The second draft of the proposed amendment to GN 156 sets out some of the key obstacles to the use of QSARs in percutaneous absorption assessments. These include the limited size and diversity of data sets used to develop the models; potential variability or insufficient knowledge of the experimental parameters from which the data derived; overlooking the concentration or dilution of the test compound; absence of consideration for other components of the formulation; and the frequent failure to predict the percentage of dermal absorption from finite or “normal exposure” doses [91]. Addressing the complexities involved in permeation modelling, Alikhan *et al.* emphasised the large number of influencing factors, including the physicochemical properties of the drug compound, the properties

of the vehicle, the structure and properties of the skin and the interactions between all of these factors [107].

3.3 Measurement of molecular transport across membranes

The fundamental process upon which permeation depends, is the concept of passive diffusion. A higher concentration of molecules increases the probability of molecular collisions. These collisions transfer momentum and ultimately cause the movement of particles down their concentration gradient. Particles separated by a permeable membrane, follow the same course of action [108].

Diffusional flux is the measurement of the number of molecules that pass through a membrane over time [109]. Fick's laws of diffusion constitute the tools used to interpret information generated by permeation experiments.

Fick's first law of diffusion describes a steady state diffusional flux and can be written:

Equation 3. 1 Fick's first law of diffusion.

$$J_{ss} = \frac{DK\Delta c}{h}$$

Where:

$J_{ss} =$ flux with units mol/cm/s
$D =$ diffusion coefficient
$K =$ vehicle – skin partition coefficient
$\Delta c =$ concentration gradient across the membrane
$h =$ diffusional path length

As explained by Hadgraft, the concentration applied to the membrane (C_{app}) is significantly higher than the concentration beneath the membrane under *in vivo* conditions [52, 53]. This is attributed to the fact that a majority of drug compounds capable of partitioning and permeating across the epidermal barrier, ultimately undergo clearance through the microvasculature and lymphatic vessels upon reaching the dermal layer. The equation can therefore also be written as:

Equation 3. 2 Fick's first law of diffusion, where there is no marked change in concentration applied to the membrane.

$$J_{ss} = k_p . c_{app}$$

Where:

$k_p = \frac{KD}{h}$

c_{app} = applied concentration.

3.4 Factors that may affect percutaneous absorption

The various components that contribute to the transport of molecules across a semi-permeable membrane are shown in Fick's 1st law of diffusion. They include the diffusion coefficient, the vehicle-skin partition coefficient, the applied concentration, and the path length. These components are influenced by the physical and chemical properties of the drug compound, its vehicle and the skin. Furthermore, the interaction between each of these factors also influences percutaneous diffusion [110].

3.4.1 Properties relating to the skin

Several membrane properties, such as thickness, donor age, and demographic background, have been explored for their potential influence on permeation.

3.4.1.1 Thickness of the *stratum corneum*

As the rate of diffusion is affected by the length of the diffusion pathway (h), as shown in Equation 3.1, the thickness of the *stratum corneum* as well as the number of cell layers are important considerations. Furthermore, when considering permeability at different locations, adjustments should be made to account for differing thickness or number of cell layers [111]. It is generally accepted that the thickness of the *stratum corneum* varies between individuals at the same site [112] and at different anatomical sites of the same individual [113-115]. However, given the many different ways of sampling the thickness of both the epidermis and the *stratum corneum*, some of which are mentioned by Holbrook and Odland [113], it is clear that different methods can result in large variations in calculated thickness. Whilst the regional variations in percentage terms should remain consistent between studies, in terms of using absolute values of thickness, it may be considered preferable to focus on the number

of cell layers. Unsurprisingly, however, cell layers are also subject to variation between individuals when considering the same location [14] and at different anatomical locations within the same individual [113]. It has been determined however, that neither age nor gender contributed to any significant differences in the number of cell layers at a particular site [116]. Regional variations have been shown to result in differences in permeation, with highest to the lowest permeation ranked as follows: genitals > head and neck > trunk > arm and leg [97].

3.4.1.2 Maturation and size of corneocytes

While the number of cell layers and *stratum corneum* thickness provide important baseline measurements for diffusion pathway calculations, recent evidence suggests that it is the maturation state and size of individual corneocytes within these layers that exerts a greater influence on barrier function.

Mature corneocytes are typically larger [117] and polygonal in shape with a more rigid cornified envelope than immature corneocytes. The latter, in contrast, are smaller, irregularly shaped and have a more fragile cornified envelope [118, 119]. The presence of immature corneocytes has been strongly associated with barrier dysfunction and increased transepidermal water loss (TEWL) [118, 120]. While immature corneocytes are often found in skin affected by inflammatory or hyperproliferative conditions, such as psoriasis [119], they also present in non-diseased skin at specific anatomical sites including the forehead, lips and cheeks [118]. They were not, however, identified on the trunk or extremities eg back, lower leg, back of hand and palm of the human body [118].

Anatomical variation in corneocyte morphology has been well documented. Early studies reported differences in corneocyte surface area [121] and thickness [122] across body regions. The possible link between surface area and percutaneous absorption was noted by Rougier *et al* [123] when it was determined that anatomical site influenced penetration. Total penetration was found to increase in the following order: back < arm < chest < thigh < abdomen < forehead, with the forehead demonstrating approximately threefold greater permeability than the back [123].

A larger study assessing 90 participants further quantified these differences, finding that corneocyte size increased progressively across the sites: forehead < wrist <

ventral wrist = ventral mid forearm close to the ventral elbow = elbow < abdomen. Correspondingly, TEWL values decreased in a reciprocal manner: forehead > wrist > ventral wrist = mid-forearm = elbow = abdomen [124]. These trends have been consistently observed in additional studies at different regional sites, including facial locations [125], reinforcing the relationship between corneocyte size, regional barrier function and TEWL [126, 127].

As corneocytes mature, their surface area increases [117, 128] contributing to an extended geometric pathlength for diffusion. Larger, more mature cells are thus associated with lower TEWL values, improved barrier properties and lower permeability [117, 124, 128]. The geometric pathlength for water efflux has been shown to be directly related to corneocyte size, with TEWL values approaching zero when corneocytes are infinitely large. It was also found that skin sites with smaller corneocytes also had fewer cell layers, contributing further to the diminished pathlength [124].

The maturation process creates distinct regions within the *stratum corneum*: the inner layers are characterised by smaller, more immature cells with fragile cornified envelopes, while the upper layers contain more resilient, more mature corneocytes with superior barrier properties [117, 129].

3.4.1.3 Age

While extrinsic and intrinsic ageing do modify the structure of the skin, it is the impact on the *stratum corneum,* as the main barrier, that is key. A number of studies report that ageing has no impact on the thickness of the *stratum corneum* [66, 67, 78] or the number of cell layers it comprises, as mentioned previously. Although lipid composition does appear to change with age, this did not impact the skin permeation of a variety of compounds [97]. Exceptions relate to preterm infants, where the *stratum corneum* has fewer cell layers and thus an underdeveloped barrier [130].

3.4.1.4 Demographic background

The influence of skin colour on permeation remains an area of ongoing investigation, with current findings yielding inconsistent and inconclusive results. Despite various studies exploring potential differences, no definitive consensus has been reached, underscoring the need for further research that accounts for biological variability, methodological rigour and inclusive sampling. [77].

3.4.2 Properties relating to the drug compound

The physicochemical properties of a drug compound including size, melting point, and ability to partition between lipid and aqueous layers all contribute to the permeation of the drug compound.

3.4.2.1 Molecular weight

A molecular mass of 500 Daltons (Da), or 500 g/mol, is considered the upper limit for the permeation of topically applied molecules [131]. This is due to the size of the intercellular spaces and the packing of the lamellar layers [62].

3.4.2.2 Melting point

A relationship between an increase in the melting point of a compound and a corresponding decrease in permeation was proposed by Kasting *et al.* [132]. This concept has also been applied by using the thermal characteristics of compounds to predict the flux of one compound relative to another [133].

3.4.2.3 Log P

Molecules with a log P of between 1 and 3 are ideal for skin permeation purposes [84, 134] as these molecules are able to partition into both the lipid and aqueous layers of the intercellular spaces. Compounds with Log P values which are lower than 1, partition less into the *stratum corneum*, resulting in fewer molecules available for diffusion. Conversely, those with Log P values above 3, may result in partition, but the molecules are more likely to remain within the lipid layers, limiting permeation [135].

3.5 Methods for increasing permeation

As mentioned above, the barrier function provided by the skin is so effective that only 1-2 % of an applied dose is generally able to permeate in topical formulations [136]. As a result, a variety of mechanisms have been used in attempts to increase permeation. These can be divided into two groups, namely active and passive techniques.

3.5.1 Active methods

Active methods are those that use physical means to overcome barriers [26], such as iontophoresis [28, 29], phonophoresis or sonophoresis [31], magnetophoresis [32], electroporation [33] and microneedles [34, 35].

3.5.2 Passive methods

Rather than using physical resources, passive methods rely on the optimisation of the formulation. Such methods include increasing the thermodynamic activity of drugs in the formulation [38], the use of skin penetration enhancers [42] and also the use of ion pairs [41].

3.5.2.1 Thermodynamic activity

Higuchi [137] explains the effects of thermodynamic activity on flux using an alternative version to Equation 1.1, shown in Equation 3.3:

Equation 3. 3 Fick's first law of diffusion expressed in terms of the thermodynamic activity of the penetrating agent in its vehicle.

$$J_{ss} = \frac{\alpha DA}{\gamma h}$$

Where:

α = the thermodynamic activity of the drug in its vehicle
γ = the effective activity coefficient of the penetrating agent in the skin barrier
A = surface area.

This equation shows how an increase in α, the thermodynamic activity of the drug in its vehicle, will increase flux. Although a saturated solution is normally considered to provide the highest thermodynamic activity, a higher energy state can be achieved by supersaturation. Supersaturation of a formulation can occur via evaporation or rapid permeation of solvents comprising the excipients of the formulation [39, 138]. Providing the stability of the formulation can be maintained, an increase in flux should result [139].

3.5.2.2 Skin penetration enhancers

Skin penetration enhancers (SPEs) and their mechanisms of action have been the subject of numerous investigations and reviews [42, 140, 141]. SPEs are excipients, generally within the formulation, that impact the permeation process in a variety of different ways. These include the alteration of lipid domains by insertion into the lipid bilayers, disrupting the packing of the bilayers and increasing the fluidity of intercellular

lipids. Interaction of SPEs with proteins within the skin barrier may result in changes to protein conformation and lead to the opening of water channels. Protein-related enhancement may also contribute to a reduction in intercellular cohesion [142]. According to the lipid-protein-partitioning theory, SPEs may also impact permeation by facilitating the partitioning of the drug compound from the formulation into the skin by modifying the nature [142] or solubility parameter of the skin.

3.5.2.3 Ion pairs

Ion pairing is an additional passive strategy employed to enhance the partitioning and permeation of drug molecules that exist in an ionised state. This method involves incorporating an ion with an opposite charge to the permeant of interest, into the drug formulation. When successful, the electrostatic attraction between these oppositely charged ions is sufficiently strong to cause them to draw together and behave as a single, unionised species. Consequently, the ion pair is able to partition into lipid environments such as the skin. It is essential to note that an ion pair does not constitute a novel chemical entity since there is no formation of ionic or covalent bonds. A comprehensive review of ion pairs is reported in Chapter 4.

4 Ion pairs for transdermal and dermal drug delivery: a review

4.1 Overview

This paper “Ion Pairs for Transdermal and Dermal Drug Delivery: A Review” was published on 20 June 2021 in *Pharmaceutics* (13, no. 6:909, https://doi.org/10.3390/pharmaceutics13060909). The co-authors and their contributions were as follows:

Cristofoli, Mignon: conceptualisation, investigation, visualisation, writing: original draft and amendments; Kung, Chin-Ping: writing - review and editing; Hadgraft, Jonathan: writing: review and editing; Lane, Majella, E.: conceptualisation, supervision, writing: review and editing; and Sil, Bruno C.: conceptualisation, supervision, writing: review and editing.

The only alterations made to this publication pertain to its formatting, which has been adjusted to enhance its readability within the main body of this thesis. Post publication updates are included in section 4.6.3.

Addressing objective 2.1.2.2, this chapter reviews the literature relating to ion pairs for topical applications. This review establishes the foundational understanding of ion pairing principles necessary to embark on the experimental ion pair work presented in Chapters 6-8.

4.2 Abstract

Ion pairing is a strategy used to increase the permeation of topically applied ionised drugs. Formation occurs when the electrostatic energy of attraction between oppositely charged ions exceeds their mean thermal energy, making it possible for them to draw together and attain a critical distance. These ions then behave as a neutral species, allowing them to partition more readily into a lipid environment. Partition coefficient studies may be used to determine the potential of ions to pair and partition into an organic phase but cannot be relied upon to predict flux. Early

researchers indicated that temperature, size of ions and dielectric constant of the solvent system all contributed to the formation of ion pairs. While size is important, this may be outweighed by improved lipophilicity of the counter ion due to increased length of the carbon chain. Organic counter ions are more effective than inorganic moieties in forming ion pairs. In addition to being used to increase permeation, ion pairs have been used to control and even prevent permeation of the active ingredient. They have also been used to stabilise solid lipid nanoparticle formulations. Ion pairs have been used in conjunction with permeation enhancers, and permeation enhancers have been used as counter ions in ion pairing. This review attempts to show the various ways in which ion pairs have been used in drug delivery via the skin. It also endeavours to extract and consolidate common approaches in order to inform future formulations for topical and transdermal delivery.

Keywords: ion pair; topical; counter ions; partition; permeation; porcine; human; skin

4.3 Introduction

The application of drugs via the skin provides a number of benefits. These include the potential to provide a steady-state release [14], the avoidance of first-pass metabolism in the case of transdermal formulations and the localisation of application for topical formulations [15]. Furthermore, the capacity for rapid cessation in cases of adverse reactions, the avoidance of side effects related to oral administration [143] and, with particular reference to non-steroidal anti-inflammatory drugs, the avoidance of gastrointestinal and renal problems [144], all contribute to the advantages of this delivery route.

Notwithstanding the many benefits, this mechanism of drug delivery needs to ensure that appropriate quantities of the drug are transported to the target site. The skin, however, does not offer an easy passage for the delivery of drugs. The outermost layer, known as the *stratum corneum* (SC), provides such an effective barrier that in the case of many topical formulations, only approximately 1–2% of the applied drug or active ingredient permeates [16].

This is partly due to the majority of pharmaceutical compounds being either weak acids or bases, with concomitant low aqueous solubility. As the most prevalent drug delivery system is oral, drugs are frequently developed as salts that ionise at physiological pH in an effort to facilitate processing and increase bioavailability. This poses a problem

for topical and transdermal drug delivery, because of the lipid-rich SC that prevents the passage of such ionised drugs at therapeutic rates. In striving to increase and also to regulate the permeation of drugs, a number of different methods have been explored. These can be divided into two groups, namely active and passive. Active methods are those that use physical means to overcome barriers, such as iontophoresis, phonophoresis and microneedles [34]. Conversely, passive methods rely on the optimisation of the formulation. Such methods include increasing the thermodynamic activity of drugs in the formulation [38], the use of skin penetration enhancers [42] and also the use of ion pairs [41].

This review considers the research pertaining to the use of ion pairs in topical and transdermal deliveries. As early permeation studies highlighted problems associated with the use of rat, mouse and snake skin, such studies have been omitted [92, 93]. In order to obtain data as best aligned to human skin responses as possible, permeation data are drawn exclusively from studies utilising human or porcine membranes [145].

4.4 Ion pairs

4.4.1 Background

Ion pairing results when individual ions behave as a neutral species or group via electrostatic interactions, without creating any ionic or covalent bonds [146]. In general, this occurs most favourably in solvents with low dielectric constants (ε), as the electrostatic interaction between ions has less competition from potential interactions with the solvent system [147]. Ions in an aqueous environment may potentially mask their charges via electrostatic interactions, allowing them to partition more readily into a lipid environment, such as the SC, than individual ions [23, 47].

The earliest theories concerning interactions between ions in electrolyte solutions included Milner's complex statistical calculation of the distribution of ions in solution, which considered both electrostatic interaction and thermal motion. Another attempt to calculate the energy of the interaction between ions was undertaken by Ghosh in 1918. The author, however, assumed that ions adopted a rigid crystal-like arrangement, ignoring the impact of thermal motion. A significant advance in the area was made by Debye and Hückel in 1923 which proposed the interaction of a central ion (m) and other ions in solution. The concept of an ionic atmosphere or cloud was

proposed by the authors suggesting that the relationship between the central ion and its neighbouring ions of opposite charge was a continuum, rather than a separate interaction.

The role of electrostatic interaction between pairs of ions was first considered by Semenchenko in 1924, but it was Bjerrum who developed the concept of ion pairs. It was suggested that at short distances, rather than the random thermal motion of ions in the ionic atmosphere, electrostatic interactions may develop between the central ion, m, and an oppositely charged ion, j. These interactions are sufficiently strong to overcome the independence of the individual ions, resulting in single-unit behaviour. When the two ions have the same number of charges, they will be considered electrically neutral. The formula for the total charge of two ion pairs was then devised according to:

Equation 4. 1 The total charge of two ion pairs.

$$(z_j - z_m)Q^0$$

Where:

z_j = charge number of the ion,

z_m = charge number of the central ion, and

Q^0 = elementary electric charge 1.602×10^{-19} C (C refers to the differential double layer capacity with the units $\mu F/cm^2$).

As theorised above, the electrostatic energy of attraction between ions needs to exceed their mean thermal energy, allowing them to draw together and attain a critical distance, resulting in ion pair formation. As the pair is linked by electrostatic forces, but not ionic or covalent bonds, the lifespan of the pairing, while greater than the contact of mere individual collisions, is susceptible to collapse during strong collisions with other particles [148].

In Untersuchungen über Ionenassoziation which can be translated as “Studies of Ion Association” [46], Bjerrum describes the activity of ions in solution using different solvents. The author showed how the association or disassociation of ions is dependent on three main factors: ε of the solvent, temperature and size of the ions [149]. However, the reliability of Bjerrum’s theory was limited, as it did not account for

elements such as solvation, concentrated solutions, solvents of high εs and hydrogen bonding [148-151]. Whilst extensions to the theory have been discussed [152], many of its basic principles are still applied for the purposes of topical and transdermal drug applications.

4.4.2 Ion pairs in topical and transdermal drug delivery

4.4.2.1 Partition coefficient

The appeal of ion pairs relates to the potential for compounds that are normally soluble in an aqueous environment, with their charges masked and enabling the partition of these systems into a subsequent lipid environment. A simple model of ion pairing would suggest that following passive diffusion into a lipid environment, the ion pairs would diffuse from areas of higher concentration to areas of lower concentration. When diffusing into an aqueous environment, the interactions with this more polar environment, comprising a higher ε, may reduce the degree of association between the ion pair, as suggested by Figure 4.1 below.

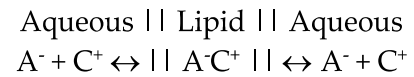

Figure 4. 1 Ions in the aqueous phase moving into the lipid phase as an ion pair.

This simple overview, however, does not account for interactions with biological membranes, different aqueous solubilities of compounds, solvent system combinations, size differences in the ion pairs and other extrinsic factors. It does, however, suggest the use of simple partition experiments to determine the potential of ion pairs to partition from aqueous into lipid environments. Such experiments have long been considered representative of hydrophobicity, an essential component of quantitative structure–activity relationships (QSARs) used to predict skin permeability [103, 153, 154].

These tests and their results are sometimes referred to as partition coefficients, apparent partition coefficients or distribution coefficients. Additionally, the logarithm of these values may be provided and are then referred to as Log P, Log P apparent or Log D. For the purposes of simplicity, this review will make reference to a partition

coefficient (PC) or PC studies and, where possible, will include the pH at which these experiments were conducted.

In general, PC measures the concentration of molecular species (S) in a non-miscible octanol (O) and aqueous (W) environment, as demonstrated in:

Equation 4. 2 Partition coefficient of S.

$$PCs = \frac{[S]_O}{[S]_W}$$

When incorporating factors such as pH and association or dissociation constants of compounds, a more representative formula for the PC of the chemical species is shown in:

Equation 4. 3 Partition coefficient of S represented by unionised, ionised and ion paired molecules.

$$PC_S = \frac{[U] + [I^-] + [I^-I^+]_O}{[U] + [I^-] + [I^-I^+]_W}$$

where:

U = unionised compound,

I^- = ionised version of the compound (anion),

I^+ = counter ion (cation), and

I^-I^+ = ion pair.

A typical example for the description of a weakly acidic compound states that there may be components of ionised, unionised and ion paired species in both the octanol and water phases. The same would hold for basic compounds that would use anionic counter ions.

PC experiments were used by Inagi *et al.* [155] to explain how indomethacin (IND), an acidic compound with an acid dissociation constant (pK_a) of 4.5 [20], was able to permeate to a greater extent than the predicted pH partition theory value would suggest. The PC of IND was tested singularly, at different pH values (2.0 – 9.0), and in conjunction with various cations. It was found that the PC for IND decreased from ~ 1.6×10^3 to 0.86 with the increase in pH (2.0 – 9.0). However, at a pH of 8.3, the PC of IND increased (~ 1.6×10^1 – ~1.7×10^3) with the increased concentration of sodium

cations (0.02–0.10 M). Conversely, an increase in IND concentration, while maintaining a constant concentration of sodium cations, did not change the PC. The authors stated that this suggested the formation of ion pair complexes between IND and sodium cations, but no association between IND molecules. Using similar experiments, they concluded that IND was able to form ion pair complexes with ammonium cations, potassium cations and triethanolamine [155].

PC studies have been used by many authors in advance of, or in conjunction with, ion pair permeation studies. PC studies undertaken by Green *et al*. [156] indicated the ability of the strong base naphazoline hydrochloride (HCl) to form ion pairs with fatty acids, and these were reflected by an increase in permeation through human skin. As shown in Table 4.1, the PC value for naphazoline HCl at a pH of 7.4 was 0.02 ± 0.01, increasing to 0.36 ± 0.04 and 0.45 ± 0.06 with the addition of oleic acid (OA) and lauric acid (LA), respectively. A PC value was reported at pH 8.0 only for neat naphazoline HCl (0.03 ± 0.01), as the increased pH caused emulsification when fatty acids were present. The permeability coefficients determined from the skin permeation studies, where the donor solution was maintained at pH 8, were approximately 0.33, 2.17 and 2.58 cm/h × 10^{-3} for naphazoline HCl, and in conjunction with OA and LA [156]. The structures of naphazoline and the fatty acid counter ions are shown in Figure 4.2.

Table 4. 1 Impact of OA and LA on the PC and permeability coefficient values for naphazoline. Concentration of naphazoline applied was 0.05 M (n = 4, values represent the mean ± S.D.) Adapted with permission from [156], Elsevier, 1988.

Partition coefficient of naphazoline	Isopropyl myristate (IPM) / buffer (pH 7.4)	0.02 ± 0.01
	OA in IPM / buffer (pH 7.4)	0.36 ± 0.04
	LA in IPM / buffer (pH 7.4)	0.45 ± 0.06
	IPM / buffer (pH 8.0)	0.03 ± 0.01
Permeability coefficient of naphazoline using human skin (cm/h x 10 $^{-3}$)	Naphazoline HCl	~ 0.33
	Naphazoline plus OA	~ 2.17
	Naphazoline plus LA	~ 2.58

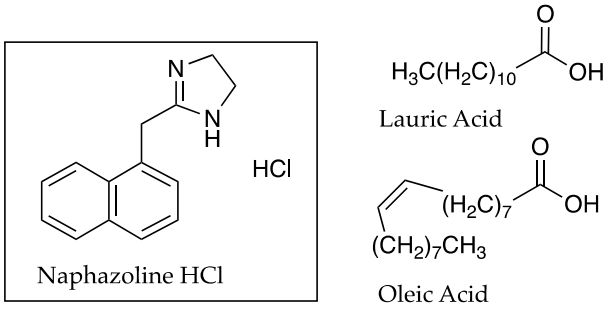

Figure 4. 2 Naphazoline HCl and the counter ions LA and OA.

Positive linear relationships were also found between experimental PC values of lignocaine HCl (0.19, 0.40 and 6.76) and corresponding flux values (1.2 ± 1.2, 13.0 ± 2.0 and 118.0 ± 30.0 μg/cm^2/h) through human skin, as seen in Table 4.2 [29]. Table 4.3 shows the results of PC experiments at pH values 5.0, 6.0 and 7.0 for benzydamine HCl. These indicate increasing PC (1.62, 5.75 and 28.18) and flux values (5.15 ± 2.42, 39.07 ± 10.50 and 269.09 ± 10.50 μg/cm^2/h) in human skin permeation experiments as the fraction of unionised drug increased with increasing pH (6.3 × 10^{-3}, 0.00631 and 0.627) [157]. Megwa [158] also reported that increases in PC results for the tertiary amine counter ions used in conjunction with salicylic acid (SA), shown in Figure 4.3, lead to increased permeation in human epidermis studies as depicted in Table 4.4.

Table 4. 2 PC and flux for lignocaine HCl at different donor pH values. For flux experiments, 2% lignocaine hydrochloride was applied in buffer solutions (n = 3, values represent the mean ± S.D.) Adapted with permission from [159], Elsevier, 2000.

pH	PC (Calculated)	Flux (μg/cm^2/h)
4.0	~ 0.19	1.2 ± 1.2
5.5	~ 0.40	13.0 ± 2.0
7.0	~ 6.76	118.0 ± 30.0

Table 4. 3 PC, unionised fractions, permeability coefficient and flux (across human skin) for benzydamine HCl at different donor pH values. For flux experiments, 2% benzydamine hydrochloride was applied in buffer solutions (n = 6, values represent the mean ± S.D.) Adapted with permission from [157], Elsevier, 2005.

pH	PC ~	Fraction unionised	Permeability Coefficient (cm/h)	Flux ($\mu g/cm^2/h$)
5.0	1.62	6.3×10^{-3}	2.6×10^{-4}	5.13 ± 2.42
6.0	5.75	0.0631	3.8×10^{-3}	39.07 ± 10.5
7.0	28.18	0.627	6.1×10^{-2}	269.09 ± 58.5

Table 4. 4 Effect of tertiary amines on the PC and the flux of SA through human epidermis. Donor phase comprised equimolar concentrations of salicylate anion and amine counter ion, with actual concentration of SA not provided by the authors; donor solvent:ethanol to propylene glycol (2:1 v/v) (n ≥ 3, values represent the mean ± S.E.M.) Adapted from[158], Wiley, 2000.

SA with counter ion:	PC in octanol- phosphate buffer (pH 5.0)	Flux ($mg/cm^2/h \times 10^{-2}$)
Triethanolamine	0.007 ± 0.00	11.90 ± 1.23
Triethylamine	0.360 ± 0.00	15.40 ± 3.85
Tripropylamine	3.180 ± 0.04	18.50 ± 2.26
Tripentylamine	109.77 ± 11.37	19.50 ± 3.63
Trihexylamine	152.17 ± 26.81	22.60 ± 1.14
Trioctylamine	140.58 ± 16.33	27.90 ± 3.98
Tridodecylamine	140.66 ± 17.23	42.70 ± 2.04

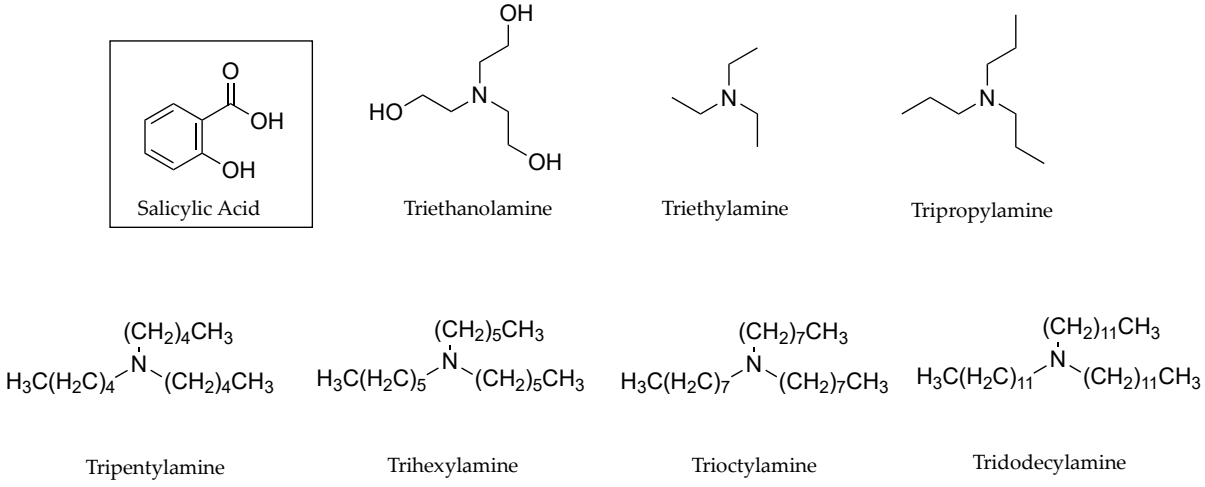

Figure 4. 3 Salicylic acid the counter ions, triethanolamine, triethylamine, tripropylamine, tripentylamine, trihexylamine, trioctylamine and tridodecylamine.

In investigating the effects of counter ions on the permeation of diclofenac (DF) through porcine membranes, it was determined that when comparing structurally related counter ions, a higher PC often corresponded to a higher permeation coefficient, as indicated in Table 4.5 below [160]. The only exception related to monoethanolamine and monoethylamine, where the PC values of 1.2 and 1.02 resulted in permeation coefficients of 0.70 and 2.00 cm/h × 10^3. Chemical structures of DF and the related counter ions are depicted in Figure 4.4.

Table 4. 5 Permeation parameters of DF salts. According to the authors, saturated solutions were applied in permeation studies (for solubility and partition experiments, n = 3; for permeation experiments used to calculate permeation coefficient n ≥ 5; values represent the mean) Adapted from [160], MDPI, 2012.

DF plus counterion:	PC	Solubility ($\mu g/cm^3 \times 10^3$)	Permeation coefficient ($cm/h \times 10^3$)
Monoethanolamine	1.20	9.9	0.70
Monoethylamine	1.02	6.1	2.00
Diethanolamine	1.20	18.0	2.80
Diethylamine	1.48	13.7	3.70
Triethanolamine	4.37	3.4	3.00
Triethylamine	7.08	6.7	3.40
N-2-hydroxyethyl pyrrolidine	1.48	20.2	9.60
Pyrrolidine	1.62	2.0	21.00
N-2-hydroxyethyl piperidine	1.95	10.7	7.70
Piperidine	9.33	4.3	20.00
N-2-hydroxyethyl morpholine	10.96	4.4	4.80
Morpholine	2.24	6.9	3.80
N-2-hydroxyethyl piperazine	1.74	12.5	13.00
Piperazine	4.68	0.4	45.00

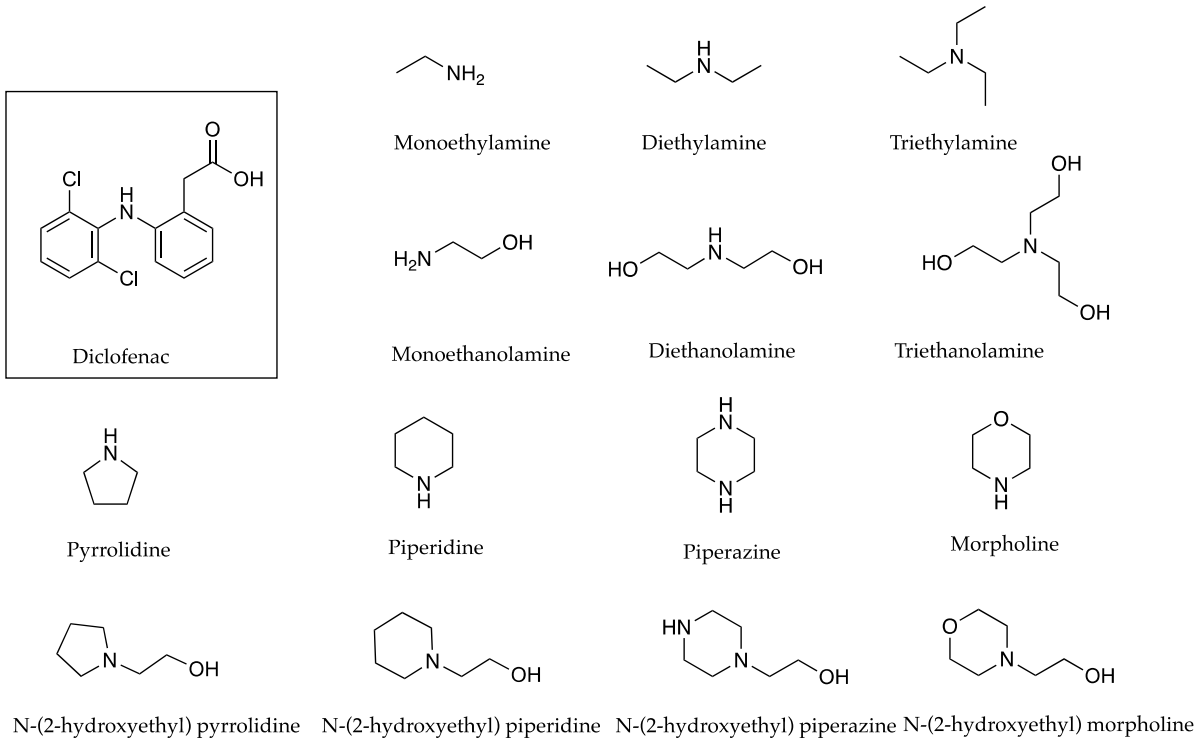

Figure 4. 4 DF with structurally related counter ions monoethylamine and monoethanolamine; diethylamine and diethanolamine; triethylamine and triethanolamine; pyrrolidine and N-(2-hydroxyethyl) pyrrolidine; piperidine and N-(2-hydroxyethyl) piperidine, piperazine and N-(2-hydroxyethyl) piperazine; and morpholine and N-(2-hydroxyethyl) morpholine.

PC has, however, not always correctly reflected the results of permeation studies [161]. No such correlation was found when counter ions were quaternary amines [158] or primary amines [162]. In the latter case, PC studies for SA using octanol and water, as opposed to isopropyl myristate (IPM) and water, toluene and propylene glycol (PG) or IPM and PG, indicated that PC values increased when SA was combined with primary amines that included alkyl chains longer than four carbons (as shown in Figure 4.5). PC values were reported for neat solutions of SA (0.550 ± 0.104) and SA in conjunction with butylamine (1.710 ± 0.108), pentylamine (5.170 ± 1.350), hexylamine (11.220 ± 1.014), heptylamine (17.950 ± 0.138), octylamine (24.340 ± 0.658), nonylamine (17.160 ± 0.416), decylamine (29.740 ± 4.330), undecylamine (22.010 ± 2.344) and dodecylamine (22.680 ± 3.452). These amounted to increases in PC values of SA from a minimum of 3 to a maximum of 54-fold. These increases in PC did not correlate with the results of human skin permeation data in which both flux values and permeability coefficients were lower than those determined for SA (0.89 ±

1.20 mg/cm/h × 10^{-1} and 8.9 cm/h × 10^{-4}). One potential reason suggested by the authors was that SA was retained in the biological membrane used in the experiments.

This was indeed the finding of Trotta *et al*. [163] who investigated the topical application of retinoic acid (RA) in conjunction with the methyl and ethyl esters of various amino acids as counter ions shown in Figure 4.6. These authors reported a linear relationship between PC results and skin accumulation in full-thickness pig ear skin. PC studies measured the partition of RA between IPM and an ethanol and pH 6.4 phosphate buffer (0.05 M) mixture, in the absence and presence of the abovementioned counter ions. A molar ratio of 1:50 (RA to potential counter ion) was used. The concentration of RA applied in the permeation experiments was 0.05% w/w. PC and skin accumulation (μg/cm^2) results were presented for neat RA (1.318 × 10^3, 1.0 ± 0.2) and RA in conjunction with tryptophan methyl ester hydrochloride (1.259 × 10^4, 2.3 ± 0.6) phenylalanine ethyl ester hydrochloride (3.090 × 10^4, 3.4 ± 0.6) and valine methyl ester hydrochloride (4.467 × 10^4, 3.7 ± 0.8). This relationship did not extend absolutely to skin flux values (μg/cm^2/h) that were reported for RA (0.13 ± 0.02), and RA in conjunction with tryptophan methyl ester hydrochloride (0.19 ± 0.02), phenylalanine ethyl ester hydrochloride (0.23 ± 0.03) and valine methyl ester hydrochloride (0.21 ± 0.03), respectively. Here, the flux value for RA in conjunction with phenylalanine ethyl ester hydrochloride (0.23 ± 0.03 μg/cm^2/h) exceeds that for the valine methyl ester hydrochloride (0.21 ± 0.03 μg/cm^2/h), despite the PC results.

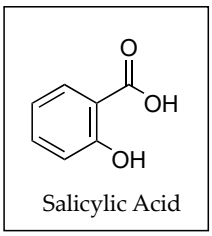

Salicylic Acid

$H_3C(H_2C)_3$-NH_2	$H_3C(H_2C)_4$-NH_2	$H_3C(H_2C)_5$-NH_2
Butylamine	Pentylamine	Hexylamine
$H_3C(H_2C)_6$-NH_2	$H_3C(H_2C)_7$-NH_2	$H_3C(H_2C)_8$-NH_2
Heptylamine	Octylamine	Nonylamine
$H_3C(H_2C)_9$-NH_2	$H_3C(H_2C)_{10}$-NH_2	$H_3C(H_2C)_{11}$-NH_2
Decylamine	Undecylamine	Dodecylamine

Figure 4. 5 SA and primary amines with alkyl chains longer than four carbons, namely butylamine, pentylamine, hexylamine, heptylamine, octylamine, nonylamine, decylamine, undecylamine and dodecylamine.

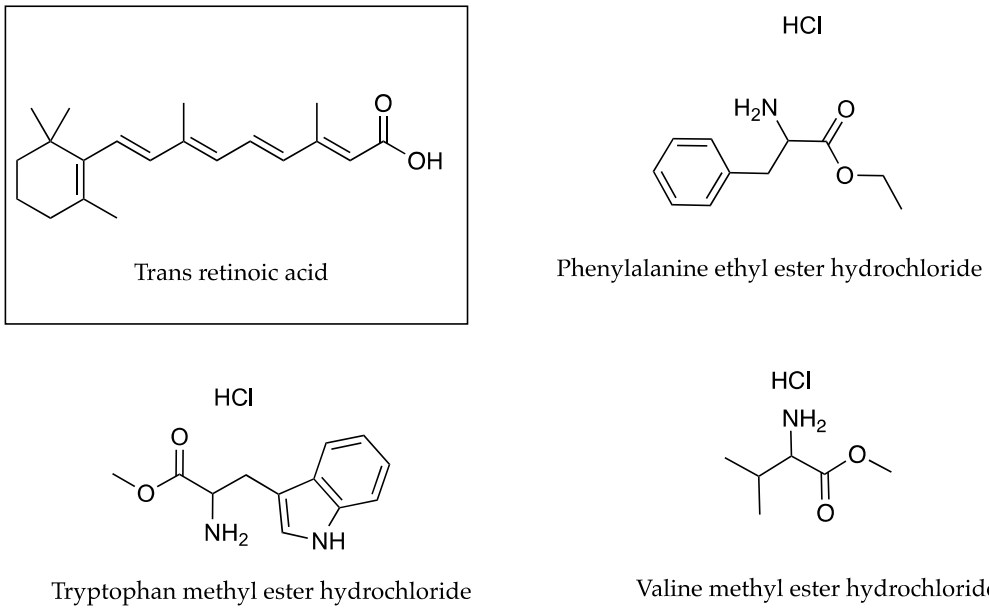

Figure 4. 6 RA and phenylalanine ethyl ester hydrochloride, tryptophan methyl ester hydrochloride and valine methyl ester hydrochloride.

Auner et al. [164] used PC studies to determine whether the lipophilicity of 5-aminolevulinic acid (ALA) could be increased by the addition of the various counter ions depicted in Figure 4.7. As ALA has two pK_a values, 4.0 and 7.9, pH values of 4.0 and pH 7.0 were employed. These resulted in an anionic charge dominating at pH 7.0 and a cationic charge dominating at pH 4.0. Results for PC studies, as seen in Table 4.6, showed that the lipophilic shift was higher in the case of pH 7.0 where ALA was tested alone (1.51), or in conjunction with cetylpyridinium chloride (CP) (9.12), cetyltrimethyl-ammonium bromide (8.13) and benzalkonium chloride (6.03). In the case of pH 4.0 where ALA was tested alone (1.20), or in conjunction with sodium-1-octanesulfonic acid (2.14), sodium-1-heptanesulfonic acid (4.68) and sodium-1-pentanesulfonic acid monohydrate (2.69), the lipophilic shift was lower. Cumulative permeation amounts of ALA through porcine skin (μg/cm^2) after 4 h showed that, with the exception of cetyltrimethylammonium bromide, all anionic and cationic counter ions increased the cumulative permeation of ALA through porcine skin. ALA at pH 4.0, without a counter ion, resulted in a cumulative amount of 5.11 μg/cm^2. This value increased with the addition of sodium-1-octanesulfonic acid (10.7 μg/cm^2), sodium-1-heptanesulfonic acid (10.0 μg/cm^2) and sodium-1-pentanesulfonic acid monohydrate (10.0 μg/cm^2), as counter ions. At pH 7.0 the cumulative amount of ALA alone was 6.5

μg/cm^2. This increased to 11.0 μg/cm^2 with CP as a counter ion and 7.0 μg/cm^2 when benzalkonium chloride was the counter ion. As mentioned previously, the cumulative amount decreased with the addition of cetyltrimethylammonium bromide to 5.0 μg/ cm^2. There appeared to be no correlation between cumulative permeation and PC values.

Table 4. 6 PC and cumulative amount permeated of pure ALA and in conjunction with various counter ions at pH 4.0 and pH 7.0. The concentration of ALA applied in the buffer solutions was 0.4 mg/mL (for permeation experiments n ≥ 3, values represent the mean ± S.D.) Adapted with permission from [164], Elsevier, 2003.

ALA plus counter ion:	pH	PC ~ (x 10^{-1})	Cumulative amount of ALA ~ (μg/cm^2) after 4 hours using porcine skin
None	4.0	1.20	5.11
Sodium-1-octanesulfonic acid	4.0	2.14	10.7
Sodium-1-heptanesulfonic acid	4.0	4.68	10.0
Sodium-1-pentanesulfonic acid monohydrate	4.0	2.69	10.0
None	7.0	1.51	6.5
Cetylpyridinium chloride	7.0	9.12	11.0
Cetyltrimethylammonium bromide	7.0	8.13	5.0
Benzalkonium chloride	7.0	6.03	7.0

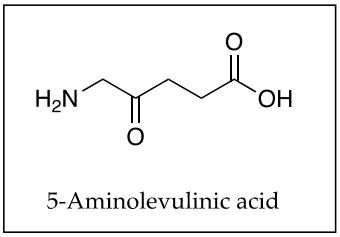

5-Aminolevulinic acid

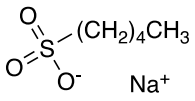

Sodium-1-pentanesulfonic acid

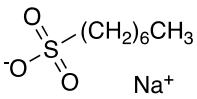

Sodium-1-heptanesulfonic acid

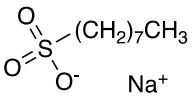

Sodium-1-octanesulfonic acid

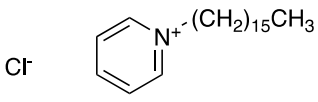

Cetylpyridinium chloride

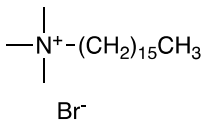

Cetyltrimethylammonium bromide

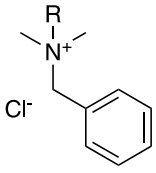

Benzalkonium chloride

Figure 4. 7 ALA and counter ions:sodium-1-pentanesulfonic acid, sodium-1-heptanesulfonic acid, sodium-1-octanesulfonic acid, cetylpyridinium chloride, cetyltrimethylammonium bromide and benzalkonium chloride.

In addition to the use of PC studies to test the partitioning abilities of counter ions, the factors described by Bjerrum as impacting their formation should not be disregarded. These included the size or radius of the counter ions as well as the ε of the solvent and temperature. A number of other areas have also been investigated in the literature such as the impact of the type of counter ions used, the influence of pH, the quantity of counter ions, the addition of permeation enhancers and the use of the latter as ion pairs.

4.4.3 Factors influencing the formation and partition of counter ions

4.4.3.1 Size and type of counter ion

Bjerrum indicated that the distance between centres of charge when ions are paired is greater for large ions and smaller for smaller ions, thus potentially affecting the "cohesion" of the ion pairs. Fini *et al.*[23] tested the ability of a number of inorganic ions ranging from lithium to caesium cations to form ion pairs with the DF anion, using PC as the main analytical tool. With the exception of lithium, the inorganic ions sodium, potassium, rubidium, and caesium were not as successful in forming ion pairs with the DF anion. An inverse correlation was indeed identified between the size of the ionic radius and the PC. Lithium, with the smallest ionic radius, exhibited the highest PC value which reduced with increasing ionic radius of the inorganic ions: PC of lithium > sodium > potassium > rubidium > caesium, while the ionic radius of lithium < sodium < potassium < rubidium < caesium [23].

In addition to the influence on potential cohesion, smaller molecular size (as determined by molecular volume or molecular weight) is also a factor recognised by QSARs as a contributor to increased permeability coefficients [103, 153, 154]. In spite of this, Megwa *et al.* [162] found that a longer chain length of tertiary alkylamines used as counter ions in conjunction with salicylic acid (SA) resulted in improved permeation results through human skin, as shown in Table 4.7 Structures for these counter ions are shown in Figure 4.3.

Table 4. 7 Impact of tertiary amines on conductivity, on the permeation of SA through human epidermis, plus physicochemical properties of tertiary counter ions (for permeation experiments n ≥ 3 ≤ 6, values represent the mean ± S.E.M.) Adapted from [162], Wiley, 2000.

Salicylic acid plus counter ion	Molecular weight of counter ion (Da)	Molal volume of counter ion (cm^3/mol)	Flux ($mg/cm^2/h$) x 10^{-2}	Conductivity (mS/cm)
None	-	-	8.90 ± 1.20	2.03 ± 0.06
Triethylamine	101.20	108.00	15.40 ± 3.85	1.77 ± 0.06
Tripropylamine	143.27	156.60	18.50 ± 2.26	1.35 ± 0.06
Tripentylamine	227.44	253.80	19.50 ± 3.63	0.90 ± 0.00
Trihexylamine	269.52	302.40	22.60 ± 1.14	0.80 ± 0.00
Trioctylamine	353.68	399.60	27.90 ± 3.98	0.60 ± 0.00
Tridodecylamine	522.00	592.50	42.70 ± 2.04	0.30 ± 0.00

The authors attributed this to the increase in lipophilicity as the alkyl chain length increased. It should also be noted that the highest molecular mass of any of the counter ions was 522 Da. While this did not appear to conform with the aforementioned rules relating to molecular size, it did result in the highest flux value. The same study also examined the effect of quaternary ammonium compounds on the permeation of SA and found that these did not impact the overall permeation of the active ingredient. It was determined that amine counter ions affect permeation through the human epidermis in the following sequence: quaternary < primary < secondary < tertiary.

The previously discussed Auner study [164] also examined the efficacy of various quaternary ammonium compounds as counter ions for ALA. As was noted, and can be seen in Table 4.6, these yielded diverse flux results in permeation tests using porcine skin. When paired with cetyltrimethylammonium bromide, despite having higher PC values than neat ALA (~8.13×10^{-1} in contrast to ~1.51×10^{-1}), it was reported to have a cumulative permeation of approximately 5 $\mu g/cm^2$ after 4 h, while the flux of ALA without the counter ion was approximately ~6.5 $\mu g/cm^2$ for the same period. Benzalkonium chloride (PC value of ~6.03×10^{-1}) and CP (PC value of ~9.12×10^{-1}) did improve the cumulative flux values with results of approximately 7 and 11 $\mu g/cm^2$, respectively, after 4 h [164]. A number of reasons for the permeation results were suggested by the authors, in accordance with studies by Takacs-Novak and Szasz [165] that examined the partition of quaternary ammonium substances. These included the influence of lipophilicity, size and flexibility, expressed as the number of

rotating carbon-carbon sigma bonds, of the counter ions. Whilst it was mentioned that no significant effect had been attributed to the type (such as aliphatic or aromatic) of quaternary nitrogen compound, much importance was attributed to the lipophilicity and association constants of ion pairs, emphasising the necessity of attaining a critical separation distance, without which ion pairs cannot be formed.

The same study also tested the use of sulfonic acid sodium salts as counter ions in conjunction with ALA (Table 4.6). While there was an increase in the cumulative permeation of ALA at pH 4.0 from ~5.11 μg/cm^2/h when counter ions were added, there was no significant difference in the cumulative permeation amounts of the different counter ions. The use of sodium-1-octanesulfonic acid resulted in the highest cumulative permeation at ~10.7 μg/cm^2/h, while sodium-1-heptanesulfonic acid and sodium-1-pentanesulfonic acid monohydrate both had cumulative permeation results of ~10.0 μg/cm^2/h.

PC investigations indicated that organic cations were more successful than inorganic cations when forming ion pairs with the DF anion [23]. It was suggested that when a salt contains both an organic anion and cation, some of the hydrophobic character remains. This was described by Minghetti and co-workers who considered the impact of four salts used in pharmaceutical applications in conjunction with DF on the permeation of the latter through human skin. The salts were described as sodium, potassium, diethylamine and epolamine (N-(2-hydroxyethyl)pyrrolidine), the structures of which can be seen in Figure 4.8. The findings suggested that associating an organic cation, such as the diethylamine and epolamine, and an organic anion in pharmaceutical salts guarantees improved permeation results. These results are contained in Table 4.10, showing the flux values for DIC (μg/cm^2/h) in conjunction with the inorganic counter ions sodium (2.29 ± 0.37) and potassium (1.35 ± 0.72) increase with the organic counter ions diethylamine (5.60 ± 2.14) and epolamine (2.90 ± 0.91), when using water as a solvent [25].

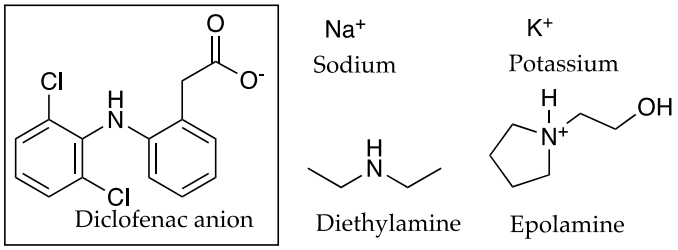

Figure 4. 8 DF anion with inorganic counter cations sodium and potassium and organic counter cations diethylamine and epolamine.

As discussed previously, Trotta used a variety of amino acid esters to increase the delivery of RA, a hydrophobic molecule that is practically insoluble in water, to the skin. Skin accumulation results (μg/cm^2) showed that valine methyl esters (3.7 ± 0.8) and phenylalanine ethyl esters (3.4 ± 0.6) were more successful than the tryptophan methyl esters (2.3 ± 0.6) in increasing the accumulation of RA in pig skin [163].

Two counter ions, benzoate (Bz) and oleate (Ol), were also considered by Cilurzo and co-workers [33] for the pairing of a chiral compound, propranolol (PR), as a racemate, RS-PR, and as a single enantiomer, S-PR (Figure 4.9 and Table 4.8). Despite partition studies reflecting a 78% increase in the PC value for RS-PR as well as an 104% increase for S-PR, when tested with the Ol counter ion, permeation data showed drug fluxes reducing in conjunction with the counter ion. The flux of the racemate in saline reduced from 18.0 ± 5.1 μg/cm^2/h to 7.0 ± 1.4 μg/cm^2/h when combined with Ol. The flux of the racemate in mineral oil (MO) decreased from 24.2 ± 4.7 μg/cm^2/h to 7.3 ± 1.4 μg/cm^2/h when combined with Ol. The S-enantiomeric form of PR showed higher flux results than the racemate when applied neat, whether in saline (44.7 ± 5.1 μg/cm^2/h) or MO (41.9 ± 1.5 μg/cm^2/h). When Ol was used as a counter ion, the flux of the S-enantiomer plummeted to 6.2 ± 0.9 μg/cm^2/h when in saline and to 11.1 ± 1.7 μg/cm^2/h when in MO. When Bz was used as the counter ion, it increased the PCs of the racemate and the S-enantiomer marginally, from 10.00 and 9.33 to 11.74 and 11.48, respectively. This again failed to translate into an increase in the flux from saline for both the racemate (18.0 ± 5.1 to 1.7 ± 0.2 μg/cm^2/h) and the S-enantiomer (44.7 ± 5.1 to 3.0 ± 0.4 μg/cm^2/h). The situation was repeated when Bz was used as the counter ion with MO was the solvent. The flux for RS-PR reduced from 24.2 ± 4.7 to 1.6 ± 0.3 μg/cm^2/h and for S-PR from 41.9 ± 1.5 to 2.9 ± 0.7 μg/cm^2/h [161].

Table 4. 8 PC values, solubility and flux values for propranolol (PR) racemate (RS), propranolol S-enantiomer (S-PR), individually and in conjunction with benzoate (Bz) and oleate (Ol) counter ions. According to the authors, saturated solutions were applied. Solubility values for (RS)-PR-Ol and (S)-PR-Ol were assumed to be 0.02 mg /mL, the concentration determined to be their critical micellular concentration (CMC). For solubility and permeation experiments n = 3, flux values represent the mean ± S.D. Adapted with permission from [161], Elsevier, 2010.

Counter Ions	PC Value ~	Solubility Saline (mg/mL)	Flux Saline (μg/cm²/h)	Solubility MO (mg/mL)	Flux MO (μg/cm²/h)
(RS) – PR	10.00	0.189	18.0 ± 5.1	1.321	24.2 ± 4.7
(S) – PR	9.33	0.432	44.7 ± 5.1	3.111	41.9 ± 1.5
(RS) – PR- Bz	11.74	4.430	1.7 ± 0.2	0.065	1.6 ± 0.3
(S) – PR Bz	11.48	9.560	3.0 ± 0.4	0.118	2.9 ± 0.7
(RS) – PR- Ol	17.78	0.020	7.0 ± 1.4	3.930	7.3 ± 1.4
(S) – PR- Ol	19.05	0.020	6.2 ± 0.9	5.874	11.1 ± 1.7

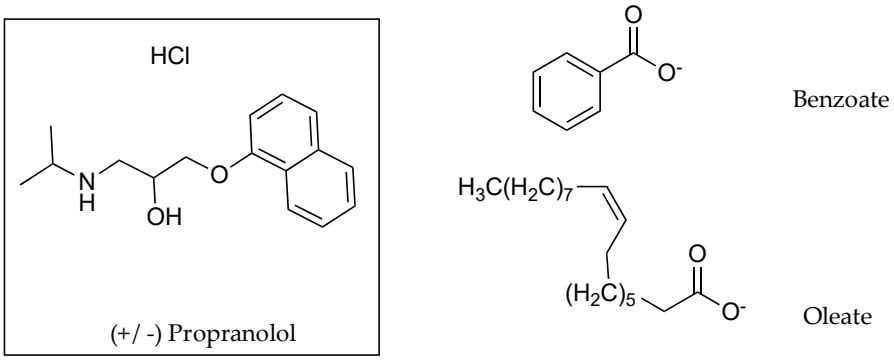

Figure 4. 9 Propranolol plus counter ions benzoate and oleate.

In 2012, Fini *et al.*[160] considered the ability of DF salts in aqueous solutions to permeate through porcine membranes. The choice of counter ions (Figure 4.4) included aliphatic alkyl amines: mono, di and tri ethyl amines, which were contrasted with mono, di and tri ethanol amines. Examples also included a range of cyclic substituents:pyrrolidine, piperidine, piperazine and morpholine. These were contrasted with structurally similar molecules that included hydroxy ethyl side chains, namely N-(2-hydroxyethyl) pyrrolidine, N-(2-hydroxyethyl) piperidine, N-(2-hydroxyethyl) piperazine and N-(2-hydroxyethyl) morpholine. The solutions used in these studies were saturated, which made the comparison of flux values challenging. Instead, flux was divided by solubility (in μg/cm^3) in order to obtain a permeability

coefficient. When comparing structurally related pairs of salts (Table 4.5), the authors ascertained that the results suggested “that a common mechanism associated with permeation is the hydrophobicity of the permeant species”. In most cases, the salt which contained the hydroxy group showed a higher aqueous solubility (when compared to the paired ion that did not contain the same hydroxy substituent), but this generally did not translate into a higher permeation coefficient. Counter ions pyrrolidine, piperidine and piperazine resulted in increased permeation coefficients when compared to their related counter ions containing hydroxy groups. Morpholine counter ions showed an affinity for the aqueous phase which reduced permeation when compared to other cyclic related salts.

The impact of one and two double bonds on an 18-carbon fatty acid counter ion on the flux of physostigmine (PHY) through porcine skin, was described in 2005 by Wang [166]. OA (C18:1) and linoleic acid (C18:2), whose structures can be seen in Figure 4.10, resulted in PC values for PHY, between IPM and PG, of 0.225 ± 0.035 and 0.219 ± 0.01, respectively. Flux values were 19.7 ± 8.2 μg/cm^2/h for the counter ion C18:1 and only 2.4 ± 0.9 μg/cm^2/h when the counter ion was C18:2, despite solubility for the two being very similar (83.9 mg/mL for C18:1 and 85.3 mg/mL for C18:2). The authors suggested that the presence of the additional unsaturation may have caused the retention of the complexes in the SC lipids [166]. Conversely, the effect of a single unsaturation on the OA structure was also mentioned by Green *et al.*[156] as a potential reason for making this a better permeation enhancer than LA, a 12-carbon saturated fatty acid.

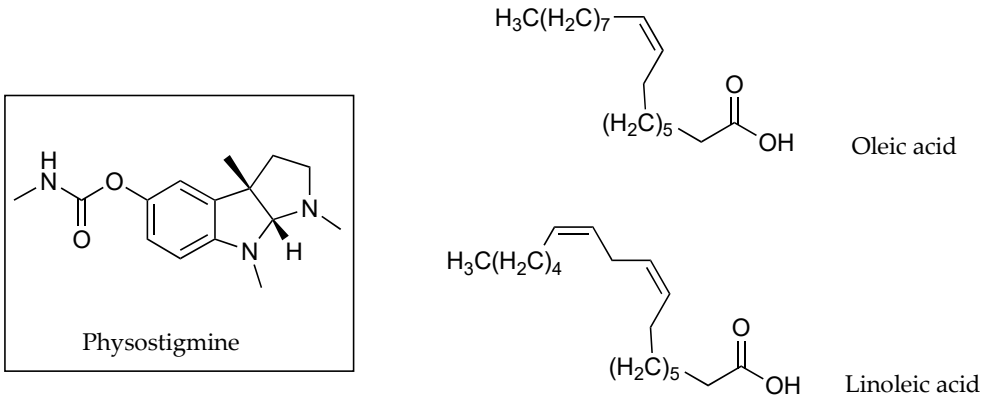

Figure 4. 10 Physostigmine and counter ions OA and LA.

More recently in 2019, In and co-workers [167] tested three different zwitterions in conjunction with carnitine Figure 4.11, which prevails as a zwitterion in weakly acidic or neutral pH solutions. Solutions comprising a 4% weight of carnitine, alone and in equimolar ratios with betaine, polyquaterium-51 or hydrogenated soya phosphatidylcholine (HSC), were used for permeation experiments. When combined with the active in solution, betaine and polyquaterium-51 reduced carnitine's percutaneous penetration, while the combination with hydrogenated soya phosphatidylcholine (HSC), a higher-molecular-mass (762.1 Da) long-chain-carbon structure, nearly tripled it. The percentage of applied carnitine found in epidermal layers of porcine skin after 24 h was approximately 9.13% when carnitine was applied without any counter ion, 4.25% when applied with betaine, 6.55% when applied with polyquaterium-51 and 23.71% when applied with HSC [167].

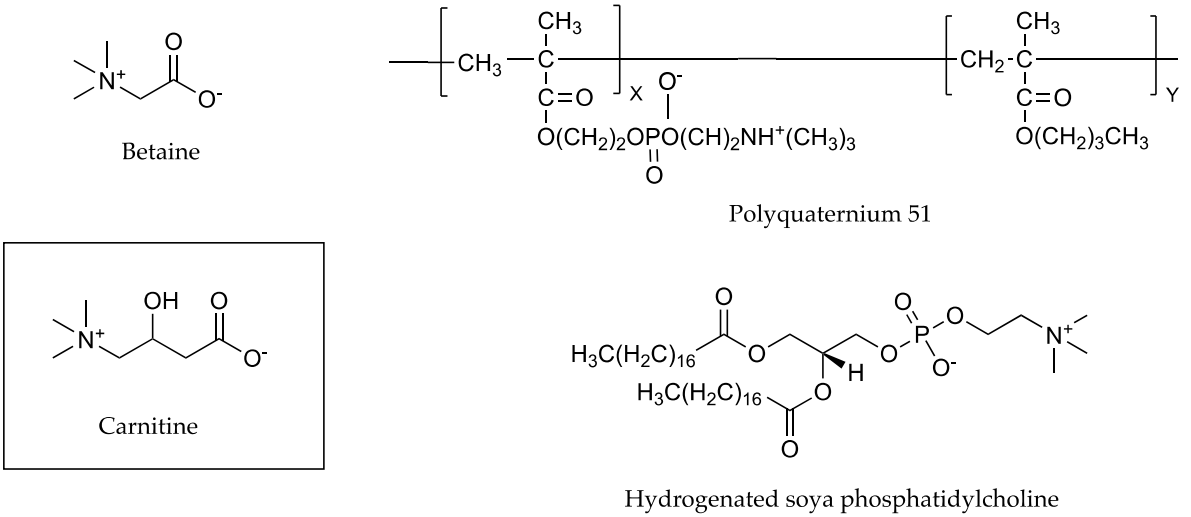

Figure 4. 11 Carnitine with 3 different zwitterion counter ions: betaine, polyquaternium-51 and HSC.

4.4.3.2 Dielectric constant (ε)

In 1956, Kraus [149] tested components of Bjerrum's theory, including the relationship between the dissociation of ion pairs to the ε of the solvent. Using water–dioxane mixtures as the solvent system and the salt tetraisoamylammonium nitrate, it was found that for values of ε greater than 44, ions were dissociated. Tetrabutylammonium bromide and sodium bromate were found to be dissociated for values of ε above 50. Irrespective of whether aqueous or organic solvents were used, there was a clear

relationship between a higher ε reducing the association between ion pairs, and a lower ε increasing the association between ion pairs.

The impact of solvents with different ε values may be tested by determining the conductivity of the ions in solution. The higher the quantity of ions in solution, the higher the conductivity. As ion pairing increases, charges become masked or neutralised, resulting in lower conductivity results [147]. The use of conductivity measurements can therefore be an important tool to test the impact of solvent adjustments on the formation of ion pairs. By increasing the proportion of a particular solvent with a lower ε, columbic interactions between the oppositely charged ions of the potential ion pairs may become more stable, resulting in the formation or stabilisation of ion pairs, and thus potentially facilitating partition.

In the early 1990s, Pardo *et al.* [168] tested IPM, isopropyl alcohol (IPA) and various mixtures of both solvents to determine the impact of solvent adjustment on the permeation of counter ions PHY and salicylate (Figure 4.12) without the use of conductivity measurements. IPA's ε, 18.62 at 20 °C [169-171], was far higher than the value determined for IPM, 3.31 at 25 °C [172]. Nonetheless, it was still only approximately one-quarter of the value of the ε of water, determined to be 80.37 at 20 °C [170]. As seen in Table 4.9, it was found that a solvent mixture comprising a 70:30 ratio of IPA to IPM had the best impact on permeation. Flux of PHY increased from 0.56 ± 0.08 × 10^4 μmol/cm^2/m at its lowest rate determined when the solvent comprised 100% of IPA, to 44.27 ± 9.16 × 10^4 μmol/cm^2/m when the solvent mixture contained 70% IPA. Flux of salicylate increased from 1.47 ± 0.11 × 10^4 μmol/cm^2/m at its lowest rate, which occurred when the solvent comprised 100% IPM to 61.66 ± 2.54 μmol/cm^2/m when the proportion of IPM was reduced to 30%.

Table 4. 9 Flux values for PHY and salicylate through excised human skin, which according to the authors, were delivered from equimolar saturated solutions of solvents consisting of IPA, IPM and their mixtures (n ≥ 3 ≤ 8, values represent the mean ± S.E.M.) Adapted from [168], Wiley, 1992.

Volume fraction of IPA in IPA-IPM solvent mixture	Flux x 10^4 µmol/cm^2/m	
	PHY	**Salicylate**
0	1.28 ± 0.35	1.47 ± 0.11
0.1	5.75 ± 0.58	6.3 ± 0.50
0.3	14.55 ± 0.71	18.2 ± 0.56
0.5	31.70 ± 3.10	47.8 ± 11.50
0.7	44.27 ± 9.16	61.66 ± 2.54
0.9	5.52 ± 0.28	17.70 ± 1.90
1	0.56 ± 0.08	1.87 ± 0.10

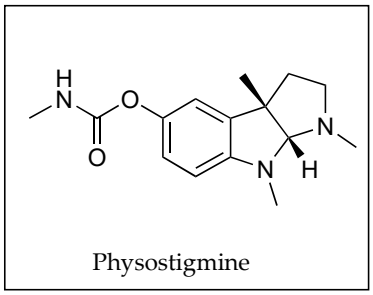

Physostigmine

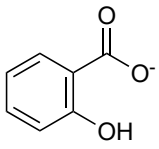

Salicylate

Figure 4. 12 Counter ions PHY and salicylate.

In early 2000, Megwa *et al.* [158] took a different approach. Instead of measuring the impact of different solvents on the conductivity of ions, the authors tested the conductivity of SA alone and in conjunction with a variety of potential counter ions in a fixed ethanol-propylene glycol (2:1 v/v) solvent combination in equimolar concentrations. As shown in Table 4.7, when the counter ions were tertiary amines, the conductivity of SA diminished with each consecutive increase in the length of the carbon chain of the counter ion. A relationship could be seen between the length of the carbon chain of the tertiary amine, conductivity, PC and flux: longer carbon chains resulted in lower conductivity, which generally represented higher PC values and higher flux, as seen in Table 4.4. However, this was limited to tertiary amines. The relationship did not extend to quaternary or primary amines [162], where, in the latter, there was very little difference in conductivity between neat SA or in conjunction with counter ions.

Four individual single solvents were tested with the inclusion of four different counter ions in conjunction with DF by Minghetti *et al.* [25]. The solvents included water, PG, Transcutol® (TC) and OA. The solubility of the drug which included its associated counter ion was generally much higher with TC and OA, yet flux values were greater when water and OA were used (Table 4.10). This research highlighted a key factor in ion pairing formulation, namely that high concentration of the drug does not guarantee an increase in flux values. The authors determined that the solubility parameters of the salts, as well as the solvents, TC and PG, were all comparable. They stated that "small differences in solubility parameters of a drug and its vehicle do not cause extensive partitioning of the drug out of its vehicle". Unsurprisingly the flux values measured in TC and PG were the lowest among the four vehicles for all the four salts, as "the lower the tendency of the solute to leave the donor phase, the lower the flux." These similar solubility parameters indicated that the solute might be more likely to be soluble in these solvents, but less likely to partition out of the vehicle. The authors concluded that permeability in permeation studies comprised two distinct features: firstly, the solubility of the solute in the donor phase and, secondly, the ability to partition out of the formulation and into the membrane.

Table 4. 10 Impact of different solvents on the solubility and flux of DF in conjunction with different salts as counter ions. According to the authors, saturated solutions of the DF salts were applied for permeation experiments (n = 3, values represent the mean ± S.D.) Adapted with permission from [25], Elsevier, 2007.

DF plus counter ion	Parameter	Solvents			
		Water	PG	TC	OA
Sodium	Solubility (µg/mL)	37 ± 10	567 ± 31	660 ± 70	25 ± 10
	Flux (µg/cm^2/h)	2.29 ± 0.37	1.21 ± 0.06	0.06 ± 0.01	1.84 ± 0.18
Potassium	Solubility (µg/mL)	218 ± 80	898 ± 79	709 ± 52	60 ± 50
	Flux (µg/cm^2/h)	1.35 ± 0.72	0.04 ± 0.02	0.84 ± 0.06	1.17 ± 0.17
Diethylamine	Solubility (µg/mL)	19 ± 10	384 ± 14	279 ± 10	63 ± 60

	Flux (μg/cm^2/h)	5.60 ± 2.14	0.35 ± 0.04	0.96 ± 0.59	2.74 ± 0.94
Epolamine	Solubility (μg/mL)	557 ±15	637 ± 60	430 ± 0.00	94 ± 70
	Flux (μg/cm^2/h)	2.90 ± 0.91	0.46 ± 0.21	0.03 ± 0.00	3.11 ± 0.18

In 2005, Wang and co-workers [166] investigated the impact of two single solvents, PG and mineral oil (MO), on the permeation of PHY in conjunction with fatty acid counter ions in porcine skin (Table 4.11). Conductivity measurements were undertaken in a manner similar to those employed by the Megwa [158] study mentioned above. The conductivity of PHY was tested alone and then in combination with a series of fatty acids of increasing carbon chain length in PG and then in MO. The main difference between the two studies was that the concentration of fatty acid:drug mixtures had a molar ratio of 50:1. Notwithstanding a low conductivity value for PHY in PG when tested in isolation, testing revealed a decrease in the conductivity of the PHY–counter ion solution, with an increase in the alkyl chain length of the fatty acid counter ion. These results for PHY, unmixed and then combined with fatty acid counter ions of carbon chain lengths: 2, 3, 8, 10, 12, 18:1 and 18:2, were ~0.25, 16, 14, 10, 9.5, 8, 3 and 4 μS/cm. Conductivity results were extremely low when conducted in MO. PHY alone in MO resulted in a conductivity value of ~9.25 × 10^{-2} μS/cm and never increased beyond ~9.4 × 10^{-2} μS/cm when combined with counter ions. The lack of any significant change in the conductivity of MO containing fatty acids when PHY was added, suggested to the authors that no ionisation of the PHY occurred, leading to an absence of ion pairing in this solvent system. Flux results were determined for saturated solutions of MO and PG. The counter ion with the longest carbon chain, OA (C18:1), consistently showed the best flux values in both solvents, 19.7 ± 8.2 μg/cm^2/h in PG and 13.9 ± 7.1 μg/cm^2/h in MO, as shown in Table 4.11. PHY together with the OA counter ion was greater than 5-fold more soluble in PG (83.9 mg/mL) than in MO (15.9 mg/mL). However, flux was only 1.4-fold greater. The lag time for the MO vehicle was ± 4.8 h whereas PG was shown to be ± 8.8 h.

Partitioning of PHY from PG was subsequently explained by the authors based on two factors. Firstly, the ion pairing that resulted in the reduced polar environment and

secondly the impact of increasing lipophilicity due to the increased carbon chain length of the counter ion. Where ion pairs were formed with short chain fatty acids, these were described as strong ion pairs, due to a higher polarity of the counter ions. The longer the alkyl chain, the weaker the ion pairing, but the more lipophilic the nature of the ion pair. A more stable ion pair was noted to have lower lipophilicity than a more unstable one, making partitioning less likely. The authors also raised the importance of concentration as a driving force for drug diffusion as well as the impact of the solvent's contribution to improving the partitioning of the drug into the skin.

Table 4. 11 Flux, conductivity (Con) and solubility (Sol) of PHY in PG and MO. According to the authors, saturated drug solutions were used in permeation experiments. Fatty acid counter ions are indicated according to length of carbon chain. 18:1 (OA, 1 double bond) and 18:2 (LA, 2 double bonds) (for conductivity and permeation experiments n = 3, values represent the mean ± S.D.) Adapted with permission from [166], Elsevier, 2005.

PHY plus fatty acid counter ion	Flux (PG) (μg/cm^2/h)	Con ~ (μS/cm) PG	Sol (mg/mL)	Flux (MO) (μg/cm^2/h)	Con ~ (μS/cm) MO x 10^{-2}	Sol (mg/mL)
None	-	0.25	71.0	2.5 ± 0.7	9.25	1.7
2	-	16	-	-	9.45	-
3	-	14	-	-	8.65	-
8	-	10	116.0	3.2 ± 0.6	9.05	5.1
10	-	9.5	80.7	6.6 ± 2.3	9.40	10.8
12	0.2 ± 0.0	8	88.7	14.0 ± 3.0	8.95	15.3
18:1	19.7 ± 8.2	3	83.9	13.9 ± 7.1	8.80	15.9
18:2	2.4 ± 0.9	4	85.3	3.9 ± 1.1	9.15	15.7

As shown in Table 4.8, MO and a saline solution were used as potential solvents when using PR as a racemic mixture or in its S-enantiomeric form, in conjunction with counter ions. PC values increased due to ion pairing with OI, from 10.00 and 9.33 for (RS)-PR and (S)-PR without OI to 17.78 and 19.05 with OI. Solubility also increased in MO from 1.321 and 3.111 mg/mL for (RS)-PR and (S)-PR without OI to 3.930 and 5.874 mg/mL with OI. Despite the increased PC and solubility values, when MO was used as the donor solvent in permeation experiments, flux values were comparatively low (7.3 ± 1.4 and 11.1 ± 1.7 μg/cm^2/h for (RS)-PR and (S)-PR in combination with OI, versus 24.2 ± 4.7 and 41.9 ± 1.5 for (RS)-PR and (S)-PR without the counter ion). The

authors concluded that this could be due to the stabilisation of the solute in the donor phase [161].

More recently, in 2019, conductivity was used in a novel fashion by In *et al.*[167], to determine the optimal molar ratio of zwitterionic ion pairs, with the lowest conductivity occurring at approximately a 1:1 ratio for the chosen counter ion. This resulted in an extension of previous approaches which considered the impact of the dielectric constants of solvents on the conductivity of ions in solution, or the impact on conductivity of using different counter ions.

4.4.3.3 Temperature

Another factor introduced by Bjerrum in the late 1920s was the impact of temperature on ion pairing. In the paper "*Evolution of the Ion-Pair Concept*", Kraus [149] explained that for solvents of a high ε value an increase in temperature caused an increase in ion pairing, whilst the converse is true for solvents with a low ε. Conductance measurements were used by Kraus as one possible method to demonstrate the increase in ion association in solvents of higher εs, with increasing temperature. The author showed that for solutions using solvents with a ε greater than ~10, and with a concentration range between 0.1 and 0.01 *N* the conductance values increase with increasing temperatures as a result of decreasing viscosity. As shown in Table 4.12, as temperature increases, the conductance increases at a decreasing rate. The conductance value reaches a maximum and then begins to decrease.

In addition, from Table 4.13, it is evident that the lower the ε, the lower the temperature of the conductance maximum, for a given concentration. Methylamine, ammonia and methanol have ε values of 9.4 at 25 °C, 22.4 at ~33.3 °C and 32.8 at 25 °C. Methylamine with the lowest ε has a conductance maximum at 15 °C. Ammonia, with a ε value approximately midway between methylamine and methanol, has its conductance maximum at 25 °C. Finally, methanol, with the highest ε of the three solvents, has a conductance maximum at 150 °C.

The author explained that as temperature rises, ion association increases until the decrease in conductivity, due to the ion association, just offsets the increase in conductivity, attributable to increasing fluidity, at the temperature of maximum conductance. From this temperature, ion association continues to increase and conductance to decrease. As the concentration of the solution is subject to very little

variance due to changes in temperature under the specified conditions, the conductance provides a guide to the increasing association attributable to increasing temperature. It was further noted that the actual extent of ion association is greater than indicated by the conductivity measurements, as the fluidity of the solution increases with the temperature, causing the conductance values to be greater than expected.

Table 4. 12 Conductance of potassium iodide in methanol at different temperatures. Units were not provided, but the trend in overall values may be used to demonstrate the concepts. Adapted from [149], American Chemical Society, 1956.

~ Temperature °C	~ Conductance
80	500×10^{6}
100	576×10^{6}
120	638×10^{6}
150	700×10^{6}
180	654×10^{6}
200	577×10^{6}
220	400×10^{6}
240	14.2×10^{-2}

Table 4. 13 The temperature at which the highest conductance value is reached for potassium iodide in solvents of different ε values:methylamine, ammonia and methanol. Adapted from [149] American Chemical Society, 1956.

Solvent	ε	Conductance maximum reached at °C
Methylamine	9.4 at 25 °C	15
Ammonia	22.4 at ~33.3 °C	25
Methanol	32.8 at 25 °C	150

4.4.3.4 pH

As previously mentioned, pH modification in given solvent systems introduces changes to PC values. In this section, some of the concepts formerly mentioned will be revisited for the purpose of clarity and contextualisation of theory.

The pH partition theory suggests that only unionised drugs can permeate lipid membranes, whilst ion pairing attempts to achieve this via the masking of charges. In order to optimise partition and permeation of several molecular compounds, pH has

been investigated in various respects. An example of this is the exploration of the slightly acidic pH values long attributed to the surface of the skin [110], and the physiological pH values associated with the lower layers of this biological membrane. Hadgraft *et al*. [173] tested whether such a pH gradient could be used to ionise the participating compounds, sodium salicylate and Ethomeen S12 (N,N-bis(2-hydroxyethyl)oleylamine), enabling the formation of ion pairs between the two. The purpose was to facilitate the transport of the active ingredient, salicylate, through the skin. Whilst this increased the transport of salicylate by approximately 3-fold when using a preparatory artificial lipid membrane and did not affect the control compound, caffeine (a weakly basic drug that was cationic at the pH values examined), the results could not be replicated when using human skin. Instead, the counter ion, Ethomeen S12, improved the transport of both salicylate and caffeine, suggesting an interference with the skin barrier.

The aforementioned studies by Green *et al.* [156] also involved the manipulation of pH. The purpose of such experiments was to facilitate the transfer of cations across human skin using ionised OA and LA as counter ions. In this study, however, the pH of the donor phase solution used in permeation experiments was higher than that of the receptor solution and also exceeded the pK_a of both LA and OA. The drug was basic in nature and ionised at the donor's pH environment. Though the counter ions, LA and OA, increased the *in vitro* skin permeation of all the permeants, it was concluded by the authors that the increased flux of the cationic naphazoline could be partly attributed to ion pairing.

Valenta and co-workers' research in the late 1990s [159] considered the permeation of lignocaine hydrochloride in human skin. These authors used a range of donor solutions with different pH values: 4.0, 5.5 and 7.0, intended to reflect various physiological conditions. As shown in Table 4.2, the flux was 1.2 ± 1.2 μg/cm^2/h at pH 4.0, 13.0 ± 2.0 μg/cm^2/h at pH 5.5 and 118.0 ± 30.0 μg/cm^2/h at pH 7.0. PC values of the lignocaine salt were 0.19 at pH 4.0, 0.40 at pH 5.5 and 6.76 at pH 7.0, both increasing with higher pH values. This was due to the increase in the amount of unionised base, consistent with the pH partition hypothesis.

Megwa and co-workers [162] demonstrated a procedure for determining the optimum pH conditions for ion pair formation between SA and various amines. The system employed was very similar to a typical PC study, with the use of toluene instead of

octanol as the lipid phase, and a range of pH buffers (pH 2.5–7.5) as the aqueous phase. Following a comparable approach to that of Green [156], the drug was dissolved in the aqueous buffers and the counter ions added to the lipid phase, as opposed to dissolving the potential counter ions in the aqueous phase only. The optimal pH for the formation of ion pairs with the amines used (methylamine, ethylamine, propylamine, butylamine, diethylamine, triethylamine and triethanolamine) was ascertained to be pH 5.0.

Further studies involving SA were also undertaken by Smith and Irwin [47] in the same year. The authors tested both solutions and saturated suspensions of SA over a range of pH values. As hypothesised, experiments showed that the flux of SA across human skin from solutions was dependent on the pH of the vehicle (Table 14). The authors also determined that the flux from saturated suspensions across human skin remained relatively constant throughout the experiments (mean flux 1.09 ± 0.202 μmol/cm^2/h) regardless of the different pH values (pH 1.84, 2.35, 2.80, 3.14, 3.45, 3.73, 4.17, 4.71). This confirmed that permeation is related to the concentration of unionised molecules and is independent of pH or pH gradients (when a saturated suspension is used). Furthermore, this study demonstrated that the solubility of unionised SA in a suspension remained constant at different pH values, indicating a method of overcoming the impact of pH on solubility and maintaining maximum solubility [174].

Table 4. 14 Flux ± standard deviation of 14.48 mM solutions of SA across human skin at a range of pH values (experiments n = 2, values represent the mean ± S.E.) Adapted with permission from [174], Elsevier, 2000.

pH	Flux (μmol/cm^2/h)
2.10	0.72 ± 0.057
2.27	0.59 ± 0.016
2.72	0.54 ± 0.009
3.13	0.25 ± 0.006
3.50	0.15 ± 0.005
3.90	0.07 ± 0.001
4.30	0.05 ± 0.001
4.71	0.04 ± 0.000
5.13	0.01 ± 0.000

A previously mentioned study by Auner *et al.*[164] involved devising optimal pH values for ion pairing which enabled the testing of both cationic (pH 7.0) and anionic (pH 4.0)

counter ions in conjunction with ALA, a molecule that comprises two pK_a values (4.0 for the carbonyl group and 7.9 for the amino group). Analysis using PC studies indicated increased lipophilicity when ALA was combined with any of the counter ions. Higher lipophilicity resulted in increased permeation through porcine skin with all counter ions, with the exception of cetyltrimethylammonium bromide, as shown in Table 4.6.

A study by Sarveiya *et al*. [157] also tested the influence of donor compartment pH values in permeation experiments on the ionisation, partitioning and flux of benzydamine HCl, as seen in Table 4.3. In human skin studies, the authors found that as the PC increased with an increase in pH, so did the flux. At pH 5.0 PC value was 1.62 and flux 5.13 ± 2.42 μg/cm^2/h; at pH 6.0 PC value was 5.75 and flux 39.07 ± 10.5 μg/cm^2/h and at pH 7.0 PC value was 28.18 and flux 269.09 ± 58.5 μg/cm^2/h. The authors did suggest, however, that as the pH increased beyond these values, although the unionised fraction and the permeability coefficient would increase too, flux would be limited due to decreasing solubility.

In research by Cázares-Delgadillo [175] that investigated the impact of sucrose esters on the permeation of lidocaine HCl (see Figure 4.13) using porcine skin, both PC and permeation experiments were considered at pH values 5.0, 7.0 and 9.0. The fraction of unionised species was derived from the Henderson–Hasselbalch equation, and it was determined that at pH 5.0 lidocaine was completely ionised, at pH 7.0, 11% was unionised and at pH 9.0, 93% was unionised. The PC studies reflected this, with higher values attributed as pH increased (0.09 ± 0.002 at pH 5.0, 1.15 ± 0.007 at pH 7.0 and 1.17 ± 0.0043 for pH 9.0). Permeation of lidocaine alone also increased when the pH value of the buffered solution increased. As all solutions were saturated, permeability coefficients were obtained by dividing the flux by the concentration of the drug in the applied formulation. As shown in Table 4.15, permeability coefficients increased as pH increased. Apparent permeability coefficients for different pH values of lidocaine HCl and in the presence of sucrose laureate (L-TC) and sucrose oleate (O-TC) are also shown in Table 4.15. It was determined that pre-treatment of the porcine ear membranes with L-TC or O-TC in Transcutol® had a surprising impact on flux, permeation coefficients and overall enhancement, as results deviated from those expected due to the abovementioned pH partition hypothesis. At pH 5.0 and pH 7.0, (where 100% and 89%, respectively, of lidocaine was ionised) L-TC enhanced the

permeability coefficient of lidocaine alone by 11.95 and 10.84-fold. At pH 9.0, where lidocaine was 100% unionised, the presence of L-TC reduced the permeability coefficient to 59% of lidocaine HCl. Conversely, the application of O-TC (while increasing the permeability coefficient by 3.77 and 3.45-fold of that of lidocaine alone at pH values 5.0 and 7.0, respectively) led to an improvement in the permeability coefficient of the unionised lidocaine by 2.67-fold at pH 9.0. Investigations by the same group also indicated that L-TC causes lipid extraction and fluidisation of the skin barrier, creating structural disorder and an increase in micropores in the membrane which may facilitate greater penetration of the ions. The authors were, however, unable to rationalise the decreased movement of unionised lidocaine through the biological membrane. Whilst this may indeed suggest the formation of ion pairs at pH values at which lidocaine is ionised, the authors considered this option unlikely [175].

Table 4. 15 Apparent permeability coefficients for different pH values for lidocaine HCl and in the presence of L-TC and O-TC. According to the authors, saturated solutions of lidocaine were used (n = 6, values represent the mean ± S.D.) Adapted with permission from [175], Elsevier, 2005.

pH	Lidocaine HCl	Lidocaine plus 2% L-TC	Lidocaine plus 2% O-TC
	Permeability coefficient x 10^4 (cm/h)	Permeability coefficient x 10^4 (cm/h)	Permeability coefficient x 10^4 (cm/h)
5.0	1.55 ± 0.31	18.46 ± 5.60	5.83 ± 0.65
7.0	1.81 ± 1.1	19.58 ± 3.82	6.24 ± 0.31
9.0	5.65 ± 1.52	3.34 ± 0.22	15.08 ± 2.30

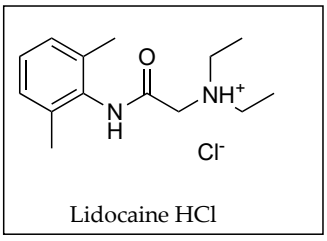

Lidocaine HCl

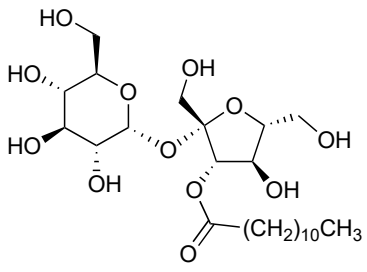

Sucrose laurate

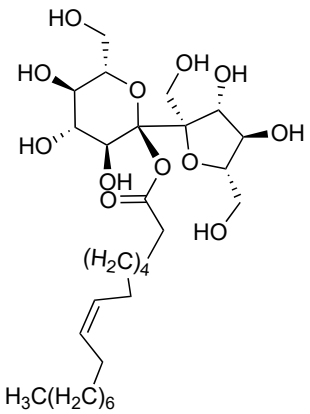

Sucrose oleate

Figure 4. 13 Lidocaine HCl with sucrose laurate and sucrose oleate.

In 2005, Wang *et al.*[166] attempted to measure pH values of fatty acids in PG and determined that shorter chain fatty acids had lower pH levels in this solvent. The authors also found that the addition of PHY increased the pH values of given formulations, suggesting neutralisation of the acid, and thus ion pairing (values not disclosed by the authors).

Vávrová and co-workers' study in 2008 described the complex molecular structures of adefovir and its proposed counter ion, 6-(dimethylamino)hexanoate (DDAK), that had previously been used by this group as a permeation enhancer (Figure 4.14). The authors tested the permeation of the adefovir ion pair through porcine skin using phosphate buffer solutions. These solutions were adjusted using phosphoric acid and sodium hydroxide to various pH values ranging from 3.4 to 7.8 as shown below in Table 4.16. It was determined that the pH value of 5.8 was optimal for permeation experiments, with most of the adefovir taking the form of a hydrogenphosphonate monoanion with the tertiary amino group of DDAK being its main proton source [176].

Table 4. 16 Flux and skin concentration of 2% adefovir with and without DDAK though porcine skin plotted against pH (n = 4 for all experiments except pH 5.8 where n = 12, values represent the mean). Adapted from [176], Elsevier, 2008.

pH Values		3.4	6.8	7.8	3.8	4.8	5.8
Flux of Adefovir ~ (μg/cm²/h)	***2% Adefovir***	0.2	3	1	2	1	4
	2% Adefovir + 1% DDAK	9.5	26.5	10	18	27	10
Adefovir Skin Concentration ~ (μg/g)	***2% Adefovir***	103	191	221	235	191	221
	2% Adefovir + 1% DDAK	412	693	538	708	771	412

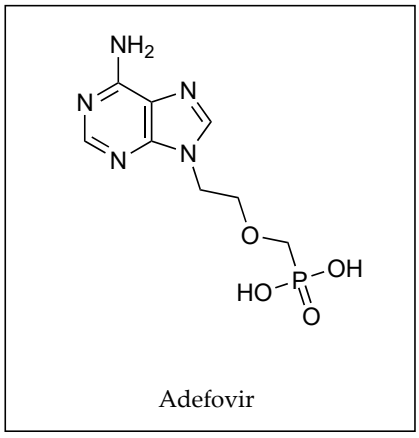

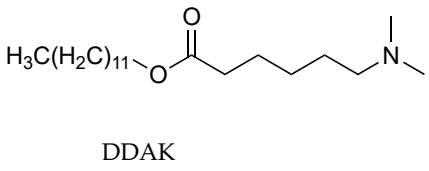

Figure 4. 14 Adefovir and DDAK.

4.4.3.5 Counter ion concentration

The effects of adding excess amounts of counter ions to saturated solutions of their salt were considered by Pardo *et al.*[168] and are shown in Table 4.17. The consequences of increasing the amount of salicylate to achieve an 8:1 salicylate–PHY molar ratio in the donor compartment of a typical permeation study, caused a decrease in the solubility of the PHY-salicylate salt. Nonetheless, this had very little effect on the flux of PHY, that changed from 44.27 ± 9.16 to 48.40 ± 9.50 μmol/cm^2/min. It did, on the other hand, increase the flux of salicylate approximately 4-fold, from 61.66 ± 2.54 to 247.30 ± 36.50 μmol/cm^2/min.

Creating an excess instead, of PHY, resulted in the equivalent of a 6.5:1 molar ratio of PHY- salicylate in the donor solution. This change in proportion had no real impact on the flux of SA (61.66 ± 2.54 to 63.90 ± 7.00 μmol/cm^2/min). It did, however, result in an increase in the flux of PHY by approximately 50% (44.27 ± 9.16 to 67.20 ± 7.70 μmol/cm^2/min).

This relatively low increase in permeation when PHY concentration was increased, versus the lack of change in flux when PHY was decreased, might be explained by the ratio of PHY cations to salicylate anions. When the number of anions decreased, the PHY cations were more likely to bind to negatively charged groups present in the porcine membrane thus limiting their movement.

Table 4. 17 Effect of solute composition on concentration (C_v), flux values and permeability coefficients of PHY and salicylate, when delivered through human skin (n ≥ 3 ≤ 8, values represent the mean ± S.E.M.). Adapted from [168], Wiley, 1992.

PHY:SA Ratio	Flux x 10^4 (μmol/cm^2/min)		Permeability coefficient x 10^4 (cm/min)		C_v (μmol/cm^3)	
	PHY	salicylate	PHY	salicylate	PHY	Salicylate
1:1	44.27 ± 9.16	61.66 ± 2.54	1.86 ± 0.39	2.60 ± 0.10	23.70 ± 0.55	23.70 ± 0.55
1:8	48.40 ± 9.50	247.30 ± 36.50	3.25 ± 0.64	2.10 ± 0.30	14.90 ± 0.40	120.00 ± 15.20
6.5:1	67.20 ± 7.70	63.90 ± 7.00	0.44 ± 0.05	2.68 ± 0.30	153.40 ± 7.70	23.70 ± 3.40

Vávrová *et al*. [176] also investigated the optimal quantity of the counter ion DDAK to be used in conjunction with adefovir, a zwitterionic drug used in the treatment of hepatitis B. This was done by maintaining the drug concentration at 2% and changing

the amount of counter ion, DDAK, to 0, 0.5, 1, 2 and 3%. Permeation studies using porcine skin indicated optimal flux values at 1% for DDAK, at which point flux values plateaued. This was demonstrated by the different amounts of permeant that surpassed the skin barrier when maintaining the drug concentration at 2% and adjusting the amount of the counter ion, DDAK. With DDAK: 0%, flux: 0 μg/cm^2/h; DDAK: 0.5%, flux: 14 μg/cm^2/h, DDAK: 1%, flux: 27 μg/cm^2/h, DDAK: 2%, flux: 26 μg/cm^2/h and when DDKA:3%, flux:26.5 μg/cm^2/h.

In 2011, Chirio *et al*. [177] used citric acid as a counter ion to increase the lipophilicity of diltiazem at a 2% *w/w* concentration (as shown in Figure 4.15) in a thermosensitive gel formulation. The different formulations devised by the authors included a 1.6% *w/w* methylcellulose gel containing diltiazem either in the absence or presence of the counter ion in a 1:4 ratio (diltiazem: citric acid). Results from permeation studies using porcine skin showed that the flux of diltiazem increased from 1.8 ± 0.3 to 2.6 ± 0.5 μg /cm^2/h when applied with the counter ion. The skin accumulation of the active also increased from 85 ± 8 to 176 ± 11 μg/cm^2 at 24 h. When the formulation was changed to a 16% *w/w* Pluronic F127 gel, flux values for diltiazem in the absence of the counter ion were shown to be 2.1 ± 0.4 μg/cm^2/h, and 3.0 ± 0.5 μg/cm/h when the counter ion was included at a 1:1 ratio. Skin accumulation also increased from 77 ± 6 to 151 ± 12 μg/cm^2 after a 24 h permeation study. The change of polymeric continuous phase of these gels resulted in a much lower concentration of counter ion being used to achieve similar permeation outcomes, demonstrating the importance of different molecular environments for ion pairing formation [177].

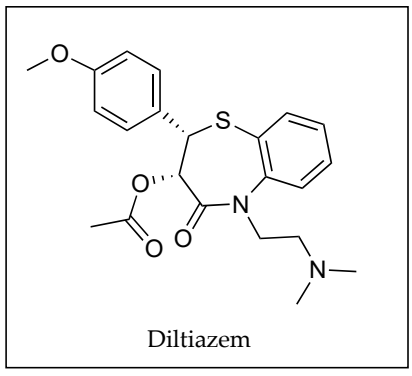

Diltiazem

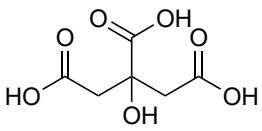

Citric acid

Figure 4. 15 Diltiazem and citric acid counter ion.

Due to the challenges involved in delivering sufficient quantities of drugs through the skin, the issue of toxicity is rarely addressed. It was, however, considered by Vávrová

et al. [176] who specifically limited the amount of adefovir to a maximum concentration of 20 mg/mL, in one set of experiments, despite drug solubility increasing up to as much as 120 mg/mL at different pH values. Fini *et al.*[160] also cautioned against the potential toxicity of the aliphatic amine counter ions used in their 2012 studies, as these do accompany the active when partitioning into the skin.

4.4.3.6 Ion pair and penetration enhancers

Penetration enhancers used as ion pairs

Green *et al.*[156] were the first to propose LA and OA as both counter ions and permeation enhancers in human skin studies in the late eighties. It was suggested that the enhanced flux of cationic naphazoline in conjunction with anionic fatty acids might be attributed to the increase in lipophilicity of naphazoline conveyed by ion pairing. This was confirmed by the results of PC studies shown previously in Table 4.1.

The counter ion, DDAK, used by Vávrová *et al*. [176] in conjunction with adefovir had previously been shown to be an effective permeation enhancer. This was demonstrated with pre-treatment of porcine skin by the counter ion in advance of the application of the adefovir solution, with results highlighted in Table 4.18. When combined with adefovir in solution, the addition of 1% of DDAK significantly reduced the solubility of adefovir at its optimal pH, 5.8, from ~124 to ~71 mg/mL. The reduction in solubility was of no consequence for this particular study, as the concentration was higher than that used in previous permeation experiments. This combination resulted in the flux increasing from ~16.5 to ~25.6 μg/cm^2/h in porcine skin experiments, when compared with pre-treatment alone. When experiments were conducted with human skin using adefovir alone, the authors observed that flux was “an order of magnitude lower” than it had been through porcine skin, but when applied in conjunction with DDAK it increased by 179-fold, from ~0.04 to 8.93 μg/cm^2/h. As mentioned previously, the authors noted that at the chosen pH value of 5.8, much of the adefovir was in the form of a hydrogenphosphonate monoanion, whilst the tertiary amino group of DDAK was protonated. They suggested that it was likely therefore, that ion pairing contributed to the reduction in solubility, and to the increased flux of the drug.

Ion pairs and the inclusion of penetration enhancers

Auner *et al.*[164] combined the use of ALA and the counter ion, cetylpyridinium chloride (CP) at pH 7, with a permeation enhancer, 6-ketocholestanol (KC). The permeation

enhancer was formulated into phosphatidylcholine liposomes. This combination increased the flux of ALA by 3.5-fold from ~6.26 to ~23.00 μg/cm^{-2} after a period of 4 h, as shown in Table 4.19.

Table 4. 18 Flux and skin concentration of adefovir after use of DDAK (for human skin experiments n ≥ 3 ≤ 4, except for 2% adefovir samples where n = 12, for porcine skin experiments n = 4, except for co-application samples where n = 12, values represent the mean). Adapted from [176] , Elsevier, 2008.

Membrane	Application	Flux ~ (μg/cm^2/h)	Skin Concentration (epidermis incl SC for human skin) ~
Porcine skin	Co-application of 2% adefovir, 1% DDAK	25.6	31.3 μg/g
	2% adefovir pre-treatment of skin with DDAK	16.5	17.1 μg/g
Human skin	Co-application of 2% adefovir, 1% DDAK	8.93	21.30 μg/cm^2
	2% adefovir, no DDAK	0.04	5.72 μg/cm^2

Table 4. 19 Permeation of ALA through porcine skin with unloaded phosphatidylcholine liposomes; with CP counter ion and unloaded phosphatidylcholine liposomes and with CP counter ion and KC loaded phosphatidylcholine liposomes. The concentration of ALA applied in the buffer solutions was 0.4 mg mL (n ≥ 3 values represent the mean). Adapted from [164], Elsevier, 2003.

ALA with:	pH	Cumulative amount of ALA ~ (μg/cm^2) after 4 hours using porcine skin
counter ion CP plus phosphatidylcholine liposomes loaded with KC	7.0	23.00
counter ion CP plus unloaded phosphatidylcholine liposomes	7.0	11.25
unloaded phosphatidylcholine liposomes	7.0	6.25

4.4.4 Ion pairs and the customisation of drug permeating amounts

Ion pairs have been used in an attempt to increase drug flux through the skin. There are occasions, however, where the permeation of active ingredients into the systemic circulation is not desirable. Vasoconstrictors (VC) have been used as ion pairs in order to increase the residence time of drugs in the skin and local tissues by reducing dermal clearance [178]. Cross and co-workers tested three different VCs in a 1:1 molar ratio with SA (Figure 4.16) using liquid paraffin as a vehicle (Table 4.20). These formulations were then applied to a human abdominal epidermal membrane using conventional *in vitro* permeation methodology. Analysis of flux values as well as skin retention of the SA and VCs was then undertaken. It was found that following absorption into the

membrane, there were unequal molar ratios of the VC and the SA in both the membrane and the receptor fluid. As shown in Table 4.20, there was greater epidermal flux and higher retention of the SA in conjunction with the VC, ephedrine. Flux of SA in combination with ephedrine was 18.6 ± 0.6 μg/cm^2/h, with naphazoline was 7.8 ± 0.8 μg/cm^2/h and with tetrahydrozoline was 1.1 ± 0.1 μg/cm^2/h. Skin retention of SA with ephedrine was 4.2 ± 0.7 μg/mg; with naphazoline, it was 3.5 ± 1.1 μg/mg; and with tetrahydrozoline, it was 2.8 ± 1.1 μg/mg.

Table 4. 20 Epidermal flux and tissue retention of VCs and SA following application to human skin. Concentrations applied were 10% w/v of equimolar amounts of SA and VC (n = 6, values represent the mean ± S.E). Used with permission from [178], Springer Nature, 2003.

VC	Flux (μg/cm^2/h)		Skin retention (μg/mg)	
	VC	SA	VC	SA
Ephedrine	11.5 ± 2.3	18.6 ± 0.6	10.0 ± 0.4	4.2 ± 0.7
Naphazoline	12.0 ± 1.6	7.8 ± 0.8	20.7 ± 6.0	3.5 ± 1.1
Tetrahydrozoline	2.9 ± 0.5	1.1 ± 0.1	3.7 ± 0.6	2.8 ± 1.1

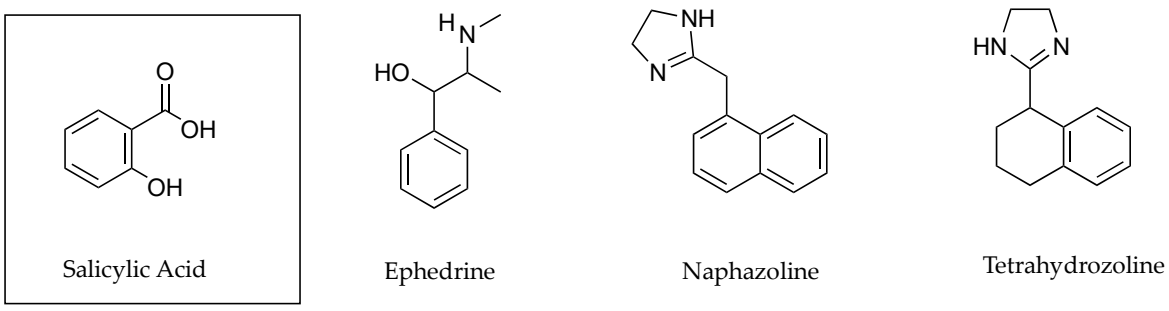

Figure 4. 16 SA and counter ions ephedrine, naphazoline and tetrahydrozoline.

In a previously discussed study by Trotta that required the maximum concentration of the RA in the skin with minimal dermal clearance, valine methyl esters and phenylalanine ethyl esters were shown to increase the permeation of the active through porcine skin as shown in Table 4.21. When RA was used in conjunction with either of these counter ions in two different oil-in-water microemulsions, RA permeation was reduced considerably, from 0.13 ± 0.02 to less than 0.01 μg/cm^2/h. There was also a corresponding increase in skin accumulation from a minimum amount of 1.0 ± 0.2 μg/cm^2 when RA permeated alone, to 13.3 ± 2.10 μg/cm^2 when

combined with the phenylalanine ethyl esters in microemulsion (a) as shown in Table 4.21. The overall increase in localised delivery using the microemulsions with ion pairs was 4 – 5-fold that of RA alone. There was also a total reduction in flux [163].

Table 4. 21 Skin accumulation and flux of RA alone and in combination with various counter ions. Formulation used for non-microemulsion studies was a 0.005% (w/w) RA in ethanol–pH 6.4 buffer solution (1:2 v/v), in the absence or presence of counter ions in a 1:50 molar ratio. Microemulsions contained 0.05% RA in the absence or presence of counter ions in a 1:50 molar ratio. Microemulsion (a) comprised 56.7% water, 8.8% IPM, 5.3% Epikuron, 13.2% Oramix and 16.0% ethanol; microemulsion (b) comprised 64.3% water, 10.0% IPM, 11.0% Epikuron, 13.6% Oramix and 9.2% ethanol (n ≥ 3, values represent the mean ± S.D.). Adapted with permission from [163], Elsevier, 2003.

RA with:	Skin accumulation after 24 hours (μg/cm$^{2)}$	Flux (μg/cm^2 /h)
alone	1.0 ± 0.2	0.13 ± 0.02
tryptophan methyl ester hydrochloride	2.3 ± 0.6	0.19 ± 0.02
phenylalanine ethyl ester hydrochloride	3.4 ± 0.6	0.23 ± 0.03
valine methyl ester hydrochloride	3.7 ± 0.8	0.21 ± 0.03
Formulated as microemulsions oil in water microemulsions (a) and (b):		
(a) Alone as microemulsion	3.3 ± 0.50	0.05 ± 0.01
(a) phenylalanine ethyl ester hydrochloride	13.3 ± 2.10	< 0.01
(a) valine methyl ester hydrochloride	8.7 ± 1.6	< 0.01
(b) Alone as microemulsion	2.3 ± 0.50	0.04 ± 0.01
(b) phenylalanine ethyl ester hydrochloride	12.6 ± 1.8	< 0.01
(b) valine methyl ester hydrochloride	10.8 ± 1.5	< 0.01

Another example of the use of a vasoconstrictor to enhance dermal accumulation was introduced by Uchino *et al.* [177] when combining DF with phenylephrine as a counter ion (seen in Figure 4.17). After a 48 h *in vitro* permeation study, the cumulative amounts of DF that had permeated after applying DF, or the ion pair complex, to pig skin were 76.1 ± 26.6 and 118.9 ± 45.8 μg/cm^2, respectively. The amounts of DF found in the epidermis as a result of the same applications, were 3.34 ± 1.04 and 5.58 ± 1.43 μg/mg, respectively. The concentrations of DF in the dermis were recorded as 0.35 ± 0.09 and 0.45 ± 0.14 μg/mg for both neat DF and the active when combined with phenylephrine as an ion pair [177, 179].

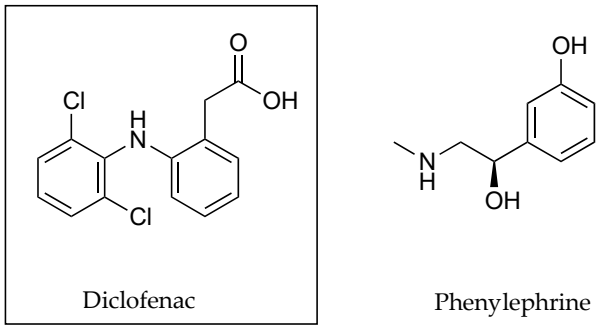

Figure 4. 17 DF and phenylephrine counter ion.

An amino acid derivative, carnitine, has been investigated as a potential alternative exfoliator, due to the side effects of conventional exfoliation methods [167]. As calcium is important in the adhesion of corneocytes, a reduction in calcium ions in the skin reduces cohesion of the corneocytes, thus improving exfoliation. The calcium chelating abilities of carnitine were considered in a recent study by In *et al*. [167]. As an amphoteric molecule, penetration of carnitine has been regarded as extremely limited. A zwitterionic counter ion, hydrogenated soya phosphatidylcholine (HSC), was utilised to both increase partitioning into the skin and to limit permeation to the epidermis. The percentage of applied carnitine (4% *w/w*), found in the epidermal layers of porcine skin after a 24 h *in vitro* permeation study was approximately 9.13% when carnitine was applied without any counter ion, and 23.71% when applied with HSC. In this study, no permeation beyond the epidermis was seen, showing the potential of ion pairs in retention of skin compounds [167].

Recently, ion pairing was used in a novel fashion by Rodrigues and co-workers to increase the lipophilicity of the hydrophobic drug, adapalene [180]. This molecule has been used for the topical treatment of acne. However, patient compliance is poor because of skin irritation. By encapsulating adapalene (0.1% *w/w*) in solid lipid nanoparticles (SLPs) in conjunction with stearylamine as a counter ion (Figure 4.18), several improvements in the formulation and delivery of adapalene were evident. According to the authors, crystals of adapalene were no longer observed in the external aqueous phase of the formulation as a result of efficient encapsulation due to ion pairing. While both compounds (i.e., adapalene and stearylamine) were considered practically insoluble in water, the interaction between these two molecular entities appeared to ensure that adapalene did not partition out of the lipid phase.

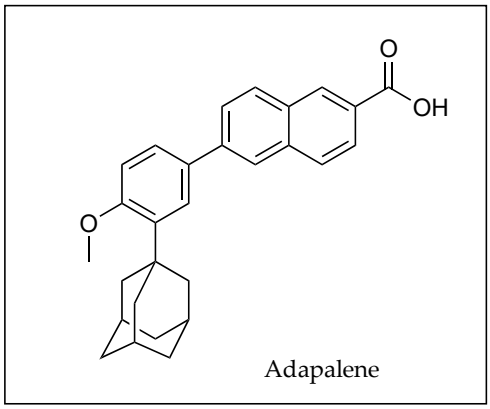

Adapalene

$H_3C(H_2C)_{17}—NH_2$

Stearylamine

Figure 4. 18 Adapalene and stearylamine counter ion.

Furthermore, the SLP formulation resulted in 4-fold more adapalene in the epidermis (16.36 ± 1.79 compared to 4.08 ± 0.22 µg/cm^2) and 7-fold more retention in the dermis (1.17 ± 0.12 compared to 0.16 ± 0.03 µg/cm^2), than the marketed gel formulation (0.1% *w/w* AD), in a porcine skin permeation study [180].

4.4.5 Kinetics

The organic ion pair, PHY–salicylate salt, was studied in human skin by Pardo *et al.* [168]. Since diffusion of the individual ion species occurred at different rates, it was concluded that while the diffusion of each component of the ion pair did follow Fick's laws of diffusion, the rate at which they occurred was influenced by a number of factors. These included the pH of the membrane, the pK_a of the individual molecules and the charge bearing groups contained within the membrane. The authors suggested that the apparent net negative charge of the skin at physiological pH, could explain the slower permeation of the positively charged PHY.

In adjusting the molar ratios of the two species to determine the impact on permeation, the authors found that increasing salicylate to achieve an 8:1 salicylate–PHY molar ratio in the donor compartment of a typical permeation study, caused a decrease in the solubility of the PHY-salicylate salt. Nonetheless, this had very little effect on the flux of PHY, which changed from 44.27 ± 9.16 to 48.40 ± 9.50 µmol/cm^2/min. It did, on the other hand, increase the flux of salicylate approximately 4-fold, from 61.66 ± 2.54 to 247.30 ± 36.50 µmol/cm^2/min. Creating an excess instead, of PHY, resulted in the equivalent of a 6.5:1 molar ratio of PHY- salicylate in the donor solution. This change in proportion had no real impact on the flux of SA (61.66 ± 2.54. to 63.90 ± 7.00 µmol/

cm^2/min). It did, however, result in an increase in the flux of PHY by approximately 50% (44.27 ± 9.16 to 67.20 ± 7.70 μmol/cm^2/min).

This relatively low increase in permeation when the PHY concentration was increased, versus no change in flux when PHY was decreased, was explained by the ratio of PHY cations to salicylate anions. When the number of anions decreased, the PHY cations were more likely to bind to negatively charged groups present in the porcine membrane thus limiting their movement. Conversely, the lack of positively charged groups in the membrane would facilitate the flux of the salicylate ion.

Other contributory factors in relation to the permeation kinetics of the permeation included solvent selection, combination and titration. The solvents IPA, with a ε of 18.62 at 20 °C [169, 170], and IPM, with a ε of 3.31 at 25 °C [172], were mixed in various combinations. As shown in Table 4.9, it was found that a solvent mixture comprising a 70:30 ratio of IPA to IPM had the best impact on permeation. Flux of PHY increased from 0.56 ± 0.08 × 10^4 μmol/cm^2/m at its lowest rate determined when the solvent comprised 100% of IPA, to 44.27 ± 9.16 × 10^4 μmol/cm^2/m when the solvent mixture contained 70% IPA. Flux of salicylate increased from 1.47 ± 0.11 × 10^4 μmol/cm^2/m at its lowest rate, which occurred when the solvent comprised 100% IPM to 61.66 ± 2.54 μmol/cm^2/m when the optimal ratio of IPA to IPM was 70:30 [168].

4.4.6 Ion pairs in marketed formulations

A commonly used NSAID, DF, is generally formulated as a salt to overcome the characteristic low solubility of the free acid. Salt forms such as sodium, epolamine (N-(2-hydroxyethyl)pyrrolidine) and diethylamine have been shown to partition from aqueous into lipid layers as ion pairs by Fini *et al.* [23, 160]. These counter ions or salts are used in a number of commercial formulations as presented in Table 4.22. Although other formulations are available on the market, these are not included in the present document.

Table 4. 22 Commercial applications of DF and counter ions sodium, epolamine and diethylammonium.

Commercial name	Active	Ion pair	Owner
Diclofenac 1% gel	DFA	Sodium	A A H Pharmaceuticals Ltd
Diclofenac 1% gel	DFA	Sodium	Actavis UK Ltd

Diclofenac 1% gel	DFA	Sodium	Alliance Healthcare (Distribution) Ltd
Diclofenac 1% gel	DFA	Sodium	Typharm Ltd
Diclofenac sodium topical gel 1%	DFA	Sodium	AvKARE
Diclofenac sodium topical gel 3%	DFA	Sodium	Taro
Diclofenac sodium topical solution (1.5 %)	DFA	Sodium	Sola Pharmaceuticals
Flector gel 1%	DFA	Epolamine, sodium	Laboratoires Genevrier
Flector EP 10 mg/ g	DFA	Epolamine	Medichemie
Flector tissugel 140 mg (medicated plaster)	DFA	Sodium	Windzor Pharma
Flector (patch)	DFA	Epolamine	Pfizer
Pennsaid® (2% solution)	DFA	Sodium	Horizon Medicines LLC
Solaraze 3% gel	DFA	Sodium	Almirall Ltd
Solacutan 3% gel	DFA	Sodium	Mibe Pharma UK Ltd
Voltarol® joint pain relief 2.32% gel	DFA	diethylammonium	GSK
Voltarol® joint 12 hour joint pain relief 2.32% gel	DFA	diethylammonium	GSK
Voltarol® osteoarthritis joint pain relief 1.16 % gel	DFA	diethylammonium	GSK
Voltarol® back and muscle pain relief 1.16% gel	DFA	diethylammonium	GSK
Voltarol®140 mg medicated plaster	DFA	Sodium	GSK

4.5 Conclusions

The literature relating to ion pairs has been examined and critically considered with the intention of elucidating common approaches used when employing ion pairing in the delivery of drugs via the skin. Not all factors influencing ion pairing, such as hydrogen bonding and solvation, were considered in the publications reviewed. Furthermore, the areas identified while examined individually, cannot be considered in isolation.

PC studies have often been undertaken to determine the ability of ions to form ion pairs and these results have sometimes, but not always, translated into increased

permeation results. While outcomes of regression analyses and QSARs have shown that the PC, as a measure of lipophilicity or hydrophobicity, is one of the most important predictors of flux, this is not always the case. This is unsurprising, given that permeation relies on both the partition and diffusion of molecules involved. Despite this, few studies considered the retention of the drug in the biological membranes in addition to flux, when considering the efficacy of PC experiments.

In terms of characteristics of the counter ion, experiments have confirmed that the ability to form ion pairs is impacted by the distance between centres of charge. Ions of a smaller radius, such as lithium, were better able to form ion pairs than those with a larger radius, such as caesium. Other observations relating to the type of counter ion, considered the degree of substitution of amine structures. The pairing efficiency of amine counter ions in conjunction with SA, in human skin permeation studies, was observed to be tertiary > secondary > primary > quaternary. Investigations also revealed organic cations to be more successful than inorganic structures in forming ion pairs. Furthermore, it was established that increasing the carbon chain length of the counter ion increased partitioning and permeation through the skin. This was attributed to increased lipophilicity of the ion pair when compared to their singular molecular constituents.

Authors have suggested that the contribution of ion pairing may be more than an electrostatic interaction. In such cases, the hydrocarbon moieties of the functional groups of counter ions may also contribute to masking or shielding the charges of the chemical composites. This conceptual experimental idea that longer alkyl chains could possibly increase such masking or shielding, would indeed explain the variety of permeation data shown by many authors.

General principles relating to solubility and the ability to partition or permeate have been analysed. The comparison of structurally related counter ions showed very clearly that while those with hydroxy groups resulted in higher aqueous solubility, this did not ordinarily translate into a higher permeation coefficient. It was confirmed that solubility of a substance in its formulation does not ensure partition into a biological membrane. Furthermore, it was indicated that where solubility parameters of the solute and the solvent are too similar, it may be concluded that partitioning of the analyte into the membrane is not assured. Importantly, it is essential to bear in mind that ion pairing strategies are always subject to all factors affecting skin permeations.

As crucial components of semi-solid formulations, solvent systems with a reduced ε value are more likely to stabilise ion pairs. The impact of different solvent combinations on the permeation of counter ions was evaluated, as was the impact of different counter ions or different quantities of counter ions, on the conductivity of the solution. However, no information has been disclosed in recent studies regarding the conductivity of various solvent systems when utilising the same counter ion combinations.

The impact of pH has also been considered by many authors in ion pair research. Although the pH partition theory considers that only unionised drugs permeate the skin, it is clear that some ionised drugs are in fact able to partition when charges are masked.

The important issue of toxicity was addressed in only two of the papers reviewed, despite the significance of this matter when selecting potential counter ions. The authors may have given no consideration to this matter, due to their experiments being initial investigations into the ability of various ions to pair, and to the impact of different structures on this ability. However, this is an important concern that should be addressed in the selection process. Furthermore, the potential for skin related irritations did not appear to be a factor when choosing possible counter ions in any of the studies reviewed. As these formulations are to be applied topically, the likelihood of skin irritation must be contemplated. One such example is benzalkonium chloride that is considered an irritant when used at a concentration of 7.5% [54,55], thus use of this compound as a counter ion should be limited.

The concept of ion pairs has developed in novel ways. This approach has not only been explored to increase permeation through the skin, but to control or limit permeation to the membrane itself. Permeation enhancers have been used as ion pairs, and ion pairs have been used in conjunction with permeation enhancers.

Ion pairs have also been used to improve the stability of solid lipid nanoparticle formulations. Thus, the formation of ion pairs is a versatile strategy, and one to be considered when formulating actives for topical and transdermal delivery. They should not be examined in isolation, because as noted, they are subject to all the factors that impact the application of drugs to or via the skin. In future investigations, it would be interesting to consider not only the impact of the solvent ε value on the conductivity of

the formulation, but also to evaluate the importance of solubility parameters of analytes and solvents used for such studies. This concept could potentially result in a formulation from which counter ions would be more likely to partition into the membrane. Additionally, mass balance studies combined with conventional permeation studies should provide additional information relating to the distribution of the pharmaceutical ingredient, bearing in mind the impact of the solubility parameters of the membrane in relation to the movement of the permeant.

4.6 Funding

This research received no external funding.

4.7 Conflicts of interest

The authors declared no conflict of interest.

4.8 Post-publication updates

According to Dimensions, as of September 2025, this review has been cited 42 times. Among these citations, six studies complied with the criteria of the original review, with only one following a "conventional" approach to ion pairing. In this investigation sodium cholate (CNa) was proposed as a counterion to enhance the partitioning of methylene blue (MB) into the skin [181]. MB is a hydrophilic molecule that has shown efficacy in the treatment of non-melanoma skin neoplasms.

The partitioning of MB between aqueous and octanol phases was evaluated in the absence of CNa and in the presence of CNa at concentrations of 0.068%, 0.135%, and 0.270% (w/v). The results demonstrated a corresponding increase in the distribution coefficient of MB with increasing CNa concentration: 0.11 ± 0.02 (0% CNa), 0.54 ± 0.17 (0.068% CNa), 1.00 ± 0.03 (0.135% CNa), and 1.43 ± 0.17 (0.270% CNa).

In vitro permeation testing (IVPT) involved the application of 300 mg of aqueous gels containing these combinations to porcine skin. Permeation amounts were below the limit of quantification. However, the addition of CNa at 0.068% w/v and 0.135% w/v increased the retention of MB in the skin by approximately 2-fold ($p < 0.01$) and 2.4-fold ($p < 0.001$) respectively, compared to MB alone (20.02 ± 6.80 μg/cm²). The addition of 0.270% (w/v) CNa did not significantly affect skin retention compared to the

control (p > 0.05). It was suggested that 0.270% (w/v) corresponded to the critical micelle concentration for CNa, above which micelles form that can partition into the octanol phase in distribution coefficient experiments but are too large to partition into the skin.

4.8.1 Updates in associated areas: new salt complexes, ionic liquids (IL) and deep eutectic solvents (DES)

4.8.1.1 Background

The phenomenon of ion pairing remains subject to ongoing debate, with certain mechanistic aspects still lacking definitive clarification. In determining whether two ions are likely to create ion pairs, many researchers have created new salt complexes comprising the oppositely charged molecules. In some cases, this has been done in an attempt to improve the solubility of the individual entities, a technique commonly used in pharmaceutical development [182]. Complexes can also be used to eliminate other ion species when combining two salts. The resulting ion pair complexes may stray into the realms of ionic liquids (IL) and deep eutectic solvents (DES), which are frequently distinguished from other salts by their low melting points. Specifically, ILs have melting points below 100 °C, while DES mixtures are characterised by significant depressions in melting points when compared to those of their individual components [183]. While both are frequently liquids at room temperature [184-186], they can be differentiated from each other on the basis of their starting materials and preparation methods. IL are described as combinations of organic heterocyclic cations and organic or inorganic anions, while DES are said to be a combination of hydrogen bond acceptors and hydrogen bond donors [185]. This commonly used reference to hydrogen bonding to define DES has however been criticised, as it would describe many ideal mixtures [187]. Regarding preparation techniques, IL typically require multiple synthetic steps and the use of various reagents, including organic solvents. These processes often generate by-products, and the reaction times can extend up to 48 hours [185]. In contrast, the production methods for DES are simpler. DES can be created by straightforward processes such as heating or grinding the compounds together, or by mixing separate aqueous solutions of the components followed by freeze-drying to yield a clear, viscous liquid [185].

When considering practical applications of these complexes, density and viscosity are their primary disadvantages. Although such challenges can be addressed by adding other solvents such as water [185], this can alter the structure of DES and IL [188]. Moreover, an excess of added solvents may completely disrupt a DES [189].

Martins *et al.* have questioned whether solutions of salts or other hydrogen bonding compounds in solvents that are liquids at room-temperature, such as water, alcohols, ethylene glycol, glycerine, and others should be classified as DES [187]. Ma however, has suggested the need for research to differentiate between aqueous DES solutions and the aqueous solutions of the individual DES components [188].

Regarding IL, studies have investigated their solubility in water and other solvents, as well as the factors influencing their hydrophilicity and hydrophobicity [189-192]. The behaviour of the ions in both pure IL, as well as aqueous and non-aqueous IL solutions, were examined by Nordness and Brennecke [193]. They described IL as dynamic systems comprising fluctuating combinations of ion pairs and charged ions. The intermolecular forces contributing to ion associations include Coulombic, hydrogen bonding, Van der Waals forces and π-π interactions, with the electrostatic interactions essential to “conventional” ion pairs dominating. Furthermore, as mentioned earlier in the context of standard ion pairs, pairing is influenced by the properties of the ions within the ion pair. Moreover, ion associations decrease with the increasing solvent concentration, transitioning from a continuous network of ions in pure IL, to free non-interacting species in infinitely diluted systems.

Notwithstanding, the classification of ILs and DES as distinct research areas, the literature does suggest that the behaviour of these complexes in solution cannot be completely separated from the concept of ion pairs as defined by Bjerrum [46].

4.8.1.2 New salt complexes

Five of the six citing publications expanded beyond the scope of the original review, employing methods and approaches that had not been addressed in the previously reviewed ion pair literature. Four of these involved new salt complexes, whilst the fifth investigated an IL.

Two of these studies were undertaken by groups at Xiangtan university and investigated the use of ion pairs to increase the permeation of strychnine [194] and diacerein [195]. Strychnine was paired with various fatty acids and the diacerein with

both organic and fatty amines. Molecular simulation was used to determine the optimal geometry between the ion pairs and confirmed hydrogen bonding between the deprotonated acid anions and protonated cations. Complexes of the ion pairs were prepared and FTIR spectra corroborated hydrogen bonding between the ions.

Infinite dose permeation studies using saturated solutions of the ion pair complexes in isopropyl myristate applied to porcine skin were undertaken in both He [194] and Liang's [195] groups. The results published by He *et al.* showed that the ion pair complexes increased the amount of strychnine that permeated by 1.5 – 7.8 times that of strychnine alone (101 ± 50.95 μg/cm^2). The highest amount that permeated at 24 h was from the strychnine-capric acid ion pair (857.54 ± 157.84 μg/cm^2).

Liang's group found greater cumulative permeation results at 24 h for diacerein-organic amines than diacerein alone (1.83 ± 0.22 μg/cm^2), with the highest amount deriving from the diacerein-triethanolamine ion pair (7.89 ± 0.38 μg/cm^2). Cumulative permeation of diacerein when combined with fatty amines was higher on average than when in combination with the organic amines (average values not provided by the authors). The greatest cumulative permeation value of diacerein occurred when the NSAID was paired with the 12-carbon laurylamine.

However, several methodological considerations warrant discussion. Although PC studies did not correlate with permeation results, in the case of diacerein, this may have been due to the method by which it was conducted. As ion pairs are generally used to facilitate the partition of ionised molecules from aqueous into organic environments, dissolving the complex initially in an aqueous phase at a given pH, followed by the addition of an organic solvent, would provide an interesting comparison to their current findings. Furthermore, in relation to both the diacerein and strychnine research, a mass balance study would have aided the explanation of the distribution of the active pharmaceutical ingredient. While permeation and PC results do not necessarily correlate, there may have been a proportion of the active ingredient that remained in the membrane, showing that it was able to partition into the lipid environment of the membrane.

Despite no apparent relationship between PC studies and the permeating amount, both publications demonstrated an additional relationship to flux based on binding energy distribution curves. It was observed that increased similarities in the binding

energy distribution curves of potential ion pairs indicated a greater compatibility between the compounds. Those compounds with enhanced compatibility, as determined by the distribution curves, also exhibited greater flux values.

Another citing study developed a salt comprising the poorly water-soluble compound, SA, together with matrine (M), to increase the water solubility of SA, decrease skin irritation and enhance its partition and permeation. IVPT entailed the application of saturated 1 mL aqueous solutions of SA and SA-M complexes, applied to porcine skin for 48 h. Ion pairing resulted in the cumulative permeation and membrane retention of SA from SA-M (± 1800 μg/cm^2 and ± 78 μg/cm^2), far exceeding the values of SA permeating and retained in the membrane from the free acid solution (± 250 μg/cm^2 and ± 20 μg/cm^2) [196].

Another paper that cited the original review that used “ion pair complexes” investigated the effect of combining tranexamic acid (TXA) and mandelic acid (MA) for the treatment of skin pigmentation [197]. The work compared individual TXA and MA solutions, physical mixtures of TXA–MA and chemically formed TXA–MA complexes. Based on zeta potential measurements, the TXA–MA complex exhibited the lowest value (-3.3 mV) compared with the TXA–MA mixture (-10.86 mV), TXA alone (-4.71 mV) and MA alone (-28.4 mV), suggesting a reduction in surface charge consistent with complex formation. FT-IR spectra further differentiated the complexes from the simple mixtures, supporting the presence of specific interactions between TXA and MA.

Although the study methods suggested that IVPT would compare TXA, TXA–MA mixtures and TXA–MA complexes, results were presented only for TXA and the TXA–MA complex. Following the application of an infinite dose (100 μL) of 3% solutions to porcine skin under occluded conditions for six hours, 10.9% of the TXA–MA complex permeated the skin compared to 7.85% from the TXA solution. The study did not report the number of replicates, standard deviations, or statistical significance. Although extraction procedures were described in the methods, no quantitative results or mass balance analyses were provided.

4.8.1.3 Recent work in the field of IL/ ion pairs

Citation of the original review included a paper published by a collaboration that included the West Pomeranian University of Technology and the Pomeranian Medical

University, both located in Szczecin, Poland [198]. These groups extended the ion pairing concept by creating counterions from the amino acids glycine, L-alanine, L-valine, L-isoleucine, L-leucine, L-serine, L-threonine, L-cysteine, L-methionine, L-aspartic acid, L-lysine, L-phenylalanine, L-proline and L-glutamic acid, which they then modified into ethyl, propyl, isopropyl and butyl esters. These cationic amino acid alkyl esters have been combined with anionic actives such as NSAIDs (including ibuprofen (IBU), ketoprofen (KETO), naproxen (NAP)) as well as salicylic acid (SA) and ferulic acid, to create new salt complexes. This was done with the purpose of improving both the aqueous solubility and the permeability of the actives. The resulting salts were considered ionic liquids due to their melting points being below 100 °C. As outlined in Tables 4.23 – 4.27, IVPT were undertaken applying infinite doses (1mL or 1g) to porcine or human skin. Concentrations ranged from 1% to saturated solutions, while vehicles comprised various bases: including Pentravan® cream with 10% ethanol; hydrogels made with Celugel® and 10% ethanol; emulsions comprising glycerin grapeseed oil and beeswax; a hydroxyethylcellulose based hydrogel; PBS (pH 7.4); or combinations of ethanol and water (70:30, v/v) [192, 198-206]. Notably, the studies using 70% ethanol solutions selected this solvent specifically for its ability to affect skin barrier properties, although this approach differs from conventional IVPT methodology where such barrier disruption is typically avoided to enable clearer assessment of the active formulation's permeation characteristics [207-210].

Unlike conventional ion pairing, where counterion addition increases partitioning of the active ingredient into the organic layer, these counterions decreased organic partitioning for all active ingredients except SA. However, the counterions increased the aqueous solubility of the APIs. As shown in Tables 4.23 – 4.27, despite this increased hydrophilicity, the vast majority of ion pair complexes demonstrated greater permeation than the active ingredients alone.

Another study by this group compared two commercial products, a gel (CG) and a cream (CC), to their own emulsion-based gel formulations. These formulations contained either an ibuprofen-L-phenylalanine ethyl ester IL complex (IB-PH), IBU alone (IBU-G) or ibuprofen sodium (IB-NA) [211]. All formulations contained the equivalent of 5% IBU. Applying 1 g of each formulation to porcine skin for 24 h, the cumulative permeation of IBU from the two salts in the emulsion-based gels (IB-NA: 1086.6 ± 245.8 μg/cm^2 and IB-PH: 948.6 ± 87.5 μg/cm^2) was significantly higher than

from the commercial products (CG: 577.9 ± 90.2 μg/cm^2 and CC: 222.2 ± 33.3 μg/cm^2). The permeation of IBU from IBU-G (909.6 ± 45.3 μg/cm^2) was comparable to IB-NA and IB-PH. Unfortunately, no mass balance studies were reported, and therefore the impact of the variations of IBU on skin accumulation could not be assessed.

The most recent IL study that cited the review considered the development of a new salt form of valsartan (VST), a poorly water-soluble drug used in the treatment of hypertension [212]. The counterion was choline (CHN), and the salt obtained was determined to be an IL. Distribution coefficient studies for both VST and VST-CHN suggested poor distribution of VST into the organic layer. The VST-CHN combination did however result in a higher log-D value (-1.0 ± 0.14) than VST alone (-1.3 ± 0.08). Occlusive, infinite dose studies applying 1 g of a 4% aqueous gel suspension to human skin for 15 hours, found no statistically significant difference in skin permeation. The VST formulation resulted in 1.727 ± 1.474 μg/mL, while the VST-CHN combination amounted to 4.769 ± 2.051 μg/mL ($p > 0.05$).

Table 4. 23 Permeation Data using porcine (P) or human (H) skin for NAP and its IL complexes. Adapted from [198], Science Direct, 2023; [199], MDPI, 2021; [204], Elsevier, 2024 and [205], MDPI, 2025.

Counterion	Log P/D	Mem-brane	Form-ulation	CP (μg/cm^2)	% applied that permeated	Ref
-	2.12 ± 0.01	P	PBS pH 7.4 saturated solution (1 mL)	45.55 ± 1.89	1.82	[199]
L-Proline ethyl ester	0.90 ± 0.02	P		277.38 ± 25.44	6.53	[199]
L-Proline propyl ester	0.99 ± 0.02	P		386.02 ± 1.57	9.64	[199]
L-Proline isopropyl ester	0.92 ± 0.04	P		389.12 ± 13.03	8.91	[199]
L-Proline butyl ester	1.09 ± 0.02	P		368.70 ± 13.85	9.07	[199]
-	2.12 ± 0.02	P	70:30 ethanol: water (v/v) [1%] (1mL)	182.27 ± 6.16	1.73 ± 0.05	[198]
L-valine propyl ester	1.24 ± 0.02	P		308.10 ± 10.05	2.71 ± 0.09	[198]
L-valine isopropyl ester	-	P		306.44 ± 7.37	3.08 ± 0.07	[198]
L-valine butyl ester	1.47 ± 0.02	P		315.21 ± 11.45	2.95 ± 0.11	[198]
L-Isoleucine propyl ester	1.17 ± 0.01	P		174.00 ± 10.34	1.45 ± 0.09	[198]

L-Isoleucine isopropyl ester	-	P		185.62 ± 6.39	1.75 ± 0.06	[198]
L-Isoleucine butyl ester	1.36 ± 0.02	P		180.28 ± 10.81	1.61 ± 0.01	[198]
L-Threonine propyl ester	0.84 ± 0.00	P		352.17 ± 6.07	3.20 ± 0.06	[198]
L-Threonine isopropyl ester	-	P		381.11 ± 6.07	3.21 ± 0.07	[198]
L-Threonine butyl ester	0.95 ± 0.00	P		313.68 ± 15.15	2.87 ± 0.63	[198]
L-Methionine propyl ester	1.33 ± 0.01	P		223.60 ± 6.42	2.09 ± 0.07	[198]
L-Methionine isopropyl ester	-	P		211.47 ± 3.74	2.14 ± 0.04	[198]
L-Methionine butyl ester	1.62 ± 0.01	P		214.68 ± 2.15	2.01 ± 0.02	[198]
-	2.36 ± 0.03	P	70:30 ethanol: water (v/v) [1%] (1mL)	112.90 ± 18.20	1.10 ± 0.18	[204]
Glycine isopropyl ester	0.24 ± 0.02	P		166.30 ± 27.10	1.70 ± 0.27	[204]
L-Leucine isopropyl ester	1.00 ± 0.00	P		130.30 ± 21.90	1.30 ± 0.22	[204]
L-Serine isopropyl ester	0.44 ± 0.01	P		186.30 ± 6.80	1.90 ± 0.07	[204]
L-Proline isopropyl ester	0.92 ± 0.04	P		246.40 ± 20.20	2.5 ± 0.20	[204]
-	-	H	Pcream [1%] (1g)[1]	339.70 ± 16.30	0.33 ± 0.02	[205]
L-prolinium isopropyl ester	-	H		791.20 ± 83.80	0.79 ± 0.08	[205]

[1.] Pentravan® cream, with 10% ethanol, 1% drug,1g applied (Pcream [1%] (1g))

Table 4. 24 Permeation Data using porcine (P) or human (H) skin for IBU and its IL complexes. Adapted from [192], MDPI, 2022; [198], Science Direct, 2023; [200], MDPI, 2021, [201] MDPI, 2021, [202], RSC, 2022; [203], MDPI, 2023.

Counterion	Log P/D	Mem-brane	Form-ulation	CP (μg/cm²)	% applied that permeated	Ref
-	2.42 ± 0.00	H	Pcream [5%](1g)	617.26 ± 13.99	-	[200]
		H	Hgel [5%](1g)	429.67 ± 60.15	-	[201]
L-Valine methyl ester	0.84 ± 0.01	H	Pcream [5%](1g)	547.90 ± 57.80	-	[200]
		H	Hgel [5%](1g)	696.68 ± 79.91	-	[201]

L-Valine ethyl ester	0.99 ± 0.00	H	Pcream [5%](1g)	698.43 ± 17.29	-	[200]
		H	Hgel [5%](1g)	611.44 ± 24.92	-	[201]
L-Valine isopropyl ester	1.25 ± 0.01	H	Pcream [5%](1g)	725.31 ± 19.79	-	[200]
		H	Hgel [5%](1g)	790.53 ± 41.43	-	[201]
L-Valine propyl ester	1.15 ± 0.00	H	Pcream [5%](1g)	803.35 ± 39.18	-	[200]
		H	Hgel [5%](1g)	682.20 ± 29.91	-	[201]
L-Valine butyl ester	1.52 ± 0.00	H	Pcream [5%](1g)	693.59 ± 37.45	-	[200]
		H	Hgel [5%](1g)	684.54 ± 5.60	-	[201]
L-Valine pentyl ester	1.75 ± 0.00	H	Pcream [5%](1g)	510.01 ± 27.91	-	[200]
		H	Hgel [5%](1g)	443.25 ± 49.60	-	[201]
L-Valine hexyl ester	1.75 ± 0.00	H	Pcream [5%](1g)	342.34 ± 20.44	-	[200]
		H	Hgel [5%](1g)	263.96 ± 36.70	-	[201]
L-Valine heptyl ester	2.00 ± 0.00	H	Pcream [5%](1g)	287.63 ± 18.27	-	[200]
		H	Hgel [5%](1g)	246.07 ± 27.52	-	[201]
L-Valine octyl ester	2.12 ± 0.00	H	Pcream [5%](1g)	195.64 ± 24.64	-	[200]
		H	Hgel [5%](1g)	206.49 ± 50.09	-	[201]
-	3.21	P	70:30 ethanol: water (v/v) [5%] (1mL)	133.35	9.33	[202]
L-Histidine propyl ester	0.96	P		335.13	7.90	[202]
L-Phenylalanine propyl ester	1.02	P		454.86	15.80	[202]
L-Tyrosine propyl ester	1.06	P		284.27	9.51	[202]
L-Tryptophan propyl ester	1.04	P		319.22	12.42	[202]
-	3.21 ± 0.00	P	PBS pH 7.4 saturated	32.00 ± 2.80	7.41 ± 0.65	[192]
Glysine isopropyl ester	0.65 ± 0.01	P		375.84 ± 12.18	7.86 ± 0.26	[192]

L-alanine isopropyl ester	0.72 ± 0.00	P	solution (1 mL)	350.10 ± 11.04	6.79 ± 0.21	[192]
L-valine isopropyl ester	1.15 ± 0.00	P		386.39 ± 31.67	13.70 ± 1.12	[192]
L-isoleucine isopropyl ester	1.65 ± 0.01	P		94.51 ± 4.79	2.32 ± 0.12	[192]
L-leucine isopropyl ester	1.39 ± 0.00	P		230.82 ± 4.92	11.08 ± 0.24	[192]
L-serine isopropyl ester	0.78 ± 0.01	P		445.22 ± 20.23	11.04 ± 0.50	[192]
L-threonine isopropyl ester	1.00 ± 0.00	P		400.94 ± 17.92	11.29 ± 0.51	[192]
L-cysteine isopropyl ester	1.43 ± 0.01	P		305.76 ± 28.03	12.21 ± 1.12	[192]
L-methionine isopropyl ester	1.51 ± 0.00	P		262.64 ± 12.38	9.57 ± 0.45	[192]
L-aspartic acid isopropyl ester	1.51 ± 0.00	P		395.80 ± 41.32	27.31 ± 2.85	[192]
L-lysine isopropyl ester	1.05 ± 0.02	P		528.64 ± 22.72	11.06 ± 0.48	[192]
L-lysine isopropyl ester*	1.06 ± 0.01	P		220.02 ± 9.81	10.62 ± 0.47	[192]
L-phenylalanine isopropyl ester	2.21 ± 0.03	P		355.09 ± 5.48	35.91 ± 0.54	[192]
L-proline isopropyl ester	1.05 ± 0.05	P		373.80 ± 10.38	15.66 ± 0.44	[192]
-	3.21 ± 0.00	P	70:30 ethanol: water (v/v) [1%] (1mL)	231.39 ± 11.92	2.22 ± 0.10	[198]
L-Valine propyl ester	1.25 ± 0.01	P		472.10 ± 50.04	4.67 ± 0.50	[198]
L-Valine isopropyl ester	-	P		455.67 ± 27.89	4.21 ± 0.26	[198]
L-valine butyl ester	1.52 ± 0.00	P		444.88 ± 72.86	4.40 ± 0.72	[198]
L-Isoleucine propyl ester	1.73 ± 0.01	P		398.54 ± 36.45	3.45 ± 0.32	[198]
L-Isoleucine isopropyl ester	-	P		416.68 ± 65.63	3.83 ± 0.60	[198]
L-Isoleucine butyl ester	1.78 ± 0.01	P		406.19 ± 11.92	3.73 ± 0.64	[198]
L-Threonine propyl ester	0.91 ± 0.02	P		480.29 ± 109.09	4.44 ± 0.74	[198]
L-Threonine isopropyl ester	-	P		529.05 ± 5.17	4.84 ± 0.64	[198]
L-Threonine butyl ester	1.21 ± 0.00	P		379.66 ± 86.71	5.01 ± 1.11	[198]

L-Methionine propyl ester	1.40 ± 0.01	P	355.83 ± 40.09	3.27 ± 0.26	[198]
L-Methionine isopropyl ester	-	P	375.33 ± 40.50	3.65 ± 0.31	[198]
L-Methionine butyl ester	2.22 ± 0.01	P	378.99 ± 99.90	3.49 ± 0.92	[198]
-	3.37 ± 0.00	P	75.00 ± 1.00	0.30 ± 0.04	[203]
L-Glutamic acid diethyl ester	2.37 ± 0.00	P	100.00 ± 1.00	0.57 ± 0.01	[203]
L-Glutamic acid dipropyl ester	2.38 ± 0.00	P	120.00 ± 4.00	0.51 ± 0.01	[203]
L-Glutamic acid diisopropyl ester	2.86 ± 0.01	P	203.00 ± 6.00	0.37 ± 0.02	[203]
L-Glutamic acid dibutyl ester	3.00 ± 0.01	P	109.00 ± 4.00	0.45 ± 0.03	[203]
L-Glutamic acid di-sec-butyl ester	3.19 ± 0.01	P	93.00 ± 12.00	0.46 ± 0.05	[203]
L-Glutamic acid dipentyl ester	2.46 ± 0.00	P	101.00 ± 12.00	0.58 ± 0.05	[203]

[1.] Pentravan® cream, with 10% ethanol, 5% drug,1g applied (Pcream [5%] (1g)); [2.] Hydrogel with Celugel® with 10% ethanol, 5% drug, 1g applied (Hgel [5%] (1g))

Table 4. 25 Permeation Data using porcine (P) skin for KETO and its IL complexes. Adapted from [198], MPDI, 2022.

Counterion	Log P/D	Mem-brane	Form-ulation	CP (μg/cm^2)	% applied that permeated
-	1.58 ± 0.01	P	70:30 ethanol: water (v/v) [1%] (1mL)	705.86 ± 6.37	6.75 ± 0.29
L-valine propyl ester	0.55 ± 0.02	P		944.50 ± 116.80	9.20 ± 1.14
L-valine isopropyl ester		P		821.45 ± 49.12	8.60 ± 0.33
L-valine butyl ester	1.00 ± 0.03	P		806.13 ± 28.38	7.73 ± 0.19
L-Isoleucine propyl ester	0.95 ± 0.01	P		823.17 ± 58.13	7.40 ± 0.67
L-Isoleucine isopropyl ester		P		742.45 ± 6.02	7.44 ± 0.06
L-Isoleucine butyl ester	1.18 ± 0.01	P		541.75 ± 38.90	5.09 ± 0.03
L-Threonine propyl ester	0.65 ± 0.03	P		1194.22 ± 56.28	12.16 ± 0.57
L-Threonine isopropyl ester		P		815.96 ± 217.73	8.12 ± 1.84

L-Threonine butyl ester	0.88 ± 0.02	P		958.31 ± 54.24	8.86 ± 1.84
L-Methionine propyl ester	1.24 ± 0.02	P		758.33 ± 45.56	7.81 ± 0.40
L-Methionine isopropyl ester		P		837.56 ± 7.66	7.78 ± 0.41
L-Methionine butyl ester	1.55 ± 0.02	P		820.46 ± 61.39	8.41 ± 0.48

Table 4. 26 Permeation Data using porcine (P) skin for SA and its IL complexes. Adapted from [198], MDPI, 2022.

Counterion	Log P/D	Mem-brane	Form-ulation	CP (μg/cm^2)	% applied that permeated
-	1.32 ± 0.02	P	70:30 ethanol: water (v/v) [1%] (1mL)	2447.85 ± 21.73	22.90 ± 0.54
L-valine propyl ester	1.51 ± 0.03	P		2894.34 ± 177.31	24.35 ± 1.49
L-valine isopropyl ester		P		4961.43 ± 285.73	44.73 ± 2.58
L-valine butyl ester	1.85 ± 0.02	P		3445.34 ± 444.43	31.41 ± 4.05
L-Isoleucine propyl ester	1.61 ± 0.01	P		3207.09 ± 224.16	30.77 ± 2.15
L-Isoleucine isopropyl ester		P		2959.26 ± 399.32	28.56 ± 3.85
L-Isoleucine butyl ester	1.84 ± 0.02	P		4257.32 ± 159.24	42.61 ± 1.59
L-Threonine propyl ester	1.50 ± 0.04	P		4818.31 ± 547.94	46.16 ± 5.25
L-Threonine isopropyl ester		P		5924.99 ± 247.47	53.12 ± 1.67
L-Threonine butyl ester	1.75 ± 0.03	P		5295.79 ± 288.08	51.95 ± 2.83
L-Methionine propyl ester	1.83 ± 0.02	P		5208.20 ± 303.94	31.89 ± 1.45
L-Methionine isopropyl ester		P		5811.84 ± 166.61	57.15 ± 3.05
L-Methionine butyl ester	2.03 ± 0.02	P		5512.88 ± 292.16	50.75 ± 1.92

Table 4. 27 Permeation Data using porcine (P) skin for ferulic acid and its IL complexes. Adapted from [206], MDPI, 2022.

Counterion	Log P/D	Membrane	Applied	CP ($\mu g/cm^2$)
-	1.643 ± 0.003	Porcine	Etoh [1%] (1mL) [1]	368.57 ± 2.94
			Emul [1%](1g)[2]	104.93 ± 7.63
			Hgel [1%](1g)[3]	289.36 ± 38.50
Glycine propyl ester	0.582 ± 0.019	Porcine	Etoh [1%] (1mL) [1]	378.26 ± 2.29
			Emul [1%](1g)[2]	101.70 ± 26.47
			Hgel [1%](1g)[3]	268.16 ± 12.71
L-leucine propyl ester	0.454 ± 0.009	Porcine	Etoh [1%] (1mL) [1]	415.12 ± 8.71
			Emul [1%](1g)[2]	119.29 ± 19.72
			Hgel [1%](1g)[3]	267.48 ± 24.57
L-proline propyl ester	0.447 ± 0.022	Porcine	Etoh [1%] (1mL) [1]	427.00 ± 4.674
			Emul [1%](1g)[2]	128.80 ± 19.86
			Hgel [1%](1g)[3]	396.86 ± 42.13

[1]70:30 ethanol: water (v/v) 1% concentration,1mL applied: Etoh [1%] (1mL); [2]Emulsion 1% concentration,1g applied: Emul [1%] (1g); [3]Hydrogel 1% concentration,1g applied: Hgel [1%] (1g)

4.8.2 Conclusion

These studies have demonstrated significant advances in the field of ion pairs. Notably, spectroscopic techniques have been employed to elucidate ion-ion interactions in ways not previously seen in ion pair studies meeting the criteria of this review. Additionally, computational modelling has identified how compounds with high energetic compatibility foster strong ion pairing and facilitate partitioning into lipophilic membranes.

The synthesis of salt forms or isolated ion-pair complexes can aid mechanistic elucidation, as they allow molecular interactions to be characterised more precisely using spectroscopic techniques such as FT-IR or NMR. However, it is important to

recognise that salt formation between an API and a counterion does not necessarily imply ion-pair formation in solution, as not all salts exhibit the electrostatic interactions required for ion pairing in this context. Consequently, evaluating the distribution coefficient at various ratios of the interacting species offers a more practical means of assessing ion-pair potential in solution.

Whilst new salt forms, whether classified as ILs, DESs or otherwise, eliminate extraneous counterions from formulations, the derivatisation of chemical structures and formation of molecular complexes create novel chemical entities. Regulatory approval for these new entities is resource-intensive and time-consuming. This raises the question of whether the same permeation enhancement could be achieved through simpler means. A comparison of individual ions combined in a formulation versus preformed ion-pair complexes would be valuable to determine whether co-formulation alone is sufficient, or whether complexation or derivatisation is necessary to achieve the desired permeation enhancement.

Despite these advances, significant methodological limitations remain. All of the studies reported here applied infinite doses of their formulations, with none progressing to finite dose application. This is particularly notable given that some research groups developed gels and creams intended for topical application, where finite dosing would reflect actual use conditions. Furthermore, whilst some studies quantified the amount of active extracted from the membrane, none presented complete mass balance calculations; explicitly identifying the amount applied, the amount remaining on the skin surface, the amount extracted from the membrane, the amount that permeated and the total percentage recovered. These omissions limit the ability to fully assess the efficiency and fate of the formulations.

5 Methodology

5.1 Overview of methodological approach

The experimental work described in this thesis was designed to systematically investigate and optimise the percutaneous delivery of diclofenac through the application of ion pairing as a passive permeation enhancement strategy. The methodological framework comprised three main parts. The first (i) involved the identification of suitable counter-ions for ion-pair formation. Following the selection of an appropriate counter-ion, the research adopted an iterative process alternating between (ii) formulation development and, (iii) *in vitro* permeation testing (IVPT). The selected counter-ion was first incorporated into basic aqueous formulations and tested using IVPT. Based on these findings, binary solvent systems were formulated and evaluated, after which alternative solvent systems were explored and tested. Finally, ternary solvent systems were developed and subjected to IVPT. This iterative cycle enabled data-driven optimisation at each stage, ensuring that subsequent formulation steps were guided by prior experimental outcomes.

Detailed experimental protocols for all analytical methods are presented in the experimental papers contained in Chapters 6-8. The following sections provide an overview of the key methodological approaches employed.

5.2 Analytical methods

5.2.1 HPLC method development and validation

Multiple compendial methods are available for the identification and quantification of diclofenac (DF), its salts, and associated pharmaceutical formulations, including the official procedure outlined in the British Pharmacopoeia. [213]. The literature also contains various alternative analytical approaches [214-219]. For this study, a single, comprehensively validated HPLC method was developed and employed to quantify diclofenac across all experimental conditions. The method was selected for its ability to detect DF in various salt forms and formulations, making it suitable for the diverse experimental requirements of this research. This method is described in detail in the first experimental paper [220] (Chapter 6), and was used consistently throughout all subsequent work.

An absorption spectrum of DNa was obtained using a Jenway 7315 UV/Vis spectrophotometer (Fisher Scientific, UK) across the range 200 – 800 nm. DNa was dissolved in the mobile phase (acetonitrile (ACN) and 0.1% trifluoroacetic acid (TFA) in water, 70:30 v/v). For HPLC quantification, a wavelength of 277 nm, corresponding to DF's second highest absorption peak, was selected. The maximum absorption wavelength (λ max) at 222 nm was not used, as methanol, a solvent employed for dilution and extraction, exhibits significant absorption between 210 - 250 nm (0.05 - 0.26 absorbance). Additionally, potential counterions also absorbed most strongly in this region, as shown in Appendix A. To minimise potential spectroscopic interference from methanol or counterions, 277 nm was adopted as the quantification wavelength.

The method employed an Agilent 1100 HPLC system equipped with a G1379A degasser, G1311A quaternary pump, G1313A autosampler, and G1316 thermostat column compartment. Data acquisition and analysis were performed using ChemStation® for LC 3D, Rev. A.09.03 (Agilent Technologies, USA). Separation was achieved using a Shiseido CAPCELL PAK C18 MGIII column (250 × 4.6 mm, 5 µm particle size, 100 Å pore size). The column was protected by a universal HPLC guard column (Phenomenex, UK) fitted with a SecurityGuard™ C18 cartridge (Phenomenex, UK). An injection volume of 10 µL and a flow rate of 1 mL/min were used at 25°C.

The method was validated in accordance with ICH (2005) guidelines for linearity, accuracy, precision, robustness, limit of detection (LOD), and limit of quantification (LOQ) [221]. Fresh calibration curves were prepared for each experimental session. Comprehensive method validation data are presented in Appendix A.

5.2.2 Solubility studies and solvent characterisation

Solubility parameters (SP) of solvents were determined using the Van Krevelen and Hoftyzer method incorporated within the Molecular Modelling Pro software (version 7.0.8). For multi-component solvent systems, SP calculations were based on volume fractions as described by equations included in experimental papers 2 [222] (Chapter 7) and 3 [223] (Chapter 8). Single solvent solubility studies employed standardised protocols with excess drug in individual solvents, maintained at 32 ± 1°C for 48 hours with continuous stirring, followed by centrifugation and HPLC analysis [222] (Chapter 7).

5.2.3 Additional analytical techniques

Supporting analytical methods were selected to provide complementary structural and physicochemical information. ^{1}H NMR spectroscopy confirmed successful synthesis of diclofenac free acid through characteristic carboxylic acid protonation signals [220] (Chapter 6), while FT-IR spectroscopy validated ion pair formation through spectral shift analysis [223] (Chapter 8). Miscibility studies employed visual inspection with methylene blue as an indicator [222, 223] (Chapters 7 & 8).

5.2.4 Quality assurance principles

Quality assurance protocols were implemented to ensure experimental consistency and reliability. A single validated HPLC method was applied across all experimental conditions to enable reliable quantification and meaningful inter-study comparisons. Standardised protocols were employed for skin preparation, IVPT procedures, sample handling, and mass balance studies [220] (Chapter 6) to minimise experimental variability. Control formulations without counter-ion were included in all experiments to provide baseline comparisons for evaluating ion-pairing effects [220, 222, 223] (Chapters 6 – 8).

5.3 Counterion identification and selection

The initial phase established a framework for counter-ion selection based on three critical criteria: (i) non-toxic profile suitable for topical application (ii) opposite charge to diclofenac at physiological pH (7.3 ± 0.2), and (iii) appropriate molecular size as smaller counter-ions are more likely to form ion pairs and reduce steric hindrance effects. The importance of molecular size was established by Bjerrum, who identified size as a factor influencing the association or dissociation of ion pairs [46], and was later confirmed by Fini *et al.* in their work examining ion pair formation of diclofenac salts in aqueous solutions [23]. Counter-ions meeting these criteria were then systematically evaluated using distribution coefficient studies between octanol and phosphate buffered saline, as detailed in the first experimental paper [220] (Chapter 6).

These specific experiments were undertaken using a pH of 7.3 ± 0.2 to mimic physiological pH. The isoelectric points (i.e., the pH at which the amino acids have no net electric charge) were higher for all potential counterions, thus ensuring ionisation

at and below this pH. While these studies were referred to as "partition coefficient studies" following nomenclature from the ion pair literature review [45] (Chapter 4), they more accurately represent distribution coefficient measurements given the pH conditions employed. L-histidine monochloride monohydrate (LHSS) emerged as the optimal counter-ion through this screening process, demonstrating superior ability to enhance drug transfer from aqueous to organic phases when used in conjunction with diclofenac sodium. It was therefore selected for subsequent IVPT in conjunction with DNa.

Distribution coefficient studies were a rapid, reliable predictor of ion pair formation potential, subsequently validated through IVPT [220, 222, 223] (Chapters 6 – 8).

5.4 Solvent system development and optimisation

The initial formulations tested comprised simple aqueous preparations (pH 7.3 ± 0.2) [220] (Chapter 6). These revealed a critical formulation challenge: DNa is sparingly soluble in water, the only solvent in which LHSS dissolves. Increasing the concentration of the counter-ion to match the ratios of the distribution coefficient studies led to precipitation. This necessitated the systematic development of multi-component solvent systems that could accommodate both drug and counter-ion while maintaining optimal thermodynamic activity for skin permeation.

The solvent development strategy progressed through increasingly sophisticated formulations:

5.4.1 Single solvent screening:

The solubility of DNa in various pharmaceutical excipients was tested [222] (Chapter 7), taking in account solubility parameter theory in an attempt to experimentally ascertain a solubility parameter value for the diclofenac salt.

5.4.2 Development of binary solvents systems

Binary solvent systems were prepared by combining water with one of three non-aqueous solvents in which DNa exhibited the highest solubility (Transcutol® (TC), dipropylene glycol (DiPG) or propylene glycol(PG)). The solvent ratios ranged from 10% to 90% (v/v) of the non-aqueous component, in 10% increments. Each combination was tested with DNa at concentrations of 5, 7.5, and 10 mg/mL, and LHSS at concentrations of 0, 10, 12.5, and 25 mg/mL [222] (Chapter 7).

After stability testing [222] (Chapter 7), various TC:water combinations were selected from formulations that exhibited no visible precipitation and remained physically stable. These were used to evaluate the ion pair, with the aim of investigating the optimal balance between solubility and the thermodynamic activity of the active within the formulation.

The effect of solvent substitution was then evaluated using a stable formulation identical in all respects to a selected TC:water formulation, except that TC was replaced with DiPG. This design allowed the specific influence of solvent identity on formulation performance to be isolated and assessed [223] (Chapter 8).

5.4.3 Ternary system exploration

Three-component solvent systems were developed to further optimise DF permeation. These comprised a combination of water with two of the non-aqueous solvents selected from those exhibiting the highest DNa solubility (TC, DiPG, and PG [223] (Chapter 8). The minimum water requirement was established at 50% v/v based on prior IVPT results using binary solvent formulations. This aqueous fraction ensured sufficient LHSS solubility, while enhancing the thermodynamic activity of DNa in the formulation.

Ternary combinations were systematically evaluated across different solvent ratios while maintaining the 50% v/v water content. The remaining 50% v/v was apportioned between the two non-aqueous solvents in various ratios to identify optimal compositions for drug delivery. Following preparation, all ternary formulations underwent stability testing prior to permeation evaluation [223] (Chapter 8). Only formulations demonstrating stability over the required timeframe, with no visible precipitation, were chosen for IVPT studies.

This approach enabled the identification of ternary systems that balanced multiple competing factors: DNa solubility, LHSS incorporation, thermodynamic activity and formulation stability, ultimately leading to optimised formulations for enhanced percutaneous delivery.

5.5 Percutaneous delivery performance evaluation

The initial aqueous formulations, as well as binary and ternary formulations developed in section 1.4, were evaluated using IVPT [220] (Chapter 6). Full thickness porcine ear

skin served as the membrane, selected as the closest available model for human skin [95, 96, 224]. Skin preparation, storage and use procedures followed standardised protocols and handling procedures [220] (Chapter 6). After the preliminary studies [220] (Chapter 6), finite doses (10 µL) were applied to mimic realistic clinical application conditions in accordance with OECD guidelines [225]. Franz diffusion cells with a diffusion area of approximately 1 cm² were used. The receptor compartment was filled with phosphate buffered saline (pH 7.3 ± 0.2). Following the first experimental paper, the receptor medium was optimised with Brij™ O20, to maintain sink conditions. The analyte stability within the receptor medium was confirmed over the experimental timeframe (Appendix B). Diffusion cells were maintained in a water bath preheated to ~ 37°C to achieve a skin surface temperature of 32 ± 1°C throughout permeation studies. Samples were collected at predetermined intervals over 24-25 hours.

Mass balance studies were conducted at the conclusion of each permeation [220] (Chapter 6) to determine drug distribution: whether it remained on the surface of the membrane, within the membrane or within the receptor solution. One modification to work after the first experimental paper was a change to the solvent used for washing and extraction. Instead of methanol alone, a methanol: water mixture (85:15 v/v) was employed, as it was found to provide superior solubility for DNa [226].

Evaluation of the initial aqueous formulations using IVPT with mass balance studies informed the development of binary solvent combinations. Evaluation of selected binary formulations in turn guided the development of ternary formulations. The IVPT and mass balance experiments also enabled comparisons between formulations, facilitated optimisation, and allowed benchmarking of these basic formulations against a more sophisticated commercial formulation.

5.6 Data analysis and statistical methods

Data analysis approaches were adapted to the specific requirements of each experimental phase. Descriptive statistics (mean ± standard deviation) were calculated for all quantitative measurements. Normality of data distribution was assessed using the Shapiro-Wilk test. For parametric data, statistical significance was evaluated using one-way analysis of variance (ANOVA) with Tukey's *post hoc* test for multiple comparisons, or independent-samples *t*-test for two-group comparisons. Non-

parametric data were analysed using the Kruskal-Wallis test with multiple pairwise comparisons or the Mann-Whitney U test for two groups. Statistical significance was set at $p < 0.05$. Detailed statistical analyses and specific software applications are described in the individual experimental papers [220, 222, 223] (Chapters 6-8).

6 A preliminary investigation into the use of amino acids as potential ion pairs for diclofenac transdermal delivery

6.1 Overview

“A Preliminary Investigation into the Use of Amino Acids as Potential Ion Pairs for Diclofenac Transdermal Delivery “ was published on 16 June 2022 in the International Journal of Pharmaceutics (623:121906, https://doi.org/10.1016/j.ijpharm.2022.121906). The co-authors and their contributions were as follows:

Cristofoli, Mignon: conceptualisation, methodology, validation, investigation, formal analysis, visualisation, writing - original draft and amendments; Hadgraft, Jonathan: conceptualisation, writing – review and editing; Lane, Majella, E.: conceptualisation, resources, supervision, writing: review and editing; and Sil, Bruno C.: conceptualisation, resources, supervision, writing: review and editing.

Addressing objectives 2.1.2.4 - 2.1.2.7, this chapter focused on establishing the foundational understanding of ion pair formation with diclofenac. The work involved characterising both diclofenac free acid (DFA) and diclofenac sodium (DNa), identifying suitable amino acid counterion candidates based on established selection criteria of size, toxicity and charge compatibility. Distribution coefficient studies were conducted to assess the partitioning behaviour of DFA and DNa between aqueous and organic phases in the presence of selected amino acids at varying concentrations. Finally, the most promising amino acid counterion combinations were evaluated using both finite and infinite dose porcine skin permeation studies to determine their potential for enhancing transdermal delivery. This chapter provides essential groundwork for the subsequent experimental work in Chapters 7 and 8.

6.2 Abstract

Ion pairing is a potential strategy used to increase the partition and permeation of ionisable drug molecules. This work outlines the process of identifying, selecting and testing potential counter ions for diclofenac (DF). Three screening criteria were considered in the initial selection process. The first, toxicity, was used to eliminate counter ion candidates that could not be used in topical formulations. The second related to the balancing of charges. As DF is a free acid in its unionised state, counter ions should be of a basic character. Finally, molecular size, as represented by molecular mass (Da), was used. Because of the impact on ion pair formation, the counter ion was required to have a lower molecular weight than diclofenac. Basic amino acids L-Arginine, L-Histidine, L-Lysine and their salts were chosen. The selection process concluded with Partition Coefficient (PC) studies. These were used to identify any counter ions able to interact electrostatically with the ionised DF, enabling the 'neutral' ion pair to partition from an aqueous into an organic layer. Permeation studies using porcine skin were performed to test the efficacy of any selected counter ion. These preliminary studies suggest that amino acids may be used as counter ions to increase the partition and permeation of ionisable drugs.

Keywords: Ion pairs; Diclofenac; Diclofenac sodium; Amino acids**;** Partition coefficient studies; Porcine skin; Permeation; Mass balance

6.3 Introduction

The topical application of drugs provides many advantages, as evidenced in the case of non-steroidal anti-inflammatory drugs (NSAIDs). A study considering hospitalisation due to adverse drug reactions (ADR) found, in the case of prescribed drugs, that NSAIDs accounted for 30% of hospital admissions. Reactions included gastrointestinal bleeding, peptic ulceration, haemorraghic cerebrovascular accident and renal damage [5]. A similar study investigated ADRs requiring hospital admissions due to over-the-counter (OTC) medication or self-medication using previously prescribed drugs. It was determined that 30% of the adverse reactions were gastrointestinal complaints caused by NSAIDs [6]. It is unsurprising therefore that in cases of osteoarthritis, the National Institute for Health and Care Excellence (NICE) recommends offering a topical NSAID (and/ or paracetamol) ahead of any oral NSAIDs, COX-2 inhibitors or opioids [9].

However, as the uppermost layer of the skin, the *stratum corneum* (SC), provides a very effective barrier to any exogenous substances, numerous strategies have been explored to increase the permeation of active ingredients. These strategies can be divided into active or passive methods. Active methods, which include iontophoresis, phonophoresis and the use of microneedles, are categorised as physical techniques used to overcome the SC [34]. Passive methods are described as those that focus on the formulation itself, i.e. the active ingredient in combination with several excipients [38, 41]. These include increasing the thermodynamic activity of drugs in the formulation [38] , the use of skin penetration enhancers [42] and also the use of ion pairs [45].

As mentioned previously [45], ion pairing has been explored to both increase and regulate the passage of ionised drugs that are applied for topical or transdermal use. This preliminary study outlines the initial steps taken to identify and test potential counter ions for the NSAID diclofenac (DF), with the purpose of increasing the permeation of this active pharmaceutical ingredient (API).

The selection of prospective counter ions for DF involved several important considerations, the first being toxicity. An understanding of the toxicity of counter ions is critical, as they may co-partition with the API into the skin [48]. Thus, a prospective counter ion that would not be acceptable from a safety perspective should be disregarded. The second factor relates to the balancing of potential ionic charges. Because the DF molecule is a free acid in its unionised state (Figure 6.1), the counter ion should be a basic molecule. With a pK_a range reported from 3.8 – 4.2 [20, 21, 227-230], DF in solution is negatively charged at physiological pH. Counter ions should therefore be positively charged. The final consideration is related to the size of the molecule. Bjerrum [231], who introduced the concept of ion pairs, identified size as a factor that influenced the association or dissociation of ion pairs [46]. This was later confirmed by Fini *et al* in their work which examined the formation of ion pairs of diclofenac salts in aqueous solutions [23].

The basic amino acids L-Arginine, L-Histidine, L-Lysine and their salts (Figure 6.2), were selected as the potential counter ions. With reference to toxicity, the amino acids and their salts are generally recognised as safe (GRAS) when used as food additives by the FDA [49]. They have also been used as cosmetic ingredients according to information given to the FDA via the Voluntary Cosmetic Registration Program

(VCRP). Human Repeat Insult Patch Test Studies have concluded that products containing these ingredients resulted in no dermal irritation or sensitisation. The Cosmetic Ingredient Review panel after studying this information, considered them to be safe in present practices of use and concentrations in cosmetics [50].

In relation to charge, Table 1 shows that the isoelectric points, (pH (I) or p(I)), i.e. the points at which these amino acids have no net electrical charge, exceed the physiological pH. For L-histidine (L-His) the pI value of 7.6 was not much greater, but it increased with L-Lysine (L-Lys) having a pI value of 9.5 and L-Arginine (L-Arg) with a pI of 10.8.

Regarding size, Table 6.2 indicates that the molecular weight (Da) of DF (296.15 Da) exceeds that of L-His (155.16 Da), L-Lys (146.19 Da) and L-Arg (174.20 Da). For the purposes of clarity, Table 3 confirms that the molecular weight (Da) of diclofenac sodium (DNa) (318.10 Da) exceeds that of L-histidine hydrochloride monohydrate (L-HSS) (209.63 Da), L-Lysine monohydrochloride (L-LSS) (182.65 Da) and L-Arginine monohydrochloride (L-ASS) (210.66 Da). These values however, are more aligned to those of the free acid and free bases, due to dissociation of the ionic salts in solution.

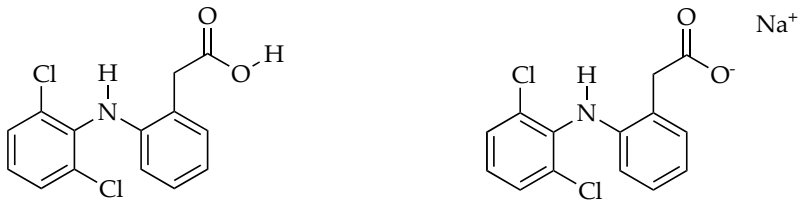

Figure 6. 1 Structures of diclofenac free acid and diclofenac sodium.

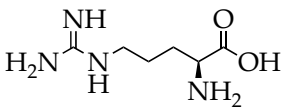

L-Arginine

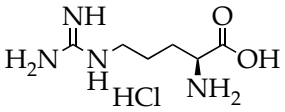

L-Arginine Monohydrochloride

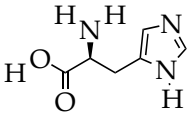

L-Histidine

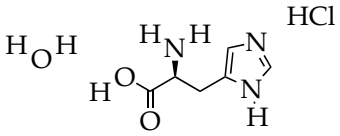

L-Histidine Hydrochloride Monohydrate

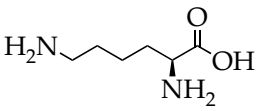

L-Lysine

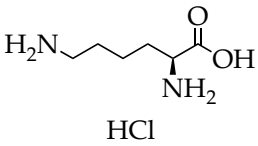

L-Lysine Monohydrochloride

Figure 6. 2 Structures of L-Arginine, L-Arginine Monohydrochloride, L-Histidine, L-Histidine Hydrochloride Monohydrate, L-Lysine and L-Lysine Monohydrochloride.

Table 6. 1 pK_a and pI values for DF, L-Arg, L-His and L-Lys

Compound	pKa	pI
Diclofenac free acid	4.2	N/A
L-Arginine	2.17, 9.04, 12.48	10.8
L-Histidine	1.82, 6.00, 9.17	7.6
L-Lysine	2.18, 8.95, 10.53	9.5

Table 6. 2 Molecular mass of DF, L-Arg, L-His and L-Lys.

Compound	Molecular mass (Da)
Diclofenac free acid	296.15
L-Arginine	174.20
L-Histidine	155.16
L-Lysine	146.19

Table 6. 3 Molecular mass of DNa, L-ASS, L-HSS and L-LSS.

Compound	Molecular mass (Da)
Diclofenac Sodium	318.10
L-Arginine Monohydrochloride	210.66
L-Histidine Hydrochloride Monohydrate	209.63
L-Lysine Monohydrochloride	182.65

The selection process concluded by testing whether the counter ion candidates could interact electrostatically with the DF anion, creating an ion pair. If successful, the apparently neutral species should be able to partition from an aqueous into an organic layer [155]. Simple partition coefficient (PC) studies, were used for this purpose. When an ion pair is formed, individual ions mask their charges through electrostatic interactions. While these experiments do not account for interactions of the molecules with biological membranes, different solvent systems and other extrinsic factors; they are useful as a screening mechanism to identify prospective ion pairs for permeation studies [156-159, 163, 164].

The aims of this work were (i) to determine the PC for DF (a) as the free acid, and in combination with the amino acid free bases and (b) as the salt form (DNa), as shown in Figure 6.1, and in combination with the amino acid salts. The combination achieving the highest PC values would then be used to (ii) investigate the effect on porcine skin permeation of DF using (a) a total amount of DF similar to that contained in a finite dose application of a 1% commercial DF-containing product (± 100 µg) and (b) a total amount of DF closer to that contained in an infinite dose application of a 1% commercial DF-containing product (± 350 µg).

6.4 Materials and methods

6.4.1 Materials

DNa 98% and the amino acids, L-Arg 98+% and L-Lys 98% were produced by Acros Organics (VWR, Leceistershire, UK). DF was synthesised and characterised in house. L-His high purity grade I was ordered from VWR (Leceistershire, UK). The amino acid salts L-ASS 98+% and L-LSS 99+% were obtained from Alfa Aesar and L-HSS 98% was from Acros Organics, all supplied by VWR (Leceistershire, UK)). High vacuum grease was obtained from Dow Corning (Seneffe, Belgium). Oxoid™ Phosphate buffered saline (PBS) tablets were purchased from Thermo Fisher Scientific (Lancashire, UK). HPLC grade acetonitrile (ACN), hydrochloric acid (HCl) (37%) and trifluoroacetic acid (TFA) were purchased from Fisher Scientific (Lancashire, UK). 1-Octanol 99% was obtained from Alfa Aesar (VWR, Leceistershire, UK). Ethanol 99.8% and 0.45 µm Millex® HV syringe filter units were supplied by Sigma Aldrich (Dorset, UK). Filter paper 150 mm diameter was obtained from Fisher Scientific (Lancashire, UK).

6.4.2 Methods

6.4.2.1 HPLC analysis

The analysis of diclofenac was performed using an Agilent 1100 HPLC. This was equipped with an Agilent G1379A degasser, a G1311A quaternary pump, a G1313A autosampler and a G1316A thermostat (Agilent Technologies, Santa Clara, CA, USA). The column used was a Shiseido CAPCELL PAK C18 MGIII, with a length of 250 mm, an internal diameter of 4.6 mm, a 5 µm particle size and 100 Å pore size (Osaka Soda, Osaka, Japan). A universal HPLC guard column (Phenomenex, Macclesfield UK) containing a SecurityGuard™ cartridge (Phenomenex, Macclesfield UK) was attached to the column. The mobile phase comprised acetonitrile (ACN):0.1% trifluoroacetic acid in water (70:30). The flow rate was 1 mL/min and the column temperature was set to 25 °C. A detection wavelength of 277 nm was chosen for the acquisition of chromatograms. The injection volume was 10 µL, with the DF peak eluting at 6 min and each sample having a total run time of 10 min. Calibration curves for the detection of diclofenac, ranging from 0.05 - 400 µg/mL were prepared using DNa. This method was validated in accordance with ICH (2005) guidelines [221] for linearity, accuracy, precision, robustness, limit of detection (LOD) and limit of quantification (LOQ). LOD was 0.12 µg/mL and LOQ was 0.37 µg/mL.

6.4.2.2 Synthesis of DF from DNa

A solution of DNa was prepared using distilled water. Various concentrations of HCl were made up, including 0.01 M, 0.5 M and 0.0001 M. HCl was slowly added dropwise to a stirring aqueous solution of DNa. At regular intervals, the pH of the solution was determined using a VWR SymPhony pH Meter (VWR, Leicestershire, UK). Once a ~ pH 4 was achieved, the solution was filtered, and the precipitate recovered. The precipitate was then washed three times using low pH (0.0001 M) HCl solution that had been maintained at a temperature of ± 8 °C. This was followed by drying using a desiccator for 24 h. Confirmation that the product, DF, had been synthesised from DNa (shown in Figure 6.S1), was obtained by use of ^{1}H-NMR. The appearance of a broad peak at approximately 12 – 13 ppm in Figure 6.S2 indicated the protonation of the carboxylic acid species confirming free acid formation.

6.4.2.3 Confirmation of the non-interference of amino acids with HPLC method for quantification of diclofenac

Absorption spectra (200 – 800 nm) were obtained for DNa, as well as the free base and salt forms of all potential amino acid counter ions, using a Jenway 7315 UV spectrophotometer (Cole-Parmer, Staffordshire, UK). Individual samples of the free bases and their salts using molar equivalent concentrations of 100 ug/mL of DF were run using the HPLC methodology described above. This was repeated after increasing the concentration of the counter ions by 50 times the previous amount. Samples containing known amounts of diclofenac with amino acids in 1:1 and 1:50 molar ratios were analysed using the HPLC method. The solvent mixture used to prepare all samples was ACN:H_2O (70:30). Solutions were filtered using a 0.45 µm Millex® HV syringe filter unit.

6.4.2.4 Measurement of partition coefficient (PC) between octanol and PBS (pH 7.3 ± 0.2)

The PCs for DF alone and with free base versions of the potential counter ions (L-Arg, L-His and L-Lys) were investigated using the counter ions at the molar ratios 1:0; 1:0.5; 1:1; 1:5; 1:10 and 1:50. As the free acid is only slightly soluble at pH 7.4 [232], DF was dissolved in ethanol. Octanol saturated PBS was added to the ethanol solution resulting in an ethanol:PBS (20:80 v/v) aqueous phase having a DF concentration of 100 µg/mL. This was divided between 6 vials, containing different concentrations of counter ions resulting in the final molar ratios of DF:amino acid 1:0; 1:0.5; 1:1; 1:5; 1:10 and 1:50. Equal amounts of the aqueous phase and PBS saturated octanol were added to screw topped glass tubes (n=3). These were sealed with Parafilm™ and shaken overnight on a Stuart Orbital Incubator S150 (Cole-Parmer, Staffordshire, UK) at 25 °C at 225 RPM. Samples were then centrifuged at 3000 RPM for 20 min at 25 °C. The PC for each combination of free acid: free base was calculated using Equation 6.1:

Equation 6. 1 Calculation of partition coefficient.

$$P_c = \frac{(C_i - C_f)}{C_f}$$

Where C_i represents the initial concentration of DF in the aqueous phase before partitioning and C_f represents the concentration in the aqueous phase after partitioning. $C_i - C_f$ corresponds to the amount that has partitioned into the octanol phase.

The same experiment was repeated using DNa with the salt versions of the basic amino acids. In this set of experiments no ethanol was used, and the aqueous phase was octanol saturated PBS.

6.4.2.5 Preparation of PBS formulations for *in vitro* permeation studies (IVPS)

For the initial permeation study (IVPS-100) a stock solution of 107.41 µg/mL of DNa in PBS (pH 7.3 ± 0.2), equivalent to 100 µg/mL of DF in PBS, was prepared. L-HSS (0.0014 g) was added to a vial containing 20 mL of the stock solution resulting in a 1:1 ratio of DF:L-HSS. L-HSS (0.0707 g) was added to a second vial containing 20 mL of the stock solution resulting in a 1:50 ratio of DF:L-HSS. These were stirred overnight.

For the second permeation study (IVPS-350) a stock solution of 376 µg/mL of DNa in PBS (pH 7.3 ± 0.2), equivalent to 350 µg/mL of DF in PBS, was prepared. L-HSS (0.0024 g) was added to a vial containing 10 mL of the stock solution resulting in a 1:1 ratio of DF:L-HSS. L-HSS (0.1238 g) was added to a second vial containing 10 mL of the stock solution resulting in a 1:50 ratio of DF:L-HSS. These were stirred overnight.

The samples representing DNa alone (DNa:L-HSS (1:0)), DNa and L-HSS at a 1:1 molar ratio (DNa:L-HSS (1:1)) and DNa and L-HSS at a 1:50 molar ratio (DNa:L-HSS (1:50)) were tested to determine the amount of DF in solution at the time of application.

For IVPS-350, samples were also filtered to determine the amount in solution at time of application.

6.4.2.6 *In vitro* porcine skin permeation studies (IVPS)

Infinite dose IVPS were conducted using vertical glass Franz diffusion cells (Soham Scientific, Cambridgeshire, UK). The diffusion area for each Franz cell was approximately 1 cm^2, as calculated using digital calipers (Fisher Scientific). The number of replicate experiments was n = 4.

Full thickness porcine ear skin, obtained from a local abattoir, was selected as the closest model for human skin [95, 96, 224]. Upon receipt, the skin was separated from the underlying tissue, wrapped in aluminium foil and stored in the freezer at -20 °C.

Immediately prior to permeation, the skin was cut to size, excess hair was trimmed, rinsed in PBS (pH 7.3 ± 0.2) and dried using filter paper. The membrane was sandwiched between the donor and receptor compartments of the pre-greased Franz cells, which were then secured with a clamp. The receptor compartment of the clamped unit was filled with approximately 2 mL of PBS (pH 7.3 ± 0.2) and stirred using a Teflon™ coated magnetic micro stirrer bar. This was placed into a Grant Sub Aqua 26 water bath (Grant Instruments, Cambridgeshire, UK) preheated to ~ 37 °C, to achieve a skin surface temperature of 32 ± 1 °C. Once the temperature of the skin was confirmed, using a Digitron TM22 digital thermometer (British Rototherm Company Ltd, Port Talbot, UK), an unfiltered 1 mL dose of the formulations was applied to the donor compartment. The donor compartment was covered using Parafilm™. Samples of 200 µL were taken hourly for 6 h for IVPS-100 and for 7 h for the IVPS-350. A final sample was taken at 24 h for both studies. Equal volumes of PBS (pH 7.3 ± 0.2), maintained at the same temperature in the water bath, replaced the sample volumes taken. All samples were analysed using the previously described HPLC method.

6.4.2.7 Mass Balance Studies

At the end of each permeation experiment a mass balance study was undertaken. Any remaining solution in the donor compartment was removed and weighed. The membrane surface was washed with methanol (1 mL) three times and dried with a cotton bud. Franz cells were disassembled, and remaining DF was extracted from the membrane using methanol (1 mL). Wash and membrane samples were placed in an orbital shaker (Orbital Mini Shaker, VWR Leceistershire, UK) overnight at room temperature. The mass balance samples were centrifuged at 13 200 rpm for 15 min at room temperature. Aliquots (200 µL) of the supernatant were taken, diluted where necessary and analysed using HPLC.

6.4.2.8 Data Analysis

Each set of experiments comprised a minimum of three replicates. The mean and standard deviation (SD) were calculated using Microsoft Excel ® version 16.55 (Microsoft Corporation, Washington, US). SPSS Statistics® Version 28.0 (IBM, New York, US) was used to perform any additional statistical analysis. The normality of distribution of the data sets was determined using the Shapiro-Wilks test. For

parametric data, a one-way analysis of variance (ANOVA) combined with Tukey's post hoc test was used to determine the statistical significance between groups. For non-parametric data, the Kruskal-Wallis one-way ANOVA (k-samples) with multiple pairwise-comparisons was performed. A probability of $p < 0.05$ was considered statistically significant.

6.5 Results and discussion

6.5.1 Confirmation of the amino acids non-interference with HPLC method for quantification of diclofenac

Absorption spectra for DF indicated two peaks, the highest at 222 nm and the second highest, chosen for analysis, at 277 nm. The λ-max values for the amino acid free bases and salts were: L-Arg 228 nm, L-ASS 225 nm, L-His 222 nm, L-HSS 223 nm, L-Lys 223 nm and L-SS 221 nm. Absorption at 277 nm was negligible and this was confirmed using the HPLC method described above. No absorption at 277 nm occurred when individual samples of the free base and salt versions of the amino acids were run at molar equivalent concentrations of 100 ug/mL of DF or at 50 times that amount. When samples combining DF and amino acid free bases in 1:1 and 1:50 molar ratios were run, amounts of DF remained constant. The same result occurred when DNa was combined with the amino acid salts.

6.5.2 Measurement of PC between octanol and PBS (pH 7.3 ± 0.2)

The results of the PC studies are shown in Tables 6.4 and 6.5. The PC of DF alone (14.21 ± 0.36 - 15.24 ± 0.33) decreased with the addition of increasing amounts of L-Arg, L-His and L-Lys. The decrease in the PC for DF was minimal as increasing amounts of L-His were added. When a DF:L-His 1:50 molar ratio was achieved, the PC was 13.32 ± 0.21. This was not the case when L-Arg (6.88 ± 0.24) and L-Lys (7.61 ± 0.20) were added at 50 times the molar concentration of DF. The reduction in the PC for DF when L-Arg and L-Lys counter ions were added at 50 times the molar ratio of DF, was 50% or greater.

Salt combinations appeared to increase, rather than decrease, the PC of diclofenac. Combinations of DNa with 50 times molar ratios of L-ASS or L-LSS resulted in modest increases in the PC of DNa:L-HSS (1:0), of approximately 10%. The combination of DNa with L-HSS provided a much greater impact relative to the PC of DNa alone,

increasing it by more than 8-fold when a 50 times molar ratio of the counter ion was used. The DNa:L-HSS combination was therefore chosen for the preliminary IVPS.

Table 6. 4 PC studies for DF and amino acid free bases in different molar ratios (n=3; mean ± SD).

Molar ratio DFA:Counter ion	DF:L-Arg	DF:L-His	DF:L-Lys
	PC ± SD	PC ± SD	PC ± SD
1:0	14.36 ± 0.27	14.21 ± 0.36	15.24 ± 0.33
1:0.5	12.85 ± 0.07	14.60 ± 0.07	14.96 ± 0.07
1:1	12.97 ± 0.26	14.42 ± 0.18	14.44 ± 0.15
1:5	8.58 ± 0.09	14.14 ± 0.23	10.33 ± 0.10
1:10	7.36 ± 0.06	14.41 ± 0.14	8.71 ± 0.15
1:50	6.88 ± 0.24	13.32 ± 0.21	7.61 ± 0.20

Table 6. 5 PC studies for DNa and amino acid salts in different molar ratios (n=3; mean ± SD).

Molar ratio DFA:Counter ion	DNa:L-ASS	DNa:L-HSS	DNa:L-LSS
	PC ± SD	PC ± SD	PC ± SD
1:0	15.33 ± 0.27	14.79 ± 0.31	17.97 ± 0.24
1:0.5	15.34 ± 0.41	16.51 ± 0.14	17.98 ± 0.20
1:1	15.38 ± 0.26	17.27 ± 0.18	17.28 ± 0.20
1:5	15.78 ± 0.13	28.72 ± 0.40	18.09 ± 0.09
1:10	15.85 ± 0.33	45.24 ± 2.76	18.18 ± 0.18
1:50	17.00 ± 0.45	121.43 ± 14.56	19.92 0.26

6.5.3 *In vitro* porcine skin permeation studies (IVPS)

6.5.3.1 IVPS-100

The concentration of DF in solution for the various formulations at the time of application was 99.63 ± 0.12 µg/mL (DNa:L-HSS (1:0)), 99.34 ± 0.38 µg/mL (DNa:L-HSS (1:1)), and 62.40 ± 0.41 µg/mL (DNa:L-HSS (1:50)). Formulations were applied unfiltered. No permeation was detected during the first six hours of sampling. As shown in Table 6. 6, at 24 h the permeation of DF from DNa:L-HSS (1:0) was comparable to that of DNa:L-HSS (1:1), namely 0.50 ± 0.20 µg/cm^2 and 0.54 ± 0.14 µg/cm^2, respectively ($p > 0.05$). The permeation from DNa:L-HSS (1:50) for the same time point was significantly higher at 5.39 ± 1.00 µg/cm^2 ($p < 0.05$). This amounted to approximately a 10-fold increase when assessed relative to the other formulations.

Likewise, when expressing cumulative permeation as a percentage (%) of the amount of DF originally detected in solution at application, there was very little difference between DNa:L-HSS (1:0) and DNa:L-HSS (1:1). These values were 0.51% and 0.54% respectively ($p > 0.05$). The value for DNa:L-HSS (1:50) was significantly higher at 8.7% ($p < 0.05$).

Figure 6.3 represents the amount (µg) of DF recovered from mass balance calculations for the various formulations. The figure distinguishes between DF retrieved through washing, extracted from the membrane, retrieved from the residual formulation in the donor compartment and the cumulative amount of DF that had permeated at 24 h.

The amounts detected in the membrane for DNa:L-HSS (1:0) and DNa:L-HSS (1:1) were 2.44 ± 0.59 µg and 2.10 ± 0.23 µg, respectively ($p > 0.05$). The amount detected in the membrane for DNa:L-HSS (1:50) was significantly higher at 8.61 ± 0.66 µg ($p < 0.05$).

Combining the amount of DF that permeated with the quantity extracted from the membrane, indicates the potential of the formulation to both partition into and permeate through the membrane. As shown in Table 6. 6, when represented as a percentage of the amount of DF in solution at the time of application, this amounts to 2.96% for DNa:L-HSS (1:0), 2.66% for DNa:L-HSS (1:1) and 22.5% for DNa:L-HSS (1:50).

DF recovered through washing and the formulation remaining in the donor compartment, amounted to 4.95 ± 1.39 µg and 92.10 ± 1.85 µg respectively for DNa:L-HSS (1:0). For DNa:L-HSS (1:1), washing accounted for 5.05 ± 3.44 µg and the remaining formulation amounted to 93.51 ± 1.32 µg DF. In the case of DNa:L-HSS (1:50) washing recovered 11.01 ± 1.22 µg while the remaining formulation comprised 60.86 ± 4.93 µg DF.

Total recovery of DF for DNa:L-HSS (1:0) was 100 ± 4.05 µg, for DNa:L-HSS (1:1) was 101 ± 5.17 µg and for DNa:L-HSS (1:50) was 85.90 ± 12.59 µg. While the recovery of DF for the first two formulations accounted for 100% and 102% of the amount in solution at the time of application, the result was much higher for the third formulation. Here, the unfiltered formulation delivered an amount of DF (85.90 ± 12.59 µg) to the donor compartments that exceeded the amount in solution at the time of application

(62.40 ± 0.41 µg). It was, however, less than the amount originally added to the formulation (100 µg). This total recovery result confirms that despite a reduced amount of DF having been applied (whether in solution or not), the use of the counter ion in a 1:50 molar ratio significantly increased the partition of DF into the membrane as well as the permeation of the drug, relative to formulations that comprised higher initial concentrations of DF, namely DNa:L-HSS (1:0) and DNa:L-HSS (1:1) .

Table 6. 6 (i) Amount of DF in solution at time of application (µg/mL) (ii) Amount of DF (µg/cm2) that permeated at 24 h after unfiltered solvents were applied and (iii) Amount of DF (µg) in membrane at 24 h (iv) Total amount of DF (µg) that permeated and in membrane at 24 h (n=4; mean ± SD).

Ratio DNa:L-HSS	Amount of DF in solution at time of application (µg/mL) ± SD	Permeation (µg/cm^2) ± SD at 24 h	Amount in membrane (µg) ± SD at 24 h	Total amount permeated and in membrane (µg) ± SD at 24 h
1:0	99.63 ± 0.12	0.50 ± 0.20	2.44 ± 0.59	2.95 ± 0.75
1:1	99.34 ± 0.38	0.54 ± 0.14	2.10 ± 0.23	2.64 ± 0.25
1:50	62.40 ± 0.41	5.39 ± 1.00	8.61 ± 0.66	14.04 ± 1.67

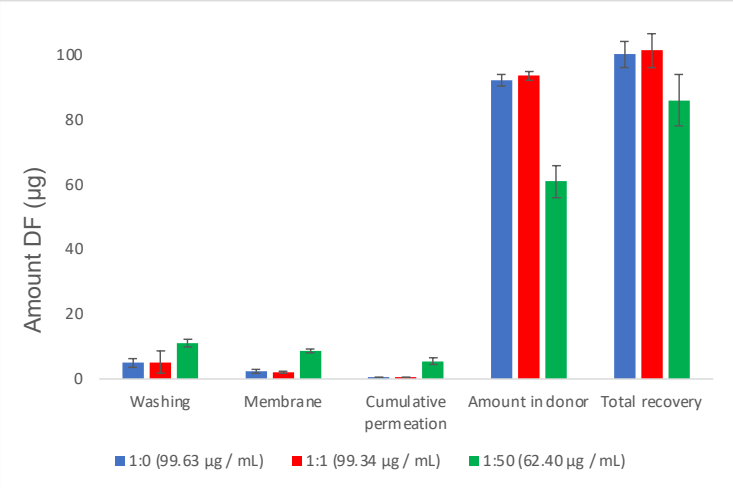

Figure 6. 3 Recovery of DF (µg) for the 3 formulations of DNa:L-HSS in the ratios 1:0, 1:1 and 1:50 following mass balance studies in porcine skin. Concentration of DF in formulations was 99.63 ± 0.12 µg/mL for DNa:L-HSS (1:0), 99.34 ± 0.38 µg/mL for DNa:L-HSS (1:1) and 62.40 ± 0.41 µg/mL for DNa:L-HSS (1:50) at time of application. Unfiltered formulations (1 mL) were applied. (n=4; mean ± SD).

6.5.3.2 IVPS-350

As shown in Table 6.7, the concentration of DF in solution for the various formulations at the time of application was 347.52 ± 0.18 µg/mL (DNa:L-HSS (1:0)), 318.94 ± 0.64 µg/mL (DNa:L-HSS (1:1)), and 9.52 ± 0.22 µg/mL (DNa:L-HSS (1:50)). The amount in solution for DNa:L-HSS (1:50) was far lower than when the equivalent of only 100 µg of DF was added. Formulations were applied unfiltered. Traces of DF were detected in receptor solutions for samples containing counter ions at 7 h. These were, however, below the limit of quantification. At 24 h, permeation from DNa:L-HSS (1:0) was 1.65 ± 0.57 µg/cm^2. This differed significantly from permeation values for both DNa:L-HSS (1:1) and DNa:L-HSS (1:50), which were 6.93 ± 2.97 µg/cm^2 and 6.91 ± 3.61 µg/cm^2, respectively ($p < 0.05$).

At 24 h, DNa:L-HSS (1:0) permeation was equivalent to 0.47% of the amount of DF in solution at application, comparable to IVPS-100 which showed 0.51% permeation. For the DNa:L-HSS (1:1) formulation, permeation appeared to increase to 2.17% compared with 0.54% for IVPS-100. In the case of the DNa:L-HSS (1:50) formulation, the cumulative amount of DF that permeated (6.91 µg) as a percentage of the amount that was in solution at the time of application (9.52 µg) was 72.55%. Despite the low amount in solution, the quantity of active that permeated was four times the amount that permeated for DNa without the presence of the counter ion.

Figure 6.4 shows the results of mass balance calculations for the various formulations. Amounts (µg) of DF recovered from washing, residual formulation in the donor compartment, cumulative permeation results (as discussed above), as well as amounts of DF detected in the membrane are presented.

The amounts of DF detected in the membrane for DNa:L-HSS (1:0), DNa:L-HSS (1:1) and DNa:L-HSS (1:50) were not significantly different at 10.01 ± 0.72 µg, 12.74 ± 3.32 µg and 13.46 ± 2.83 µg ($p > 0.05$).

The combination of the amount of DF that permeated together with the amount extracted from the membrane indicates the potential of the formulation to both partition into and to permeate through the membrane. As shown in Table 6.7, the total for DNa:L-HSS (1:0) amounts to 11.66 ± 0.38 µg. This is significantly lower ($p < 0.05$) than the comparable amounts of 19.67 ± 5.19 µg for DNa:L-HSS (1:1) and 20.37 ± 2.49 µg for DNa:L-HSS (1:50) ($p > 0.05$).

Washing and the amount of DF formulation remaining in the donor compartment for DNa:L-HSS (1:0) accounted for 10.75 ± 4.12 µg and 328.27 ± 9.66 µg of DF respectively. For DNa:L-HSS (1:1), washing accounted for 7.47 ± 1.09 µg and the remaining formulation contained 320.61 ± 8.05 µg of DF. In the case of DNa:L-HSS (1:50), washing recovered 36.87 ± 12.02 µg and the remaining formulation included 17.34 ± 0.67 µg DF.

Total recovery of DF for DNa:L-HSS (1:0) was 350.68 ± 6.59 µg, equivalent to the total amount applied, and slightly higher than the amount originally detected in solution (347.52 ± 0.18 µg). For DNa:L-HSS (1:1) the total amount recovered, 347.75 ± 2.82 µg, exceeded the amount in solution at the time of application (318.94 ± 0.64 µg). This suggested that the unfiltered DNa:L-HSS (1:1) formulation that was applied to the donor compartments of the Franz cells, contained a quantity of DF that was not in solution. The total recovery of DF for the final formulation, DNa:L-HSS (1:50), was 74.58 ± 11.33 µg, notably less than the 85.90 ± 12.59 µg recovered from the IVPS-100. Despite the low quantity retrieved, it greatly exceeded the amount detected in solution at the time of application, namely 9.52 ± 0.22 µg. Notwithstanding the exceptionally low amount of DF added to the donor compartments for DNa:L-HSS (1:50), both the amount of DF in the membrane and amount permeated are comparable to those DNa:L-HSS (1:1) where much higher quantities were applied. Furthermore, the use of the counter ion at both a 1:1 and 1:50 molar ratio significantly increased the combined partition of DF into the membrane and permeation of the drug, relative to the formulation that contained no L-HSS ($p < 0.05$).

Table 6. 7 (i) Amount of DF in solution at time of application (µg/mL) (ii) Amount of DF (µg/cm2) that permeated at 24 h after unfiltered solvents were applied and (iii) Amount of DF (µg) in membrane at 24 h (iv) Total amount of DF (µg) that permeated and in membrane at 24 h (n=4; mean ± SD).

Ratio DNa:L-HSS	Amount of DF in solution at time of application (µg/mL) ± SD	Permeation (µg/cm^2) ± SD at 24 h	Amount in membrane (µg) ± SD at 24 h	Total amount permeated and in membrane (µg) ± SD at 24 h
1:0	347.52 ± 0.18	1.65 ± 0.57	10.01 ± 0.72	11.66 ± 0.38
1:1	318.94 ± 0.64	6.93 ± 2.97	12.74 ± 3.32	19.67 ± 5.19
1:50	9.52 ± 0.22	6.91 ± 3.61	13.46 ± 2.83	20.37 ± 2.49

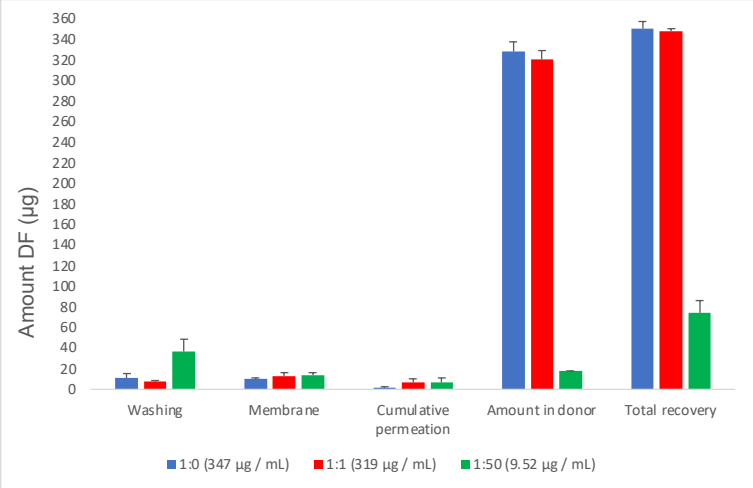

Figure 6. 4 Recovery of DF (µg) for the 3 formulations of DF:L-HSS in the ratios 1:0, 1:1 and 1:50 following mass balance studies in porcine skin. Concentration of DF in formulations was 347.52 ± 0.18 µg/mL for DNa:L-HSS (1:0), 318.94 ± 0.64 µg/mL for DNa:L-HSS (1:1) and 9.52 ± 0.22 µg/mL for DNa:L-HSS (1:50) at time of application. Unfiltered formulations (1 mL) were applied. (n=4; mean ± SD).

6.6 Conclusion

This study outlined the process of identifying, selecting and testing potential counter ions for DF. Screening criteria based on molecules of required charge, size and toxicity were used to identify potential counter ion candidates. This process was subsequently followed by PC studies which concluded the selection procedure. The results suggested that a combination of DNa and L-HSS were able to interact electrostatically within an aqueous solution, resulting in the masking of charges and enabling the partition of the apparently neutral species into an organic phase. This ion pair combination was tested using IVPS.

Despite a reduction in the solubility of DF as the amount of the counter ion increased, the IVPS clearly showed the potential indicated by the PC experiments to increase the partition of DF. Reduced amounts of DF both in solution and applied, as confirmed by mass balance studies, prevented an effective comparison of the impact of the counter ion. Notwithstanding, the addition of the counter ion increased both the ability of DF to partition into the membrane and to permeate through it. For IVPS-100, the amount of DF that permeated with the DNa:L-HSS (1:50) formulation was ~11 times greater than the amount that permeated without the counter ion. The amount of DF in the membrane was 3.5 times greater in the DNa:L-HSS (1:50) samples, than for DNa:L-HSS (1:0).

In relation to IVPS-350, the very low amount of DF applied to the DNa:L-HSS (1:50) samples resulted in less extreme differences in the results. The amount that permeated with the DNa:L-HSS (1:50) formulation was four times greater than the amount that permeated without the counter ion. The amount in the membrane was also 1.3-fold greater. This should, however, be considered in context. For the DNa:L-HSS (1:50) samples, only 9.52 ± 0.22 µg was in solution at the time of application and the total amount of DF applied was 74.58 ± 11.33 µg.

While a 1:1 DF:counter ion ratio may not be optimal, the effect of increasing solubility was outlined in IVPS-350, where DF:L-HSS (1:1) increased the amount in the membrane significantly (19.67 ± 5.19 µg), when compared with DF:L-HSS (1:0) (11.66 ± 0.38) ($p < 0.05$). As large quantities of L-HSS hindered the solubility of DNa, future work should consider different ratios of DNa:L-HSS to determine the efficacy of lower quantities of L-HSS. This could be done by performing additional PC studies using the DF:L-HSS molar ratios of 1:20; 1:30 and 1:40, to supplement the existing ones, namely 1:0; 1:0.5; 1:1; 1:5; 1:10 and 1:50. The impact of each increase on the gradient of a curve can be used to determine at what point increasing the amount of the counter ion reduces the rate at which the PC increases. Furthermore, solvent systems that facilitate the solubility of both DF and L-HSS require investigation and are on-going in our laboratory. This is being done with a view to creating simple solvent systems as potential precusors to topical formulations.

Because of the well-documented adverse effects of oral NSAIDs, topically-applied NSAID preparations are increasingly being used as alternatives. These investigations suggest a simple approach to identifying and selecting sustainable counter ions that may be used to increase the partition and permeation of a topically-applied NSAID. The use of ion pairs may therefore increase both the efficacy of formulations and/or result in a reduction in the amount of the active pharmaceutical ingredient being required. Moreover, the use of amino acids as potential counter ions not only satisfy toxicity requirements, but comply with the need to use renewable resources that are economical and have a low environmental impact.

6.7 Funding

This research received no external funding.

6.8 Conflicts of interest

The authors declared no conflict of interest.

6.9 Supplementary information

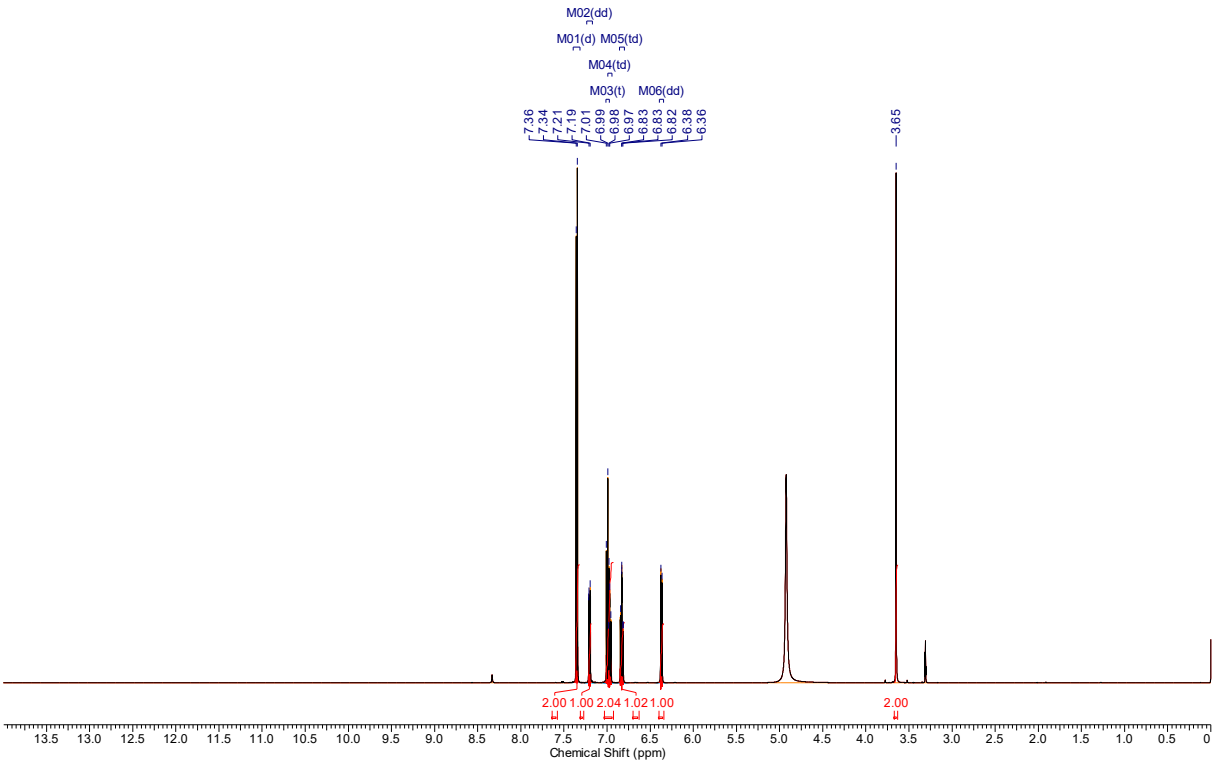

Figure 6.S 1 ^{1}H-NMR spectrum: diclofenac sodium

^{1}H NMR (500 MHz, METHANOL-d_4) d ppm 6.37 (dd, *J*=8.04, 1.10 Hz, 1 H) 6.83 (td, *J*=7.41, 1.26 Hz, 1 H) 6.97 (td, *J*=7.72, 1.58 Hz, 1 H) 6.99 (t, *J*=8.04 Hz, 1 H) 7.20 (dd, *J*=7.57, 1.26 Hz, 1 H) 7.35 (d, *J*=8.20 Hz, 2 H).

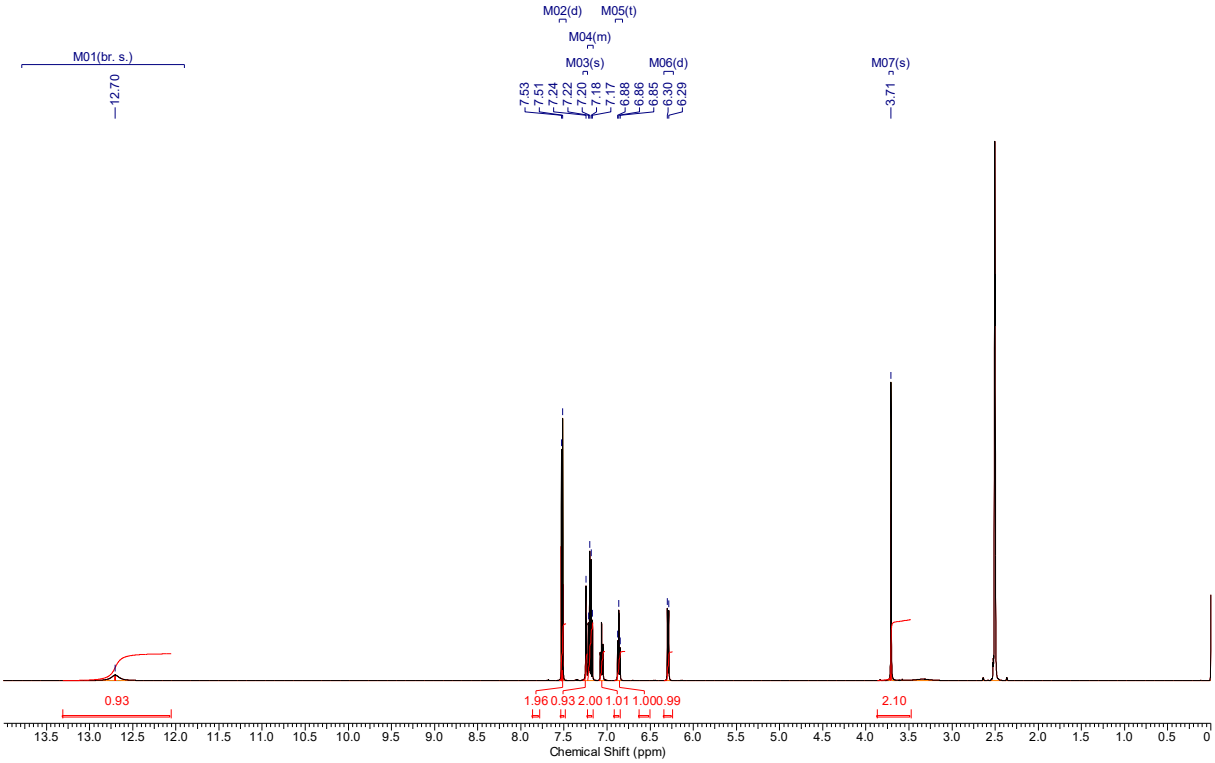

Figure 6.S 2 ^{1}H-NMR spectrum: diclofenac free acid

^{1}H NMR (500 MHz, DMSO-d_6) d ppm 3.71 (s, 2 H) 6.29 (d, *J*=7.88 Hz, 1 H) 6.86 (t, *J*=7.41 Hz, 1 H) 7.16 - 7.23 (m, 2 H) 7.24 (s, 1 H) 7.52 (d, *J*=7.88 Hz, 2 H) 12.70 (br. s., 1 H).

7 A model binary system for the evaluation of novel ion pair formulations of diclofenac

7.1 Overview

“A model binary system for the evaluation of novel ion pair formulations of diclofenac” was published on 9 April 2024 in the Royal Society of Chemistry: Pharmaceutics, Volume 1, Issue 2, pages 234 - 244, DOI:10.1039/D4PM00063C. The co-authors and their contributions were as follows:

Cristofoli, Mignon: conceptualisation, methodology, validation, investigation, formal analysis, visualisation, writing - original draft and amendments; Hadgraft, Jonathan: conceptualisation, writing; Lane, Majella, E.: conceptualisation, resources, supervision, writing: review and editing; and Sil, Bruno C.: conceptualisation, resources, supervision, writing: review and editing.

Addressing objectives 2.1.2.8 - 2.1.2.9, this chapter built upon the findings of Chapter 6 by tackling the solubility challenges associated with DNa-amino acid ion pair formulations. The work involved assessing DNa solubility across various solvents and identifying those miscible with water, the only solvent in which LHSS dissolves. A model binary system was then developed specifically for evaluating ion pair formulations of DNa and L-histidine hydrochloride monohydrate (LHSS), using porcine skin IVPT under finite dose conditions. This binary system formed the foundation from which alternative solvents were tested and from which ternary solvent systems were developed in Chapter 8.

7.2 Abstract

Diclofenac (DF) is well established as a topical treatment option for conditions such as osteoarthritis. In investigating novel DF ion pairs for topical delivery, studies to determine the impact of various amino acids on the distribution of DF between octanol

and aqueous environments were conducted. These studies identified the amino acid L-histidine hydrochloride monohydrate (LHSS) as an ion pair candidate for diclofenac sodium (DNa). Preliminary porcine skin permeation studies indicated that the addition of LHSS to DNa solutions increased the amount of DF that permeated through porcine skin. With increasing amounts of LHSS added, greater amounts of DF precipitated out of solution. In the present work, the solubility of DNa in various solvents was assessed, with the intention of identifying solvents in which DNa was most soluble. Binary systems comprising water and selected solvents were tested for both miscibility and the solubility of DNa and LHSS. The model system selected to evaluate novel ion pair formulations using porcine skin *in vitro permeation testing* under finite dose (10 µL) conditions comprised Transcutol® (TC) and water. The tested formulations contained DNa at concentrations of 5, 7.5 and 10 mg/ mL. Higher LHSS concentrations were possible when the DNa concentrations were lower and ranged from 10 – 25 mg/mL. However, increasing the DNa concentration to 10 mg/mL, with 10 mg/mL LHSS, resulted in a significant reduction in the amount of DF that partitioned and permeated, relative to formulations that contained either 5 mg/mL DNa in combination with LHSS (at 12.5 or 25 mg/mL), or 7.5 mg/mL DNa together with 12.5 mg/mL LHSS. The current work confirms previous investigations, suggesting that the addition of LHSS to DNa in a formulation may increase the partition and permeation of DF.

7.3 Introduction

Osteoarthritis (OA) is a painful and degenerative condition of the joints, affecting the hips, knees and hands. According to the Global Burden of Disease study, the condition affects approximately 7% of the world's population, amounting to more than 500 million people [7]. Direct costs associated with OA are estimated at 1 – 2% of the Gross National Product of countries with established market economies, including the UK, the USA, Canada and Australia [8]. Indirect costs such as the loss of productivity and early retirement, serve to exacerbate the already substantial economic implications.

Various organisations worldwide have published guidelines relating to the treatment of OA [233, 234]. In the UK, topical non-steroidal anti-inflammatory drugs (NSAIDs) are considered first-line pharmacological treatment options for OA, due to the adverse drug reactions associated with other options such as opioids and oral NSAIDs [9]. The European Society for Clinical and Economic Aspects of Osteoporosis, Osteoarthritis

and Musculoskeletal Diseases have strongly recommended the use of topical NSAIDs, particularly where so-called symptomatic slow-acting drugs such as chondroitin sulfate and prescription crystalline glucosamine sulfate, in conjunction with paracetamol, have not relieved the symptoms of OA [10]. In the US, the use of topical NSAIDs for the treatment of OA has been endorsed by the American College of Rheumatology in conjunction with the Arthritis Foundation [11] as well as the American Academy of Orthopaedic Surgeons [235]. The global organisation, Osteoarthritis Research Society International, have also strongly recommended the use of topical NSAIDs as a treatment option for OA of the knee [12]. As the most prescribed NSAID worldwide [19], it is unsurprising therefore that topical formulations using diclofenac (DF) are widely recognised as effective treatment options for OA [236]. Unfortunately, due to the efficacy of the barrier properties of the *stratum corneum*, only a small percentage of topically applied pharmaceutical salt preparations partition into the skin. Consequently, much of the applied pharmaceutical product never reaches its target site. Rational formulation design of topical DF products offers the potential for both economic savings as well as an opportunity to demonstrate commitment to reducing the environmental consequences of conscious formulation choices. This is consistent with the policies of many large pharmaceutical companies (such as Astra Zeneca [51], Novartis [52] and Roche [53, 54]) who are committed to reducing, where possible, the presence of pharmaceuticals in the environment.

Strategies to overcome the skin barrier are frequently categorised into two groups. The first comprises active or physical methods [26, 27] such as ionotophoresis [28-30], sonophoresis [31], microneedles [34-37], magnetophoresis [32] and electroporation [33]. The second consists of passive techniques that focus specifically on the formulation. Examples include increasing the thermodynamic activity of the active pharmaceutical ingredient [38-40, 138], the inclusion of various excipients as skin penetration enhancers [38, 42-44, 237] and the use of ion pairs to address ionised drug molecules [45].

Previously the amino acid L-histidine hydrochloride monohydrate (LHSS) was identified as an ion pair candidate for diclofenac sodium (DNa) [220]. This determination resulted from studies performed to investigate the impact of LHSS on the distribution of DF between octanol and aqueous environments. Experiments comprised DNa and LHSS in various ratios, namely 1:0.5; 1:1; 1:5, 1:10 and 1:50. The

results suggested that increasing the quantity of LHSS relative to DNa, would result in an increase in the amount of DF that partitioned into an organic medium. Preliminary porcine skin permeation studies confirmed that the addition of LHSS to DNa aqueous solutions also increased the amount of DF that permeated through porcine skin. The formulations used comprised DF at 100 µg/mL and 350 µg/mL. LHSS was either not included, for the purposes of a control (1:0) or added at 1:1 or 1:50 molar ratios. The more LHSS that was added, however, the more DF precipitated out of solution. This was particularly evident at the higher concentration of DF [220]. As LHSS is only soluble in water and DNa has very low solubility in water, a binary solvent system was developed. The aims of the present study, therefore, were to build upon the previous investigations [220] with two main objectives: (i) to address the issue of the solubility of both DNa and LHSS and (ii) to develop a model binary system to evaluate novel DNa:LHSS ion pair formulations, using porcine skin *in vitro permeation testing* (IVPT) under finite dose (10 µL) conditions.

7.4 Materials and methods

7.4.1 Materials

DNa 98% and the amino acid salt, LHSS, were supplied by VWR (Leicestershire, UK). High vacuum grease was obtained from Dow Corning (Seneffe, Belgium). Oxoid™ phosphate buffered saline (PBS) tablets were purchased from Thermo Fisher Scientific (Lancashire, UK). Filter paper, 150 mm diameter, as well as HPLC grade acetonitrile (ACN) and trifluoroacetic acid (TFA), were purchased from Fisher Scientific (Lancashire, UK). Propylene glycol was supplied by Merck Life Sciences (Poole, UK). Hexylene glycol, butylene glycol and dipropylene glycol were supplied by VWR (Leicestershire, UK). Isopropyl alcohol was purchased from Honeywell (Berkshire, UK). Dimethyl isosorbide, isopropyl myristate and mineral oil were obtained from Thermo Fisher Scientific (Lancashire, UK). Diethylene glycol monoethyl ether (Transcutol®), propylene glycol monocaprylate type II (Capryol 90®), propylene glycol monolaurate type 1 (Lauroglycol 90®) and medium chain triglycerides (Labrafac Lipophile W1349®) were kind donations from Gattefosse (St. Priest, France).

7.4.2 HPLC analysis

The detection and quantification of DF was performed using the method previously reported. This method was validated in accordance with ICH (2005) guidelines (International Conference on Harmonisation Expert Working Group, 2005) for linearity, accuracy, precision, robustness, limit of detection (LOD) and limit of quantification (LOQ) [220]. The mobile phase was made up of acetonitrile (ACN):0.1% trifluoroacetic acid in water (70:30). Calibration curves for the detection of diclofenac were prepared using DNa. They ranged from 0.05 to 100 µg/mL. The LOD was 0.03 µg/mL and LOQ was 0.10 µg/mL [220].

7.4.3 Solubility studies, solubility parameters (SP) of solvents, miscibility studies and stability studies

7.4.3.1 Single solvent solubility studies

Individual solvents (2 mL) were added to screw cap glass vials. An excess of DNa and a Teflon® coated magnetic stirrer bar were added to each solvent. The vials were subsequently sealed with Parafilm® and placed in a Grant Sub Aqua 26 water bath (Grant Instruments, Cambridgeshire, UK) at 32 ± 1 ˚C for 48 h with continuous stirring. The samples were inspected periodically to ensure that DNa remained visibly in excess. Where this was not the case, further DNa was added. After 48 h, approximately 1 mL of each solvent was transferred into a micro centrifuge tube. These tubes were then centrifuged for 15 min at 12 000 rpm, at a temperature of 32 ± 1 ˚C. The pipette tips and centrifuge tubes used to perform these tasks were maintained at 32 ± 1 ˚C in an oven for at least 30 min prior to use. Samples were diluted where required and analysed by HPLC.

7.4.3.2 Solubility parameters (SP) of solvents

SPs of single solvents were determined using the Van Krevelen and Hoftyzer method, incorporated within the Molecular Modelling Pro software, version 7.0.8 (Norgwyn Montgomery Software Inc., Pennsylvania, USA). The saturated solubility of DNa in each solvent was plotted against the SPs of each solvent using OriginPro® 2022 software (OriginLab Corporation, USA). Where the SP of binary solvents were considered, calculations were based on the volume fraction of the solvent as shown in equation 7.1**:**[238-240].

Equation 7. 1 Calculation of SP of a binary solvent system.

$$(\delta)^n = \frac{(\delta^i * \Phi^i) + (\delta^j * \Phi^j)}{(\Phi^i + \Phi^j)}$$

Where $(\boldsymbol{\delta})^{\boldsymbol{n}}$represents the SP of the solvent mixture, δ^i and δ^jcorrespond to the SP of the individual solvents, while Φ^i and Φ^jrefer to the volume fraction of each solvent.

7.4.3.3 Miscibility testing of drug-loaded binary solvent systems

As LHSS is only soluble in water, binary solvent combinations comprised water and one other solvent in the ratios 10:90, 20:80, 30:70, 40:60, 50:50, 60:40, 70:30, 80:20 and 90:10 (v/v). The non-aqueous solvent options were identified through the single solvent solubility studies mentioned above. As shown in Figure 7.1, DNa was determined to be most soluble in Transcutol® (TC), dipropylene glycol (DiPG) and propylene glycol (PG), which were selected for this study. Methylene blue was added to all samples to confirm miscibility. These studies were carried out using DNa at fixed concentrations of 1.00%, 0.75% and 0.50% (w/v). Stock solutions containing 50 mg/mL and 25 mg/mL of LHSS in water were prepared. In contrast to the fixed concentrations of DNa, the concentration of LHSS in the samples increased or decreased relative to the volume of LHSS stock solution contained in the sample. Samples were sealed with Parafilm® and shaken for 24 h using an orbital shaker (VWR, Leicestershire, UK) set to 32 ˚C and 800 rpm. The samples were then left at room temperature and evaluated at 24 h and 72 h.

7.4.3.4 Stability testing of binary formulations

The stability of selected formulations was evaluated for a period of 72 h. These binary formulations were added to Eppendorf® tubes or glass vials containing micro stirrer bars. They were sealed with Parafilm® and placed in a Grant Sub Aqua 26 water bath (Grant Instruments, Cambridgeshire, UK) at 32 ± 1 ˚C. At 24, 48 and 72 h samples were visually inspected for precipitation. Where precipitation occurred, formulations were not taken forward for investigation. Where no precipitation was evident, samples were analysed using HPLC.

7.4.4 Finite dose (10 µL) porcine skin *in vitro* permeation testing (IVPT) and mass balance studies

All porcine skin IVPT used full thickness porcine skin. Preparation of the membrane as well as IVPT and mass balance studies, were conducted in accordance with the methods used in previous work [220]. The only change related to the solvent used for the washing of the membrane and extraction of DNa. Instead of pure methanol, a mixture of methanol and water (85:15 v/v), was used due the increased solubility of DNa [226].

7.4.5 Data analysis

Microsoft Excel® version 16.55 (Microsoft Corporation, Washington, U.S.) was used to calculate the mean and standard deviation (SD) of the data. Additional statistical analysis was carried out using IBM® SPSS Statistics® Version 28.0 (IBM, New York, US). Evaluation of the normality of distribution of the data sets was performed using the Shapiro-Wilk test. The statistical significance of parametric data was analysed using a one-way analysis of variance (ANOVA) combined with Tukey's post hoc test or the independent-samples *t*-test for only two samples. For non-parametric data, statistical significance was assessed using the Kruskal-Wallis one-way ANOVA (k-samples) with multiple pairwise-comparisons or the Mann-Whitney U test for two samples. Probability values where $p < 0.05$ were considered statistically significant.

7.5 Results and discussion

7.5.1 Solubility studies, SP of solvents, drug-loaded miscibility studies and stability studies

7.5.1.1 Single solvent solubility studies

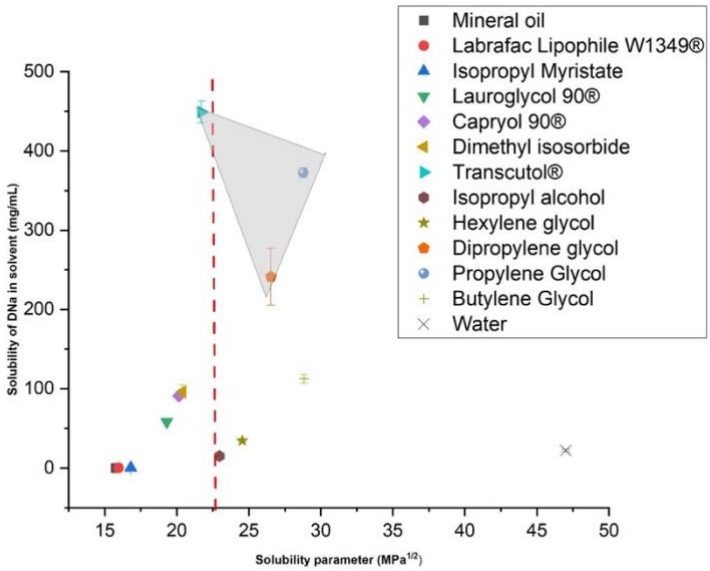

Figure 7. 1 The results of the saturated solubility of DNa in individual solvents are plotted against their SPs (n ≥ 3; mean ± SD). The dashed red line represents the SP of DNa determined by Barra et al [44].

The results of the saturated solubility of DNa in each solvent are plotted against the SP of the solvent in Figure 7.1. The SP reflects the cohesive energy density of the molecules in question. It has been suggested that materials exhibiting closely matched SPs have a strong affinity for one another, with the degree of similarity between these parameters directly influencing the extent of their interaction [241]. Therefore, liquids with similar SPs should be miscible [241] and compounds [242] should dissolve in solvents with comparable SPs. It is important to acknowledge, however, that practical observations do not always align perfectly with SP values. Furthermore, neither the Van Krevelen and Hoftyzer nor any of the standard contribution methods are applicable to the determination of the SPs of salts [243]. Nonetheless, they remain a useful starting point when screening solvents for solubility and miscibility purposes. The grey triangulated area in Figure 7.1 identifies the three solvents in which DNa was most soluble. These include Transcutol® (TC), propylene glycol (PG) and dipropylene

glycol (DiPG) with corresponding SPs of 21.72, 28.78 and 26.54 $MPa^{1/2}$. Applying the principles of SPs, high solubility equates to high affinity, which in turn suggests similar SPs [241]. It is possible, therefore, that the SP of DNa could lie within the aforementioned triangulated shaded area (Figure 7.1). This is corroborated in work published by Bustamante and Barra *et al* [243, 244]. Their research group expanded on existing SP methods enabling the evaluation of the SPs of certain sodium salts. The SP value for DNa determined by the cohort, using the van Krevelen group contribution method, equated to 22.65 $MPa^{1/2}$. This value corresponds very closely to the SP of TC, the solvent in which DNa was most soluble, and is represented in Figure 7.1 by a dashed red line.

As a result of the single solvent solubility studies, which indicated that DNa exhibited the highest solubility in TC, PG and DiPG, these solvents were chosen for the subsequent phase of formulation development. They are shown alongside water and DNa in Table 7.1 together with their CAS numbers, chemical structures, molecular weights, dielectric constant values at 25 °C and SPs. The solvents, selected primarily to maximise the solubility of DNa, are reported to function as permeation enhancers [42], and are also commonly used as excipients in topically applied pharmaceutical formulations. One such example is the inclusion of PG in the commercial formulation, Voltaren® 1% gel (GSK Consumer Health, New Jersey, USA). As such, they appear in the FDA Inactive Ingredients Database. Currently the maximum daily exposure (MDE) for TC (CAS 111-90-0) in topical applied gels is 1500 mg and the maximum potency per unit dose (MPPUD) for transdermal systems is 430 mg. PG (CAS 57-55-6) has a MDE for topically applied creams of 6113 mg and a MPPUD of 65% (w/w) for topical ointments. DiPG (CAS 25265-71-8) has a 296 mg MDE for extended-release films for transdermal use, while general transdermal systems are limited to 6 mg. No MPPUD is currently listed for DiPG contained in transdermal systems.

While these solvents were chosen specifically due to their efficacy as solubilisers of DNa, the work by Minghetti *et al* revealed the need for caution when focusing primarily on solubility. It was ascertained that DNa was far more soluble in PG (567 ± 31 µg/mL) and TC (660 ± 70 µg/mL) than oleic acid (25 ± 10 µg/mL) or water (37 ± 10 µg/mL). Despite the application of saturated solutions, the flux from water (2.29 ± 0.37 $\mu g/cm^2/h$) and oleic acid (1.84 ± 0.18 $\mu g/cm^2/h$) was greater than the flux from PG (1.21 ± 0.06 $\mu g/cm^2/h$) and TC (0.06 ± 0.01 $\mu g/cm^2/h$) [25]. The study demonstrated

that the assumption of equivalent thermodynamic activity for saturated solutions is negated when the activity coefficients of the solute in the solvents vary [25]. This was addressed by Higuchi, who explained that a high affinity between solute and vehicle translates into low activity coefficients. This in turn results in reduced rates of partition of the solute from the vehicle into the membrane [137]. Minghetti described this affinity as a very small difference between the SP of the active pharmaceutical ingredient (API) and the solvents, PG and TC, which reduced the ability of the API to partition into the membrane [25]. This study indicated that a similarity in SPs could cause a reduction in the activity coefficient and therefore the thermodynamic activity of the active in the formulation. While this would suggest potential challenges for single solvent systems, or combinations of the solvents selected for maximum DNa solubility, the inclusion of water should mitigate any such concerns. The SP of water (47.00 $MPa^{1/2}$) is distinct from that of PG (28.78 $Mpa^{1/2}$), DiPG (26.54 $Mpa^{1/2}$) and TC (21.72 $Mpa^{1/2}$), and therefore should result in a higher activity coefficient, thermodynamic activity and ability to partition into the membrane. The dielectric constants of solvents and solvent systems should also be considered due to their bearing on the stability of ion pairs. In general at lower dielectric constants, the association between ion pairs increases, while the converse is true for higher dielectric constants [46, 149]. The three solvents TC, PG and DiPG have dielectric constants of 14.1[245], 28.95 [246] - 30.2 [247] and 19.8 [248] respectively, at 25 °C. These values are lower than that of water which exhibits a dielectric constant of 78.3 at the same temperature [249]. Thus, the addition of any of the selected solvents would result in a reduction in the dielectric constant and polarity of water alone. As the organic component of the formulation increases, the electrostatic attraction generated by the solvent system diminishes in relation to the ions. This reduction leads to decreased interference in the electrostatic attraction between the ion pairs [147].

Table 7. 1 Chemical structures and molecular mass (g/mol) of DNa and the solvents DiPG, PG, TC and water. The table also contains the dielectric constants (ε) and SP ($MPa^{1/2}$) of the solvents.

Compound name	CAS	Chemical structure	Molar Mass (g/mol)	Dielectric constant of solvent (ε) at 25 °C	Solubility parameter ($MPa^{1/2}$) of solvents
DNa	15307-79-6	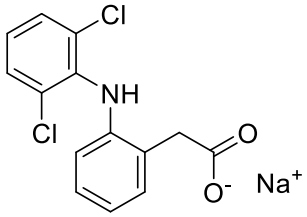	318.13	n/a	n/a
DiPG	25265-71-8	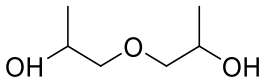	134.17	19.80[248]	26.54
PG	57-55-6	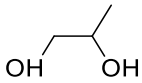	76.09	28.95[246] - 30.20[247]	28.78
TC	111-90-0	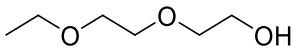	134.18	14.10[245]	21.72
Water	7732-18-5		18.02	78.30[249]	47.00

7.5.1.2 Miscibility studies for drug-loaded binary solvent systems

Table 7. 2 Miscible binary solvent combinations comprising TC, PG or DiPG and water, that had no apparent precipitation following drug-loaded miscibility testing. Results include the percentage concentration of DNa (w/v) in the sample as well as the molar ratio of LHSS relative to DNa in the sample. Formulations in italics were removed after precipitation was detected during stability testing. Formulations in bold appeared stable after stability tests and were selected for use in IVPT.

LHSS solution 50 mg/mL											
% DNa	Solvent % (v/v)		Mols LHSS/ mol DNa	% DNa	Solvent % (v/v)		Mols LHSS/ mol DNa	% DNa	Solvent % (v/v)		Mols LHSS/ mol DNa
	TC	Water			DiPG	Water			PG	Water	
0.75	*50*	*50*	*4.71*	*1.00*	*50*	*50*	*3.53*	0.50	60	40	5.65
0.50	**50**	**50**	**7.06**	*0.75*	*50*	*50*	*4.71*	0.50	80	20	2.83
0.50	*40*	*60*	*8.48*	0.50	50	50	7.06	0.50	90	10	1.41
				0.50	*40*	*60*	*8.48*				
LHSS solution 25 mg/mL											
% DNa	Solvent % (v/v)		Mols LHSS/ mol DNa	% DNa	Solvent % (v/v)		Mols LHSS/ mol DNa	% DNa	Solvent % (v/v)		Mols LHSS/ mol DNa
	TC	Water			DiPG	Water			PG	Water	
1.00	50	50	1.77	1.00	60	40	1.41	*1.00*	*70*	*30*	*1.06*
1.00	**60**	**40**	**1.41**	1.00	70	30	1.06	1.00	80	20	0.71
1.00	70	30	1.06	1.00	80	20	0.71	1.00	90	10	0.35
0.75	**50**	**50**	**2.35**	1.00	90	10	0.35	0.50	60	40	2.83
0.75	60	40	1.88	0.75	70	30	1.41	0.50	70	30	2.12
0.75	70	30	1.41	0.75	80	20	0.94	0.50	80	20	1.41
0.50	40	60	4.24	0.75	90	10	0.47	0.50	90	10	0.71

0.50	**50**	**50**	**3.53**	0.50	50	50	3.53	
0.50	60	40	2.83	0.50	60	40	2.83	
				0.50	70	30	2.12	

As LHSS is only soluble in water, the binary systems comprised TC, PG or DiPG in combination with an aqueous fraction in ratios of 10:90, 20:80, 30:70, 40:60, 50:50, 60:40, 70:30, 80:20 and 90:10 (v/v). DNa was included in fixed concentrations of 1.00%, 0.75% and 0.50% (w/v). The concentration of LHSS varied according to the volume of 50 mg/mL or 25 mg/mL LHSS solution added to the sample. Methylene blue was used to confirm miscibility. Table 7.2 indicates all miscible solvent combinations, at specific concentrations of DNa and LHSS that showed no apparent precipitation.

7.5.1.3 Binary solvent selection and stability testing

Stability testing was conducted to identify suitable formulations for permeation experiments, resulting in the exclusion of formulations marked in italics in Table 7.2. TC:water was selected as a model binary system as it facilitated comparisons where concentrations of DF, as well as solvent ratios, remained constant while the concentration of the counter ion was varied. This system also contained stable combinations of increased concentrations of DF at the same and different solvent ratios, as shown in Table 7.2. DiPG:water systems were not selected, as they did not comprise a sufficient number of stable formulations appropriate for comparative purposes. This was particularly relevant in relation to formulations containing an aqueous content of 50% (v/v), where the concentration of LHSS would be maximised. PG:water systems were not considered due to their consistently low aqueous content, limiting the quantity of LHSS. Formulations shown in bold were selected for IVPT as they appeared to be stable after 72 h and were therefore suitable for comparative purposes.

7.5.2 Results of finite dose (10 µL) binary IVPT and mass balance studies

7.5.2.1 Binary solvents: TC and water (50:50 v/v), containing 5 mg/mL DNa and 25 mg/mL LHSS (5DL25), 12.5 mg/mL LHSS (5DL12.5) or 0 mg/mL LHSS (5DL0)

Table 7. 3 Results for the finite dose (10 µL) porcine IVPT using binary solvent formulations produced from TC and water (50:50 v/v), containing 5 mg/mL DNa and 0, 12.5 or 25 mg/mL LHSS. The table shows (i) cumulative permeation of DF (µg/cm^2) at 25 h as well as the percentages of DF applied that (ii) permeated, (iii) remained on the skin surface, (iv) remained in the membrane, (v) permeated plus remained in the membrane and (vi) were recovered. In addition, the table contains a reference to the molar ratio of LHSS relative DNa, that was applied (4 ≤ n ≤ 5; mean ± SD).

Amount DF partitioned and permeated	DNa 5 mg/mL:LHSS 25 mg/mL (5DL25)	DNa 5 mg/mL:LHSS 12.5 mg/mL (5DL12.5)	DNa 5 mg/mL:LHSS 0 mg/mL (5DL0)
Cumulative permeation µg/cm^2 at 25 h	1.52 ± 0.32	1.48 ± 0.65	0.79 ± 0.62
Permeated 25 h %	3.49 ± 0.73	3.47 ± 1.56	1.76 ± 1.37
Retained on the skin surface %	65.53 ± 17.57	84.28 ± 2.90	85.02 ± 5.83
Retained in the membrane %	11.00 ± 7.21	8.79 ± 2.05	7.60 ± 1.19
Retained in membrane plus permeated %	14.49 ± 7.76	12.26 ± 3.06	9.36 ± 2.49
Recovery %	80.02 ± 11.39	96.54 ± 1.81	94.38 ± 6.01
DNa:LHSS molar ratio	1:7.1	1:3.5	1:0

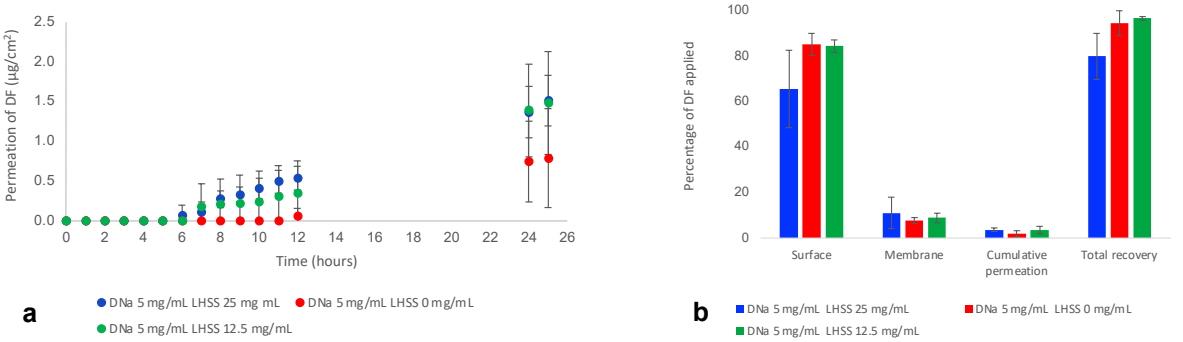

Figure 7. 2 (a) Cumulative permeation of DF from IVPT using porcine skin. A finite dose (10 µL) of the binary solvent formulation comprising TC and water (50:50 v/v) containing 5 mg/mL DNa and 0, 12.5 or 25 mg/mL LHSS, was applied (4 ≤ n ≤ 5; mean ± SD) (b) Percent recovery (mean ± SD) of DF from mass balance studies, following porcine IVPT using 10 µL of the binary solvent formulations produced from TC and water (50:50 v/v), containing 5 mg/mL DNa and 0, 12.5 or 25 mg/mL LHSS.

The data observed in Table 7.3 and Figure 7.2(a) suggests that the addition of LHSS enhanced the permeation of DF across porcine skin at 25 h, relative to the control formulation containing no LHSS. The variations, however, were not statistically significant ($p > 0.05$). Cumulative permeation of DF at 25 h ranged from 0.79 ± 0.62 µg/cm^2, (5DL0), to comparable amounts of 1.48 ± 0.65 µg/cm^2 and 1.52 ± 0.32 µg/cm^2 for the 5DL12.5 and 5DL25 formulations, respectively ($p > 0.05$). The percentage value of DF that permeated followed the same order, amounting to between 1.76 ± 1.37% for the control sample increasing to 3.47 ± 1.56% (5DL12.5) and 3.49 ± 0.73% (5DL25) ($p > 0.05$). All formulations resulted in comparable percentages of DF being

extracted from the membrane, varying from 7.60 ± 1.19% - 11.00 ± 7.21% ($p > 0.05$). To obtain a clearer picture of the total drug compound partitioning and permeating, the values for membrane retention and permeation were combined. Again, the results for all formulations were comparable, with the total percentages of DF amounting to 9.36 ± 2.49% (5DL0), 12.26 ± 3.06% (5DL12.5) and 14.49 ± 7.76% (5DL25, $p > 0$). Despite these amounts representing increases of approximately 55% (5DL25) and 30% (5DL12.5) relative to the control, they were not statistically significant ($p > 0.05$).

As mentioned previously, TC was selected due to its proficiency as a solubiliser, particularly in relation to compounds exhibiting poor water-solubility [250-252]. Despite its capacity to partition into and permeate through human skin as a neat solvent [253], high solubility of active ingredients in TC has not always resulted in high permeation values [25, 254, 255]. The incorporation of water to create binary solvent systems, however, has frequently served to increase the permeation of the active compound [250, 256]. This has been corroborated by investigations concerning the solubility and thermodynamic activity of various low water-soluble compounds in TC, water and binary combinations thereof [240, 257-261]. In these studies, the compounds exhibited high solubility in TC and had SPs that closely aligned with that of TC. A clear relationship emerged with the introduction of water, whereby an increase in the mole fraction of water corresponded to an elevated activity coefficient of the compound in the solvent system. As both the experimental and calculated SP [243, 244] of DNa is reported to be similar to that of TC, the addition of water increases the thermodynamic activity of the active in the formulation [261]. Thus, the selection of a binary solvent system comprising a 50:50 (v/v) ratio of TC:water, balances the requirement of solubility for both DNa and LHSS while addressing the issue of the thermodynamic activity of DNa in the formulation.

Recovery of DF was 94.38 ± 6.01% where no LHSS was used (5DL0), increasing to 96.54 ± 1.81% for the formulation containing 12.5 mg/mL LHSS (5DL12.5). Significantly less DF (80.02 ± 11.39% $p < 0.05$) was recovered from the final formulation, L5DL25.

7.5.2.2 Binary solvents: TC and water (50:50 v/v), containing 7.5 mg/mL DNa and 0 mg/mL LHSS (7.5DL0) or 12.5 mg/mL LHSS (7.5DL12.5)

Table 7. 4 Results for the finite dose (10 µL) porcine IVPT using binary solvent formulations produced from TC and water (50:50 v/v), containing 7.5 mg/mL DNa and 0 or 12.5 mg/mL LHSS. The table shows (i) cumulative permeation of DF (µg/cm^2) at 25 h as well as the percentages of DF applied that (ii) permeated, (iii) remained on the skin surface, (iv) remained in the membrane, (v) permeated plus remained in the membrane and (vi) were recovered. In addition, the table contains a reference to the molar ratio of LHSS relative to DNa, that was applied (3 ≤ n ≤ 4; mean ± SD).

Amount DF partitioned and permeated	DNa 7.5 mg/mL:LHSS 12.5 mg/mL (7.5DL12.5)	DNa 7.5 mg/mL:LHSS 0 mg/mL (7.5DL0)
Cumulative permeation µg/cm^2 at 25 h	1.49 ± 0.76	0.22 ± 0.19
Permeated 25 h %	2.24 ± 1.15	0.35 ± 0.30
Retained on the skin surface %	88.18 ± 4.41	94.64 ± 5.66
Retained in the membrane %	8.14 ± 2.24	3.95 ± 0.12
Retained in membrane plus permeated %	10.38 ± 2.49	4.30 ± 0.42
Recovery %	98.56 ± 4.89	98.94 ± 6.08
DNa:LHSS molar ratio	1:2.35	1:0

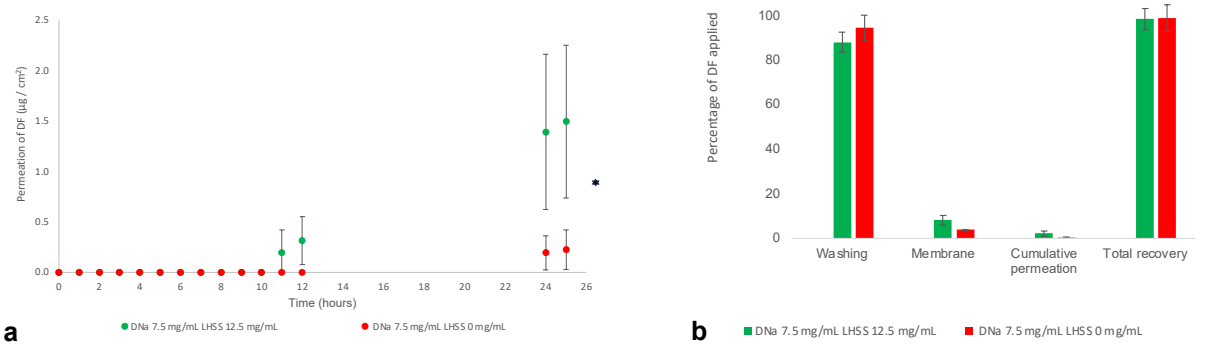

Figure 7. 3 (a) Cumulative permeation of DF from IVPT using porcine skin. A finite dose (10 µL) of the binary solvent formulation comprising TC and water (50:50 v/v) containing 7.5 mg/mL DNa and 0 or 12.5 mg/mL LHSS, was applied. (3 ≤ n ≤ 4; mean ± SD, *p < 0.05). (b) Percentage recovery (mean ± SD) of DF from mass balance studies, following porcine IVPT using 10 µL of the binary solvent formulations produced from TC and water (50:50 v/v), containing 7.5 mg/mL DNa and 0 or 12.5 mg/mL LHSS.

The results of the permeation study, as shown in Table 7.4 and Figures 7.3(a) & (b), indicate that the addition of 12.5 mg/mL LHSS to a higher concentration of DNa (7.5 mg/mL), significantly increased the permeation of DF at 25 h relative to the control. Permeation values for the LHSS-containing formulation (7.5DL12.5) amounted to 1.49 ± 0.76 µg/cm^2 while the control (7.5DL0) was 0.22 ± 0.19 µg/cm^2 ($p < 0.05$).

Although one of the previous formulations tested (5DL12.5 shown in Table 7.3) contained an equivalent quantity of LHSS (12.5 mg/mL LHSS), the increase in the concentration of DNa from 5 – 7.5 mg/mL, resulted in a change to the DNa:LHSS

molar ratio. Previously (5DL12.5) this ratio was 1:3.5, reducing to 1:2.35 (7.5DL12.5), as a result of the increase in DNa concentration. These changes appeared to have no significant impact on the cumulative permeation of DF from the 7.5DL12.5 formulation (1.49 ± 0.76 μg/cm^2) relative to the 5DL12.5 experiment (1.48 ± 0.65 μg/cm^2, $p > 0.05$). When viewed as a percentage of the DF applied, the amount reduced from 3.47 ± 1.56% (5DL12.5) to 2.24 ± 1.15% (7.5DL12.5), however this was not considered statistically significant ($p > 0.05$). When considering the quantity of DF in the membrane, the addition of LHSS in the current experiment (7.5 mg/mL DNa) resulted in a significantly higher percentage being extracted (8.14 ± 2.24%) when compared to the control (3.95 ± 0.12%, $p < 0.05$). This remained consistent when the percentage of DF that permeated was added to that extracted from the membrane, with values of 10.38 ± 2.49% for the LHSS formulation and 4.30 ± 0.42% for the control ($p < 0.05$).

A comparison of the percentage of DF extracted from the membrane for the 5DL12.5 samples (8.79 ± 2.05%) with the results of the 7.5DL12.5 samples (8.14 ± 2.24%), showed no significant differences ($p > 0.05$). Moreover, the combination of the amount of DF that permeated with that extracted from the membrane amounted to 12.26 ± 3.06% for the 5DL12.5 formulation, which was comparable to 10.38 ± 2.29% for the 7.5DL12.5 preparation ($p > 0.05$). Recovery of DF was approximately 98% for both the 7.5 mg/mL DNa formulation containing LHSS as well as the control. This was consistent with the range recommended by the OECD guidelines.[88]

7.5.2.3 Binary solvents: TC and water (60:40 v/v), containing 10 mg/mL DNa and 0 mg/mL LHSS (10DL0) or 10 mg/mL LHSS (10DL10)

Table 7. 5 Results for the finite dose (10 µL) porcine IVPT using binary solvent formulations produced from TC and water (60:40 v/v), containing 10 mg/mL DNa and 0 or 10 mg/mL LHSS. The table shows (i) cumulative permeation of DF (µg/cm^2) at 25 h as well as the percentages of DF applied that (ii) permeated, (iii) remained on the skin surface, (iv) remained in the membrane, (v) permeated plus remained in the membrane and (vi) were recovered. In addition, the table contains a reference to the molar ratio of LHSS relative DNa, that was applied (n = 5; mean ± SD).

Amount DF partitioned and permeated	DNa 10 mg/mL:LHSS 10 mg/mL (10DL10)	DNa 10 mg/mL:LHSS 0 mg/mL (10DL0)
Cumulative permeation µg/cm^2 at 25 h	1.01 ± 0.91	0.36 ± 0.44
Permeated 25 h %	1.10 ± 0.98	0.41 ± 0.49
Retained on the skin surface %	93.55 ± 1.90	93.43 ± 5.49
Retained in the membrane %	4.31 ± 1.34	4.39 ± 0.95
Retained in membrane plus permeated %	5.41 ± 2.21	4.80 ± 1.08
Recovery %	98.96 ± 0.86	98.23 ± 5.13
DNa:LHSS molar ratio	1:1.41	1:0

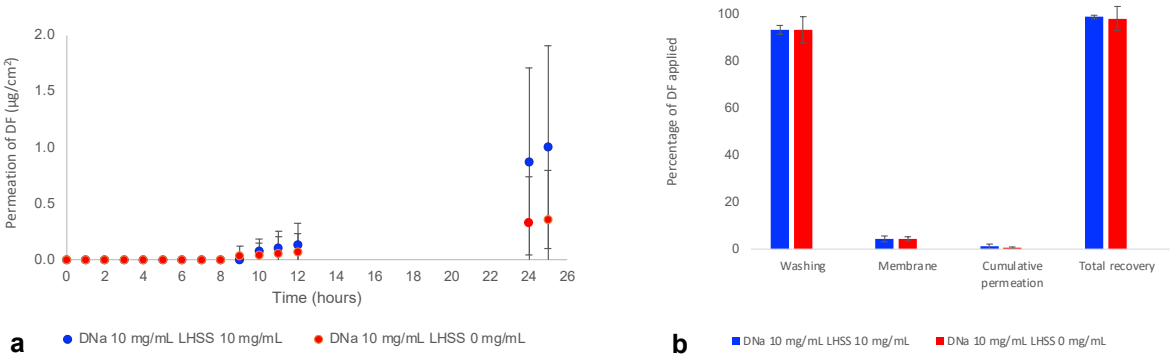

Figure 7. 4 (a) Cumulative permeation of DF from IVPT using porcine skin. A finite dose (10 µL) of the binary solvent formulation comprising TC and water (60:40 v/v) containing 10 mg/mL DNa and 0 or 10 mg/mL LHSS, was applied. (n = 5; mean ± SD) (b) Percentage recovery (mean ± SD) of DF from mass balance studies, following porcine IVPT using 10 µL of the binary solvent formulations produced from TC and water (60:40 v/v), containing 10 mg/mL DNa and 0 or 10 mg/mL LHSS.

To ascertain the impact of increasing the concentration of DNa to 10 mg/mL while reducing LHSS to an equivalent amount, further IVPT were performed. In addition to changes in the amounts of DNa and LHSS, the solvent ratios of TC:water were modified from 50:50 (v/v) to 60:40 (v/v). Although cumulative permeation profiles shown in Figure 7.4(a) suggest enhanced permeation of DF from the LHSS-containing vehicle at 25 h, differences were not statistically significant ($p > 0.05$). As shown in Table 7.5, permeation of DF at 25 h from the control (10DL0) was 0.36 ± 0.44 µg/cm^2, equivalent to 0.41 ± 0.49% of the DF applied. This was consistent with the values of

the LHSS formulation (10DL10), where permeation of DF was 1.01 ± 0.91 μg/cm^2 or 1.10 ± 0.97% of the DF applied ($p > 0.05$).

Furthermore, the percentage and actual amounts (μg/cm^2) of DF that permeated from 10DL10 and 10DL0 were comparable to both 7.5 mg DNa formulations as well as the 5 mg DNa formulation control formulations ($p > 0.05$). However, percentages of DF that permeated from the 5 mg/mL formulations, 5DL12.5 (3.47 ± 1.56%) and 5DL25 (3.49 ± 0.73%), were significantly greater than the 1.10 ± 0.98% that permeated from 10DL10 ($p < 0.05$).

Analysis of the percentage of DF retained within the skin for the 10 mg/mL DNa formulations, revealed no significant differences between 10DL10 (4.31 ± 1.34%) and 10DL0 (4.39 ± 0.95%, $p > 0.05$). Furthermore, the combined values of DF extracted from the membrane and permeating, amounted to 5.41 ± 2.21% (10DL10) and 4.80 ± 1.08% (10DL0), were not significantly different ($p > 0.05$). This suggests that the molar ratio of DNa:LHSS (1:1.41), did not impact either partition into the skin or permeation in this solvent system. Comparisons of the amounts of DF retained in the membrane for 7.5 and 10 mg/mL DNa formulations did, however, reveal significant differences when LHSS was included. The reduction of LHSS (12.5 – 10 mg/mL), while simultaneously varying the solvent ratio (TC:water from 50:50 – 60:40), caused a significant decrease in the percentage of DF retained in the membrane. This amount reduced from 8.14 ± 2.24% (7.5DL12.5) to 4.31 ± 1.34% (10DL10) despite the increase in DNa concentration (7.5 – 10 mg/mL, $p < 0.05$). This was not the case, however in relation to the 7.5DL0, where the DF retained in the membrane was comparable to that of the 10DL10 formulation ($p > 0.05$). As mentioned previously, this could indicate that the molar quantity of LHSS was not high enough relative to that of DNa, to result in an increase in penetration of the active. The total percentage of DF that partitioned and permeated reflected a similar pattern, significantly decreasing from 10.38 ± 2.49% (7.5DL12.5) to 5.41 ± 2.21% (10DL10) ($p < 0.05$). There was no significant difference in the percentages that partitioned and permeated from the 7.5DL0 (4.30 ± 0.42%) and 10DL10 (5.41 ± 2.21%) formulations ($p > 0.05$).

Differences in the amounts of DF retained in the membrane between the two 5 mg/mL preparations and the 10 mg/mL formulation containing LHSS, were also statistically different ($p < 0.05$). Notwithstanding the increase in the concentration of DNa (5 – 10 mg/mL), the quantity of DF extracted from the membrane reduced from 8.79 ± 2.05%

(5DL12.5) and 11.00 ± 7.21% (5DL25) to 4.31 ± 1.34% for the 10DL10 formulation. When the amount of DF permeating was added to that recovered from the skin, the results followed the same pattern. Values reduced from 12.26 ± 3.06% (5DL12.5) and 14.49 ± 7.76% (5DL25) when the concentration of DNa applied was 5 mg/mL to 5.41 ± 2.21% (10DL10) when the concentration of DNa increased to 10 mg/mL ($p < 0.05$). Values of DF for 5DL0 (9.35 ± 2.49%) and 10DL10 (5.41 ± 2.21%) were comparable ($p > 0.05$).

The observed changes can be partially attributed to the adjustment of the TC:water solvent ratio from 50:50 to 60:40 (v/v). This modification directly impacts the SP of the solvent system[259, 260], reducing it from 34.36 to 31.83 $MPa^{1/2}$, bringing it closer to the SPs of TC and DNa. The thermodynamic consequences of increasing the TC fraction in binary TC:water systems, where the permeant is sparingly soluble in water, but freely soluble in TC, were investigated using paracetamol [262], DNa [261, 262] and various other active ingredients [240, 257-260]. It was shown that increasing TC relative to water decreased the thermodynamic activity of the active ingredients within the solvent systems. This effect was demonstrated by Bialik *et al* with IVPT using ibuprofen [256]. Due to its low solubility in water (0.021 mg/mL) relative to TC (400 mg/mL) [250]. ibuprofen permeation decreased with increasing TC concentration, due to the alteration of the permeant's thermodynamic activity in the vehicle [256].

Apart from the alteration in solvent ratio, the reduction in the DNa:LHSS molar ratio to (1:1.41) could have contributed to a decrease in DF partitioning and permeation. This may indicate that a minimum amount of LHSS is required to achieve any increased partition and permeation results. Prior studies have indicated a correlation between DF partitioning and increased LHSS counter ion concentration [220].

Finally, as shown in Table 7.5, recovery of the DF applied exceeded 98% for both the 10DL10 and the control sample sets, satisfying the guidelines set out by the OECD [88].

7.6 Conclusion

Building on previous research, the current study has addressed challenges pertaining to solubility and identified a binary solvent model comprising TC and water to evaluate DNa:LHSS ion pairs. The tested formulations included (i) fixed concentrations of DNa (5 mg/mL) and solvent ratios (50:50 (v/v)) while varying the counter ion concentration

(12.5 or 25 mg/mL), (ii) an increased concentration of DNa (7.5 mg/mL) at fixed solvent ratios (50:50 (v/v)) and counter ion concentrations (12.5 mg/mL), and (iii) increasing the concentration of DNa (10 mg/mL) while varying the TC:water solvent ratio (60:40 (v/v)) and decreasing the counter ion concentration (10 mg/mL). All formulations complied with the MDE and MPPUD for TC outlined in the FDA's Inactive Ingredient Database.

The selection of TC, a solvent with a SP similar to that reported for DNa, resulted in a large increase in the solubility of the active when compared to our previous work. Challenges associated with this choice, such as a reduction in the activity coefficient of DNa in the solvent system and its ability to partition out of the formulation and into the membrane, were addressed by the inclusion of water. The effect of reducing the water content was demonstrated by the alteration of the TC:water ratio from 50:50 to 60:40 (v/v). Although the increase in TC enabled the DNa concentration to be doubled (5 – 10 mg/mL), this had no significant effect on the actual amount of DF partitioning and permeating from the 10DL0 system, relative to any of the other control samples. Furthermore, the reduction in the dielectric constant of the solvent system attributable to the increase in the TC fraction, was not able to offset the drop in the quantity of LHSS from 25 mg/mL and 12.5 mg/mL to 10 mg/mL. This was evidenced by the significant reduction the amount of DF partitioning and permeating from the 10DL0 formulation relative to the 5DL12.5, 5DL25 and 7.5DL12.5 samples.

The studies showed that while the inclusion of LHSS at 5 mg/mL increased the partition and permeation of DF by approximately 30% (5DL12.5) and 55% (5DL25) relative to the control; this was not statistically significant. However, when the concentration of DNa was increased to 7.5 mg/mL (7.5DL12.5), the inclusion of LHSS significantly enhanced the amount of DF that partitioned and permeated (approximately 145%), when compared to the control formulation. The increase in the amount of DNa from 5 - 7.5 mg/mL had no significant effect on the partition and permeation of DF, when the quantity of LHSS remained constant at 12.5 mg/mL.

In accordance with our previous investigations, the current work suggests that the inclusion of LHSS with DNa in a formulation may increase the partition and permeation of DF. This represents a further step in the development of an ion pair formulation where less DNa may be required within the preparation to achieve a therapeutic result. In continuing this process, the solubility of the active and the counter ion require further

consideration, particularly in relation to the ratio in which they are most effective. Additionally, the importance of the activity coefficient of the active in the formulation should be balanced with the potential to stabilise the ion pairs, by increasing the use of solvents with a lower dielectric constant than water. Further work has already commenced exploring the implications of substituting TC with an alternative solvent, DiPG, as the DNa-solubiliser. This substitution should enable the impact of a solvent change on IVPT results to be determined. Additional investigations will incorporate more than one solvent into the DNa-solubilising fraction. These ternary systems will be tested via IVPT to further optimize the ion pair formulation.

7.7 Funding

This research received no external funding.

7.8 Conflicts of interest

The authors declared no conflict of interest.

8 Ion pairing as a strategy to enhance the delivery of diclofenac

8.1 Overview

“Ion pairing as a strategy to enhance the delivery of diclofenac” was published on 3 August 2025 in the Royal Society of Chemistry: Pharmaceutics 2 (2025): 1163 - 1174, DOI:10.1039/D5PM00096C. The co-authors and their contributions were as follows:

Mignon Cristofoli: conceptualisation, methodology, validation, investigation, formal analysis, visualisation, writing - original draft and amendments; Jonathan Hadgraft: conceptualisation; Majella, E. Lane: conceptualisation, resources, supervision, writing - review and editing; and Sil, Bruno C.: conceptualisation, resources, supervision, writing - review and editing.

Addressing objectives 2.1.2.10 - 2.1.2.13, this chapter developed the work relating to the binary system described in Chapter 7 by examining solvent substitution effects. Ternary formulations were developed to further enhance DF delivery. The formulation that performed best in terms of overall delivery was compared to a commercial product containing 1% DNa. FT-IR characterisation of ion pairs was undertaken as an additional method to confirm ion pair formation.

8.2 Abstract

This study explores the use of ion pairing and solvent selection to enhance the percutaneous delivery of diclofenac (DF) from topical formulations. Previous investigations identified L-histidine monochloride monohydrate (LHSS) as an ion pair candidate for diclofenac sodium (DNa). Initial *in vitro* permeation tests (IVPT) demonstrated that while LHSS increased DF permeation, it caused DF precipitation at higher concentrations. As DNa is sparingly soluble in water, the only solvent in which LHSS dissolves, its solubility was tested in alternative solvents. The highest solubility

was observed in Transcutol® (TC), dipropylene glycol (DiPG) and propylene glycol (PG). Building on earlier research using TC:water binary systems to evaluate ion pairs, this study assessed: (i) the substitution of TC with DiPG in binary formulations, (ii) the development of ternary systems comprising water, TC and either DiPG or PG, and (iii) their impact on DF delivery using finite dose IVPT with porcine skin. The inclusion of LHSS (10 mg/mL) with DNa (10 mg/mL) in a DiPG:water (60:40 v/v) binary system significantly enhanced DF delivery (2.69 ± 1.01%), relative to the LHSS-free control (1.02 ± 0.44%, $p < 0.05$.). However, this was significantly lower than in TC:water binary formulations (4.80 ± 1.08 - 5.41 ± 2.21%; $p < 0.05$). Similarly, ternary formulations containing DiPG (5 mg/mL DNa; 12.5 mg/mL LHSS; DiPG:TC:water; 10:40:50 v/v/v) resulted in lower DF delivery (5.62 ± 2.78%) compared to the corresponding TC:water (50:50 v/v) binary formulation (12.26 ± 3.06%, 5 mg/mL DNa; 12.5 mg/mL LHSS, $p < 0.05$). Conversely, replacing DiPG with PG in the ternary formulation (PG:TC:water; 10:40:50 v/v/v) containing 25 mg/mL LHSS, significantly enhanced DF permeation (4.26 ± 1.41 μg/cm^2) compared to all binary (0.14 ± 0.28 – 1.52 ± 0.32 μg/cm^2) and ternary formulations (0.21 ± 0.36 – 1.72 ± 1.06 μg/cm^2, $p < 0.05$). This formulation also outperformed a recognised commercial product (1.74 ± 0.6 μg/cm^2) by 145%, despite containing only half the DNa concentration and resulted in the highest total DF uptake as a percentage of the applied dose (27.25 ± 2.61%). This work builds on previous findings, confirming that LHSS enhances DF delivery in combination with DNa. By examining solvent systems and counterion effects, it provides a deeper understanding of formulation strategies to optimise the percutaneous delivery of DF.

8.3 Introduction

Osteoarthritis (OA) affects over 500 million people worldwide, with substantial direct and indirect economic costs [7, 8]. Topical non-steroidal anti-inflammatory drugs (NSAIDs), and diclofenac (DF) in particular, are widely recommended for the treatment of OA due to their effectiveness and lower risk of adverse effects compared to oral NSAIDs and opioids [9-12, 263]. However, due to the barrier function of the skin's *stratum corneum* (SC), only a small fraction of the applied drug penetrates effectively, leaving much of it unable to reach the target site. Improved formulation of DF products could lead to both cost savings and reduced environmental impact by minimising excess drug waste. This aligns with the environmental initiatives of major

pharmaceutical companies, like Astra Zeneca [51], Novartis [52] and Roche [53, 54], which aim to reduce pharmaceutical residues in the environment where possible.

Previous research by the authors investigated ion pairing to enhance the percutaneous delivery of DF [220, 222]. Initial distribution coefficient studies showed that adding L-histidine monochloride monohydrate (LHSS) to aqueous diclofenac sodium (DNa) solutions increased the amount of DF partitioning from the aqueous to the organic phase, with higher LHSS amounts leading to greater DF transfer to the organic layer. Subsequent infinite dose *in vitro* permeation tests (IVPT) using porcine skin indicated that incorporating LHSS in DNa formulations enhanced DF permeation compared to formulations without LHSS. The aqueous formulations investigated also highlighted solubility challenges. As DNa is only sparingly soluble in water [261], the sole solvent in which LHSS dissolves, its solubility was tested in various alternative solvents. Of these, Transcutol® (TC), propylene glycol (PG) and dipropylene glycol (DiPG) were identified as the solvents in which DNa was most soluble [222].

The authors identified TC:water as a model binary solvent system for the evaluation of the DNa:LHSS ion pairs, as it enabled the comparison of a variety of formulations. This selection of TC as a solvent resulted in a large increase in the solubility of DNa [222], addressing a major challenge identified in earlier experimental work [220]. However, when TC exceeded a 50:50 (v/v) ratio in TC:water, it appeared to reduce the thermodynamic activity of DNa in the formulation. This in turn led to a significant reduction in the movement of DF into and through the membrane, indicating the importance of optimising for the competing aspects of solubility and thermodynamic activity when choosing the solvents for a formulation. To further investigate the effects of solvents on the DNa-LHSS ion pair, this study has three objectives:(i) to replace TC with an alternative solvent in a binary formulation; (ii) to develop ternary systems incorporating water and solvents in which DNa has previously shown high solubility; and (iii) to conduct IVPT, applying finite doses (10 µL) to porcine skin to evaluate the impact of these formulations on the percutaneous delivery of DF.

8.4 Materials and methods

8.4.1 Materials

Diclofenac sodium (DNa) 98%, L-histidine monochloride monohydrate (LHSS) and dipropylene glycol (DiPG) were produced by Acros Organics and supplied by VWR

(Leceistershire, UK). Voltaren® 1% gel (Haleon, New Jersey, USA) was purchased from Walgreens (New York, USA). High vacuum grease was obtained from Dow Corning (Seneffe, Belgium). Oxoid™ Phosphate buffered saline (PBS) tablets were purchased from Thermo Fisher Scientific (Lancashire, UK). HPLC grade acetonitrile (ACN), trifluoroacetic acid (TFA), methanol and 150 mm diameter filter paper, were purchased from Fisher Scientific (Lancashire, UK). Propylene glycol (PG) was produced by Sigma-Aldrich and supplied by Merck Life Sciences (Poole, UK). Diethylene glycol monoethyl ether, with the trade name Transcutol® (TC), was kindly donated by Gattefossé (St. Priest, France). Ion pairs were generated in situ, with formation confirmed by FT-IR spectroscopy (Supplementary Information).

8.4.2 HPLC analysis

Detection and quantification of DF was carried out using the method previously reported by the authors [220, 222]. Validation for linearity, accuracy, precision and robustness, as well as limits of detection and quantification was performed in accordance with the International Conference on Harmonisation Expert Working Group (ICH) guidelines (2005) [221]. The mobile phase comprised acetonitrile and 0.1% trifluoroacetic acid in water, in a ratio of 70:30 (v/v). The injection volume was 10 µL and the flow rate was 1 mL/min. A detection wavelength of 277 nm was selected for the acquisition of chromatograms. Calibration curves ranging from 0.05 – 100 µg/mL DF, were prepared using DNa. The limit of detection was 0.03 µg/mL, while the limit of quantification was 0.10 µg/ mL.

8.4.3 Binary solvent systems

To determine the effects of a non-aqueous solvent substitution on the movement of DF into and through the membrane, TC was replaced with DiPG. Studies previously identified DiPG as one of three solvents in which DNa exhibited the highest solubility relative to the other solvents tested [222]. The original binary solvent formulations comprising TC and water (60:40 v/v), and containing 10 mg/mL DNa, and either 0 or 10 mg/mL LHSS [222] were selected for TC substitution. In the modified formulations, TC was replaced with DiPG while maintaining the 60:40 (v/v) solvent ratio with water (60:40 v/v) [222].

8.4.4 Miscibility testing of drug-loaded ternary solvent systems

Ternary solvent combinations comprised an aqueous component ranging from 50 – 80% (v/v). The minimum water requirement was previously established to ensure a sufficient quantity of LHSS in the preparation, as well as to enhance the thermodynamic activity of DNa in the formulation [222]. Where the aqueous fraction amounted to 50% (v/v), the remaining 50% (v/v) was apportioned between the non-aqueous solvents in ratios of 40:10, 30:20, 20:30 and 10:40 (v/v). When the aqueous volume represented 60% (v/v), the 40% (v/v) attributable to non-aqueous solvents was divided on a 30:10, 20:20 and 10:30 (v/v) basis. When the aqueous fraction was 70% (v/v), the non-aqueous fraction comprised the combinations 20:10 and 10:20 (v/v). Finally, when the aqueous proportion was 80% (v/v), the non-aqueous solvents each represented 10% (v/v). Methylene blue was added to the solvent combinations to confirm miscibility.

The studies were performed using DNa in fixed concentrations of 1.00%, 0.75% and 0.50% (w/v). Stock solutions of LHSS in water were prepared at concentrations of 50 mg/mL and 25 mg/mL. Like the previously conducted binary studies [222], the concentration of DF remained constant, regardless of the solvents used. As LHSS was prepared in stock solutions, its concentration varied depending on the volume of the LHSS stock solution included in the sample. All samples were sealed using Parafilm® and shaken at 800 rpm on an orbital shaker (VWR, Leicestershire, UK) set at 32 °C for 24 h. The samples were kept at room temperature and assessed at 24 h and 72 h.

8.4.5 Stability testing of formulations

Prior to use in IVPT, the stability of all formulations was evaluated for 72 h. Stability testing was undertaken using the method previously reported by the authors [222]. Any formulations where precipitation was visually detected, were disregarded. Where no precipitation was apparent, samples were analysed using HPLC.

8.4.6 Solubility parameters (SP) of solvents

SPs of single solvents were determined previously [222] using the Van Krevelen and Hoftyzer method, incorporated within the Molecular Modelling Pro software, version 7.0.8 (Norgwyn Montgomery Software Inc., Pennsylvania, USA). The calculation of SP values for binary or ternary solvents were based on the volume fraction of the solvent as shown in eqn (8.1) [238-240]:

Equation 8. 1 Calculation of SP of a ternary solvent system.

$$(\delta)^n = \frac{\left(\delta^i \times \phi^i\right) + \left(\delta^j \times \phi^j\right) + (\delta^k \times \phi^k)}{(\phi^i + \phi^j + \phi^k)}$$

where $(\delta)^n$ denotes the SP of the solvent mixture, δ^i, δ^j and δ^k represents the SP of the individual solvents, and Φ^i, Φ^j and Φ^k refers to the volume of each solvent.

8.4.7 Finite dose (10 µL) porcine skin IVPT and mass balance studies

IVPT and mass balance studies were conducted as previously reported [220, 222]. IVPT was conducted using vertical glass Franz diffusion cells (Soham Scientific, Cambridgeshire, UK), with receptor medium consisting of 6% w/v Brij™ O20 in phosphate-buffered saline (pH 7.3 ± 0.2) to maintain sink conditions. Diffusion cells were placed in a Grant Sub Aqua 26 water bath (Grant Instruments, Cambridgeshire, UK) preheated to ~37 °C to achieve a skin surface temperature of 32 ± 1 °C. Finite doses (10 µL) of formulations were applied. Final samples were collected at 25 h. Membranes were washed three times and extracted with a mixture of methanol and water (85:15 v/v).

8.4.8 Data analysis

The mean and standard deviation (SD) of the data was calculated using Microsoft Excel ® version 16.94 (Microsoft Corporation, Washington, U.S.). IBM ® SPSS Statistics ® Version 29.0.1.1 (IBM, New York, US) was used to carry out further statistical analysis. The normality of distribution of the data sets was evaluated using the Shapiro-Wilk test. For parametric data, statistical significance was analysed using a one-way analysis of variance (ANOVA), combined with Tukey's *post hoc* test. Where only two samples were compared, the independent-samples *t*-test was used. Statistical significance of non-parametric data was assessed using the Kruskal-Wallis one-way ANOVA (*k*-samples) with multiple pairwise-comparisons where there were more than two samples. Alternatively, for two samples, the Mann-Whitney *U* test was used. Probability values where $p < 0.05$ were considered statistically significant.

8.5 Results and discussion

8.5.1 Binary solvents: effect of solvent substitution

The formulations applied comprised DiPG and water (60:40, v/v) and contained 10 mg/mL DNa and either 10 or 0 mg/mL LHSS. To assess the influence of alternative non-aqueous solvents on the percutaneous delivery of DF, a study involving solvent substitution was conducted. Earlier work had identified, but not tested, a binary system containing 60% DiPG and 40% water (v/v) with 10 mg/mL DNa and either 0 or 10 mg/mL LHSS [222]. As this system corresponded to a previously evaluated formulation with 60% TC and 40% water (v/v) at the same DNa and LHSS concentrations (10 mg/mL DNa; 10 or 0 mg/mL LHSS; TC:water; 60:40; v/v), it was selected to determine the impact of solvent substitution.

Table 8.1 and Figure 8.1 show that the addition of LHSS at 10 mg/mL to the formulation containing 10 mg/mL DNa and comprising DiPG:water (60:40, v/v), resulted in a DF permeation value of 0.53 ± 0.34 µg/cm², amounting to 0.62 ± 0.42% of the applied dose. While this was higher than the amount of DF permeating from the DiPG:water (60:40 v/v) control (10 mg/mL DNa; 0 mg/mL LHSS; DiPG:water; 60:40; v/v) at 0.14 ± 0.28 µg/cm² (0.16 ± 0.32%), the difference was not statistically significant ($p > 0.05$). As reported in Table 8.S1, permeation values for the corresponding TC:water (60:40, v/v) study, were 1.01 ± 0.91 µg/cm² for the LHSS containing formulation (10 mg/mL DNa; 10 mg/mL LHSS; TC:water; 60:40; v/v) and 0.36 ± 0.44 µg/cm² for the control (10 mg/mL DNa; 0 mg/mL LHSS; TC:water; 60:40; v/v). These results were determined to be comparable to the DiPG:water (60:40, v/v) permeation values ($p > 0.05$).

Table 8. 1 Results for finite dose (10 µL) porcine skin IVPT. Formulations were prepared with DiPG and water (60:40 v/v); 10 mg/mL DNa; and 0 or 10 mg/mL LHSS (n = 5; mean ± SD).

Amount DF retained in the membrane and permeated	DiPG:water (60:40 v/v)	
	DNa 10 mg/mL: LHSS 10 mg/mL	DNa 10 mg/mL LHSS 0 mg/mL
Cumulative permeation µg/cm^2 at 25 h	0.53 ± 0.34	0.14 ± 0.28
Permeated 25 h %	0.62 ± 0.42	0.16 ± 0.32
Retained on skin surface %	99.86 ± 3.84	101.38 ± 6.41
Retained in membrane %	2.07 ± 0.71	0.87 ± 0.23
Retained in membrane plus permeated %	2.69 ± 1.01	1.02 ± 0.44
Recovery %	102.55 ± 3.32	102.41 ± 6.10
DNa:LHSS molar ratio	1:1.41	1:0

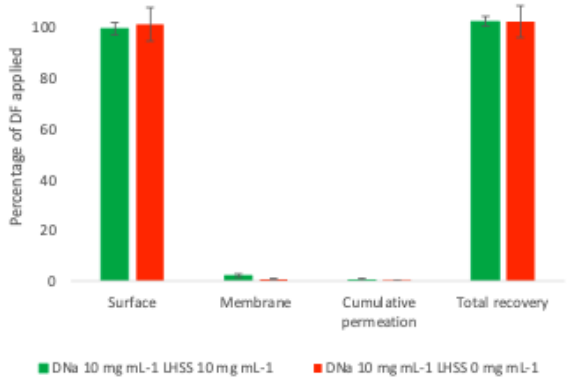

Figure 8. 1 Percentage recovery (mean ± SD) of DF from mass balance studies, following porcine IVPT. Finite doses (10 µL) of the binary solvent formulations prepared with DiPG and water (60:40 v/v), containing 10 mg/mL DNa and 0 or 10 mg/mL LHSS, were applied (n = 5; mean ± SD).

The percentage of DF extracted from the membrane, however, was significantly higher for the DiPG:water (60:40, v/v) formulation containing LHSS (2.07 ± 0.71%, 10 mg/mL DNa; 10 mg/mL LHSS; DiPG:water; 60:40; v/v), than for the DiPG:water (60:40, v/v) control formulation (0.87 ± 0.23%, 10 mg/mL DNa; 0 mg/mL LHSS; DiPG:water; 60:40; v/v, $p < 0.05$). Nonetheless, when compared to the TC:water (60:40, v/v) system, it was determined that the percentages of DF extracted from both the LHSS-containing formulation (10 mg/mL DNa; 10 mg/mL LHSS; TC:water; 60:40; v/v, 4.31 ± 1.34%) and the control (10 mg/mL DNa; 0 mg/mL LHSS; TC:water; 60:40; v/v, 4.39 ± 0.95%), were significantly greater ($p < 0.05$).

The total percentage of DF applied that was retained in the membrane and permeated from the DiPG:water (60:40, v/v) system was significantly higher when the counterion was included (10 mg/mL DNa; 10 mg/mL LHSS; DiPG:water; 60:40; v/v), 2.69 ± 1.01%, relative to the control (10 mg/mL DNa; 0 mg/mL LHSS; DiPG:water; 60:40; v/v), 1.02 ± 0.44% ($p < 0.05$). Similarly, these values were significantly lower than those observed for the TC:water solvent system, where the inclusion of LHSS (10 mg/mL DNa; 10 mg/mL LHSS; TC:water; 60:40; v/v) resulted in a total percentage of 5.41 ± 2.21% and the control (10 mg/mL DNa; 0 mg/mL LHSS; TC:water; 60:40; v/v) 4.80 ± 1.08% ($p < 0.05$).

Thus the incorporation of the counterion in the DiPG:water (60:40, v/v) formulations (10 mg/mL DNa; 10 mg/mL LHSS; DiPG:water; 60:40; v/v) significantly increased the

total percentage of DF that moved into and through the skin, when compared to the control (10 mg/mL DNa; 0 mg/mL LHSS; DiPG:water; 60:40; v/v). Conversely, when examining the equivalent TC:water (60:40, v/v) formulations, the addition of LHSS (10 mg/mL DNa; 10 mg/mL LHSS; TC:water; 60:40; v/v) had no significant effect on the total percentage of DF that was extracted from the membrane and permeated. Despite this, the TC:water (60:40, v/v) formulations, whether including or excluding LHSS, resulted in significantly higher percentages of DF that was retained in the membrane and permeated, than the DiPG:water (60:40, v/v) formulations.

An initial analysis of the SPs and their effects on the solute's thermodynamic activity in the solvent system, did not entirely account for the observed results. The calculated [243] and experimentally determined [222] SP for the active (22.65 $MPa^{½}$) is more closely aligned to that of the TC:water binary solvent system (31.83 $MPa^{½}$) than the DiPG:water system (34.73 $MPa^{½}$). Thus, the DiPG:water system would be expected to facilitate greater movement of the active into the skin due to a higher thermodynamic activity of the solute in the solvent system [137]. However, this was not supported by the experimental data. One potential explanation for this discrepancy is that treating the solvent system as a uniform whole overlooks the influence of individual excipients, which may have their own effects [264]. When examined separately, DiPG has a solubility parameter (SP) of 26.54 $MPa^{½}$, while TC has an SP of 21.72 $MPa^{½}$. The value for TC is similar to both the amount estimated for the skin (20.46 $MPa^{½}$) [265] and that determined for the active. Moreover, evidence from various finite-dose IVPT using multiple formulations containing TC as an excipient, supports this idea. In these studies approximately 40–60% of the TC included in the applications was either extracted from the membrane or permeated [266]. As the total recovery of TC was never greater than 1% more than the amount that had partitioned and permeated, the studies were repeated under occlusive conditions. The total recovery of TC increased to between 85 and 93%, with the loss attributed to evaporation [266]. Published data using dynamic vapour sorption (DVS) [267-271] and IVPT studies [267, 271] confirm that TC [268-270] evaporates more rapidly than DiPG [268] due to its higher vapour pressure [272, 273], resulting in an overall lower recovery. Consequently, TC primarily evaporates or penetrates into the skin, whereas DiPG with its lower volatility, remains largely recoverable from the surface [269]. As TC leaves the formulation, whether by skin absorption or evaporation, the relative water content increases. Since the drug is

only sparingly soluble in water [261], this shift enhances its thermodynamic activity [240, 256, 259-262], thereby promoting drug penetration into the skin [256].

Additionally, it has been suggested that TC's lower dielectric constant, 14.10 at 25 °C [245], in contrast to DiPG's higher value, 19.80 at 25 °C [248], suppresses the complete ionisation of salts by promoting ion pairing within the salts themselves [250]. This might reduce the need for the ion pair, LHSS, and could partially explain why there was no significant difference between the TC formulations that contained LHSS and the control (absence of LHSS).

In addition to TC's influence on charge reduction and its impact on the thermodynamic driving force of the active, it has been suggested that TC also acts upon the SC in various ways [250]. It has been associated with an increase in the solubility of actives in the *stratum corneum* [274], and has been shown to interact with several SC proteins and lipids, potentially increasing their mobility [275]. The increased mobility of ceramide headgroups has been linked to a disruption in the packing of the interfacial headgroup regions of the lipid layers [275]. Such disruptions have been associated with an increase in the diffusion of active ingredients [276]. However, such published mechanistic studies do not represent finite dose applications but rather reflect the impact on the SC under saturated conditions [274, 275]. Nonetheless, a number of publications that have considered the distribution of excipients, in addition to the active pharmaceutical ingredient (API), have reported that the permeation of the API has closely followed the permeation of TC in both single [267, 270, 277] and binary [270] solvent systems.

In the present study, the percentage recovery of the DF applied was within the range recommended by the OECD guidelines [88], at 102.55 ± 3.32% for the LHSS-containing formulation (10 mg/mL DNa; 10 mg/mL LHSS; DiPG:water; 60:40; v/v) and 102.41 ± 6.10% for the control (10 mg/mL DNa; 0 mg/mL LHSS; DiPG:water; 60:40; v/v).

8.5.2 Ternary DNa-LHSS loaded miscibility studies

The three solvents in which DNa was most soluble, were selected for use in ternary DNa-LHSS miscibility tests. As DNa was most soluble in TC, non-aqueous fractions comprised TC with either DiPG or PG.

DiPG:TC:water (10:40:50, v/v/v) combinations contained DNa at 7.5 and 5 mg/mL, and L-HSS at 12.5 or 0 mg/mL.

Alternative ternary solvent systems comprised PG:TC:water (10:40:50, v/v/v) and included DNa at 5 mg/mL and L-HSS at either 25 mg/mL, 12.5 or 0 mg/mL. The selected ternary systems were miscible and had no visible precipitation.

8.5.3 Finite dose (10 µL) ternary IVPT and mass balance studies

8.5.3.1 Ternary solvents DiPG:TC:water (10:40:50, v/v/v) containing 7.5 mg/mL DNa and either 12.5 or 0 mg/mL LHSS

As shown in Table 8.2 the addition of LHSS (7.5 mg/mL DNa; 12.5 mg/mL LHSS; DiPG:TC:water; 10:40:50; v/v/v) resulted in an increase of approximately 36% in the permeation of DF (1.48 ± 1.13 µg/cm2 or 2.20 ± 1.68% of DF applied) when compared to the control formulation (1.09 ± 0.82 µg/cm2 or 1.63 ± 1.22% of DF applied, 7.5 mg/mL DNa; 0 mg/mL LHSS; DiPG:TC:water; 10:40:50; v/v/v). This increase was not considered statistically significant ($p > 0.05$). Furthermore, these results were considered comparable to binary permeation experiments using 7.5 mg/mL DNa and combining TC and water (50:50 v/v, $p > 0.05$). As shown in Table 8.S1, the LHSS-containing TC:water binary formulations (7.5 mg/mL DNa; 12.5 mg/mL LHSS; TC:water; 50:50; v/v) resulted in a permeation of 1.49 ± 0.75 µg/cm² (2.24% of the DF applied), while the formulation without LHSS (7.5 mg/mL DNa; 0 mg/mL LHSS; TC:water; 50:50; v/v) showed a permeation of 0.22 ± 0.19 µg/cm² (0.35% of the DF applied, $p > 0.05$).

Table 8. 2 Results for finite dose (10 µL) porcine IVPT. Ternary solvent formulations were prepared with DiPG:TC:water (10:40:50, v/v/v), 7.5 mg/mL DNa and 0 or 12.5 mg/mL LHSS (n = 5; mean ± SD).

Amount DF retained in the membrane and permeated	DiPG:TC:water (10:40:50, v/v/v)	
	DNa 7.5 mg/mL: LHSS 12.5 mg/mL	DNa 7.5 mg/mL: LHSS 0 mg/mL
Cumulative permeation µg/cm^2 at 25 h	1.48 ± 1.13	1.09 ± 0.82
Permeated 25 h %	2.20 ± 1.68	1.63 ± 1.22
Retained on skin surface %	90.87 ± 2.51	94.45 ± 1.40
Retained in membrane %	4.98 ± 0.61	4.76 ± 0.89
Retained in membrane plus permeated %	7.18 ± 1.86	6.39 ± 2.02
Recovery %	98.05 ± 1.60	100.84 ± 2.43
DNa:LHSS molar ratio	1:2.35	1:0

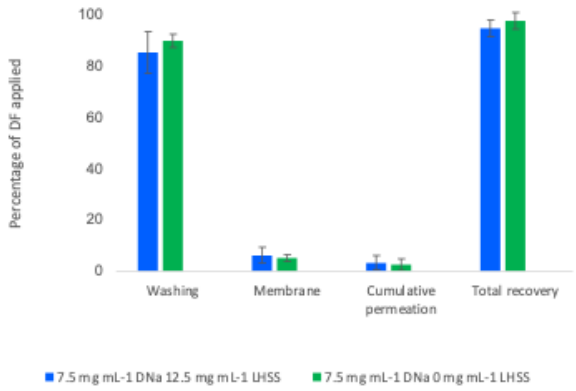

Figure 8. 2 Percentage recovery (mean ± SD) of DF from mass balance studies, following porcine IVPT. Finite doses (10 µL) of the ternary solvent formulations prepared with DiPG:TC:water (10:40:50, v/v/v), containing 7.5 mg/mL DNa and 0 or 12.5 mg/mL LHSS (n = 5; mean ± SD).

Similarly, the percentages of DF extracted from the membrane were comparable for the ternary formulation containing LHSS (7.5 mg/mL DNa; 12.5 mg/mL LHSS; DiPG:TC:water; 10:40:50; v/v/v), 6.37 ± 3.14% and the ternary control (7.5 mg/mL DNa; 0 mg/mL LHSS; DiPG:TC:water; 10:40:50; v/v/v), 5.27 ± 1.37% ($p > 0.05$). No significant differences were observed between LHSS-containing binary (8.14 ± 2.24%, 7.5 mg/mL DNa; 12.5 mg/mL LHSS; TC:water; 50:50; v/v) and ternary (6.37 ± 3.14%, 7.5 mg/mL DNa; 12.5 mg/mL LHSS; DiPG:TC:water; 10:40:50; v/v/v) formulations ($p > 0.05$), or binary (3.95 ± 0.12%, 7.5 mg/mL DNa; 0 mg/mL LHSS; TC:water; 50:50; v/v) and ternary (5.27 ± 1.37%, 7.5 mg/mL DNa; 0 mg/mL LHSS; DiPG:TC:water; 10:40:50; v/v/v) control formulations ($p > 0.05$).

Likewise, the ternary formulation with LHSS (9.66 ± 5.77%, 7.5 mg/mL DNa; 12.5 mg/mL LHSS; DiPG:TC:water; 10:40:50; v/v/v) was comparable to the ternary control (7.83 ± 3.67%, 7.5 mg/mL DNa; 0 mg/mL LHSS; DiPG:TC:water; 10:40:50; v/v/v, $p > 0.05$). This extended to comparisons between the binary (10.38 ± 2.49%, 7.5 mg/mL DNa; 12.5 mg/mL LHSS; TC:water; 50:50; v/v) and ternary (9.66 ± 5.77%, 7.5 mg/mL DNa; 12.5 mg/mL LHSS; DiPG:TC:water; 10:40:50; v/v/v) formulations containing the ion pair ($p > 0.05$). Similarly, the binary (4.30 ± 0.42%, 7.5 mg/mL DNa; 0 mg/mL LHSS; TC:water; 50:50; v/v) and ternary (7.83 ± 3.67%, 7.5 mg/mL DNa; 0 mg/mL LHSS; DiPG:TC:water; 10:40:50; v/v/v) control formulations were also comparable ($p > 0.05$).

The recovery of DF conformed with recommendations outlined in the OECD guidelines [88]. This can be seen in both Table 8.2 and Figure 8.2 representing mass balance

results, which indicate that the recovery of DF was 98.05 ± 1.60% (7.5 mg/mL DNa; 12.5 mg/mL LHSS; DiPG:TC:water; 10:40:50; v/v/v) and 100.84 ± 2.43% (7.5 mg/mL DNa; 0 mg/mL LHSS; DiPG:TC:water; 10:40:50; v/v/v) respectively.

8.5.3.2 Ternary solvents DiPG:TC:water (10:40:50 v/v/v), containing 5 mg mL^{-1} DNa and either 12.5 or 0 mg/mL LHSS

Although the decrease in concentration of DNa resulted in an increase in the DNa:LHSS molar ratio from 1:2.35 to 1:3.5, there was no significant difference in the total percentage of DF that was extracted from the membrane and permeated for the 5 and 7.5 mg/mL DiPG-containing ternary samples ($p > 0.05$).

As shown in Table 8.3 and Figure 8.3 the cumulative permeation of DF for the LHSS-containing ternary formulation with 5 mg/mL DNa (5 mg/mL DNa; 12.5 mg/mL LHSS; DiPG:TC:water; 10:40:50; v/v/v) was 0.21 ± 0.42 μg/cm^2. This value was almost identical to that of the corresponding ternary control formulation (5 mg/mL DNa; 0 mg/mL LHSS; DiPG:TC:water; 10:40:50; v/v/v) which measured 0.21 ± 0.36 μg/cm^2. These amounts represented 0.47 ± 0.93% and 0.48 ± 0.80% of the DF applied, respectively, with no significant difference between them ($p > 0.05$). As shown in Table 8.S1, the binary formulation containing LHSS (1.48 ± 0.65 μg/cm^2, 5 mg/mL DNa; 12.5 mg/mL LHSS; TC:water; 50:50; v/v) resulted in significantly higher permeation values for DF than the equivalent ternary formulation (5 mg/mL DNa; 12.5 mg/mL LHSS; DiPG:TC:water; 10:40:50; v/v/v, $p < 0.05$). However, the results for the control formulations (5 mg/mL DNa; 0 mg/mL LHSS; TC:water; 50:50; v/v, 0.79 ± 0.62 μg/cm2 and 5 mg/mL DNa; 0 mg/mL LHSS; DiPG:TC:water; 10:40:50; v/v/v) were comparable ($p > 0.05$).

Table 8. 3 Results for the finite dose (10 μL) porcine IVPT. Ternary solvent formulations prepared with DiPG:TC:water (10:40:50 v/v/v), 5 mg/mL DNa and 0 or 12.5 mg/mL LHSS. (4 ≤ n ≤ 5; mean ± SD).

Amount DF retained in the membrane and permeated	**DiPG:TC:water (10:40:50 v/v/v)**	
	DNa 5 mg/mL: LHSS 12.5 mg/mL	**DNa 5 mg/mL: LHSS 0 mg/mL**
Cumulative permeation μg/cm^2 at 25 h	0.21 ± 0.42	0.21 ± 0.36
Permeated 25 h %	0.47 ± 0.93	0.48 ± 0.80
Retained on skin surface %	93.49 ± 5.03	93.99 ± 1.75
Retained in membrane %	5.15 ± 1.99	5.71 ± 1.17
Retained in membrane plus permeated %	5.62 ± 2.78	6.20 ± 1.60
Recovery %	99.11 ± 2.31	100.19 ± 1.87
DNa:LHSS molar ratio	1:3.5	1:0

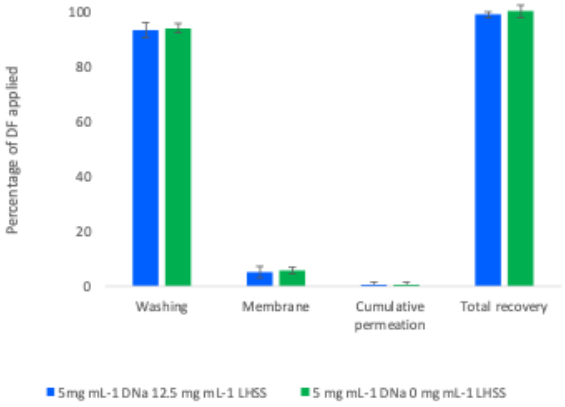

Figure 8. 3 Percentage recovery (mean ± SD) of DF from mass balance studies, following porcine IVPT. Finite doses (10 µL) of the ternary solvent formulations were prepared with DiPG:TC:water (10:40:50 v/v/v), containing 5 mg/mL DNa and 0 or 12.5 mg/mL LHSS (4 ≤ n ≤ 5; mean ± SD).

When examining the percentage of DF extracted from the membrane, no significant differences were detected between the ternary formulation containing LHSS (5.15 ± 1.99%, DiPG:TC:water; 10:40:50; v/v/v) and the corresponding ternary control formulation (5.71 ± 1.17%, 5 mg/mL DNa; 0 mg/mL LHSS; DiPG:TC:water; 10:40:50; v/v/v). However, the percentage of DF retained in the membranes of both ternary formulations (5 mg/mL DNa; 12.5 mg/mL LHSS; DiPG:TC:water; 10:40:50; v/v/v and 5 mg/mL DNa; 0 mg/mL LHSS; DiPG:TC:water; 10:40:50; v/v/v) was significantly lower than that of the equivalent binary formulations (8.79 ± 2.05% , 5 mg/mL DNa; 12.5 mg/mL LHSS; TC:water; 50:50; v/v and 7.60 ± 1.19%, 5 mg/mL DNa; 0 mg/mL LHSS; TC:water; 50:50; v/v, $p < 0.05$).

As with the previous results, the total DF value for the ternary sample containing the ion pair (5 mg/mL DNa; 12.5 mg/mL LHSS; DiPG:TC:water; 10:40:50; v/v/v) was 5.62 ± 2.78%, which was comparable to that of the ternary control formulation (5 mg/mL DNa; 0 mg/mL LHSS; TC:water; 50:50; v/v) which had a value of 6.20 ± 1.60% ($p > 0.05$). Similarly, the total DF value for the ternary control formulation (5 mg/mL DNa; 0 mg/mL LHSS; TC:water; 50:50; v/v) was similar to that of the binary control formulation (5 mg/mL DNa; 0 mg/mL LHSS; TC:water; 50:50; v/v), which resulted in 9.36± 2.49% ($p > 0.05$). However, when LHSS was included, the total DF value for the ternary formulation (5 mg/mL DNa; 12.5 mg/mL LHSS; DiPG:TC:water; 10:40:50; v/v/v) was

significantly lower than that observed for the binary formulation (5 mg/mL DNa; 12.5 mg/mL LHSS; TC:water; 50:50; v/v) which reached 12.26 ± 3.06% ($p < 0.05$).

Similar to the 7.5 mg/mL formulations, no statistically significant differences were observed between the ternary samples ($p > 0.05$). However, the impact of TC replacement was more evident in the 5 mg/mL samples. The inclusion of DiPG significantly reduced the total amount of DF extracted and permeated in the ternary formulation containing LHSS (5.62 ± 2.78%, 5 mg mL^{-1} DNa; 12.5 mg mL^{-1} LHSS; DiPG:TC:water; 10:40:50; v/v/v) compared to the corresponding binary formulation (5 mg mL^{-1} DNa; 12.5 mg mL^{-1} LHSS; TC:water; 50:50; v/v), which reached 12.26 ± 3.06% ($p < 0.05$).

The recovery of DF was consistent with OECD guidelines [88], with 99.11 ± 2.31% recovered for the LHSS-containing preparation (5 mg/mL DNa; 12.5 mg/mL LHSS; DiPG:TC:water; 10:40:50; v/v) and 100.19 ± 1.87% for the control (5 mg/mL DNa; 0 mg/mL LHSS; DiPG:TC:water; 10:40:50; v/v).

8.5.3.3 Ternary solvents PG:TC:water (10:40:50 v/v), containing 5 mg/mL DNa and either 25, 12.5 or 0 mg/mL LHSS

The final ternary system studied maintained the concentration of DNa at 5 mg/mL, while varying the LHSS concentration across the three sample types: 25 mg/mL, 12.5 mg/mL and a control group with no LHSS. The primary modification involved replacing DiPG with PG, resulting in a solvent mixture of PG:TC:water (10:40:50 v/v/v).

Figure 8.4 and Table 8.4 summarise the cumulative permeation data for DF, as well as the results of mass balance investigations. The cumulative permeation of DF from samples containing 25 mg/mL LHSS (5 mg/mL DNa; 25 mg/mL LHSS; PG:TC:water; 10:40:50; v/v/v) amounted to 4.26 ± 1.41 μg/cm^2. This was significantly greater ($p < 0.05$) than the permeation from samples containing 12.5 mg/mL LHSS (1.72 ± 1.06 μg/cm^2, 5 mg/mL DNa; 12.5 mg/mL LHSS; PG:TC:water; 10:40:50; v/v/v) and the control samples (0.66 ± 0.30 μg/cm^2, 5 mg/mL DNa; 0 mg/mL LHSS; PG:TC:water; 10:40:50; v/v/v), which were comparable ($p > 0.05$). These permeation amounts corresponded to 10.33 ± 3.27% (5 mg/mL DNa; 25 mg/mL LHSS; PG:TC:water; 10:40:50; v/v/v), 3.95 ± 2.43% (5 mg/mL DNa; 12.5 mg/mL LHSS; PG:TC:water; 10:40:50; v/v/v) and 1.51 ± 0.69% (5 mg/mL DNa; 0 mg/mL LHSS; PG:TC:water; 10:40:50; v/v/v) of the DF applied.

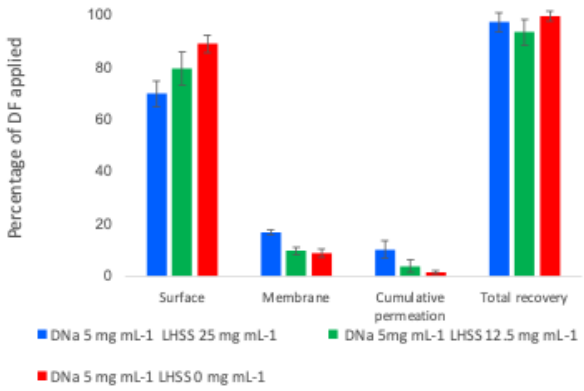

Figure 8. 4 Percentage recovery (mean ± SD) of DF from mass balance studies, following porcine IVPT using 10 µL of the ternary solvent formulations prepared with PG:TC:water (10:40:50 v/v/v), containing 5 mg/mL DNa and 0, 12.5 or 25 mg/mL LHSS (4 ≤ n ≤ 5; mean ± SD).

Table 8. 4 Results for the finite dose (10 µL) porcine IVPT. Ternary solvent formulations prepared with PG:TC:water (10:40:50 v/v/v), 5 mg/mL DNa and 0, 12.5 or 25 mg mL LHSS and (4 ≤ n ≤ 5; mean ± SD).

Amount DF retained in the membrane and permeated	PG:TC:water (10:40:50 v/v/v)		
	DNa 5 mg/mL:LHSS 25 mg/mL	DNa 5 mg/mL:LHSS 12.5 mg/mL	DNa 5 mg/mL:LHSS 0 mg/mL
Cumulative permeation µg/cm^2 at 25 h	4.26 ± 1.41	1.72 ± 1.06	0.66 ± 0.30
Permeated 25 h %	10.33 ± 3.27	3.95 ± 2.43	1.51 ± 0.69
Retained on skin surface %	69.91 ± 4.92	79.53 ± 6.24	88.99 ± 4.21
Retained in membrane %	16.92 ± 1.04	9.87 ± 1.46	8.96 ± 1.49
Retained in membrane plus permeated %	27.25 ± 2.61	13.82 ± 3.57	10.47 ± 2.09
Recovery %	97.16 ± 3.51	93.35 ± 4.76	99.47 ± 2.74
DNa:LHSS molar ratio	1:7.1	1:3.5	1:0

Table 8. 5 Results for the finite dose (10 µL) porcine IVPT using the commercial formulation containing 10 mg/mL DNa (n = 4; mean ± SD).

Amount DF retained in the membrane and permeated	**DNa 10 mg/mL**
Cumulative permeation µg/cm^2 at 24 h	1.74 ± 0.60
Permeated 24 h %	2.10 ± 0.72
Retained on skin surface %	69.91 ± 4.92
Retained in membrane %	6.06 ± 0.67
Retained in membrane plus permeated %	8.20 ± 1.37
Recovery %	102.74 ± 4.23

Figure 8.4 and Table 8.4 summarise the cumulative permeation data for DF, as well as the results of mass balance investigations. The cumulative permeation of DF from samples containing 25 mg/mL LHSS (5 mg/mL DNa; 25 mg/mL LHSS; PG:TC:water; 10:40:50; v/v/v) amounted to 4.26 ± 1.41 μg/cm^2. This was significantly greater ($p < 0.05$) than the permeation from samples containing 12.5 mg/mL LHSS (1.72 ± 1.06 μg/cm^2, 5 mg/mL DNa; 12.5 mg/mL LHSS; PG:TC:water; 10:40:50; v/v/v) and the control samples (0.66 ± 0.30 μg/cm^2, 5 mg/mL DNa; 0 mg/mL LHSS; PG:TC:water; 10:40:50; v/v/v), which were comparable ($p > 0.05$). These permeation amounts corresponded to 10.33 ± 3.27% (5 mg/mL DNa; 25 mg/mL LHSS; PG:TC:water; 10:40:50; v/v/v), 3.95 ± 2.43% (5 mg/mL DNa; 12.5 mg/mL LHSS; PG:TC:water; 10:40:50; v/v/v) and 1.51 ± 0.69% (5 mg/mL DNa; 0 mg/mL LHSS; PG:TC:water; 10:40:50; v/v/v) of the DF applied.

The DF permeation from the PG-containing ternary formulation comprising LHSS at 25 mg/mL (4.26 ± 1.41 μg/cm^2, 5 mg/mL DNa; 25 mg/mL LHSS; PG:TC:water; 10:40:50; v/v/v) was significantly greater than that from any of the 5 mg/mL, 7.5 mg/mL and 10 mg/mL DNa formulations, whether binary (0.14 ± 0.28 - 1.52 ± 0.32 μg/cm^2) or ternary (0.21 ± 0.36 – 1.72 ± 1.06 μg/cm^2) solvent systems were used.

Furthermore, this ternary formulation (5 mg/mL DNa; 25 mg/mL LHSS; PG:TC:water; 10:40:50; v/v/v) resulted in approximately 2.5 times (145% more) the DF permeation of a commercial 1% DNa formulation (1.74 ± 0.6 μg/cm² at 24 h) under finite dose conditions, as shown in Table 8.5. Notably, this was observed despite containing only half the active concentration of the commercial formulation. When expressed as a percentage of the DF applied, permeation from the ternary formulation (10.33 ± 3.27%, 5 mg/mL DNa; 25 mg/mL LHSS; PG:TC:water; 10:40:50; v/v/v) was significantly greater than that from the commercial formulation (2.10 ± 0.72%, $p < 0.05$).

No significant difference was observed in DF permeation between the PG-ternary formulations containing 12.5 mg/mL LHSS (1.72 ± 1.06 μg/cm^2, 5 mg/mL DNa; 12.5 mg/mL LHSS; PG:TC:water; 10:40:50; v/v/v) or no LHSS (0.66 ± 0.30 μg/cm^2, 5 mg/mL DNa; 0 mg/mL LHSS; PG:TC:water; 10:40:50; v/v/v) and the equivalent 5 mg/mL DNa DiPG-ternary formulations (0.21 ± 0.42 μg/cm^2, 5 mg/mL DNa; 12.5 mg/mL LHSS; DiPG:TC:water; 10:40:50; v/v/v and 0.21 ± 0.36 μg/cm^2, 5 mg/mL DNa; 0 mg/mL LHSS; DiPG:TC:water; 10:40:50; v/v/v $p > 0.05$).

Membrane retention of DF was 16.92 ± 1.04%, 9.87 ± 1.46% and 8.96 ± 1.49% of the DF applied for PG-containing ternary samples with 25 mg/mL, 12.5 mg/mL and 0 mg/mL LHSS respectively. The total percentage of DF recovered through extraction from the membrane and permeation was significantly higher for the 25 mg/mL LHSS formulation (27.25 ± 2.61%, 5 mg/mL DNa; 25 mg/mL LHSS; PG:TC:water; 10:40:50; v/v/v, $p < 0.05$) than for the 12.5 mg/mL LHSS (13.82 ± 3.57%, 5 mg/mL DNa; 12.5 mg/mL LHSS; PG:TC:water; 10:40:50; v/v/v) and control (10.47 ± 2.09%, 5 mg/mL DNa; 0 mg/mL LHSS; PG:TC:water; 10:40:50; v/v/v) formulations, which were comparable ($p > 0.05$).

The percentage of DF extracted from the membrane, as well as the total percentage of DF retained in the membrane and permeated, were significantly greater for the PG ternary formulation containing 25 mg/mL LHSS (16.92 ± 1.04% and 27.25 ± 2.61%, 5 mg/mL DNa; 25 mg/mL LHSS; PG:TC:water; 10:40:50; v/v/v) than for other binary and ternary formulations (0.87 ± 0.23% - 8.79 ± 2.05% and 1.02 ± 0.44% - 12.26 ± 3.06%), with only one exception. The binary TC:water formulation also containing 25 mg/mL LHSS (5 mg/mL DNa; 25 mg/mL LHSS; TC:water; 50:50; v/v), was considered comparable for these values (11.00 ± 7.21% and 14.49 ± 7.76%, $p > 0.05$).

When compared to the commercial formulation, the PG ternary formulation (5 mg/mL DNa; 25 mg/mL LHSS; PG:TC:water; 10:40:50; v/v/v) showed significantly greater membrane retention (16.92 ± 1.04% VS 6.06 ± 0.67%) and total DF extracted from the membrane and permeated (27.25 ± 2.61% VS 8.20 ± 1.37%, $p < 0.01$).

Furthermore, the percentages of DF retained within the membrane, and the total DF retained plus permeated, were significantly greater from the PG-ternary formulations with either 12.5 mg/mL LHSS (9.87 ± 1.46% and 13.82 ± 3.57%, 5 mg/mL DNa; 12.5 mg/mL LHSS; PG:TC:water; 10:40:50; v/v/v) or no LHSS (8.96 ± 1.49% and 10.47 ± 2.09%, 5 mg/mL DNa; 0 mg/mL LHSS; PG:TC:water; 10:40:50; v/v/v) when compared to other DiPG-ternary (5.62 ± 2.78% - 7.18 ± 1.86%) systems ($p < 0.05$). However, no significant difference was observed when comparing these PG-ternary formulations (5 mg/mL DNa; 12.5 mg/mL LHSS; PG:TC:water; 10:40:50; v/v/v and 5 mg/mL DNa; 0 mg/mL LHSS; PG:TC:water; 10:40:50; v/v/v) with TC:water (50:50 v/v) binary samples (5 mg/mL DNa; 12.5 mg/mL LHSS; TC:water; 50:50; v/v and 5 mg/mL DNa; 0 mg/mL LHSS; TC:water; 50:50; v/v), in which case the values ranged from 8.14 ± 2.24% -

11.00 ± 7.21% for membrane retention, and 10.38 ± 2.49% - 14.49 ± 7.76% for total DF recovery from membrane retention and permeation ($p > 0.05$).

The replacement of 10 % (v/v) DiPG with 10 % (v/v) PG had significant effects on the amounts of DF retained in the membrane, as well as the combined amounts attributable to membrane extraction and permeation ($p < 0.05$).

While the impact of the dielectric constant values of solvents should always be considered when investigating ion pair behaviour [46, 149], the replacement of DiPG [248] with PG [278] would be unlikely to facilitate ion pairing due to its higher value. Furthermore, while the slightly higher SP value for the PG-ternary system (35.06 $MPa^{1/2}$), relative to the DiPG-ternary system (34.84 $MPa^{1/2}$), may contribute to the increased uptake of DF, analysis of the individual solvents suggests a more complex account. Notwithstanding its SP of 28 $MPa^{½}$, PG was found to be a more effective solubiliser for the active (SP 22.65 $MPa^{1/2}$) [222, 243] than DiPG, which has a SP value of 26.54 $MPa^{½}$. This higher affinity should correspond to a reduction in the thermodynamic activity of the active in the solvent system [137]. However, although the skin's SP [265] is more closely aligned with DiPG than PG, finite dose studies investigating excipient behaviour produced results contrary to these numerical predictions. Specifically, single-solvent studies showed that 98.9% of DiPG remained on the skin surface after 48 hours, compared to less than 7% of PG [267]. While this result may be attributed in part to evaporation, due to PG's higher vapour pressure [279] relative to DiPG's [273], the quantities of solvent that moved into and through the membrane suggested a greater affinity between PG and the skin than between DiPG and the skin [267]. This movement of PG into the skin combined with possible evaporation could contribute to an increase in the water portion of the solvent system. As DF is sparingly soluble in water [261] this would enhance its thermodynamic activity in the changing vehicle, and promote its rate of penetration into the SC.

The mechanism of action of PG has been widely debated. It has been suggested that it enhances drug solubility in the skin [280-282], influences partitioning behaviour of actives [281, 282], and disrupts the barrier properties of the SC under occluded infinite dose conditions [283].

It has also been proposed that PG facilitates the movement of drugs through the skin by solvating alpha-keratin and inhabiting hydrogen-bonding sites, resulting in a

reduction to drug-membrane bonds [284]. Differential scanning calorimetry (DSC) studies in human skin suggest that PG behaves like water, forming hydrogen-bonds with polar head groups. This results in a loosening of the lipid packing and a reduction in intermolecular forces, potentially facilitating drug migration [284]. Findings on PG's impact on lipid organisation remain inconsistent. Bouwstra *et al* [285] proposed that PG and water integrate into polar head group regions without altering bilayer spacing, while Brinkman and Müller-Goymann observed vertical and horizontal integration, resulting in an increase in the distance between the repeating bilayers [286]. In contrast, Moghadam and colleagues found that PG resulted in no structural changes to SC lipids [287]. More recently, however, Synchrotron-Based Fourier Transform Infrared Spectroscopy indicated that PG resulted in alterations to the bilayer structure of intercellular lipids, with disorder occurring on an increasing basis from the *stratum corneum* to the deeper regions of the viable epidermis and the dermis [288].

Despite the variable explanations for its mechanism of action, PG is widely used in topical formulations, with percutaneous absorption frequently reported [267, 271, 289-292]. It has been used to increase the solubility of actives and as a permeation enhancer [42, 142, 269, 270, 280, 284, 288, 293-295]. It has also been proposed as a "carrier solvent", provided the PG was able to partition out of the formulation and into the skin [289].

Various infinite [281, 282, 296] and finite dose [293] studies using human skin have reported correlations between PG application and drug permeation. This has been confirmed using confocal raman spectroscopy (CRS) [297].

When PG was combined with water in infinite dose *in vivo* [281] and *in vitro* [282, 298] applications, the permeation of various compounds were shown to increase with rising concentrations of PG. Furthermore, PG has demonstrated synergistic effects when combined with other permeation enhancers such as terpenes [299], fatty acids [296] and amides [284]. It is unsurprising therefore that the combination of PG and TC has been reported to enhance the uptake of active pharmaceutical ingredients, when compared to the individual solvents, in finite dose applications [270, 295, 300]. PG, which permeates more gradually than TC [267], has also been shown to augment the permeation of TC [270]. Our studies demonstrate the significant increase in the total percentage of DF moving into and through the membrane for all ternary samples containing PG (PG:TC:water; 10:40:50; v/v/v) relative to all binary and ternary

formulations containing DiPG (DiPG:water; 60:40; v/v and DiPG:TC:water; 10:40:50; v/v/v).

The synergistic behaviour of TC and PG also helps to explain the increase in permeation of DF from the ternary formulation containing PG and LHSS at 25 mg/mL LHSS (5 mg/mL DNa; 25 mg/mL LHSS; PG:TC:water; 10:40:50; v/v/v) relative to the binary formulation that contained no PG (5 mg/mL DNa; 25 mg/mL LHSS; TC:water; 50:50; v/v).

As shown in Figure 8.4, recovery of DF through mass balance studies was within the guidelines set by the OECD [88]. The amount of DF was 97.16 ± 3.51% for the 25 mg/mL LHSS samples (5 mg/mL DNa; 25 mg/mL LHSS; PG:TC:water; 10:40:50; v/v/v), 93.35 ± 4.76% for the 12.5 mg/mL LHSS samples (5 mg/mL DNa; 12.5 mg/mL LHSS; PG:TC:water; 10:40:50; v/v/v) and 99.47 ± 2.74% for the control samples (5 mg/mL DNa; 0 mg/mL LHSS; PG:TC:water; 10:40:50; v/v/v).

8.6 Conclusions

The aim of this study was to continue the investigation into the impact of solvents on DNa:LHSS ion pair formulations. Replacing TC with DiPG resulted in a binary solvent system comprising DiPG and water (60:40 v/v). While the inclusion of the counterion in the DiPG formulation (10 mg/mL DNa; 10 mg/mL LHSS; DiPG:water; 60:40; v/v) significantly enhanced the total percentage of DF that passed into and through the skin, when compared to the DiPG control (10 mg/mL DNa; 0 mg/mL LHSS; DiPG:water; 60:40; v/v), the solvent substitution significantly reduced the membrane retention and total DF extracted from the membrane and permeated when compared to the original TC formulations (10 mg/mL DNa; 10 mg/mL or 0 mg/mL LHSS; TC:water; 60:40; v/v, $p < 0.05$).

The investigation into the use of ternary systems produced further insights. When considering the 7.5 mg/mL DNa formulations, the inclusion of DiPG had no significant effect on the movement of DF into and through porcine skin, whether comparing L-HSS-containing ternary and binary preparations (7.5 mg/mL DNa; 12.5 mg/mL LHSS; DiPG:TC:water; 10:40:50; v/v/v and 7.5 mg/mL DNa; 12.5 mg/mL LHSS; TC:water; 50:50; v/v, $p > 0.05$) or their controls (7.5 mg/mL DNa; 0 mg/mL LHSS; DiPG:TC:water; 10:40:50; v/v/v and 7.5 mg/mL DNa; 0 mg/mL LHSS; TC:water; 50:50; v/v, $p > 0.05$).

For the ternary system comprising 5 mg/mL DNa, the effects of replacing TC with DiPG were more apparent. At this concentration of DNa, amounts of DF moving into and through the membrane from the LHSS-containing ternary formulation (5 mg/mL DNa; 12.5 mg/mL LHSS; DiPG:TC:water; 10:40:50; v/v/v) were significantly less than from the binary TC:water formulation containing the counterion (5 mg/mL DNa; 12.5 mg/mL LHSS; TC:water; 50:50; v/v, $p < 0.05$).

In contrast to DiPG, which exhibited some limiting effects on the percutaneous delivery of DF, its substitution with PG (10% v/v), resulted in significant improvements. These included higher percentages of DF retained in the membrane and increased total values attributed to membrane extraction and permeation, compared to all DiPG binary and ternary formulations ($p < 0.05$).

Moreover, the addition of LHSS in the ternary formulation containing PG (5 mg/mL DNa; 25 mg/mL LHSS; PG:TC:water; 10:40:50; v/v/v) resulted in significantly higher DF permeation values than any other binary or ternary formulation ($p < 0.05$). It also delivered approximately 2.5 times (145%) more DF when compared to a commercial 1% DNa formulation, despite containing only half the DNa concentration.

Additionally, the PG ternary formulation containing 25 mg/mL LHSS produced the highest total DF total uptake as a percentage of the applied dose ($p < 0.05$), comparable only to the one other preparation which contained LHSS at the same 25 mg/mL concentration (5 mg/mL DNa; 25 mg/mL LHSS; TC:water; 50:50; v/v).

When examining the impact of solvent substitutions in formulations containing TC and DiPG, the analysis of individual solvents revealed complexities beyond those predicted by the SP of the overall solvent system. Such an approach would overlook the influence of individual excipients, which may exert their own effects. Instead, when evaluated separately, TC has a SP more closely aligned with DNa and the skin, than DiPG.

A similar approach was required when analysing PG and DiPG in ternary systems. Despite PG's lower predicted affinity for both the active and the skin relative to DiPG, PG proved to be a more effective solvent for DNa. Like TC, PG's ability to penetrate into the skin coupled with its higher volatility relative to DiPG, may contribute to an increase in the water content of the system. This in turn would increase the

thermodynamic activity of DNa in the changing vehicle, as it is sparingly soluble in water, thereby increasing its rate of penetration into the SC.

An assessment of dielectric constant values showed that TC's lower dielectric constant is more effective at both suppressing ionisation and promoting ion pairing, than DiPG. In contrast, while PG has a higher dielectric constant value than DiPG, any influence in the ternary system may be limited by its relatively low proportion in the solvent composition (10% v/v).

This work demonstrates how passive enhancement methods, such as counterion use and solvent selection, can be effectively combined to improve the percutaneous delivery of a topically applied pharmaceutical salt. A non-toxic, economical, and sustainably produced counterion was identified, which significantly increased DF penetration. The role of various solvents in maximising the solubility of the API and counterion was also explored, focusing on their potential as permeation enhancers and their impact on the thermodynamic activity of the API within formulations.

Using a commercial formulation as a benchmark suggests that this approach could reduce the required API concentration in formulations, offering both economic and environmental advantages. Future work could involve optimising the current formulations by experimenting with additional solvents to improve the solubility and stability of the API within the formulation. Supplementary adjustments to the concentration of LHSS could further enhance the delivery of the API. In addition, this approach could serve as a versatile framework for other topically applied NSAIDs. This includes APIs formulated as salts (e.g., ketorolac tromethamine) or those that undergo ionisation, expanding the potential applications of the method to a wider range of drugs with similar delivery challenges.

8.7 Abbreviations

Acetonitrile	ACN
Active pharmaceutical ingredient	API
Analysis of variance	ANOVA
Diclofenac	DF
Diclofenac sodium	DNa

Differential scanning calorimetry	DSC
Dipropylene glycol	DiPG
Dynamic vapour sorption	DVS
L-histidine monochloride monohydrate	LHSS
International Conference on Harmonisation Expert Working Group	ICH
In vitro permeation testing	IVPT
Non-steroidal anti-inflammatory drugs	NSAIDs
Osteoarthritis	OA
Phosphate buffered saline	PBS
Propylene glycol	PG
Solubility parameters	SP
Standard deviation	SD
Transcutol®	TC
Trifluoroacetic acid	TFA

8.8 Funding

This research received no external funding.

8.9 Conflicts of interest

The authors declared no conflict of interest.

8.10 Supplementary information

8.10.1 Results from previous binary studies

Table 8.S 1 Results for the finite dose (10 µL) porcine IVPT using binary solvent formulations prepared of TC and water. Formulations were prepared with TC:water at 50:50 (v/v), containing 5 or 7.5 mg/mL DNa and 0, 12.5 or 25 mg/mL LHSS; and TC:water at 60:40 (v/v), containing 10 mg/mL DNa and 0 or 10 mg/mL LHSS.Data are presented as mean ± SD) (3 ≤ n ≤ 5).

Amount DF retained in the membrane and permeated	DNa 5 mg/mL:LHSS 25 mg/mL	DNa 5 mg/mL:LHSS 12.5 mg/mL	DNa 5 mg/mL:LHSS 0 mg/mL	DNa 7.5 mg/mL:LHSS 12.5 mg/mL	DNa 7.5 mg/mL:LHSS 0 mg/mL	DNa 10 mg/mL:LHSS 10 mg/mL	DNa 10 mg/mL:LHSS 0 mg/mL
Cumulative permeation µg/cm^2 at 25 h	1.52 ± 0.32	1.48 ± 0.65	0.79 ± 0.62	1.49 ± 0.76	0.22 ± 0.19	1.01 ± 0.91	0.36 ± 0.44
Permeated 25 h %	3.49 ± 0.73	3.47 ± 1.56	1.76 ± 1.37	2.24 ± 1.15	0.35 ± 0.30	1.10 ± 0.98	0.41 ± 0.49
Retained on the skin surface %	65.53 ± 17.57	84.28 ± 2.90	85.02 ± 5.83	88.18 ± 4.41	94.64 ± 5.66	93.55 ± 1.90	93.43 ± 5.49
Retained in the membrane %	11.00 ± 7.21	8.79 ± 2.05	7.60 ± 1.19	8.14 ± 2.24	3.95 ± 0.12	4.31 ± 1.34	4.39 ± 0.95
Retained in membrane plus permeated %	14.49 ± 7.76	12.26 ± 3.06	9.36 ± 2.49	10.38 ± 2.49	4.30 ± 0.42	5.41 ± 2.21	4.80 ± 1.08
Recovery %	80.02 ± 11.39	96.54 ± 1.81	94.38 ± 6.01	98.56 ± 4.89	98.94 ± 6.08	98.96 ± 0.86	98.23 ± 5.13
DNa:LHSS molar ratio	1:7.1	1:3.5	1:0	1:2.35	1:0	1:1.41	1:0

8.10.2 Confirmation of ion pairs using FT-IT spectroscopy

8.10.2.1 Methods

Formation of DNa:LHSS salt

Equimolar amounts of DNa and LHSS were dissolved in deionised water to form a homogeneous aqueous solution. An equal volume of chloroform was added to this solution. The mixture was shaken overnight on a Stuart Orbital Incubator S150 (Cole-Parmer, Staffordshire, UK) at 25°C at 225 rpm to promote interaction between DNa and LHSS.

Following the shaking period, the mixture was transferred to a separating funnel and allowed to settle until the layers clearly separated. The lower chloroform layer was carefully collected and placed in a fume hood to evaporate at room temperature. Upon complete evaporation of the chloroform, a solid residue identified as the DNa:LHSS salt was obtained.

To monitor the efficiency of extraction and ensure complete transfer of components into the organic phase, the aqueous layer was sampled before, during and at the end of the extraction. These samples were analysed using high-performance liquid

chromatography (HPLC), to confirm the partition of diclofenac from the aqueous into the organic phase.

The three salts, LHSS, DNa and DNa:LHSS were analysed using FT-IR. Spectra were recorded on an Agilent Technologies Cary 630 FT-IR spectrophotometer (Agilent, Santa Clara, CA, USA).

8.10.2.2 Results and discussion

L-histidine salt

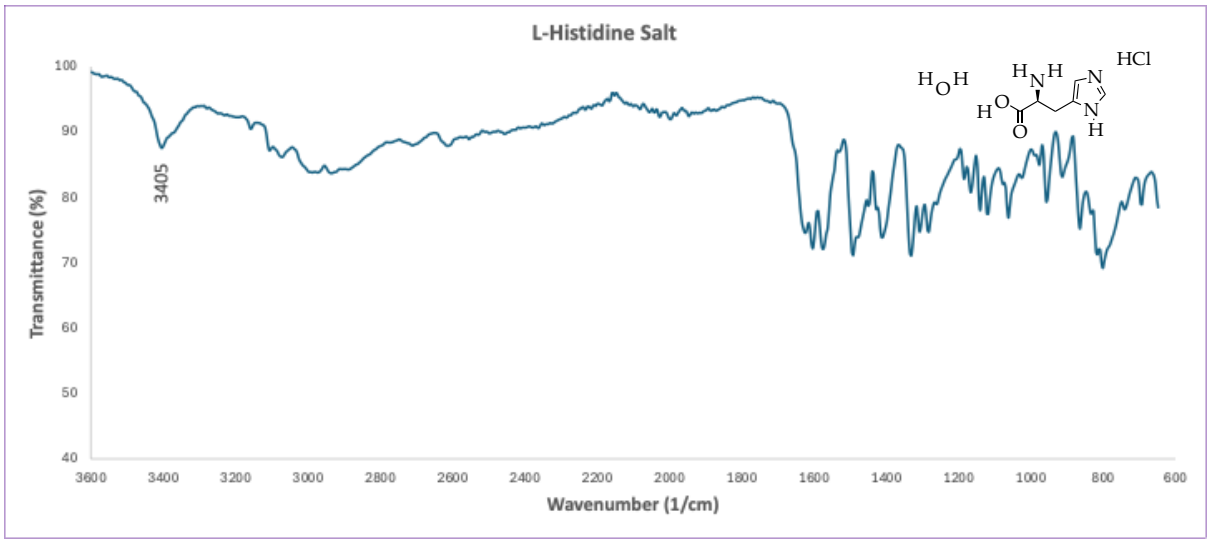

Figure 8.S 1 FT-IR spectrum of L-histidine salt.

Reference peak:

3405 cm^{-1}:sharp N-H stretch from protonated amino group and/or imidazole NH^+

The fingerprint region is quite congested with many absorptions. There is some overlap and clustering that occurs.

~1600-1550 cm^{-1}:Strong absorption (carboxylate asymmetric stretch) - visible as intense peaks

~1400 cm^{-1}:Prominent peak (carboxylate symmetric stretch) - clearly visible

~1300-1200 cm^{-1}:Multiple overlapping peaks of varying intensities (C-N stretches, imidazole vibrations)

~1100-900 cm^{-1}:Series of medium-intensity peaks (C-H bending, ring deformations)

Diclofenac sodium

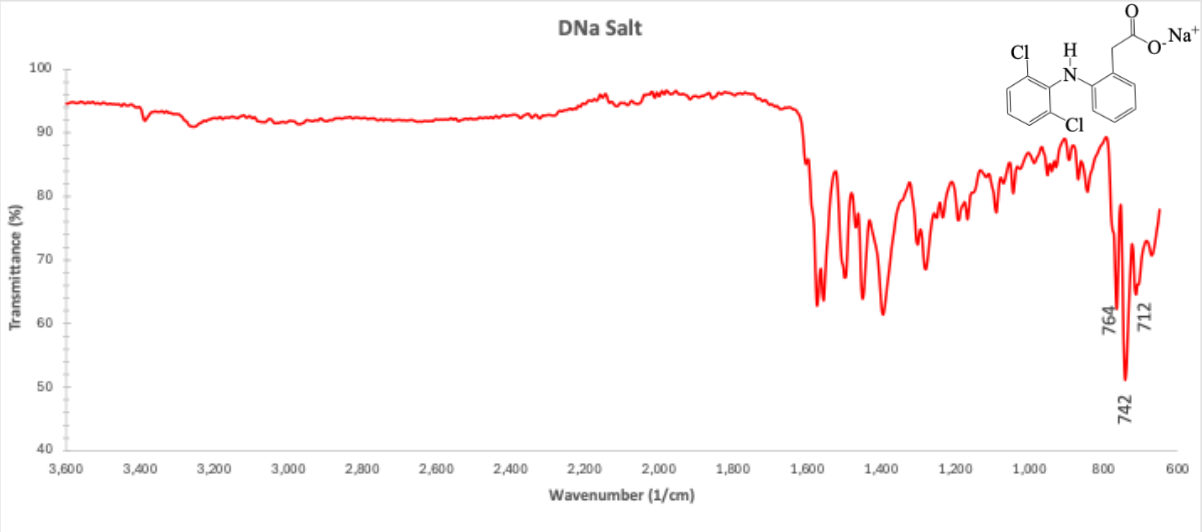

Figure 8.S 2 FT-IR spectrum of diclofenac sodium.

N-H Stretching Region: DNa is very flat, with almost no absorption in 3200-3600 cm^{-1} region

Fingerprint region is less complex than LHSS salt, however there are several distinct, peaks

~1600-1580 cm^{-1}: Strong sharp peak, COO^- asymmetric stretch

~1500-1450 cm^{-1}: Aromatic C=C stretches (benzene rings), clearly separated

~1400 cm^{-1}: Distinct COO^- symmetric stretch

~1300-1250 cm^{-1}: Sharp, isolated C-N stretches (aniline portion)

712, 742, and 764 cm^{-1}: **Multiple C-Cl stretches** from dichloroaniline portion, with 742 cm^{-1} being the most intense

DNa:LHSS salt

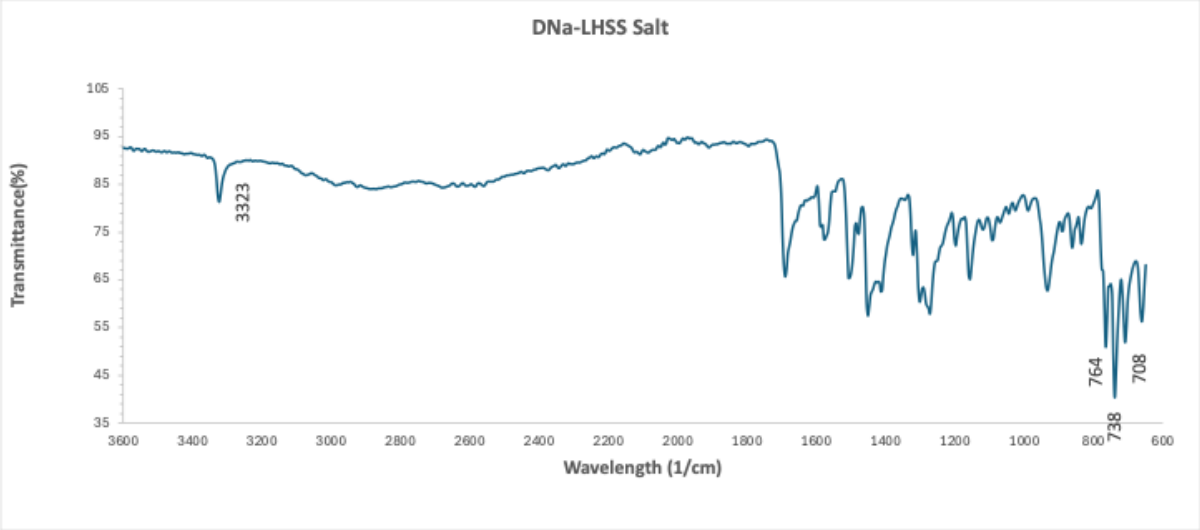

Figure 8.S 3 FT-IR spectrum of DNa-LHSS salt.

N-H stretching changes:

L-histidine salt: Sharp peak at ~3405 cm^{-1}

DNa-LHSS salt: Sharp peak at ~3323 cm^{-1}

The appearance of N-H stretching in the ion pair confirms histidine incorporation

The shift from 3405 to **3323 cm^{-1}** may be due to the histidine N-H groups being in a different hydrogen bonding environment due to interaction with the diclofenac carboxylate rather than chloride ions.

Fingerprint region (800-1600 cm^{-1}):

Combines features from both molecules. It shows a congested pattern similar to histidine but with some of the sharp, well-defined peaks characteristic of diclofenac

~1600-1400 cm^{-1}: Complex overlapping pattern (both carboxylate environments)

~800-750 cm^{-1}: Retains the characteristic diclofenac C-Cl stretch at 764, 738 and 708 cm^{-1}.

The FTIR evidence demonstrates successful ion pair formation between DNa and LHSS. The significant N-H frequency shift (from 3405 cm^{-1} - 3323 cm^{-1}) indicates histidine N-H groups are hydrogen bonding with diclofenac carboxylate rather than chloride ions. While there is a slight shift in some of the C-Cl frequencies (742 - 738

cm^{-1} and 712 - 708 cm^{-1}), with the 764 cm^{-1} remaining unchanged, the retention of characteristic C-Cl stretches confirms diclofenac incorporation in a new molecular environment consistent with ion pair formation. The altered complexity of the fingerprint region further suggests molecular interaction, rather than physical mixing.

Importantly, LHSS is only soluble in water, while DNa has minimal solubility in chloroform (0.3 mg/mL at 32°C). The formation of a chloroform-soluble product from these water-soluble starting materials provides compelling evidence for the creation of a new chemical entity with fundamentally altered physicochemical properties.

This is further supported by HPLC analysis of the aqueous phase, which confirmed progressive reduction in diclofenac concentration over the extraction period, indicating ongoing ion pair formation and transfer to the organic phase.

Together the spectroscopic evidence, altered solubility properties and extraction behaviour provides robust confirmation of successful DNa:LHSS ion pair formation.

9 Conclusion

This thesis achieved its primary aim of exploring a novel amino acid-based ion pair strategy to enhance the percutaneous delivery of DF. Through a systematic investigation of rationally selected counterions and solvents, followed by strategic formulation development, the work establishes a framework for amino acid ion pairing. This approach addresses the fundamental challenge of limited skin penetration in topical pharmaceutical formulations containing ionised active pharmaceutical ingredients.

All research objectives outlined in Chapter 2 were achieved, following a logical investigative progression. Essential context was provided in Chapter 3 by examining the skin as both a pathway and destination for drug delivery (objective 2.1.2.1). Chapter 4 established the theoretical foundation via a comprehensive review of ion pairs for topical applications (objective 2.1.2.2).

Building on this foundation, the experimental work began in Chapter 6 with the identification of potential amino acid counterion candidates based on size, toxicity and charge compatibility criteria (objective 2.1.2.5). Distribution coefficient studies were then used to assess their effectiveness in enhancing DF partitioning from aqueous to organic phases (objective 2.1.2.6). These experiments identified LHSS as the optimal counterion for DNa, resulting in more than an 8-fold increase in the distribution coefficient when a 50 times molar ratio of LHSS was used (121.43 ± 14.56 compared to 14.79 ± 0.31 for DNa alone). This was subsequently validated through porcine skin IVPT (objective 2.1.2.7). When formulations contained 100 µg/mL DF, the application of DNa:LHSS (1:50) showed more than a 10-fold increase in permeation (5.39 ± 1.00 µg/cm^2/h) compared with no LHSS (0.5 ± 0.2 µg/cm^2/h).

Chapter 7 commenced by addressing critical solubility challenges. DNa solubility was assessed across a range of pharmaceutical solvents, identifying TC, PG and DiPG as the most suitable based on their favourable solubility-miscibility profiles (objective 2.1.2.8). These outcomes informed the development of a model TC:water binary system capable of accommodating both DNa and the counterion LHSS, while maintaining formulation stability (objective 2.1.2.9). Subsequent IVPT using this binary system confirmed that incorporating LHSS with DNa increased DF permeation. For example, the addition of 12.5 mg/mL LHSS to a formulation containing 7.5 mg/mL DNa

increased the permeation of DF to 1.49 ± 0.76 μg/cm^2/h relative to 0.22 ± 0.19 μg/cm^2/h for the control, representing a 6.8-fold enhancement. Total permeation and retention improved from 4.30 ± 0.42% to 10.38 ± 2.49% ($p < 0.05$).

Formulation optimisation was pursued in Chapter 8, beginning with investigations into the impact of solvent substitution within the binary system (objective 2.1.2.10). These solvent substitution studies revealed that individual solvent properties, rather than overall system solubility parameters (SP), governed formulation performance. This was confirmed in the ternary solvent systems, which formed the next stage of optimisation (objective 2.1.2.11). After evaluating DiPG-containing ternary systems and subsequently testing PG in place of DiPG with varying LHSS concentrations, the optimal formulation was developed. This formulation (PG:TC:water; 10:40:50 v/v/v) containing 5 mg/mL DNa and 25 mg/mL LHSS was compared to a commercial 1% DNa product (objective 2.1.2.12). Finite dose IVPT showed that 145% more DF permeated from the PG:TC:water; 10:40:50 v/v/v system comprising 5 mg/mL DNa and 25 mg/mL LHSS (4.26 ± 1.41 μg/cm^2/h), than from the commercial 1% DNa product (1.74 ± 0.6 μg/cm^2/h) despite using only half the DNa concentration ($p < 0.05$).

Supporting these investigations, various characterisations were undertaken throughout the work. ^{1}H NMR spectroscopy was used in Chapter 6 to confirm DF synthesis (objective 2.1.2.4), while FT-IR spectroscopy was employed in Chapter 8 as additional confirmation to IVPT of successful ion pair formation (objective 2.1.2.13).

Beyond these quantitative outcomes, several mechanistic insights, relevant to ion-pair formulation design, emerged. Most significantly, solubility parameter approaches alone that treat solvent combinations as uniform entities, appeared ineffective in predicting formulation performance for ion pair systems. When examining the impact of solvent substitutions in preparations containing TC and DiPG, the analysis of individual solvents revealed complexities not predicted by the SP of the overall solvent system. Instead, when evaluated separately, TC exhibited a SP more closely aligned with DNa (22.65 MPa$^{1/2}$) and skin (20.46 MPa$^{1/2}$) than DiPG, explaining its superior performance despite overall predictions suggesting otherwise.

A similar principle governed the behaviour of PG and DiPG in ternary systems. Despite PG's lower predicted affinity for both the active and skin relative to DiPG, replacing DiPG with PG in the ternary system proved more effective for DNa delivery. This

enhanced performance resulted from PG's ability to penetrate into the skin coupled with its higher volatility relative to DiPG, contributing to an increase in the water content of the system. As DNa is sparingly soluble in water, this shift enhanced DNa's thermodynamic activity within the changing vehicle, thereby increasing its rate of penetration into the *stratum corneum*.

An assessment of dielectric constant values provided additional insights into ion pair stability and formation. The inclusion of organic solvents reduced the overall dielectric constant of the aqueous system, promoting ion pair formation by decreasing the electrostatic interference from the solvent environment. While DiPG (19.80 at 25°C) and PG (28.95 at 25°C) exhibited higher dielectric constants than TC (14.10 at 25°C), all organic solvents remained significantly lower than water (78.3 at 25°C), contributing to enhanced ion pair stability within the formulations.

The integration of these findings shows how passive enhancement methods, in this case counterion selection and solvent optimisation, can be effectively combined to improve the percutaneous delivery of topically applied pharmaceutical salts. Identifying LHSS as a non-toxic, economical and sustainably produced counterion that significantly enhances DF penetration demonstrates the potential of amino acid-based approaches in topical drug delivery.

Building on the framework established in this work, future research could pursue several directions. Formulation optimisation could be advanced by evaluating a wider range of solvents to enhance both solubility and stability of APIs and counterions. Fine-tuning LHSS concentrations could further improve delivery efficiency, while complementary stability studies under varied storage conditions would provide critical insights for practical implementation.

Beyond the present model compound, the amino acid ion-pairing strategy could be applied to a broader range of topically administered pharmaceuticals. Logical candidates include other ionisable NSAIDs (e.g., ketorolac tromethamine) and pharmaceutical salts that undergo ionisation. Extending this framework could lead to more predictive strategies for rational solvent selection in topical applications.

This approach offers substantial environmental and economic benefits without compromising therapeutic efficacy. By reducing the API concentration by half whilst achieving 145% greater DF permeation than the commercial product, this strategy

could significantly minimise pharmaceutical waste entering the environment. This reduction of drug use aligns with the environmental initiatives of major pharmaceutical companies including AstraZeneca, Novartis and Roche, who are committed to reducing pharmaceutical residues in the environment where possible. Economic benefits include immediate reduction of expensive raw material costs through lower API requirements whilst maintaining superior therapeutic performance. Finally, this strategy leverages existing compounds and excipients, offering a regulatory-compliant alternative to developing novel compounds.

10 References

1. *Martindale: The Complete Drug Reference*. 39th ed. Edited by Brayfield, A. London: London Pharmaceutical Press, 2017, 1 - 4160.
2. Grand Review Research. *Non-Steroidal Anti-Inflammatory Drugs Market Size, Share & Trends Analysis Report by Disease Indication (Arthritis, Ophthalmic Diseases), by Route of Administration, by Distribution Channel, by Region, and Segment Forecasts, 2025–2030.* 2024. https://www.grandviewresearch.com.
3. Barkin, R. L. "Topical Nonsteroidal Anti-Inflammatory Drugs: The Importance of Drug, Delivery, and Therapeutic Outcome." *American Journal of Therapeutics* 22 (2015): 388-407. https://doi.org/10.1097/MJT.0b013e3182459abd.
4. Evans, J., McGregor, E., McMahon, A. D., McGilchrist, M. M., Jones, M. C., White, G., McDevitt, D. G. and MacDonald, T. M. "Non-Steroidal Anti-Inflammatory Drugs and Hospitalization for Acute Renal Failure." *QJM: An International Journal of Medicine* 88 (1995): 551-57. https://doi.org/10.1186/s12882-017-0673-8.
5. Pirmohamed, M., James, S., Meakin, S., Green, C., Scott, A. K., Walley, T. J., Farrar, K., Park, B. K. and Breckenridge, A. M. "Adverse Drug Reactions as Cause of Admission to Hospital: Prospective Analysis of 18 820 Patients." *British Medical Journal* 329 (2004): 15-19. https://doi.org/10.1136/bmj.329.7456.15.
6. Schmiedl, S., Rottenkolber, M., Hasford, J., Rottenkolber, D., Farker, K., Drewelow, B., Hippius, M., Saljé, K. and Thürmann, P. "Self-Medication with over-the-Counter and Prescribed Drugs Causing Adverse-Drug-Reaction-Related Hospital Admissions: Results of a Prospective, Long-Term Multi-Centre Study." *Drug Safety* 37 (2014): 225-35. https://doi.org/10.1007/s40264-014-0141-3.
7. Hunter, D. J., March, L. and Chew, M. "Osteoarthritis in 2020 and Beyond: A Lancet Commission." *Lancet* 396 (2020): 1711-12. https://doi.org/10.1016/S0140-6736(20)32230-3.
8. Leifer, V. P., Katz, J. N. and Losina, E. "The Burden of OA-Health Services and Economics." *Osteoarthritis and Cartilage* 30 (2022): 10-16. https://doi.org/10.1016/j.joca.2021.05.007.
9. The National Institute for Health and Care Excellence (NICE). *Osteoarthritis in over 16s: Diagnosis and Management*. 2022, 12 - 14.
10. Bruyère, O., Honvo, G., Veronese, N., Arden, N. K., Branco, J., Curtis, E. M., Al-Daghri, N. M., Herrero-Beaumont, G., Martel-Pelletier, J. and Pelletier, J.-P. "An Updated Algorithm Recommendation for the Management of Knee Osteoarthritis from the European Society for Clinical and Economic Aspects of Osteoporosis, Osteoarthritis and Musculoskeletal Diseases (ESCEO)." *Seminars in Arthritis and Rheumatism* 49 (2019): 337-50. https://doi.org/10.1016/j.semarthrit.2019.04.008.
11. Kolasinski, S. L., Neogi, T., Hochberg, M. C., Oatis, C., Guyatt, G., Block, J., Callahan, L., Copenhaver, C., Dodge, C. and Felson, D. "2019 American College of Rheumatology/Arthritis Foundation Guideline for the Management of Osteoarthritis of the Hand, Hip, and Knee." *Arthritis & Rheumatology* 72 (2020): 220-33. https://doi.org/ 10.1002/art.41142.
12. Bannuru, R. R., Osani, M., Vaysbrot, E., Arden, N., Bennell, K., Bierma-Zeinstra, S., Kraus, V., Lohmander, L. S., Abbott, J. and Bhandari, M. "Oarsi Guidelines for the Non-Surgical Management of Knee, Hip, and Polyarticular Osteoarthritis." *Osteoarthritis and Cartilage* 27 (2019): 1578-89. https://doi.org/10.1016/j.joca.2019.06.011.
13. Leppert, W., Malec–Milewska, M., Zajaczkowska, R. and Wordliczek, J. "Transdermal and Topical Drug Administration in the Treatment of Pain." *Molecules* 23 (2018): 681. https://doi.org/10.3390/molecules23030681.

14. Kligman, A. M. "Skin Permeability: Dermatologic Aspects of Transdermal Drug Delivery." *American Heart Journal* 108 (1984): 200-06. https://doi.org/10.1016/0002-8703(84)90576-3.
15. Kulkarni, V. S. *Handbook of Non-Invasive Drug Delivery Systems: Science and Technology*. Elsevier, 2009, 1 - 36.
16. Hadgraft, J. and Lane, M. E. "Advanced Topical Formulations " *International Journal of Pharmaceutics* 514 (2016): 52-57. https://doi.org/ 10.1016/j.ijpharm.2016.05.065
17. IMARC Research Group. *Pharmaceutical Drug Delivery Market Size, Share, Trends, and Forecast by Route of Administration, Application, End User, and Region, 2025-2033.* 2025, http://www.imarcgroup.com.
18. Heinrich Stahl, P. and Wermuth, C. G. "Handbook of Pharmaceutical Salts." *Properties, Selection, and Use, VHCA and Wiley-VCH* (2008): 1 -13. https://doi.org/10.1021/jm030019n.
19. McGettigan, P. and Henry, D. "Use of Non-Steroidal Anti-Inflammatory Drugs That Elevate Cardiovascular Risk: An Examination of Sales and Essential Medicines Lists in Low-, Middle-, and High-Income Countries." *PLoS Medicine* 10 (2013): e1001388. https://doi.org/10.1371/journal.pmed.1001388.
20. *Clarke's Analysis of Drugs and Poisons*. 4th ed. Edited by Moffat, A. C., Osselton, M. D. and Widdop, B. London: Pharmaceutical Press, 2011, 1 - 2736.
21. Sallmann, A. R. "The History of Diclofenac." *American Journal of Medicine* 80 (1986): 29-33. https://doi.org/ 10.1016/0002-9343(86)90076-8.
22. *Martindale: The Complete Drug Reference*. 39th ed. Edited by Brayfield, A. London: London Pharmaceutical Press, 2017, 1 - 4160.
23. Fini, A., Fazio, G., Gonzalez-Rodriguez, M., Cavallari, C., Passerini, N. and Rodriguez, L. "Formation of Ion-Pairs in Aqueous Solutions of Diclofenac Salts." *International Journal of Pharmaceutics* 187 (1999): 163-73. https://doi.org/10.1016/S0378-5173(99)00180-5.
24. *The Merck Index: An Encyclopedia of Chemicals, Drugs, and Biologicals*. 15th ed. Edited by O''Neil, M. J. Cambridge, UK Royal Society of Chemistry, 2013, 1 - 2708.
25. Minghetti, P., Cilurzo, F., Casiraghi, A., Montanari, L. and Fini, A. "Ex Vivo Study of Transdermal Permeation of Four Diclofenac Salts from Different Vehicles." *Journal of Pharmaceutical Sciences* 96 (2007): 814-23. https://doi.org/10.1002/jps.20770.
26. Gao, Y., Du, L., Li, Q., Li, Q., Zhu, L., Yang, M., Wang, X., Zhao, B. and Ma, S. "How Physical Techniques Improve the Transdermal Permeation of Therapeutics: A Review." *Medicine* 101 (2022): e29314. https://doi.org/10.1097/MD.0000000000029314.
27. Coulman, S., Allender, C. and Birchall, J. "Microneedles and Other Physical Methods for Overcoming the Stratum Corneum Barrier for Cutaneous Gene Therapy." *Critical Reviews in Therapeutic Drug Carrier Systems* 23 (2006): 205-58. https://doi.org/10.1615/critrevtherdrugcarriersyst.v23.i3.20.
28. Wang, Y., Thakur, R., Fan, Q. and Michniak, B. "Transdermal Iontophoresis: Combination Strategies to Improve Transdermal Iontophoretic Drug Delivery." *European Journal of Pharmaceutics and Biopharmaceutics* 60 (2005): 179-91. https://doi.org/ 10.1615/critrevtherdrugcarriersyst.v23.i3.20.
29. Dixit, N., Bali, V., Baboota, S., Ahuja, A. and Ali, J. "Iontophoresis-an Approach for Controlled Drug Delivery: A Review." *Current Drug Delivery* 4 (2007): 1-10. https://doi.org/ 10.2174/1567201810704010001.
30. Delgado-Charro, M. B. and Guy, R. H. "Iontophoresis: Applications in Drug Delivery and Noninvasive Monitoring." In *Transdermal Drug Delivery Systems*. CRC Press, 2002, 199-224. https://doi.org/10.1124/pharmrev.123.000549.
31. Vranić, E. "Sonophoresis-Mechanisms and Application." *Bosnian J. Basic Med. Sci.* 4 (2004): 25. https://doi.org/ 10.17305/bjbms.2004.3410.
32. Murthy, S. N., Sammeta, S. M. and Bowers, C. "Magnetophoresis for Enhancing Transdermal Drug Delivery: Mechanistic Studies and Patch Design." *Journal of*

Controlled Release 148 (2010): 197-203. https://doi.org/10.1016/j.jconrel.2010.08.015.
33. Chen, X., Zhu, L., Li, R., Pang, L., Zhu, S., Ma, J., Du, L. and Jin, Y. "Electroporation-Enhanced Transdermal Drug Delivery: Effects of Log P, Pka, Solubility and Penetration Time." *European Journal of Pharmaceutical Sciences* 151 (2020): 105410. https://doi.org/ 10.1016/j.ejps.2020.105410.
34. Mitragotri, S. "Devices for Overcoming Biological Barriers: The Use of Physical Forces to Disrupt the Barriers." *Advanced Drug Delivery Reviews* 65 (2013): 100-03. https://doi.org/10.1016/j.addr.2012.07.016.
35. Jung, J. H. and Jin, S. G. "Microneedle for Transdermal Drug Delivery: Current Trends and Fabrication." *J. Pharm. Invest.* (2021): 1-15. https://doi.org/10.1007/s40005-021-00512-4.
36. Tuan-Mahmood, T.-M., McCrudden, M. T., Torrisi, B. M., McAlister, E., Garland, M. J., Singh, T. R. R. and Donnelly, R. F. "Microneedles for Intradermal and Transdermal Drug Delivery." *European Journal of Pharmaceutical Sciences* 50 (2013): 623-37. https://doi.org/10.1016/j.ejps.2013.05.005.
37. Ita, K. "Transdermal Delivery of Drugs with Microneedles—Potential and Challenges." *Pharmaceutics* 7 (2015): 90-105. https://doi.org/10.3390/pharmaceutics7030090.
38. Hadgraft, J. "Passive Enhancement Strategies in Topical and Transdermal Drug Delivery." *International Journal of Pharmaceutics* 184 (1999): 1-6. https://doi.org/10.1016/S0378-5173(99)00095-2.
39. Santos, P., Watkinson, A. C., Hadgraft, J. and Lane, M. E. "Influence of Penetration Enhancer on Drug Permeation from Volatile Formulations." *International Journal of Pharmaceutics* 439 (2012): 260-68. https://doi.org/10.1016/j.ijpharm.2012.09.031.
40. Tapfumaneyi, P., Imran, M., Alavi, S. E. and Mohammed, Y. "Science of, and Insights into, Thermodynamic Principles for Dermal Formulations." *Drug Discovery Today* 28 (2023): 103521-21. https://doi.org/10.1016/j.drudis.2023.103521.
41. Lane, M. E., Santos, P., Watkinson, A. C. and Hadgraft, J. *Passive Skin Permeation Enhancement*. Hoboken, NJ, USA: Hoboken, NJ, USA: John Wiley & Sons, Inc, 2011, 23-42. https://doi.org/ 10.1002/9781118140505.ch2.
42. Lane, M. E. "Skin Penetration Enhancers." *International Journal of Pharmaceutics* 447 (2013): 12-21. https://doi.org/10.1016/j.ijpharm.2013.02.040.
43. Williams, A. C. and Barry, B. W. "Penetration Enhancers." *Adv Drug Deliv Rev* 56 (2004): 603-18. https://doi.org/10.1016/j.addr.2003.10.025.
44. Marwah, H., Garg, T., Goyal, A. K. and Rath, G. "Permeation Enhancer Strategies in Transdermal Drug Delivery." *Drug Delivery* 23 (2016): 564-78. https://doi.org/10.3109/10717544.2014.935532.
45. Cristofoli, M., Kung, C.-P., Hadgraft, J., Lane, M. E. and Sil, B. C. "Ion Pairs for Transdermal and Dermal Drug Delivery: A Review." *Pharmaceutics* 13 (2021): 909. https://doi.org/10.3390/pharmaceutics13060909.
46. Bjerrum, N. *Untersuchungen Über Ionenassoziation*. AF Høst, 1926, 6, 14, 32-36, 46-47.
47. Cavallari, C., Passerini, N., Fini, A., Fazio, G., Cini, M. and Rodrigeuz, L. "Partition of Diclofenac Salts as Ion-Pairs " *European Journal of Pharmaceutical Sciences* 6 (1998): S63-S63. https://doi.org/10.1016/S0928-0987(98)91451-8.
48. Fini, A., Cavallari, C., Monastero, A. and Bassini, G. "Diclofenac Salts, Viii. Effect of the Counterions on the Permeation through Porcine Membrane from Aqueous Saturated Solutions." *Pharmaceutics* 4 (2012): 413-29. https://doi.org/10.3390/pharmaceutics4030413.
49. Office of the Federal Register National Archives and Records Administration. *21 Cfr 172.320 - Amino Acids*. USA: 2011.
50. Burnett, C. L., Heldreth, B., Bergfeld, W. F., Belsito, D. V., Hill, R. A., Klaassen, C. D., Liebler, D. C., Marks, J. G., Shank, R. C., Slaga, T. J.*, et al.* "Safety Assessment

of A-Amino Acids as Used in Cosmetics." *International Journal of Toxicology* 32 (2013): 41S-64S. https://doi.org/10.1177/1091581813507090.
51. Astra Zeneca. *Pharmaceuticals in the Environment Statement*. Cambridge, U.K.: 2024, 1-6.https://www.astrazeneca.com
52. Novartis AG. *Pharmaceuticals in the Environment*. Basel, Switzerland: 2006. https://www.novartis.com
53. F. Hoffmann-La Roche AG. *Roche Position on Pharmaceuticals in the Environment (Pie)*. Basel, Switzerland: 2011, 1-5. https://www.assets.roche.com
54. F. Hoffmann-La Roche AG. *Roche Position on Product Stewardship*. Basel, Switzerland: 2017, 1-6. https://www.assets.roche.com
55. Singh, P. and Roberts, M. "Skin Permeability and Local Tissue Concentrations of Nonsteroidal Anti-Inflammatory Drugs after Topical Application." *Journal of Pharmacology and Experimental Therapeutics* 268 (1994): 144-51. https://doi.org/10.1016/S0022-3565(25)38459-4.
56. Rehfeld, A., Nylander, M., Karnov, K., Rehfeld, A., Nylander, M. and Karnov, K. "The Integumentary System." *Compendium of Histology: A Theoretical and Practical Guide* (2017): 411-32.
57. Mitchell, B. S. *Histology : An Illustrated Colour Text.* Edinburgh, New York: Churchill Livingstone, 2009, 42 - 48.
58. Mills, S. E. *Histology for Pathologists*. Wolters Kluwer Health, 2012, 1 - 142.
59. Albanna, M. and Holmes, J. H. *Skin Tissue Engineering and Regenerative Medicine*. Elsevier Science, 2016, 4 - 11.
60. Venus, M., Waterman, J. and McNab, I. "Basic Physiology of the Skin." *Surgery (Oxford)* 28 (2010): 469-72. https://doi.org/ 10.1016/J.MPSUR.2010.07.011
61. Griffiths, C., Barker, J., Bleiker, T., Chalmers, R. and Creamer, D. *Rook's Textbook of Dermatology* Ninth edition. Chichester, West Sussex, Hoboken, NJ John Wiley & Sons Inc., 2016, 49 - 106.
62. Chilcott, R. P., Price, S. *Principles and Practice of Skin Toxicology* Chichester, West Sussex, England, Hoboken, NJ. : John Wiley & Sons, 2008, 6 - 50.
63. "Skin, Hair and Nails: Structure and Function."Edited by Forslind, B., & Lindberg, M.Boca Raton, FL: CRC Press, 2003.
64. Sprowls, J. B. and Dittert, L. W. *Sprowls' American Pharmacy: An Introduction to Pharmaceutical Techniques and Dosage Forms*. Lippincott, 1974, 237.
65. Mogensen, M., Morsy, H. A., Thrane, L. and Jemec, G. B. E. "Morphology and Epidermal Thickness of Normal Skin Imaged by Optical Coherence Tomography." *Dermatology* 217 (2008): 14-20. https://doi.org/10.1159/000118508.
66. Sandby-Møller, J., Poulsen, T. and Wulf, H. C. "Epidermal Thickness at Different Body Sites: Relationship to Age, Gender, Pigmentation, Blood Content, Skin Type and Smoking Habits." *Acta Dermato-Venereologica* 83 (2003): 410. https://doi.org/10.1080/00015550310015419.
67. Neerken, S., Lucassen, G. W., Bisschop, M. A., Lenderink, E. and Nuijs, T. A. M. "Characterization of Age-Related Effects in Human Skin: A Comparative Study That Applies Confocal Laser Scanning Microscopy and Optical Coherence Tomography." *Journal of Biomedical Optics* 9 (2004): 274. https://doi.org/10.1117/1.1645795.
68. Marks, R. "Measurement of Biological Ageing in Human Epidermis." *British Journal of Dermatology* 104 (1981): 627-33. https://doi.org/10.1111/j.1365-2133.1981.tb00748.x.
69. Nishibu, A., Ward, B. R., Jester, J. V., Ploegh, H. L., Boes, M. and Takashima, A. "Behavioral Responses of Epidermal Langerhans Cells in Situ to Local Pathological Stimuli." *Journal of Investigative Dermatology* 126 (2006): 787-96. https://doi.org/10.1038/sj.jid.5700107.
70. West, H. C. and Bennett, C. L. "Redefining the Role of Langerhans Cells as Immune Regulators within the Skin." *Frontiers in Immunology* 8 (2018): 1941. https://doi.org/10.3389/fimmu.2017.01941.

71. Romani, N., Brunner, P. M. and Stingl, G. "Changing Views of the Role of Langerhans Cells." *Journal of Investigative Dermatology* 132 (2012): 872-81. https://doi.org/10.1038/jid.2011.437.
72. Nesterova, A. P., Yuryev, A., Klimov, E. A., Zharkova, M., Shkrob, M., Ivanikova, N. V., Sozin, S. and Sobolev, V. *Disease Pathways: An Atlas of Human Disease Signaling Pathways*. Elsevier, 2019, 524 - 525.
73. Elias, P. M. and Feingold, K. R. *Skin Barrier*. CRC Press, 2005, 66.
74. Halprin, K. M. "Epidermal “Turnover Time”—a Re-Examination." *British Journal of Dermatology* 86 (1972): 14-19. https://doi.org/10.1111/j.1365-2133.1972.tb01886.x
75. Bergstresser, P. R. and Taylor, R. J. "Epidermal ‘Turnover Time’—a New Examination." *British Journal of Dermatology* 96 (1977): 503-06. https://doi.org/10.1111/j.1365-2133.1977.tb07152.x.
76. Iizuka, H. "Epidermal Turnover Time." *Journal of Dermatological Science* 8 (1994): 215-17. https://doi.org/10.1016/0923-1811(94)90057-4.
77. Walters, K. A. *Dermatological and Transdermal Formulations*. New York: M. Dekker, 2002, 1 - 40.
78. Grove, G. L. and Kligman, A. M. "Age-Associated Changes in Human Epidermal Cell Renewal." *Journal of Gerontology* 38 (1983): 137. https://doi.org/10.1093/geronj/38.2.137https://doi.org/10.1093/geronj/38.2.137.
79. Hall, B. J., Hall, J.C. *Sauer's Manual of Skin Diseases*. 10th Philadelphia, USA: Lippincott Williams & Wilkins, 2010, 3.
80. Kawai, M., Imokawa, G. and Mizoguchi, M. "Physiological Analysis of the Facial Skin by Corneocyte Morphology and Stratum Corneum Turnover." *Nihon Hifuka Gakkai zasshi. The Japanese Journal of Dermatology* 99 (1989): 999-1006.
81. Cherkashina, O., Tsitrina, A., Abolin, D., Morgun, E., Kosykh, A., Sabirov, M., Vorotelyak, E. and Kalabusheva, E. "The Recovery of Epidermal Proliferation Pattern in Human Skin Xenograft." *Cells* 14 (2025): 448. https://doi.org/10.3390/cells14060448.
82. Scheuplein, R. J. and Blank, I. H. "Permeability of the Skin." *Physiological reviews* 51 (1971): 702. https://doi.org/10.1152/physrev.1971.51.4.702.
83. Michaels, A. S., Chandrasekaran, S. K. and Shaw, J. E. "Drug Permeation through Human Skin: Theory and in Vitro Experimental Measurement." *AIChE Journal* 21 (1975): 985-96. https://doi.org/10.1002/aic.690210522.
84. Albery, W. J. and Hadgraft, J. "Percutaneous Absorption: In Vivo Experiments." *Journal of Pharmacy and Pharmacology* 31 (1979): 140-47. https://doi.org/10.1111/j.2042-7158.1979.tb13456.x.
85. Hadgraft, J. "Skin, the Final Frontier (Product Review)." *International Journal of Pharmaceutics* 224 (2001): 1-18. https://doi.org/10.1016/S0378-5173(01)00731-1.
86. Scheuplein, R. J. "A Personal View of Skin Permeation (1960-2013)." *Skin Pharmacology and Physiology* 26 (2013): 199-212. https://doi.org/10.1159/000351954.
87. OECD. *Test No. 427: Skin Absorption: In Vivo Method*. 2004, 1 - 8.
88. OECD. *Test Guideline 428: Skin Absorption: In Vitro Method*. Paris: OECD, 2004, 1 - 8.
89. OECD. *OECD Guidelines for the Testing of Chemicals*. Paris: OECD Publishing, 2004.
90. OECD. *Guidance Notes on Dermal Absorption, Series on Testing and Assessment No. 156*. 36. 2011, 1-72.
91. OECD. *Guidance Notes on Dermal Absorption, Series on Testing and Assessment No. 156 Draft Second Edition*. 36. 2019, 1-66.
92. Rigg, P. C. and Barry, B. W. "Shed Snake Skin and Hairless Mouse Skin as Model Membranes for Human Skin During Permeation Studies." *Journal of Investigative Dermatology* 94 (1990): 235-40. https://doi.org/10.1111/1523-1747.ep12874561.
93. Bond, J. R. and Barry, B. W. "Limitations of Hairless Mouse Skin as a Model for in Vitro Permeation Studies through Human Skin: Hydration Damage." *Journal of*

Investigative Dermatology 90 (1988): 486. https://doi.org/10.1111/1523-1747.ep12460958.
94. Dick, I. P. and Scott, R. C. "Pig Ear Skin as an in-Vitro Model for Human Skin Permeability." *Journal of Pharmacy and Pharmacology* 44 (1992): 640-45. https://doi.org/10.1111/j.2042-7158.1992.tb05485.x.
95. Starr, N. J., Khan, M. H., Edney, M. K., Trindade, G. F., Kern, S., Pirkl, A., Kleine-Boymann, M., Elmse, C., O'Mahony, M. M. and Bell, M. "Elucidating the Molecular Landscape of the Stratum Corneum." *Proceedings of the National Academy of Sciences* 119 (2022): e2114380119 https://doi.org/ 10.1073/pnas.2114380119.
96. Jacobi, U., Kaiser, M., Toll, R., Mangelsdorf, S., Audring, H., Otberg, N., Sterry, W. and Lademann, J. "Porcine Ear Skin: An in Vitro Model for Human Skin." *Skin Research and Technology* 13 (2007): 19-24. 10.1111/j.1600-0846.2006.00179.x.
97. Benson, H. A. E. and Watkinson, A. C. *Topical and Transdermal Drug Delivery Principles and Practice* Hoboken, N.J: Wiley, 2011, 1 - 409.
98. Sarmento, B., Albuquerque, J. *Concepts and Models for Drug Permeability Studies: Cell and Tissue Based in Vitro Culture Models* Amsterdam: Elsevier Ltd, 2016, 155 - 167.
99. Bhatia, S. N. and Ingber, D. E. "Microfluidic Organs-on-Chips." *Nature Biotechnology* 32 (2014): 760-72. https://doi.org/ 10.1038/nbt.2989.
100. Sung, J. H., Wang, Y. I., Narasimhan Sriram, N., Jackson, M., Long, C., Hickman, J. J. and Shuler, M. L. "Recent Advances in Body-on-a-Chip Systems." *Analytical Chemistry* 91 (2018): 330-51. https://doi.org/10.1021/acs.analchem.8b05293.
101. Picollet-D'hahan, N., Zuchowska, A., Lemeunier, I. and Le Gac, S. "Multiorgan-on-a-Chip: A Systemic Approach to Model and Decipher Inter-Organ Communication." *Trends in Biotechnology* 39 (2021): 788-810. https://doi.org/10.1016/j.tibtech.2020.11.014.
102. Risueño, I., Valencia, L., Jorcano, J. and Velasco, D. "Skin-on-a-Chip Models: General Overview and Future Perspectives." *APL bioengineering* 5 (2021):
103. Potts, R. O. and Guy, R. H. "Predicting Skin Permeability." *Pharmaceutical Research* 9 (1992): 663-69. https://doi.org/10.1023/A:1015810312465.
104. Sun, Y., Moss, G. P., Prapopoulou, M., Adams, R., Brown, M. B. and Davey, N. "Prediction of Skin Penetration Using Machine Learning Methods." Presented at 2008 Eighth IEEE International Conference on Data Mining, 2008. IEEE, 1049-54.
105. Cherkasov, A., Muratov, E. N., Fourches, D., Varnek, A., Baskin, I. I., Cronin, M., Dearden, J., Gramatica, P., Martin, Y. C. and Todeschini, R. "Qsar Modeling: Where Have You Been? Where Are You Going To?" *Journal of Medicinal Chemistry* 57 (2014): 4977-5010. https://doi.org/10.1021/jm4004285.
106. Wu, Y.-W., Ta, G. H., Lung, Y.-C., Weng, C.-F. and Leong, M. K. "In Silico Prediction of Skin Permeability Using a Two-Qsar Approach." *Pharmaceutics* 14 (2022): 961. https://doi:10.3390/pharmaceutics14050961.
107. Alikhan, A., Farahmand, S. and Maibach, H. I. "Correlating Percutaneous Absorption with Physicochemical Parameters in Vivo in Man: Agricultural, Steroid, and Other Organic Compounds." *Journal of Applied Toxicology* 29 (2009): 590-96. https://doi.org/ 10.1002/jat.1445.
108. *Cell Physiology Sourcebook: A Molecular Approach*. Edited by Sperelakis, N. Orlando, FL: Academic Press, 2001.
109. Steffansen, B., Brodin, B., Nielsen, C. U., European University Consortium for Advanced Pharmaceutical, E. and Research. *Molecular Biopharmaceutics : Aspects of Drug Characterisation, Drug Delivery and Dosage Form Evaluation*. London: Pharmaceutical Press, 2010.
110. Katz. "Absorption of Drugs through the Skin." *Concepts in Biochemical Pharmacology* (1971): 103. https://doi.org/10.1007/978-3-642-65052-9_7.
111. Baker, H. and Kligman, A. M. "A Simple in Vivo Method for Studying the Permeability of the Human Stratum Corneum." *Journal of Investigative Dermatology* 48 (1967): 273-74. https://doi.org/10.1038/jid.1967.46.

112. Anderson, R. L. and Cassidy, J. M. "Variations in Physical Dimensions and Chemical Composition of Human Stratum Corneum." *Journal of Investigative Dermatology* 61 (1973): 30-32. https://doi.org/10.1111/1523-1747.ep12674117.
113. Holbrook, K., A. and Odland, G., F. . "Regional Differences in the Thickness (Cell Layers) of the Human Stratum Corneum: An Ultrastructural Analysis." *Journal of Investigative Dermatology* 62 (1974): 415. https://doi.org/10.1111/1523-1747.ep12701670.
114. Gorcea, M., Lane, M. E. and Moore, D. J. "Exploratory in Vivo Biophysical Studies of Stratum Corneum Lipid Organization in Human Face and Arm Skin." *International Journal of Pharmaceutics* 622 (2022): 121887. https://doi.org/10.1016/j.ijpharm.2022.121887
115. Jeong, K. M., Seo, J. Y., Kim, A., Kim, Y. C., Baek, Y. S., Oh, C. H. and Jeon, J. "Ultrasonographic Analysis of Facial Skin Thickness in Relation to Age, Site, Sex, and Body Mass Index." *Skin Research and Technology* 29 (2023): e13426. https://doi.org/10.1111/srt.13426
116. Ya-Xian, Z. "Number of Cell Layers of the Stratum Corneum in Normal Skin - Relationship to the Anatomical Location on the Body, Age, Sex and Physical Parameters." *Archives of dermatological research* 291 (1999): 555-9. https://doi.org/ 10.1007/s004030050453.
117. Mohammed, D., Matts, P., Hadgraft, J. and Lane, M. "Depth Profiling of Stratum Corneum Biophysical and Molecular Properties." *British Journal of Dermatology* 164 (2011): 957-65. https://doi.org/ 10.1111/j.1365-2133.2011.10211.x.
118. Hirao, T., Denda, M. and Takahashi, M. "Identification of Immature Cornified Envelopes in the Barrier-Impaired Epidermis by Characterization of Their Hydrophobicity and Antigenicities of the Components." *Experimental Dermatology* 10 (2001): 35-44. https://doi.org/ 10.1034/j.1600-0625.2001.100105.x
119. Michel, S., Schmidt, R., Shroot, B. and Reichert, U. "Morphological and Biochemical Characterization of the Cornified Envelopes from Human Epidermal Keratinocytes of Different Origin." *Journal of Investigative Dermatology* 91 (1988): 11-15. https://doi.org/10.1111/1523-1747.ep12463281.
120. Kunii, T., Hirao, T., Kikuchi, K. and Tagami, H. "Stratum Corneum Lipid Profile and Maturation Pattern of Corneocytes in the Outermost Layer of Fresh Scars: The Presence of Immature Corneocytes Plays a Much More Important Role in the Barrier Dysfunction Than Do Changes in Intercellular Lipids." *British Journal of Dermatology* 149 (2003): 749-56. https://doi.org/ 10.1046/j.1365-2133.2003.05545.x.
121. Plewig, G. and Marples, R. R. "Regional Differences of Cell Sizes in the Human Stratum Corneum. Part I." *Journal of Investigative Dermatology* 54 (1970): 13-18. https://doi.org/10.1111/1523-1747.ep12551482.
122. Plewig, G., Scheuber, E., Reuter, B. and Waidelich, W. "Thickness of Corneocytes." In *Stratum Corneum*. Springer, 1983, 171-74.
123. Rougier, A., Dupuis, D., Lotte, C., Roguet, R., Wester, R. and Maibach, H. "Regional Variation in Percutaneous Absorption in Man: Measurement by the Stripping Method." *Archives of Dermatological Research* 278 (1986): 465-69. https://doi.org/10.1007/BF00455165.
124. Machado, M., Salgado, T. M., Hadgraft, J. and Lane, M. E. "The Relationship between Transepidermal Water Loss and Skin Permeability." *International Journal of Pharmaceutics* 384 (2010): 73-77. https://doi.org/ 10.1016/j.ijpharm.2009.09.044.
125. Schnetz, E., Kuss, O., Schmitt, J., Diepgen, T., Kuhn, M. and Fartasch, M. "Intra-and Inter-Individual Variations in Transepidermal Water Loss on the Face: Facial Locations for Bioengineering Studies." *Contact Dermatitis* 40 (1999): 243-47. https://doi.org/10.1111/j.1600-0536.1999.tb06057.x.
126. Marrakchi, S. and Maibach, H. I. "Biophysical Parameters of Skin: Map of Human Face, Regional, and Age-Related Differences." *Contact Dermatitis* 57 (2007): 28-34. https://doi.org/10.1111/j.1600-0536.2007.01138.x.

127. Jang, H.-Y., Park, C.-W. and Lee, C.-H. "A Study of Transepidermal Water Loss at Various Anatomical Sites of the Skin." *Korean Journal of Dermatology* (1996): 402-06.
128. Mohammed, D., Matts, P. J., Hadgraft, J. and Lane, M. E. "Variation of Stratum Corneum Biophysical and Molecular Properties with Anatomic Site." *The AAPS journal* 14 (2012): 806-12. https://doi.org/ 10.1208/s12248-012-9400-3
129. Évora, A. S., Adams, M. J., Johnson, S. A. and Zhang, Z. "Corneocytes: Relationship between Structural and Biomechanical Properties." *Skin Pharmacology and Physiology* 34 (2021): 146-61. https://doi.org/10.1159/000513054.
130. Hoath, S. B., Maibach, H.I. *Neonatal Skin: Structure and Function*. 2nd. Boca Raton, Florida, USA: Taylor & Francis, 2003, 264 - 308.
131. Bos, J. D. and Meinardi, M. M. "The 500 Dalton Rule for the Skin Penetration of Chemical Compounds and Drugs." *Experimental Dermatology: Viewpoint* 9 (2000): 165-69. https://doi.org/10.1034/j.1600-0625.2000.009003165.x.
132. Kasting, G. B., Smith, R. L. and Cooper, E. "Effect of Lipid Solubility and Molecular Size on Percutaneous Absorption." *Skin pharmacokinetics* 1 (1987): 138-53.
133. Touitou, E., Chow, D. D. and Lawter, J. R. "Chiral B-Blockers for Transdermal Delivery." *International Journal of Pharmaceutics* 104 (1994): 19-28. https://doi.org/ 10.1016/0378-5173(94)90333-6.
134. Hadgraft, J. and Lane, M. E. "Skin Permeation: The Years of Enlightenment." *International Journal of Pharmaceutics* 305 (2005): 2-12. https://doi.org/10.1016/j.ijpharm.2005.07.014.
135. Guy, R. H. and Hadgraft, J. "The Effect of Penetration Enhancers on the Kinetics of Percutaneous Absorption." *Journal of controlled release* 5 (1987): 43-51. https://doi.org/10.1016/0168-3659(87)90036-8.
136. Hadgraft, J. and Lane, M. E. "Skin: The Ultimate Interface." *Physical Chemistry Chemical Physics* 13 (2011): 5215-22. https://doi.org/10.1039/c0cp02943b.
137. Higuchi, T. "Physical Chemical Analysis of Percutaneous Absorption Process from Creams and Ointments." *Journal of the Society of Cosmetic Chemists* 11 (1960): 85-97.
138. Santos, P., Watkinson, A., Hadgraft, J. and Lane, M. "Formulation Issues Associated with Transdermal Fentanyl Delivery." *International Journal of Pharmaceutics* 416 (2011): 155-59. https://doi.org/10.1016/j.ijpharm.2011.06.024.
139. Cilurzo, F., Casiraghi, A., Selmin, F. and Minghetti, P. "Supersaturation as a Tool for Skin Penetration Enhancement." *Current Pharmaceutical Design* 21 (2015): 2733-44. https://doi.org/ 10.2174/1381612821666150428125046.
140. Suhonen, T. M., Bouwstra, J. A. and Urtti, A. "Chemical Enhancement of Percutaneous Absorption in Relation to Stratum Corneum Structural Alterations." *Journal of controlled release* 59 (1999): 149-61. https://doi.org/ 10.1016/s0168-3659(98)00187-4.
141. Kováčik, A., Kopečná, M. and Vávrová, K. "Permeation Enhancers in Transdermal Drug Delivery: Benefits and Limitations." *Expert opinion on drug delivery* 17 (2020): 145-55. https://doi.org/ 10.1080/17425247.2020.1713087
142. Barry, B. "Lipid-Protein-Partitioning Theory of Skin Penetration Enhancement." *Journal of Controlled Release* 15 (1991): 237-48. https://doi.org/10.1016/0168-3659(91)90115-T.
143. Song, T., Quan, P., Xiang, R. and Fang, L. "Regulating the Skin Permeation Rate of Escitalopram by Ion-Pair Formation with Organic Acids." *AAPS PharmSciTech* 17 (2016): 1267-73. https://doi.org/10.1208/s12249-015-0474-y.
144. Singh, P. and Roberts, M. S. "Skin Permeability and Local Tissue Concentrations of Nonsteroidal Antiinflammatory Drugs after Topical Application." *Journal Of Pharmacology And Experimental Therapeutics* 268 (1994): 144-51. https://doi.org/ 10.1016/S0022-3565(25)38459-4.

145. Steiling, W., Kreutz, J. and Hofer, H. "Percutaneous Penetration/Dermal Absorption of Hair Dyes in Vitro." *Toxicology in Vitro* 15 (2001): 565-70. https://doi.org/ https://doi.org/10.1016/S0887-2333(01)00062-5.
146. McNaught, A. D. and Wilkinson, A. "Iupac. Compendium of Chemical Terminology." Oxford: Blackwell Scientific Publications, 1997. https://goldbook.iupac.org/terms. 2nd ed.
147. Levine, I. N. *Physical Chemistry* 6th ed., International ed. London, U.K.: McGraw-Hill Higher Education, 2009, 315.
148. Bagoțskiĭ, V. S. *Fundamentals of Electrochemistry* 2nd ed. Hoboken, N.J.: Wiley-Interscience, 2006, 124 - 125.
149. Kraus, C. A. "The Ion-Pair Concept, Its Evolution and Some Applications." *Journal of Physical Chemistry* 60 (1956): 129-41. https://doi.org/10.1021/j150536a001.
150. Lee, S. J., Kurihara-Bergstrom, T. and Kim, S. W. "Ion-Paired Drug Diffusion through Polymer Membranes." *International Journal of Pharmaceutics* 39 (1987): 59-73. https://doi.org/10.1016/0378-5173(87)90199-2.
151. Squire, P. *A Companion to the British Pharmacopoeia : Comparing the Strength of the Various Preparations with Those of the London, Edinburgh, and Dublin, United States and Other Foreign Pharmacopoeias with Practical Hints on Prescribing*. London: J. Churchill and Sons, 1864.
152. Byberg, J., Jensen, S. J. K. and Kläning, U. K. "Extension of the Bjerrum Theory of Ion Association." *Transactions of the Faraday Society* 65 (1969): 3023-31. https://doi.org/10.1039/TF9696503023.
153. Cronin, M. T., Dearden, J. C., Moss, G. P. and Murray-Dickson, G. "Investigation of the Mechanism of Flux across Human Skin in Vitro by Quantitative Structure-Permeability Relationships." *European Journal of Pharmaceutical Sciences : Official Journal of the European Federation for Pharmaceutical Sciences* 7 (1999): 325-30. https://doi.org/10.1016/s0928-0987(98)00041-4.
154. Patel, H., Berge, W. t. and Cronin, M. T. D. "Quantitative Structure–Activity Relationships (Qsars) for the Prediction of Skin Permeation of Exogenous Chemicals." *Chemosphere* 48 (2002): 603-13. https://doi.org/10.1016/S0045-6535(02)00114-5.
155. Inagi, T., Muramatsu, T., Nagai, H. and Terada, H. "Mechanism of Indomethacin Partition between N-Octanol and Water." *Chemical & Pharmaceutical Bulletin* 29 (1981): 2330-37. https://doi.org/10.1248/cpb.29.2330.
156. Green, P. G., Guy, R. H. and Hadgraft, J. "*In Vitro* and *in Vivo* Enhancement of Skin Permeation with Oleic and Lauric Acids." *International Journal of Pharmaceutics* 48 (1988): 103-11. https://doi.org/10.1016/0378-5173(88)90252-9.
157. Sarveiya, V., Templeton, J. F. and Benson, H. A. E. "Effect of Lipophilic Counter-Ions on Membrane Diffusion of Benzydamine." *European Journal of Pharmaceutical Sciences* 26 (2005): 39-46. https://doi.org/10.1016/j.ejps.2005.04.013.
158. Megwa, S. A., Cross, S. E., Benson, H. A. E. and Roberts, M. S. "Ion-Pair Formation as a Strategy to Enhance Topical Delivery of Salicylic Acid." *Journal of Pharmacy and Pharmacology* 52 (2000): 919-28. https://doi.org/10.1211/0022357001774804.
159. Valenta, C., Siman, U., Kratzel, M. and Hadgraft, J. "The Dermal Delivery of Lignocaine: Influence of Ion Pairing." *International Journal of Pharmaceutics* 197 (2000): 77-85. https://doi.org/10.1016/S0378-5173(99)00453-6.
160. Fini, A., Bassini, G., Monastero, A. and Cavallari, C. "Diclofenac Salts, Viii. Effect of the Counterions on the Permeation through Porcine Membrane from Aqueous Saturated Solutions." *Pharmaceutics* 4 (2012): 413. https://doi.org/10.3390/pharmaceutics4030413.
161. Cilurzo, F., Minghetti, P., Alberti, E., Gennari, C. G. M., Pallavicini, M., Valoti, E. and Montanari, L. "An Investigation into the Influence of Counterion on the Rs-Propranolol and S- Propranolol Skin Permeability." *Journal of Pharmaceutical Sciences* 99 (2010): 1217-24. https://doi.org/10.1002/jps.21891.

162. Megwa, S. A., Cross, S. E., Whitehouse, M. W., Benson, H. A. E. and Roberts, M. S. "Effect of Ion Pairing with Alkylamines on the in-Vitro Dermal Penetration and Local Tissue Disposition of Salicylates." *Journal of Pharmacy and Pharmacology* 52 (2000): 929-40. https://doi.org/10.1211/0022357001774813.
163. Trotta, M., Ugazio, E., Peira, E. and Pulitano, C. "Influence of Ion Pairing on Topical Delivery of Retinoic Acid from Microemulsions." *Journal of Controlled Release* 86 (2003): 315-21. https://doi.org/10.1016/S0168-3659(02)00416-9.
164. Auner, B., Valenta, C. and Hadgraft, J. "Influence of Lipophilic Counter-Ions in Combination with Phloretin and 6-Ketocholestanol on the Skin Permeation of 5-Aminolevulinic Acid." *International Journal of Pharmaceutics* 255 (2003): 109-16. https://doi.org/10.1016/S0378-5173(03)00053-X.
165. Takács-Novák, K. and Szász, G. "Ion-Pair Partition of Quaternary Ammonium Drugs: The Influence of Counter Ions of Different Lipophilicity, Size, and Flexibility." *Pharmaceutical Research* 16 (1999): 1633-38. https://doi.org/10.1023/A:1018977225919.
166. Wang, M. Y., Yang, Y. Y. and Heng, P. W. S. "Skin Permeation of Physostigmine from Fatty Acids-Based Formulations: Evaluating the Choice of Solvent." *International Journal of Pharmaceutics* 290 (2005): 25-36. https://doi.org/10.1016/j.ijpharm.2004.10.027.
167. In, S., Yook, N., Kim, J.-H., Shin, M., Tak, S., Jeon, J. H., Ahn, B., Park, S.-G., Lee, C.-K. and Kang, N.-G. "Enhancement of Exfoliating Efficacy of L- Carnitine with Ion-Pair Method Monitored by Nuclear Magnetic Resonance Spectroscopy." *Scientific Reports* 9 (2019): 13507-9. https://doi.org/10.1038/s41598-019-49818-2.
168. Pardo, A., Shiri, Y. and Cohen, S. "Kinetics of Transdermal Penetration of an Organic Ion Pair: Physostigmine Salicylate." *Journal of Pharmaceutical Sciences* 81 (1992): 990-95. https://doi.org/10.1002/jps.2600811006.
169. Rowe, R. C., Shesky, P. J., Cook, W. G. and Fenton, M. E. *Handbook of Pharmaceutical Excipients*. 7th. UK: Pharmaceutical Press, 2012.
170. Akerlof, G. "Dielectric Constants of Some Organic Solvent-Water Mixtures at Various Temperatures." *Journal of the American Chemical Society* 54 (1932): 4125-39. https://doi.org/10.1021/ja01350a001.
171. Rowe, R. C., Sheskey, P. and Quinn, M. *Handbook of Pharmaceutical Excipients*. Libros Digitales-Pharmaceutical Press, 2009, 346.
172. Harada, S., Takahashi, Y., Nakagawa, H., Yamashita, F. and Hashida, M. "Effect of Vehicle Properties on Skin Penetration of Emedastine." *Biological & Pharmaceutical Bulletin* 23 (2000): 1224-28. https://doi.org/10.1248/bpb.23.1224.
173. Hadgraft, J., Walters, K. A. and Wotton, P. K. "Facilitated Percutaneous Absorption: A Comparison and Evaluation of Two in Vitro Models." *International Journal of Pharmaceutics* 32 (1986): 257-63. https://doi.org/10.1016/0378-5173(86)90187-0.
174. Smith, J. C. and Irwin, W. J. "Ionisation and the Effect of Absorption Enhancers on Transport of Salicylic Acid through Silastic Rubber and Human Skin." *International Journal of Pharmaceutics* 210 (2000): 69-82. https://doi.org/10.1016/S0378-5173(00)00561-5.
175. Cázares-Delgadillo, J., Naik, A., Kalia, Y. N., Quintanar-Guerrero, D. and Ganem-Quintanar, A. "Skin Permeation Enhancement by Sucrose Esters: A Ph - Dependent Phenomenon." *International Journal of Pharmaceutics* 297 (2005): 204-12. https://doi.org/10.1016/j.ijpharm.2005.03.020.
176. Vávrová, K., Lorencová, K., Novotný, J., Holý, A. and Hrabálek, A. "Permeation Enhancer Dodecyl 6-(Dimethylamino)Hexanoate Increases Transdermal and Topical Delivery of Adefovir: Influence of Ph, Ion-Pairing and Skin Species." *European Journal of Pharmaceutics and Biopharmaceutics* 70 (2008): 901-07. https://doi.org/10.1016/j.ejpb.2008.07.002.
177. Uchino, T., Miyazaki, Y., Ishikawa, A. and Kagawa, Y. "Development of a Novel Simple Gel Formulation Containing an Ion-Pair Complex of Diclofenac and

Phenylephrine." *Skin Pharmacology and Physiology* 32 (2019): 318-27. https://doi.org/10.1159/000501734.
178. Cross, S. E., Thompson, M. J. and Roberts, M. S. "Transdermal Penetration of Vasoconstrictors - Present Understanding and Assessment of the Human Epidermal Flux and Retention of Free Bases and Ion-Pairs." *Pharmaceutical Research* 20 (2003): 270-74. https://doi.org/10.1023/A:1022235507186.
179. Chirio, D., Trotta, M., Gallarate, M., Peira, E. and Carlotti, M. E. "Thermosensitive Gels for the Topical Administration of Diltiazem." *Journal of Dispersion Science and Technology* 32 (2011): 320-25. https://doi.org/10.1080/01932691003659684.
180. Rodrigues, L. B. O., Lima, F. A., Alves, C. P. B., Martins-Santos, E., Aguiar, M. M. G., Oliveira, C. A., Oréfice, R. L., Ferreira, L. A. M. and Goulart, G. A. C. "Ion Pair Strategy in Solid Lipid Nanoparticles: A Targeted Approach to Improve Epidermal Targeting with Controlled Adapalene Release, Resulting Reduced Skin Irritation." *Pharmaceutical Research* 37 (2020). https://doi.org/10.1007/s11095-020-02866-0.
181. Tavares, E. B., Paiva, M. C. E., Lobo, G. D., Martins, T. S., Segura, W. D. and Garcia, M. T. J. "Sodium Cholate-Mediated Ion-Pairing for Skin Delivery of Methylene Blue: Physicochemical Characterization and Influence on Skin Barrier and Skin Penetration." *AAPS PharmSciTech* 26 (2025): 1-17.
182. Gupta, D., Bhatia, D., Dave, V., Sutariya, V. and Varghese Gupta, S. "Salts of Therapeutic Agents: Chemical, Physicochemical, and Biological Considerations." *Molecules* 23 (2018): 1719. https://doi.org/10.1208/s12249-025-03072-0.
183. Hansen, B. B., Spittle, S., Chen, B., Poe, D., Zhang, Y., Klein, J. M., Horton, A., Adhikari, L., Zelovich, T. and Doherty, B. W. "Deep Eutectic Solvents: A Review of Fundamentals and Applications." *Chemical Reviews* 121 (2020): 1232-85. https://doi.org/10.1021/acs.chemrev.0c00385.
184. El Achkar, T., Greige-Gerges, H. and Fourmentin, S. "Basics and Properties of Deep Eutectic Solvents: A Review." *Environmental Chemistry Letters* 19 (2021): 3397-408. https://doi.org/10.1007/s10311-021-01225-8.
185. Płotka-Wasylka, J., De la Guardia, M., Andruch, V. and Vilková, M. "Deep Eutectic Solvents Vs Ionic Liquids: Similarities and Differences." *Microchemical Journal* 159 (2020): 105539. https://doi.org/10.1016/j.microc.2020.105539.
186. Marcus, Y. and Marcus, Y. "Deep Eutectic Solvents in Extraction and Sorption Technology." *Deep Eutectic Solvents* (2019): 153-83. https://doi.org/10.1007/978-3-030-00608-2_5.
187. Martins, M. A., Pinho, S. P. and Coutinho, J. A. "Insights into the Nature of Eutectic and Deep Eutectic Mixtures." *Journal of Solution Chemistry* 48 (2019): 962-82. https://doi.org/10.1007/s10953-018-0793-1.
188. Ma, C., Laaksonen, A., Liu, C., Lu, X. and Ji, X. "The Peculiar Effect of Water on Ionic Liquids and Deep Eutectic Solvents." *Chemical Society Reviews* 47 (2018): 8685-720. https://doi.org/10.1039/C8CS00325D.
189. Rodrigues, R. F., Freitas, A. A., Canongia Lopes, J. N. and Shimizu, K. "Ionic Liquids and Water: Hydrophobicity Vs. Hydrophilicity." *Molecules* 26 (2021): 7159. https://doi.org/10.3390/molecules26237159.
190. Klähn, M., Stüber, C., Seduraman, A. and Wu, P. "What Determines the Miscibility of Ionic Liquids with Water? Identification of the Underlying Factors to Enable a Straightforward Prediction." *The Journal of Physical Chemistry B* 114 (2010): 2856-68. https://doi.org/10.1021/jp1000557.
191. Domańska, U., Królikowski, M., Pobudkowska, A. and Bocheńska, P. "Solubility of Ionic Liquids in Water and Octan-1-Ol and Octan-1-Ol/Water, or 2-Phenylethanol/Water Partition Coefficients." *The Journal of Chemical Thermodynamics* 55 (2012): 225-33. https://doi.org/10.1016/j.jct.2012.06.003.
192. Ossowicz-Rupniewska, P., Klebeko, J., Świątek, E., Bilska, K., Nowak, A., Duchnik, W., Kucharski, Ł., Struk, Ł., Wenelska, K. and Klimowicz, A. "Influence of the Type of Amino Acid on the Permeability and Properties of Ibuprofenates of Isopropyl Amino

Acid Esters." *International Journal of Molecular Sciences* 23 (2022): 4158. https://doi.org/10.3390/ijms23084158.
193. Nordness, O. and Brennecke, J. F. "Ion Dissociation in Ionic Liquids and Ionic Liquid Solutions." *Chemical Reviews* 120 (2020): 12873-902. https://doi.org/10.1021/acs.chemrev.0c00373.
194. He, L., Xiong, D., Ma, L., Liang, Y., Zhang, T., Wu, Z., Tang, H. and Wu, X. "Ion-Pair Compounds of Strychnine for Enhancing Skin Permeability: Influencing the Transdermal Processes in Vitro Based on Molecular Simulation." *Pharmaceuticals (Basel, Switzerland)* 15 (2021): 34. https://doi.org/10.3390/ph15010034.
195. Liang, Y., Duan, M., Yi, W., Zhang, T., Wang, Y., Wu, Z. and Tang, H. "Ion-Pair Compounds of Diacerein for Enhancing Skin Permeability in Vitro: The Compatibility–Permeability Relationship of Counter Ion and Diacerein." *Drug Delivery* 29 (2022): 499-505. https://doi.org/10.1080/10717544.2022.2032877.
196. Wang, M., Wang, Z., Zhang, J., Zhang, L., Wang, W., Zhan, J., Liao, Y., Wu, C., Yu, W. and Zhang, J. "A Matrine-Based Supramolecular Ionic Salt That Enhances the Water Solubility, Transdermal Delivery, and Bioactivity of Salicylic Acid." *Chemical Engineering Journal* 468 (2023): 143480. https://doi.org/10.1016/j.cej.2023.143480.
197. Jeon, H., Park, N., Won, J. G., Shin, Y. W., Choi, J., Min, K., Choi, E., Kim, C. K., Park, S. W. and Son, N. S. "Enhanced Skin Permeation and Pigmentation Reduction Effects of a Novel Tranexamic Acid-Mandelic Acid Ion-Pairing Complex." *Skin Research and Technology* 31 (2025): e70222. https://doi.org/10.1111/srt.70222.
198. Klebeko, J., Ossowicz-Rupniewska, P., Nowak, A., Kucharska, E., Kucharski, Ł., Duchnik, W., Struk, Ł., Klimowicz, A. and Janus, E. "Cations of Amino Acid Alkyl Esters Conjugated with an Anion from the Group of NSAIDs–as Tunable Pharmaceutical Active Ionic Liquids." *Journal of Molecular Liquids* 384 (2023): 122200. https://doi.org/10.1016/j.molliq.2023.122200.
199. Świątek, E., Ossowicz-Rupniewska, P., Janus, E., Nowak, A., Sobolewski, P., Duchnik, W., Kucharski, Ł. and Klimowicz, A. "Novel Naproxen Salts with Increased Skin Permeability." *Pharmaceutics* 13 (2021): 2110. https://doi.org/10.3390/pharmaceutics13122110.
200. Ossowicz-Rupniewska, P., Nowak, A., Klebeko, J., Janus, E., Duchnik, W., Adamiak-Giera, U., Kucharski, Ł., Prowans, P., Petriczko, J. and Czapla, N. "Assessment of the Effect of Structural Modification of Ibuprofen on the Penetration of Ibuprofen from Pentravan®(Semisolid) Formulation Using Human Skin and a Transdermal Diffusion Test Model." *Materials* 14 (2021): 6808. https://doi.org/10.3390/ma14226808.
201. Klebeko, J., Ossowicz-Rupniewska, P., Nowak, A., Janus, E., Duchnik, W., Adamiak-Giera, U., Kucharski, Ł., Prowans, P., Petriczko, J. and Czapla, N. "Permeability of Ibuprofen in the Form of Free Acid and Salts of L-Valine Alkyl Esters from a Hydrogel Formulation through Strat-M™ Membrane and Human Skin." *Materials* 14 (2021): 6678. https://doi.org/10.3390/ma14216678.
202. Ossowicz-Rupniewska, P., Szczepkowska, K., Bednarczyk, P., Nowak, M., Nowak, A., Duchnik, W., Kucharski, Ł., Struk, Ł., Klimowicz, A. and Czech, Z. "New Amino Acid Propyl Ester Ibuprofenates from Synthesis to Use in Drug Delivery Systems." *RSC advances* 12 (2022): 35779-92. https://doi.org/10.1039/D2RA05804A.
203. Witkowski, K., Nowak, A., Duchnik, W., Kucharski, Ł., Struk, Ł. and Ossowicz-Rupniewska, P. "Exploring Alkyl Ester Salts of L-Amino Acid Derivatives of Ibuprofen: Physicochemical Characterization and Transdermal Potential." *Molecules* 28 (2023): 7523. https://doi.org/10.3390/molecules28227523.
204. Kopciuch, E., Janus, E., Ossowicz-Rupniewska, P., Nowak, A., Duchnik, W., Kucharski, Ł., Adamiak-Giera, U. and Lendzion-Bieluń, Z. "Characterization of Naproxen Salts with Amino Acid Esters and Their Application in Topical Skin Preparations." *European Journal of Pharmaceutics and Biopharmaceutics* 204 (2024): 114505. https://doi.org/ 10.1016/j.ejpb.2024.114505.
205. Kopciuch, E., Ossowicz-Rupniewska, P., Adamiak-Giera, U., Nowak, A., Wilpiszewska, K., Białecka, M., Kucharski, Ł., Muzykiewicz-Szymańska, A., Miernik,

M. and Halczak, M. "Topical Pentravan® Based Compositions with Naproxen and Its Proline Ester Derivative—a Comparative Study of Physical Properties and Permeation of Naproxen through the Human Skin." *Applied Sciences (2076-3417)* 15 (2025): 1-16. https://doi.org/10.3390/app15031338.
206. Janus, E., Pinheiro, L. R., Nowak, A., Kucharska, E., Świątek, E., Podolak, N., Perużyńska, M., Piotrowska, K., Duchnik, W. and Kucharski, Ł. "New Ferulic Acid and Amino Acid Derivatives with Increased Cosmeceutical and Pharmaceutical Potential." *Pharmaceutics* 15 (2022): 117. https://doi.org/10.3390/pharmaceutics15010117.
207. Bommannan, D., Potts, R. O. and Guy, R. H. "Examination of the Effect of Ethanol on Human Stratum Corneum in Vivo Using Infrared Spectroscopy." *Journal of Controlled Release* 16 (1991): 299-304. https://doi.org/10.1016/0168-3659(91)90006-Y.
208. Berner, B., Mazzenga, G. C., Otte, J. H., Steffens, R. J., Juang, R. H. and Ebert, C. D. "Ethanol: Water Mutually Enhanced Transdermal Therapeutic System Ii: Skin Permeation of Ethanol and Nitroglycerin." *Journal of Pharmaceutical Sciences* 78 (1989): 402-07. https://doi.org/10.1002/jps.2600780512.
209. Kurihara-Bergstrom, T., Knutson, K., DeNoble, L. J. and Goates, C. Y. "Percutaneous Absorption Enhancement of an Ionic Molecule by Ethanol–Water Systems in Human Skin." *Pharmaceutical Research* 7 (1990): 762-66. https://doi.org/10.1023/A:1015879925147.
210. Megrab, N. A., Williams, A. C. and Barry, B. W. "Oestradiol Permeation across Human Skin, Silastic and Snake Skin Membranes: The Effects of Ethanol/Water Co-Solvent Systems." *International Journal of Pharmaceutics* 116 (1995): 101-12. https://doi.org/10.1016/0378-5173(94)00321-U.
211. Agboola, A. A., Nowak, A., Duchnik, W., Kucharski, Ł., Story, A., Story, G., Struk, Ł., Antosik, A. K. and Ossowicz-Rupniewska, P. "Emulsion-Based Gel Loaded with Ibuprofen and Its Derivatives." *Gels* 9 (2023): 391. https://doi.org/10.3390/gels9050391.
212. Hamdan, I. I., El-Sabawi, D., Ramazanov, R. R., Lantushenko, A., Evstigneev, M., Altaher, A., Mansour, R. and Bani-Jaber, A. "Valsartan–Choline: Preparation, Characterization, and Transdermal Permeation." *Journal of Molecular Liquids* 419 (2025): 126827. https://doi.org/10.1016/j.molliq.2024.126827.
213. British Pharmacopoeia Commission. *British Pharmacopoeia 2018*. London: London : The Stationery Office on behalf of the Medicines and Healthcare products Regulatory Agency MHRA, 2017.
214. Bucci, R., Magrì, A. D. and Magrì, A. L. "Determination of Diclofenac Salts in Pharmaceutical Formulations." *Fresenius J Anal Chem* 362 (1998): 577-82. https://doi.org/10.1007/s002160051127.
215. Bhattacharya, S. S., Banerjee, S., Ghosh, A. K., Chattopadhyay, P., Verma, A. and Ghosh, A. "A Rp-Hplc Method for Quantification of Diclofenac Sodium Released from Biological Macromolecules." *International Journal of Biological Macromolecules* 58 (2013): 354-59. https://doi.org/10.1016/j.ijbiomac.2013.03.065.
216. Chaudhary, H., Kohli, K., Amin, S., Arora, S., Kumar, V., Rathee, S. and Rathee, P. "Development and Validation of Rp-Hplc Method for Simultaneous Estimation of Diclofenac Diethylamine and Curcumin in Transdermal Gels." *Journal of Liquid Chromatography & Related Technologies* 35 (2012): 174-87. https://doi.org/10.1080/10826076.2011.597068.
217. Hamad, Z. S. and Yahya, B. M. "High Performance Liquid Chromatographic Determination of Diclofenac Sodium in Plasma of the Rat." *Iraqi Journal of Veterinary Sciences* 27 (2013): 103-07. https://doi.org/10.33899/ijvs.2013.82815.
218. Mulgund, S., Phoujdar, M., Londhe, S., Mallade, P., Kulkarni, T., Deshpande, A. and Jain, K. "Stability Indicating Hplc Method for Simultaneous Determination of Mephenesin and Diclofenac Diethylamine." *Indian Journal of Pharmaceutical Sciences* 71 (2009): 35-40. https://doi.org/10.4103/0250-474X.51950.

219. Yilmaz, B., Asci, A. and Palabiyik, S. S. "Hplc Method for Determination of Diclofenac in Human Plasma and Its Application to a Pharmacokinetic Study in Turkey." *Journal of Chromatographic Science* 49 (2011): 422-27. https://doi.org/10.1093/chrsci/49.6.422.
220. Cristofoli, M., Hadgraft, J., Lane, M. E. and Sil, B. C. "A Preliminary Investigation into the Use of Amino Acids as Potential Ion Pairs for Diclofenac Transdermal Delivery." *International Journal of Pharmaceutics* 623 (2022): 121906-06. https://doi.org/10.1016/j.ijpharm.2022.121906.
221. International Conference on Harmonisation Expert Working Group. "Validation of Analytical Procedures: Text and Methodology Q2 (R1)." Presented at International Conference on Harmonization of Technical Requirements for Registration of Pharmaceuticals for Human Use, Geneva, Switzerland, 2005.
222. Cristofoli, M., Hadgraft, J., Lane, M. E. and Sil, B. C. "A Model Binary System for the Evaluation of Novel Ion Pair Formulations of Diclofenac." *RSC Pharmaceutics* 1 (2024): 234 - 244. https://doi.org/10.1039/D4PM00063C.
223. Cristofoli, M., Hadgraft, J., Lane, M. E. and Sil, B. C. "Ion Pairing as a Strategy to Enhance the Delivery of Diclofenac." *RSC Pharmaceutics* 2 (2025): 1163-1174 https://doi.org/10.1039/D5PM00096C.
224. Dick, I. P. and Scott, R. C. "Pig Ear Skin as an *in Vitro* Model for Human Skin Permeability." *Journal of Pharmacy and Pharmacology* 44 (1992): 640-45. https://doi.org/10.1111/j.2042-7158.1992.tb05485.x.
225. OECD, T. G. "428: Skin Absorption: In Vitro Method." *OECD Guidelines for the Testing of Chemicals, Section* 4 (2004): 1 - 8.
226. Saei, A. A., Jabbaribar, F., Fakhree, M. A. A., Acree, W. E. and Jouyban, A. "Solubility of Sodium Diclofenac in Binary Water + Alcohol Solvent Mixtures at 25°C." *Journal of Drug Delivery Science and Technology* 18 (2008): 149-51. https://doi.org/10.1016/S1773-2247(08)50024-4.
227. Chiarini, A., Tartarini, A. and Fini, A. "Ph-Solubility Relationship and Partition Coefficients for Some Anti-Inflammatory Arylaliphatic Acids." *Archiv der Pharmazie* 317 (1984): 268-73. https://doi.org/10.1002/ardp.19843170314.
228. Fini, A., Fazio, G. and Feroci, G. "Solubility and Solubilization Properties of Non-Steroidal Anti-Inflammatory Drugs." *International Journal of Pharmaceutics* 126 (1995): 95-102. https://doi.org/10.1016/0378-5173(95)04102-8.
229. Avdeef, A., Box, K., Comer, J., Hibbert, C. and Tam, K. "Ph-Metric Logp 10. Determination of Liposomal Membrane-Water Partition Coefficients of Ionizable Drugs." *Pharmaceutical Research* 15 (1998): 209-15. https://doi.org/10.1023/A:1011954332221.
230. Llinàs, A., Burley, J. C., Box, K. J., Glen, R. C. and Goodman, J. M. "Diclofenac Solubility: Independent Determination of the Intrinsic Solubility of Three Crystal Forms." *Journal of Medicinal Chemistry* 50 (2007): 979. https://doi.org/10.1021/jm0612970.
231. Bjerrum, N. *Untersuchungen Über Ionenassoziation*. AF Høst, 1926, 6, 14, 32-36, 46-47.
232. Durairaj, C., Kim, S. J., Edelhauser, H. F., Shah, J. C. and Kompella, U. B. "Influence of Dosage Form on the Intravitreal Pharmacokinetics of Diclofenac." *Investigative Ophthalmology and Visual Science* 50 (2009): 4887-97. https://doi.org/10.1167/iovs.09-3565.
233. Primorac, D., Molnar, V., Matišić, V., Hudetz, D., Jeleč, Ž., Rod, E., Čukelj, F., Vidović, D., Vrdoljak, T. and Dobričić, B. "Comprehensive Review of Knee Osteoarthritis Pharmacological Treatment and the Latest Professional Societies' Guidelines." *Pharmaceuticals* 14 (2021): 205. https://doi.org/ 10.3390/ph14030205.
234. Rannou, F., Pelletier, J.-P. and Martel-Pelletier, J. "Efficacy and Safety of Topical NSAIDs in the Management of Osteoarthritis: Evidence from Real-Life Setting Trials and Surveys." *Seminars in Arthritis and Rheumatism* 45 (2016): S18-S21. https://doi.org/ 10.1016/j.semarthrit.2015.11.007.

235. American Academy of Orthopaedic Surgeons (AAOS). "Treatment of Osteoarthritis of the Knee: Evidence-Based Guideline." *Journal of the American Academy of Orthopaedic Surgeons* 21 (2013): 577-9. https://doi.org/10.5435/JAAOS-21-09-571.
236. Bariguian Revel, F., Fayet, M. and Hagen, M. "Topical Diclofenac, an Efficacious Treatment for Osteoarthritis: A Narrative Review." *Rheumatology and Therapy* 7 (2020): 217-36. https://doi.org/ 10.1007/s40744-020-00196-6.
237. Lane, M. E., Santos, P., Watkinson, A. C. and Hadgraft, J. "Passive Skin Permeation Enhancement." In *Topical and Transdermal Drug Delivery.* Hoboken, NJ, USA: John Wiley & Sons, Inc., 2012. https://doi.org/10.1002/9781118140505.
238. Barton, A. F. *CRC Handbook of Solubility Parameters and Other Cohesion Parameters*. 2nd ed. New York: CRC Press, 1991.
239. Louwerse, M. J., Maldonado, A., Rousseau, S., Moreau-Masselon, C., Roux, B. and Rothenberg, G. "Revisiting Hansen Solubility Parameters by Including Thermodynamics." *Chemphyschem* 18 (2017): 2999-3006. https://doi.org/10.1002/cphc.201700408.
240. Alshehri, S. and Shakeel, F. "Solubility Determination, Various Solubility Parameters and Solution Thermodynamics of Sunitinib Malate in Some Cosolvents, Water and Various (Transcutol+ Water) Mixtures." *Journal of Molecular Liquids* 307 (2020): 112970. https://doi.org/ 10.1016/j.molliq.2020.112970.
241. Hansen, C. M. *Hansen Solubility Parameters: A User's Handbook*. CRC press, 2007, 1.
242. Hancock, B. C., York, P. and Rowe, R. C. "The Use of Solubility Parameters in Pharmaceutical Dosage Form Design." *International Journal of Pharmaceutics* 148 (1997): 1-21. https://doi.org/ 10.1016/S0378-5173(96)04828-4.
243. Barra, J., Peña, M.-A. and Bustamante, P. "Proposition of Group Molar Constants for Sodium to Calculate the Partial Solubility Parameters of Sodium Salts Using the Van Krevelen Group Contribution Method." *European Journal of Pharmaceutical Sciences* 10 (2000): 153-61. https://doi.org/10.1016/S0928-0987(00)00061-0.
244. Bustamante, P., Peña, M. A. and Barra, J. "Partial-Solubility Parameters of Naproxen and Sodium Diclofenac." *J. Pharm. Pharmacol.* 50 (1998): 975-82. https://doi.org/10.1111/j.2042-7158.1998.tb06911.x.
245. Gattefossé SAS. *Transcutol® P for Efficient Drug Solubilization and Skin Penetration*. 2018, 1-24.
246. Vishwam, T., Shihab, S., Murthy, V. K., Tiong, H. S. and Sastry, S. S. "Microwave Dielectric Relaxation Spectroscopy Study of Propylene Glycol/Ethanol Binary Mixtures: Temperature Dependence." *Spectrochim. Acta, Part A* 179 (2017): 74-82. https://doi.org/ 10.1016/j.saa.2017.02.023.
247. Sengwa, R. "A Comparative Dielectric Study of Ethylene Glycol and Propylene Glycol at Different Temperatures." *Journal of Molecular Liquids* 108 (2003): 47-60. https://doi.org/10.1016/S0167-7322(03)00173-9.
248. Ikada, E. "Dielectric Properties of Some Diols." *Journal of Physical Chemistry* 75 (1971): 1240-46. https://doi.org/ https://doi.org/10.1021/j100679a012.
249. Malmberg, C. and Maryott, A. "Dielectric Constant of Water from 0 to 100 C." *J. Res. Natl. Bur. Stand. (U. S.)* 56 (1956): 1-8.
250. Osborne, D. W. and Musakhanian, J. "Skin Penetration and Permeation Properties of Transcutol®—Neat or Diluted Mixtures." *AAPS PharmSciTech* 19 (2018): 3512-33. https://doi.org/10.1208/s12249-018-1196-8.
251. Ha, E.-S., Lee, S.-K., Choi, D. H., Jeong, S. H., Hwang, S.-J. and Kim, M.-S. "Application of Diethylene Glycol Monoethyl Ether in Solubilization of Poorly Water-Soluble Drugs." *J. Pharm. Invest.* 50 (2020): 231-50. https://doi.org/10.1007/s40005-019-00454-y.
252. Hashemzadeh, N. and Jouyban, A. "Review of Pharmaceutical Applications of Diethylene Glycol Monoethyl Ether: Pharmaceutical Applications of Carbitol." *Journal of Pharmacy & Pharmaceutical Sciences* 25 (2022): 340-53.

253. Dugard, P. H., Walker, M., Mawdsley, S. J. and Scott, R. C. "Absorption of Some Glycol Ethers through Human Skin in Vitro." *Environmental Health Perspectives* 57 (1984): 193-97. https://doi.org/10.1289/ehp.845719.
254. Kikwai, L., Kanikkannan, N., Babu, R. and Singh, M. "Effect of Vehicles on the Transdermal Delivery of Melatonin across Porcine Skin in Vitro." *Journal of Controlled Release* 83 (2002): 307-11. https://doi.org/ 10.1016/S0168-3659(02)00202-X.
255. Csizmazia, E., Erős, G., Berkesi, O., Berkó, S., Szabó-Révész, P. and Csányi, E. "Penetration Enhancer Effect of Sucrose Laurate and Transcutol on Ibuprofen." *Journal of Drug Delivery Science and Technology* 21 (2011): 411-15. https://doi.org/10.1016/S0168-3659(02)00202-X.
256. Bialik, W., Walters, K., Brain, K. and Hadgraft, J. "Some Factors Affecting the in Vitro Penetration of Ibuprofen through Human Skin." *International Journal of Pharmaceutics* 92 (1993): 219-23. https://doi.org/10.1016/0378-5173(93)90283-L.
257. Shakeel, F. and Alshehri, S. "Solubilization, Hansen Solubility Parameters, Solution Thermodynamics and Solvation Behavior of Flufenamic Acid in (Carbitol+ Water) Mixtures." *Processes* 8 (2020): 1204. https://doi.org/ 10.3390/pr8101204.
258. Shakeel, F., Haq, N., Alanazi, F. K., Alanazi, S. A. and Alsarra, I. A. "Solubility of Sinapic Acid in Various (Carbitol+ Water) Systems: Computational Modeling and Solution Thermodynamics." *Journal of Thermal Analysis and Calorimetry* 142 (2020): 1437-46. https://doi.org/10.1007/s10973-020-09451-y.
259. Shakeel, F., Kazi, M., Alanazi, F. K. and Alam, P. "Solubility of Cinnarizine in (Transcutol+ Water) Mixtures: Determination, Hansen Solubility Parameters, Correlation, and Thermodynamics." *Molecules* 26 (2021): 7052. https://doi.org/10.3390/molecules26227052.
260. Shakeel, F., Haq, N. and Alshehri, S. "Solubility Data of the Bioactive Compound Piperine in (Transcutol+ Water) Mixtures: Computational Modeling, Hansen Solubility Parameters and Mixing Thermodynamic Parameters." *Molecules* 25 (2020): 2743. https://doi.org/10.3390/molecules25122743.
261. Shazly, G., Haq, N. and Shakeel, F. "Solution Thermodynamics and Solubilization Behavior of Diclofenac Sodium in Binary Mixture of Transcutol-Hp and Water." *Die Pharmazie-An International Journal of Pharmaceutical Sciences* 69 (2014): 335-39. https://doi.org/10.1691/ph.2014.3208.
262. Shakeel, F., Alanazi, F. K., Alsarra, I. A. and Haq, N. "Solubilization Behavior of Paracetamol in Transcutol–Water Mixtures at (298.15 to 333.15) K." *Journal of chemical and engineering data* 58 (2013): 3551-56. https://doi.org/10.1021/je4008525.
263. Brown, G. A. "Aaos Clinical Practice Guideline: Treatment of Osteoarthritis of the Knee: Evidence-Based Guideline." *JAAOS-Journal of the American Academy of Orthopaedic Surgeons* 21 (2013): 577-79. https://doi.org/ 10.5435/JAAOS-21-09-577
264. Golightly, L. K., Smolinske, S. S., Bennett, M. L., Sutherland, E. W. and Rumack, B. H. "Pharmaceutical Excipients: Adverse Effects Associated with Inactive Ingredients in Drug Products (Part I)." *Medical Toxicology and Adverse Drug Experience* 3 (1988): 128-65. https://doi.org/10.1007/BF03259937.
265. Liron, Z. and Cohen, S. "Percutaneous Absorption of Alkanoic Acids Ii: Application of Regular Solution Theory." *Journal of Pharmaceutical Sciences* 73 (1984): 538-42. https://doi.org/10.1002/jps.2600730426.
266. Scientific Commitee on Consumer Products. *Opinion on Diethylene Glycol Monoethyl Ether (Degee)*. European Commission, 2006.
267. Haque, T., Rahman, K. M., Thurston, D. E., Hadgraft, J. and Lane, M. E. "Topical Delivery of Anthramycin I. Influence of Neat Solvents." *European Journal of Pharmaceutical Sciences* 104 (2017): 188-95. https://doi.org/10.1016/j.ejps.2017.03.043.

268. Iliopoulos, F., Sil, B. C., Al Hossain, A. M., Moore, D. J., Lucas, R. A. and Lane, M. E. "Topical Delivery of Niacinamide: Influence of Neat Solvents." *International Journal of Pharmaceutics* 579 (2020): 119137. https://doi.org/10.1016/j.ijpharm.2020.119137.
269. Hossain, A. M. A., Sil, B. C., Iliopoulos, F., Lever, R., Hadgraft, J. and Lane, M. E. "Preparation, Characterisation, and Topical Delivery of Terbinafine." *Pharmaceutics* 11 (2019): 548. https://doi.org/10.3390/pharmaceutics11100548.
270. Kung, C.-P., Zhang, Y., Sil, B. C., Hadgraft, J., Lane, M. E., Patel, B. and McCulloch, R. "Investigation of Binary and Ternary Solvent Systems for Dermal Delivery of Methadone." *International Journal of Pharmaceutics* 586 (2020): 119538. https://doi.org/10.1016/j.ijpharm.2020.119538.
271. Haque, T., Thurston, D., Rahman, K., Hadgraft, J. and Lane, M. "Topical Delivery of Anthramycin II. Influence of Binary and Ternary Solvent Systems." *European Journal of Pharmaceutical Sciences* 121 (2018): 59-64. https://doi.org/10.1016/j.ejps.2018.05.002.
272. National Center for Biotechnology Information. *Pubchem Compound Summary for Diethylene Glycol Monoethyl Ether.* United States National Library of Medicine (NLM), 2024.
273. National Center for Biotechnology Information *Pubchem Compound Summary for Dipropylene Glycol.* United States National Library of Medicine (NLM), 2024.
274. Harrison, J. E., Watkinson, A. C., Green, D. M., Hadgraft, J. and Brain, K. "The Relative Effect of Azone® and Transcutol® on Permeant Diffusivity and Solubility in Human Stratum Corneum." *Pharmaceutical Research* 13 (1996): 542-46. https://doi.org/10.1023/A:1016037803128.
275. Björklund, S., Pham, Q. D., Jensen, L. B., Knudsen, N. Ø., Nielsen, L. D., Ekelund, K., Ruzgas, T., Engblom, J. and Sparr, E. "The Effects of Polar Excipients Transcutol and Dexpanthenol on Molecular Mobility, Permeability, and Electrical Impedance of the Skin Barrier." *Journal of colloid and interface science* 479 (2016): 207-20. https://doi.org/10.1016/j.jcis.2016.06.054.
276. Hadgraft, J. "Skin, the Final Frontier" *International Journal of Pharmaceutics* 224, no. 1-2 (2001) 1-18. https://doi.org/10.1016/S0378-5173(01)00731-1.
277. Oliveira, G., Hadgraft, J. and Lane, M. "The Role of Vehicle Interactions on Permeation of an Active through Model Membranes and Human Skin." *International Journal of Cosmetic Science* 34 (2012): 536-45. https://doi.org/10.1111/j.1468-2494.2012.00753.x.
278. Sastry, S. S., Sarma, N., Vishwam, T. and Murthy, V. "Dielectric Relaxation Studies of Acetonitrile/Propylene Glycol and Their Binary Mixtures." *Indian Journal of Pure & Applied Physics (IJPAP)* 55 (2017): 403-12. https://doi.org/10.1016/j.saa.2017.02.023.
279. Daubert, T. E. "Physical and Thermodynamic Properties of Pure Chemicals: Data Compilation." *Design Institute for Physacal Property Data (DIPPR)* (1989).
280. Kasting, G. B., Francis, W. R. and Roberts, G. E. "Skin Penetration Enhancement of Triprolidine Base by Propylene Glycol." *Journal of Pharmaceutical Sciences* 82 (1993): 551-52. https://doi.org/ 10.1002/jps.2600820525.
281. Herkenne, C., Naik, A., Kalia, Y. N., Hadgraft, J. and Guy, R. H. "Effect of Propylene Glycol on Ibuprofen Absorption into Human Skin in Vivo." *Journal of Pharmaceutical Sciences* 97 (2008): 185-97. https://doi.org/10.1002/jps.20829.
282. Watkinson, R., Guy, R., Hadgraft, J. and Lane, M. "Optimisation of Cosolvent Concentration for Topical Drug Delivery–Ii: Influence of Propylene Glycol on Ibuprofen Permeation." *Skin Pharmacology and Physiology* 22 (2009): 225-30. https://doi.org/10.1159/000231528.
283. Mohammed, D., Hirata, K., Hadgraft, J. and Lane, M. E. "Influence of Skin Penetration Enhancers on Skin Barrier Function and Skin Protease Activity." *European Journal of Pharmaceutical Sciences* 51 (2014): 118-22. https://doi.org/10.1016/j.ejps.2013.09.009.

284. Barry, B. W. "Mode of Action of Penetration Enhancers in Human Skin." *Journal of controlled release* 6 (1987): 85-97. https://doi.org/10.1016/0168-3659(87)90066-6.
285. Bouwstra, J., De Vries, M., Gooris, G., Bras, W., Brussee, J. and Ponec, M. "Thermodynamic and Structural Aspects of the Skin Barrier." *Journal of Controlled Release* 15 (1991): 209-19. https://doi.org/10.1016/0168-3659(91)90112-Q.
286. Brinkmann, I. and Müller-Goymann, C. "An Attempt to Clarify the Influence of Glycerol, Propylene Glycol, Isopropyl Myristate and a Combination of Propylene Glycol and Isopropyl Myristate on Human Stratum Corneum." *Die Pharmazie-An International Journal of Pharmaceutical Sciences* 60 (2005): 215-20.
287. Moghadam, S. H., Saliaj, E., Wettig, S. D., Dong, C., Ivanova, M. V., Huzil, J. T. and Foldvari, M. "Effect of Chemical Permeation Enhancers on Stratum Corneum Barrier Lipid Organizational Structure and Interferon Alpha Permeability." *Molecular Pharmaceutics* 10 (2013): 2248-60. https://doi.org/10.1021/mp300441c.
288. Carrer, V., Alonso, C., Pont, M., Zanuy, M., Córdoba, M., Espinosa, S., Barba, C., Oliver, M. A., Martí, M. and Coderch, L. "Effect of Propylene Glycol on the Skin Penetration of Drugs." *Archives of Dermatological Research* 312 (2020): 337-52. https://doi.org/10.1007/s00403-019-02017-5.
289. Hoelgaard, A. and Møllgaard, B. "Dermal Drug Delivery—Improvement by Choice of Vehicle or Drug Derivative." *Journal of Controlled Release* 2 (1985): 111-20. https://doi.org/10.1016/0168-3659(85)90037-9.
290. Fasano, W. J., ten Berge, W. F., Banton, M. I., Heneweer, M. and Moore, N. P. "Dermal Penetration of Propylene Glycols: Measured Absorption across Human Abdominal Skin in Vitro and Comparison with a Qsar Model." *Toxicology in Vitro* 25 (2011): 1664-70. https://doi.org/10.1016/j.tiv.2011.07.003.
291. Guo, X., Guo, Z., Wei, H., Yang, H., He, Y., Xie, S., Wu, G., Zhong, H., Li, L. and Zhao, Q. "In Vivo Quantification of Propylene Glycol, Glucose and Glycerol Diffusion in Human Skin with Optical Coherence Tomography." *Laser physics* 20 (2010): 1849-55. https://doi.org/10.1134/S1054660X10170032.
292. Mohammed, D., Matts, P., Hadgraft, J. and Lane, M. "In Vitro–in Vivo Correlation in Skin Permeation." *Pharmaceutical Research* 31 (2014): 394-400. https://doi.org/10.1007/s11095-013-1169-2.
293. Trottet, L., Merly, C., Mirza, M., Hadgraft, J. and Davis, A. "Effect of Finite Doses of Propylene Glycol on Enhancement of in Vitro Percutaneous Permeation of Loperamide Hydrochloride." *International Journal of Pharmaceutics* 274 (2004): 213-19. https://doi.org/10.1016/j.ijpharm.2004.01.013.
294. Williams, A. C. and Barry, B. W. "Penetration Enhancers." *Advanced Drug Delivery Reviews* 64 (2012): 128-37. https://doi.org/10.1016/j.addr.2012.09.032.
295. Paz-Alvarez, M., Pudney, P. D., Hadgraft, J. and Lane, M. E. "Topical Delivery of Climbazole to Mammalian Skin." *International Journal of Pharmaceutics* 549 (2018): 317-24. https://doi.org/10.1016/j.ijpharm.2018.07.058.
296. Schneider, I.-M., Dobner, B., Neubert, R. and Wohlrab, W. "Evaluation of Drug Penetration into Human Skin Ex Vivo Using Branched Fatty Acids and Propylene Glycol." *International Journal of Pharmaceutics* 145 (1996): 187-96. https://doi.org/10.1016/S0378-5173(96)04768-0.
297. Bonnist, E., Gorce, J.-P., Mackay, C., Pendlington, R. and Pudney, P. "Measuring the Penetration of a Skin Sensitizer and Its Delivery Vehicles Simultaneously with Confocal Raman Spectroscopy." *Skin Pharmacology and Physiology* 24 (2011): 274-83. https://doi.org/10.1159/000328729.
298. Zhang, Q., Li, P. and Roberts, M. S. "Maximum Transepidermal Flux for Similar Size Phenolic Compounds Is Enhanced by Solvent Uptake into the Skin." *Journal of Controlled Release* 154 (2011): 50-57. https://doi.org/10.1016/j.jconrel.2011.04.018.
299. Yamane, M. A., Williams, A. C. and Barry, B. W. "Terpene Penetration Enhancers in Propylene Glycol/Water Co-Solvent Systems: Effectiveness and Mechanism of Action." *J Pharm Pharmacol* 47 (1995): 978-89. https://doi.org/10.1111/j.2042-7158.1995.tb03282.x.

300. Paz-Alvarez, M., Tang, C. F., Pudney, P. D. and Lane, M. E. "Rational Development of Topical Climbazole Formulations." *International Journal of Pharmaceutics* 653 (2024): 123886. https://doi.org/10.1016/j.ijpharm.2024.123886.
301. US Food and Drug Administration. *Analytical Procedures and Methods Validation for Drugs and Biologics : Guidance for Industry*. Silver Spring: US Department of Health and Human Services, 2015, 1 - 15.
302. Center for Drug Evaluation and Research. *Reviewer Guidance: Validation of Chromatographic Methods*. Washington: CDER, 1994, 1 - 30.
303. United States Pharmacopoeial Convention. *First Supplement to Usp 40 - Nf 35, <1225> Validation of Compendial Prodecures*. Rockville: United States Pharmacopeial Convention, 2017, 877 - 81.
304. Ueda, C. T., Shah, V. P., Derdzinski, K., Ewing, G., Flynn, G., Maibach, H., Marques, M., Rytting, H., Shaw, S. and Thakker, K. "Topical and Transdermal Drug Products." Presented at Pharmacopeial Forum, 2009. 35, 750-64.
305. Swartz, M. E. and Krull, I. S. *Analytical Method Development and Validation*. CRC Press, 2018.
306. "Analytical Method Validation, Verification and Transfer." In *Pharmaceutical Analysis for Small Molecules*. Edited by Davani,B. Hoboken, New Jersey: John Wiley and Sons, 2017, 69 - 83.
307. OECD. *Guidance Document for the Conduct of Skin Absorption Studies*. Paris: 2004, 1-31.

11 Appendices

Appendix A: Method Validation

A.1 Introduction

Validation of an HPLC method essentially comprises “the process of demonstrating that an analytical procedure is suitable for its intended purpose” [301]. Guidance for this undertaking was obtained from a variety of complementary sources including the United States Food and Drug Administration (FDA) “Guidance for industry:analytical procedures and methods validation for drugs and biologics” [301], The International Council for Harmonisation of Technical Requirements for Pharmaceuticals for Human Use (ICH) guideline “Validation of Analytical Procedures: Text and Methodology Q2 (R1)” [221] (ICH Q2 (R1), the FDA’s “Reviewer Guidance, validation of chromatographic methods” [302] as well as chapter <1225> of the United States Pharmacopeia (USP) [303].

A.2 Materials and methods

A.2.1 Materials

Diclofenac sodium (DNa) 98% and the amino acids, L-arginine (L-Arg) 98+%, L-lysine (L-Lys) 98% and L-histidine monochloride monohydrate (LHSS) 98% were purchased from Acros Organics (VWR, Leceistershire, UK). L-histidine (L-His) high purity grade I was ordered from VWR (Leceistershire, UK). The amino acid salts L-arginine monohydrochloride (L-ASS) 98+% and L-lysine monohydrochloride (L-LSS) 99+% were obtained from Alfa Aesar also supplied by VWR (Leceistershire, UK). High vacuum grease was obtained from Dow Corning (Seneffe, Belgium). Oxoid™ Phosphate buffered saline (PBS) tablets were purchased from Thermo Fisher Scientific (Lancashire, UK). Voltarol® 1.16% Emulgel was purchased from Boots pharmacy (Nottingham, UK). HPLC grade acetonitrile and methanol were purchased from Fisher Scientific (Lancashire, UK). Trifluoroacetic acid was purchased from VWR (Leceistershire, UK). Brij® O20 and 0.45 µm Millex® syringe filters were obtained from Sigma Aldrich (Dorset, UK).

A.2.2 Methods

In order to demonstrate that a method is able to fulfil its purpose, a number of method validation characteristics have been outlined by the FDA [301]. These include

specificity, linearity, accuracy, precision, range, quantitation limit and detection limit. They also require a robustness evaluation, unless the method in question is compendial and has no deviations. The FDA refers to the ICH Q2 (R1) as the primary reference for recommendations and definitions on validation characteristics and also includes the FDA guidance for industry on “Validation of Chromatographic methods” [302].

These requirements, known as the “eight steps of method validation”, have also been set out in USP Chapter <1225> [303], and are considered in turn, below.

A.2.2.1 Specificity

Specificity refers to the capacity to analyse the analyte in question despite the presence of other components in the sample such as impurities, excipients and degradation products. It is therefore important to identify the analyte and illustrate the ability to accurately determine the content of an analyte in a sample.

The ICH [221] suggests a two-stage process. The first is identification, which can be accomplished by discriminating between closely related structures, or by comparison to known reference materials. Here, DNa was obtained as the reference material, from which diclofenac (DF) was identified. The identification element of specificity is satisfied within the linearity and range requirement.

The second part of the process requires either the acquisition of impurity tests to ensure the exact amounts of anything that is “non-analyte” or an assay that enables an accurate statement of the content of the analyte in the sample. For the purposes of this study, the content of the analyte was determined by utilising the drug substance as a reference to create an assay. It was then used to quantify the content of the drug product, which contains a defined quantity of DF, as shown below in the accuracy requirement.

As DNa and DF would be included in formulations containing potential counterions, additional tests were carried out to ensure non-interference of the counterions with the detection and quantification of DF. Absorption spectra of the potential counter ions, as free bases (L-Arg, L-His, L-Lys) or in their salt form (L-AS, L-HSS, L-LS) were obtained and compared to the absorption spectrum of DF and DNa. Samples of different molar concentrations of drug and counter ion, separately and in combination, were analysed using the HPLC method.

A.2.2.1 (a) Absorption spectra

Absorption spectra between 200 and 800 nm were recorded for DF, DNa, the free base forms of the counter ions (L-Arg, L-His, and L-Lys), and their corresponding salt forms (L-AS, L-HSS, and L-LS). The solvent system was identical to the mobile phase described in the method outlined in chapter 5, but without TFA, resulting in a mixture of ACN and water (70:30, v/v). This solvent mixture was also used as the blank. Absorbance at 277 nm, the wavelength applied for DF detection, was specifically determined.

A.2.2.1 (b) Analysis of samples using HPLC

All samples were prepared using ACN and water (70:30, v/v) as the solvent. DF was prepared at a concentration of 100 µg/mL, while DNa was prepared at a concentration equivalent to the molar amount of DF. Each amino acid, in both free base and salt forms, was also prepared individually at molar equivalence to DF and at a 50-fold molar excess relative to DF.

In addition to the individual solutions, combination samples were prepared. DF was combined with each of the free base amino acids (L-Arg, L-His, and L-Lys) at two molar ratios, 1:1 and 1:50 (DF:amino acid), with the final DF concentration adjusted to 50 µg/mL. Separately, DNa was combined with each of the amino acid salts (L-ASS, L-HSS, and L-LSS) at the same molar ratios (1:1 and 1:50). For these mixtures, DNa was added at a concentration providing a molar equivalent to 50 µg/mL DF.

Prior to HPLC analysis, all solutions were filtered through a 0.45 µm Millex® filter unit.

A.2.2.2 Linearity and range

The linearity of the procedure indicates its ability to obtain results that are directly proportional to the concentration of the analyte in the sample within a given range [221]. A minimum of five concentrations of the analyte are required to obtain responses, represented in this case by the area under the curve (AUC) [221]. The linear relationship can then be evaluated by obtaining a correlation coefficient (R^2 value), as well as the y-intercept and the slope of the regression line.

Responses (AUC) for nine different concentrations of DNa (0.05 to 100 µg/mL) were obtained using the HPLC conditions mentioned in Table A1. These DNa concentrations corresponded to a range of 0.05 – 93.10 µg/mL of DF. The AUC values represent the average obtained for three replicates. ICH guidelines require a

concentration range that represents a minimum of 80 – 120% of all test concentrations. As the purpose of this method is the quantification of DF permeating through porcine skin as well as mass balance studies, the range may vary from very small amounts to much larger amounts. The maximum amount that would generally be applied is an infinite dose, which equates to approximately 370 µg of DF[1]. In these cases, samples would be diluted. The ultimate objective of these studies was to represent normal conditions of exposure and thus to work with finite dose studies. This is defined as 1 - 5 mg of drug substance per cm^2 of skin for a solid product and up to 10 µL/cm^2 of skin for liquids [88]. This would equate to a maximum concentration in the region of 74 µg of DF, hence the range chosen.

A.2.2.3 Accuracy

Accuracy is defined in the Validation of Chromatographic Methods [302], as the measure of how close the experimental value is to the true value. It recommends that data is obtained representing 80, 100 and 120% of the label claim. As mentioned previously, due to the nature of the experiments undertaken, namely the permeation of DF and its salts through porcine skin together with mass balance studies, a variety of concentrations are analysed. For the drug substance the concentrations are 1, 25 and 50 µg/mL of DNa which equate to 0.93, 23.27 and 46.55 µg/mL of DF. For the drug product, the concentrations of DF analysed were 14.84, 42.68 and 94.63 µg/mL.

The ICH sets out several different methods for establishing the accuracy of drug substances and drug products. The methods for determining the accuracy of drug substances include (i) applying the analytical procedure to an analyte of known purity; (ii) comparing the results of the proposed analytical procedure with another independent procedure whose accuracy is already established or (iii) accuracy can be inferred once precision, linearity and specificity have been established.

Methods for the determination of a drug product include (i) using analytical procedures to analyse synthetic mixtures of drug product components to which known quantities of the drug substance to be analysed has been added; (ii) where samples of all components of the drug product cannot be obtained, it is acceptable to add known quantities of the drug substance or analyte to the drug product or to compare the

[1] This equates to the amount of a diclofenac in DNa soluble in approximately 1 mL of PBS or contained in 50 µl of a commercial gel comprising 1.16% diclofenac salt

results of the proposed analytical procedure with another independent procedure whose accuracy is already established or (iii) accuracy can be inferred once precision, linearity and specificity have been established.

Accuracy should be assessed in all cases using a minimum of 3 concentrations each comprising 3 replicates and should be presented as a percentage recovery (see equation A1).

Equation A 1

$$\%\ Recovery = \frac{measured\ value}{expected\ value}\ x\ 100$$

The Pharmacopeial Forum on Topical and Transdermal Drug Products [304] states that the drug content of drug products packaged in tubes should fall within a range of 90 – 110% of the label claim. Furthermore, the guideline states that when testing uniformity of content, the average relative standard deviation should not be greater than 6%.

The British Pharmacopeia [213] states that DF gel containing diethylamine (DEA) should contain 95 – 105% of the stated amount.

A purity correction factor should also be allowed for when comparing the standard (drug substance) which guarantees only 98% purity to the commercially available drug product.

A.2.2.3 (a) Accuracy of a drug substance

In this case the accuracy was tested by applying the analytical procedure to an analyte of known purity. A stock solution of DNa and water was made up. Three different concentrations namely 1, 25 and 50 µg/mL representing 0.93, 23.27 and 46.55 µg/mL of DF, each comprising three replicates, were then tested using the analytical method described above in section 5.2.1.

A.2.2.3 (b) Accuracy of a drug product

Rather than using synthetic mixtures of the drug product components, three different sample concentrations of an actual commercial formulation were obtained. This ensured that the method was validated under operationally relevant conditions while also satisfying the second stage of the specificity requirement, namely the

determination of the content of the drug product. Amounts of 1.6, 4.6 and 10.2 mg of the commercial drug product were weighed out. This corresponded to concentrations of 14.84, 42.68 and 94.63 µg/mL of DF within each sample[2]. The DF present in the commercially available topical gel was extracted using methanol. The samples plus solvent mixture were placed in a bench shaker at room temperature for 1 hour. The samples were then centrifuged for 15 minutes at 13 200 rpm and the supernatant was tested. The three different concentrations, each comprising three replicates, were analysed.

A.2.2.4 Precision

Precision indicates how close the values for the area under the curve are to one another, when samples of the same concentrations are measured using the same analytical conditions [302]. Investigations of precision comprises a number of different aspects including (i) repeatability, (ii) intermediate precision and (iii) reproducibility. Standard deviation, relative standard deviation and confidence intervals should be reported for each aspect of precision considered (Guidance, 1994; Guideline 2005).

Standard deviation is calculated as shown in equation A2:

Equation A 2

$$Standard\ deviation = \sqrt{\frac{1}{n-1}\sum_{i=1}^{n}(x_i - \bar{x})^2}$$

Where n = sample size, $\bar{x}$ = mean of the sample, i = the first sample and x_i = the value of the first sample.

Relative standard deviation, also known as percentage relative standard deviation or coefficient of variation is calculated as follows:

Equation A 3

$$\%\ Relative\ standard\ deviation = \frac{standard\ deviation}{mean}\ x\ 100$$

[2] The amount of drug product x 1.16% = the amount (g) of diclofenac diethylamine in the sample. In order to obtain the amount of diclofenac, this was divided by the molecular mass of diclofenac diethylamine (370.294 g / mol) and multiplied by the molecular mass of diclofenac (296.147 g / mol).

A.2.2.4 (a) Repeatability

One of the aspects of measuring precision is repeatability over a short time interval using the same conditions. In this case, three different concentrations of DNa, namely 1, 25 and 50 µg/mL representing 0.93, 23.27 and 46.55 µg/mL of DF, each comprising three replicates, were tested intraday.

The same intraday study was performed quantifying diclofenac in a drug product, a commercially available gel. Three different concentrations of diclofenac present in the commercially available gel, namely 14.84, 42.68 and 94.63 µg/mL, each comprising three replicates, were tested intraday.

A.2.2.4 (b) Intermediate precision

Intermediate precision refers to in-lab variations [305]. One method of determining intermediate precision is to determine any differences caused by different experimental periods.

With respect to the intermediate precision of DNa, three different concentrations 1, 25 and 50 µg/mL representing 0.93, 23.27 and 46.55 µg/mL of DF, each comprising three replicates, were analysed on different days.

The same analysis was performed using diclofenac in a commercial gel formulation using theoretical concentrations of 14.84, 42.68 and 94.63 µg/mL.

A.2.2.4 (c) Reproducibility

This refers to precision between laboratories at different sites [306]. Whilst the methods have been used in two laboratories, the results have not been compared.

A.2.2.5 Robustness

The robustness of a method refers to its ability to withstand small, but deliberate variations. Sequential changes to the original method included adjustments to wavelength, injection volume, solvent ratios, temperature of column and flow rate.

A.2.2.6 Limit of detection (LOD) and limit of quantification (LOQ)

Limits of detection (LOD) refer to the lowest concentration of the analyte being investigated that can be detected, but not necessarily quantified. There are numerous ways in which this can be determined. The ICH recognises three methods, including the expression of the LOD as a signal-to-noise ratio, visual non-instrumental methods

such as thin layer chromatography (TLC) or based on the standard deviation of the response and the slope. It is the final method that has been used here.

The detection limit (DL) is determined using the following equation:

Equation A 4

$$DL = \frac{3.3\,\sigma}{S}$$

Where:

σ = standard deviation of the response and

S = the slope of the calibration curve

Limit of quantification (LOQ) refers to the lowest concentration of an analyte that can be quantified with accuracy and precision using the method. The ICH recognises various approaches for determining the LOQ including those mentioned above for LOD. The standard deviation of the response and the slope have been used here. The equation used to determine the LOQ is:

Equation A 5

$$LOQ = \frac{10\,\sigma}{S}$$

The estimate of the standard deviation of the response can be based on the standard deviation of the blank or based on the calibration curve. When using the calibration curve option, the standard deviation of y-intercepts of regression lines (ie the residual standard deviation) serves as the estimate of response variability.

The formulae for residual and residual standard deviation are as follows:

Equation A 6

$$Residual = Y - Y_{est}$$

Equation A 7

$$S_{res} = \sqrt{\frac{\sum(Y - Y_{est})^2}{n - 2}}$$

Where:

S_{res} = residual standard deviation (σ = standard deviation of the response)

Y = observed value

Y_{est} = projected value using the calibration curve

n = data points in the population

S_{res} = σ for the purposes of these calculations

Values for all three potential calibration curves were obtained.

A.2.2.7 System suitability

This requirement could also be included under repeatability, as seen in the Validation of Chromatographic Methods [302]. It measures the ability of the instrument to repeatedly reproduce multiple injections of a homogeneous sample. The smaller the percentage RSD, the more sensitive results will be to any variations. The Validation of Chromatographic Methods suggests a minimum of 6-10 injections for methods validation with a percentage RSD of ≤ 1%. The ability of the instrument to reproduce consistent results was tested using 6 samples.

1.8 A.3 Results

A.3.1. Validation of HPLC analytical method for the detection and quantification of DF

A.3.1.1 Linearity, range and specificity (identification element)

The responses for the nine different concentrations of DNa, and the quantities of DF contained therein, can be seen in Table A1 below:

Table A 1 Concentration of samples and responses represented as the area under the curve (AUC).

Concentration of DNa µg/mL	Quantity of DF µg/mL	AUC
100.00	93.10	2149.27
75.00	69.82	1608.27
50.00	46.55	1062.03
25.00	23.27	524.60
10.00	9.31	211.87

5.00	4.65	105.87
1.00	0.93	22.47
0.50	0.47	11.97
0.05	0.05	1.5

Using all nine DF concentrations results in a calibration curve represented by the equation y = 23.052x - 2.5264. Despite a correlation coefficient (R^2) of 1, the calibration curve does not provide fully accurate quantifications at lower concentrations. This was tested by inputting the acquired responses (AUC) into the equation to determine the concentration used[3]. In order to obtain the best possible results for the quantification of DF, the values obtained have been used in two separate calibration curves, each comprising five concentration values. The first curve utilises the concentrations from 10 to 100 µg/mL of DNa, equivalent to 9.31 – 93.10 µg/mL of DF (Table A2).

[3] When all nine concentrations were used for one calibration curve, the resulting equation was y = 23.052x - 2.5264 having an R^2 value = 1. When the calibration curve was tested using calculated responses (AUC) to obtain concentration, values for the lower concentrations, whilst detectable, were not accurately quantified.

Actual concentration	Area under the curve (response)	Concentration based on y = 23.052x - 2.5264	|Difference between actual and calculated concentration|
93.10	2149.27	93.35	0.25
69.82	1608.27	69.88	0.05
46.55	1062.03	46.18	0.37
23.27	524.60	22.87	0.41
9.31	211.87	9.30	0.01
4.65	105.87	4.70	0.05
0.93	22.47	1.08	0.15
0.47	11.97	0.63	0.16
0.05	1.5	0.17	0.13

When two separate calibration curves are used, the responses are improved:

Actual concentration	Area under the curve (response)	Concentration based on y = 23.169x – 10.435	|Difference between actual and calculated concentration|
93.10	2149.27	93.22	0.12
69.82	1608.27	69.86	0.04
46.55	1062.03	46.29	0.26
23.27	524.60	23.09	0.18
9.31	211.87	9.59	0.28
Actual concentration	**Area under the curve (response)**	**Concentration based on y = 22.631x + 0.9929**	**|Difference between actual and calculated concentration|**
9.31	211.87	9.32	0.01
4.65	105.87	4.63	0.02
0.93	22.47	0.95	0.02
0.47	11.97	0.48	0.02
0.05	1.5	0.02	0.02

Table A 2 Response values in the form of area under the curve (AUC) for concentrations of DF ranging from 9.31 – 93.10 µg/mL.

Concentration µg/mL	AUC
93.10	2149.27
69.82	1608.27
46.55	1062.03
23.27	524.60
9.31	211.87

These values result in the linear equation y = 23.169x – 10.435 (Figure A1). It has a correlation coefficient (R^2) of 1, a slope of 23.169 and a y-intercept of -10.435. This curve is far more accurate in the range 23.27 - 93.10 µg/mL, than the single curve.

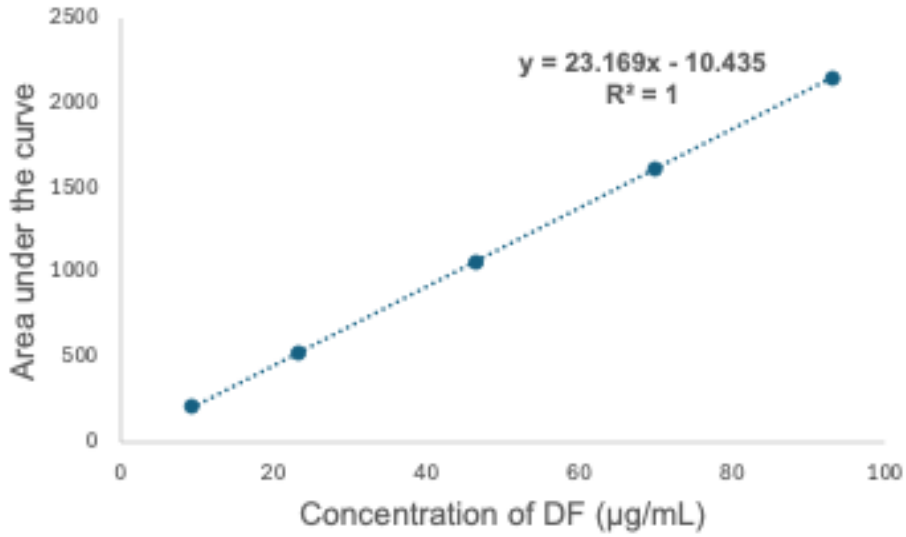

Figure A 1 Calibration curve for DF representing concentrations of DF ranging from 9.31 – 93.10 µg/mL.

The second curve comprises concentrations of DF from 0.05 – 9.31 µg/mL (Table A3). It has a correlation coefficient (R^2) of 1, a slope of 22.631 and a y-intercept of 0.9929 as seen in Figure A2. This calibration curve provides more accurate results for the range of concentrations 0.05 – 9.31 µg/mL than the single calibration curve (footnote 3).

Table A 3 Response values in the form of area under the curve (AUC) for concentrations for DF ranging from 0.05 – 9.31 µg/mL.

Concentration µg/mL	AUC
9.31	211.87
4.65	105.87
0.93	22.47
0.47	11.97
0.05	1.5

Figure A 2 Calibration curve for DF representing concentrations of DF ranging from 0.05 – 9.31 µg/mL.

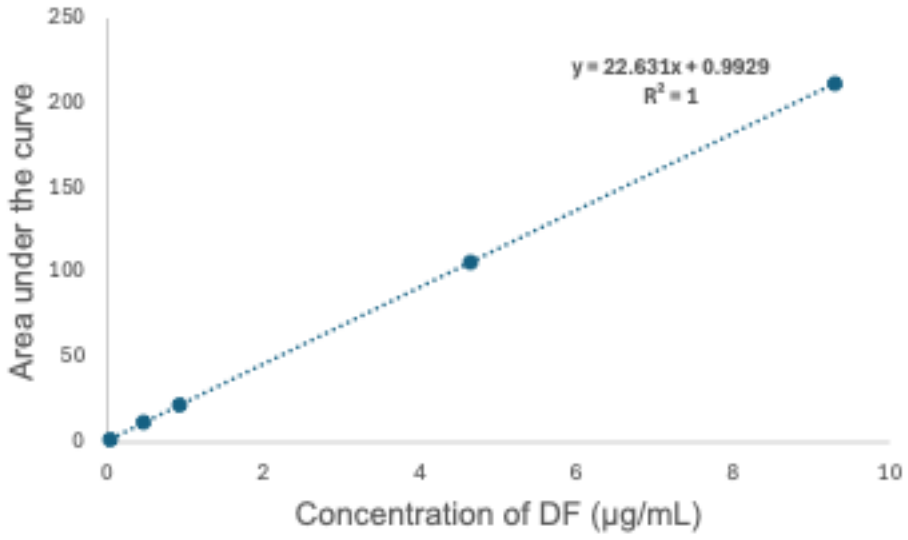

Both calibration curves show correlation coefficients (R^2) of 1, which confirms good linearity.

The identification element of the specificity requirement was fulfilled when utilising DNa as a reference material from which DF was identified. This was repeated by obtaining responses to 9 different concentrations of DNa and the DF contained therein.

A.3.1.2 Accuracy and specificity (quantification of analyte within a sample)

A.3.1.2 (a) Accuracy of drug substance

Accuracy was tested by applying the analytical procedure to an analyte of known purity. A stock solution of DNa and water was made up. Three replicates of three

different concentrations namely 1, 25 and 50 µg/mL of DNa, representing 0.93, 23.27 and 46.55 µg/mL of DF, were then tested using the analytical method. The results of this recovery study are included in Table A4 showing recovery rates of 102.39%, 99.90% and 99.56% as well as percentage RSD values of 0.54, 0.01 and 0.08% respectively. The mean value for the percentage recovery is 100.62% and the mean value of the percentage RSD is 0.21%.

Table A 4 Accuracy validation for the quantification of DF in DNa (n=3; mean ± SD).

Theoretical concentration DF (µg/mL)	Measured concentration DF (µg/mL)	Recovery (%)	RSD (%)
0.93	0.95 ± 0.01	102.39	0.54
23.27	23.25 ± 0.00	99.90	0.01
46.55	46.35 ± 0.04	99.56	0.08
		Mean 100.62 ± 1.55	Mean 0.21 ± 0.29

The results for the mean value indicate that accuracy requirement is satisfied for this method, whilst the relative standard deviation of less than 1% suggests fulfilment of the precision element of sample analysis.

A.3.1.2 (b) Accuracy of detection from within a commercial drug product

Three different sample concentrations of the actual drug product were obtained corresponding to concentrations of 14.84, 42.68 and 94.63 µg/mL of DF within each sample[4]. Accuracy was tested by applying the analytical procedure to the drug samples. The results of this recovery study are included in Table A5, showing recovery rates of 91.83, 101.13 and 101.72 % as well as percentage RSD values of 0.16, 0.19 and 0.23% respectively. The mean value for the percentage recovery is 98.23% and the mean value of the percentage RSD is 0.19%.

[4] The amount of drug product x 1.16% = the amount (g) of diclofenac diethylamine in the sample. In order to obtain the amount of diclofenac, this was divided by the molecular mass of diclofenac diethylamine (370.294 g / mol) and multiplied by the molecular mass of diclofenac (296.147 g / mol).

Table A 5 Accuracy validation for the quantification of DF in a commercially available product (n=3; mean ± SD)

Theoretical concentration DF (µg/mL)	Measured concentration DF (µg/mL)	Recovery (%)	RSD (%)
14.84	13.63 ± 0.02	91.83	0.16
42.68	43.16 ± 0.08	101.13	0.19
94.63	92.26 ± 0.22	101.72	0.23
		Mean 98.23 ± 5.55	Mean 0.19 ± 0.04

The results for the mean recovery values indicate that the accuracy requirement was satisfied for this method, as it falls within the non-compendial requirements of 90 - 110 %. Due to the exceptionally small samples taken, it did not comply with compendial requirements of 95 – 105 %. The relative standard deviation is under 1% indicating compliance with the precision element of sample analysis.

The ability to quantify the analyte from within the drug product also satisfied the second part of the specificity requirement.

A.3.1.2 (c) Accuracy of detection from samples containing counterions

A.3.1.2 (c)(i) Absorption spectra

Results of absorption spectra for DF (a) and DNa (b) indicate absorption peaks at 222 and 277 respectively.

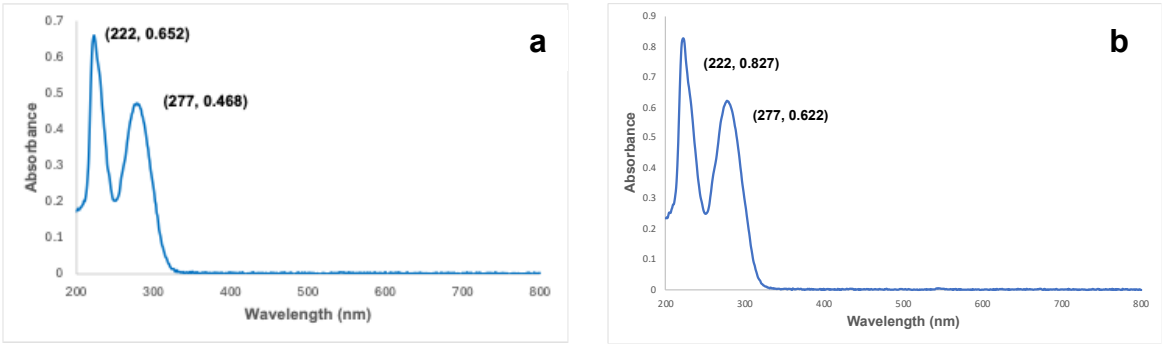

Figure A 3 Absorption spectrum between 200 - 800 nm of (a) DF and (b) DNa

Figures A4 - A6 show the absorption spectra of (a) the free base forms and (b) the salt forms of the amino acids. All spectra exhibited absorption maxima between 222 and

228 nm. At 277 nm, the wavelength used for DF detection, absorbance values were low, ranging from 0.005 to 0.031. These results indicate that interference with the quantification of DF at 277 nm is unlikely.

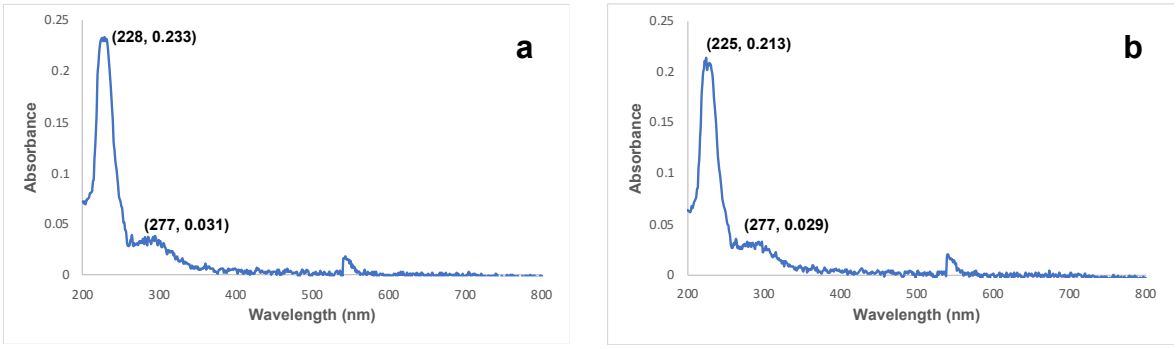

Figure A 4 Absorption spectrum between 200 - 800 nm of (a) L-Arg and (b) L-ASS

b

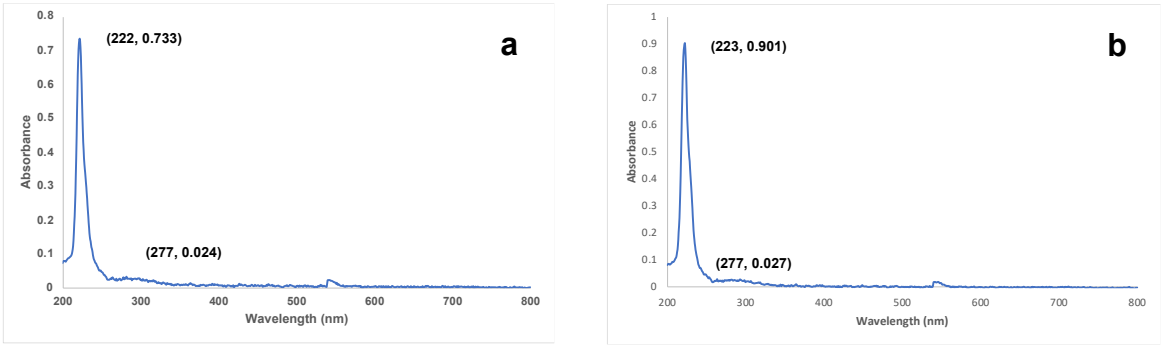

Figure A 5 Absorption spectrum between 200 - 800 nm of (a) L-His and (b) L-HSS

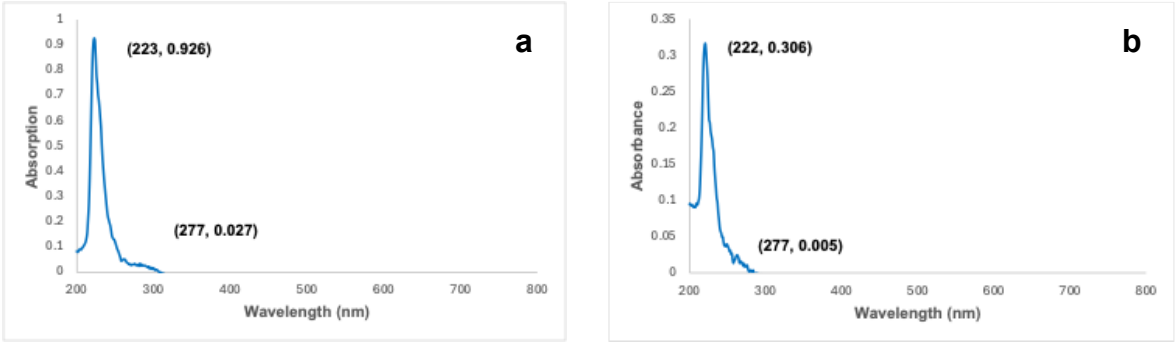

Figure A 6 Absorption spectrum between 200 - 800 nm of (a) L-Lys and (b) L-LSS

A.3.1.2 (c)(ii) Analysis of samples containing counterions

The absence of interference in the detection and quantification of DF was confirmed by analysing individual and combined samples of DF, DNa, and the free base and salt forms of the amino acids. Individual samples of DF, DNa, and the amino acids were analysed at equimolar concentrations relative to DF (100 µg/mL). As shown in Table A6, the AUC values were 2276.63 ± 0.38 for DF, 2294.43 ± 1.53 for DNa, and 0 for all amino acid forms. These values corresponded to calculated concentrations of 97.81 ± 0.02 µg/mL for DF and 98.58 ± 0.07 µg/mL (DF equivalent) for DNa. Even when the amino acid counter ions were present at a 50-fold molar excess, no signals were detected at the relevant elution times.

Table A 6 Absorption of individual samples of DF, DNa, and the amino acids at 277nm. Samples of the amino acids were tested at (i) equimolar concentrations relative to DF at 100 µg/ mL and (ii) 50-fold molar concentrations relative to DF at 100 µg/ mL (n=3; mean ± SD).

Solute	Molar ratio relative to DF	Time	AUC	DF µg/ mL
DF	1	6.43 ± 0.00	2276.63 ± 0.38	97.81 ± 0.02
DNa	1	6.38 ± 0.00	2294.43 ± 1.53	98.58 ± 0.07
L-Arg	1	-	0.00	0.00
L-ASS	1	-	0.00	0.00
L-His	1	-	0.00	0.00
L-HSS	1	-	0.00	0.00
L-Lys	1	-	0.00	0.00
L-LSS	1	-	0.00	0.00
L-Arg	50	-	0.00	0.00
L-ASS	50	-	0.00	0.00
L-His	50	-	0.00	0.00
L-HSS	50	-	0.00	0.00
L-Lys	50	-	0.00	0.00
L-LSS	50	-	0.00	0.00

Combinations of DF with the amino acid free bases and DNa with the amino acid salts were analysed at equimolar ratios, based on a DF concentration of 50 µg/mL. As shown in Table A7, the AUC values for the equimolar mixtures ranged from 1143.67 ± 1.66 to 1151.30 ± 1.65, corresponding to calculated DF concentrations of 48.91 ± 0.07 to 49.31 ± 0.07 µg/mL. When the counter ion concentrations were increased to a 50-

fold molar excess, the AUC values ranged from 1151.30 ± 3.22 to 1170.40 ± 0.44, equating to concentrations of 49.24 ± 0.14 to 50.07 ± 0.02 µg/mL.

These results demonstrate that neither equimolar amounts of the amino acid counter ions nor a 50-fold molar excess interfered with the detection or quantification of DF. The measured concentrations remained consistent with the expected DF concentration of 50 µg/mL across all combinations, confirming the selectivity of the method.

Table A 7 Absorption at 277 nm for combinations of DF with amino acid free bases and DNa with amino acid salts at 1:1 and 1:50 molar ratios, based on a DF concentration of 50 µg/mL (n = 3; mean ± SD).

Solute	Molar ratio relative to DF	Time	AUC	DF µg/ mL
DF + L-Arg	1:1	6.38 ± 0.00	1151.30 ± 1.65	49.31 ± 0.07
DF + L-Arg	1:50	6.38 ± 0.00	1151.30 ± 1.88	49.24 ± 0.08
DF + L-His	1:1	6.43 ± 0.00	1143.70 ± 5.34	48.91 ± 0.23
DF + L-His	1:50	6.38 ± 0.00	1170.40 ± 0.44	50.07 ± 0.02
DF + L-Lys	1:1	6.38 ± 0.00	1151.30 ± 0.79	49.24 ± 0.03
DF + L-Lys	1:50	6.37 ± 0.00	1151.30 ± 3.22	49.24 ± 0.14
DNa + L-ASS	1:1	6.45 ± 0.00	1143.67 ± 1.66	48.91 ± 0.07
DNa + L-ASS	1:50	6.37 ± 0.00	1157.37 ± 0.87	49.50 ± 0.04
DNa + L-HSS	1:1	6.37 ± 0.00	1151.30 ± 0.15	49.24 ± 0.01
DNa + L-HSS	1:50	6.37 ± 0.00	1151.30 ± 1.08	49.24 ± 0.05
DNa + L-LSS	1:1	6.38 ± 0.00	1149.17 ± 0.64	49.15 ± 0.03
DNa + L-LSS	1:50	6.37 ± 0.00	1161.00 ± 1.47	49.66 ± 0.06

A.3.1.3 Precision

A.3.1.3 (a) Repeatability

The repeatability aspect of precision was determined using three different concentrations of DNa, namely 1, 25 and 50 µg/mL, representing 0.93, 23.27 and 46.55 µg/mL of DF. Three replicates of each concentration were tested intraday.

Table A 8 Summary of the intraday variability data for DF in DNa (n=3; mean ± SD)

Theoretical concentration DF (µg/mL)	Measured concentration DF (µg/mL)			
	First set		Second set	
	Mean ± SD	% RSD	Mean ± SD	% RSD
0.93	0.95 ± 0.01	0.54	0.96 ± 0.00	0.46
23.27	23.25 ± 0.00	0.01	23.27 ± 0.00	0.01
46.55	46.35 ± 0.04	0.08	46.46 ± 0.02	0.05

Table A 9 Average intraday values for DF (n=3; mean ± SD). Confidence intervals 95% and 99% were obtained across all samples

Theoretical concentration DF (µg/mL)	Intraday measured concentration DF (µg/mL)		95% Confidence interval	99% Confidence interval
	Mean ± SD	% RSD		
0.93	0.96 ± 0.00	0.05	0.003	0.005
23.27	23.26 ± 0.00	0.01	0.010	0.016
46.55	46.40 ± 0.03	0.06	0.071	0.111

The same intraday study was performed quantifying DF in a drug product, a commercially available emulgel.

Table A 10 Summary of the intraday variability data for DF in a commercial emulgel (n=3; mean ± SD)

Theoretical concentration DF (µg/mL)	Measured concentration DF (µg/mL)			
	First set		Second set	
	Mean ± SD	% RSD	Mean ± SD*	% RSD
14.84	13.63 ± 0.02	0.16	13.64 ± 0.05	0.38
42.68	43.16 ± 0.08	0.19	43.15 ± 0.08	0.18
94.63	96.26 ± 0.22	0.23	95.97 ± 0.03	0.03

Table A9 Average intraday values for DF contained within the commercial emulgel (n=3; mean ± SD). Confidence intervals 95% and 99% were obtained across all samples.

Theoretical concentration DF (µg/mL)	Intraday measured concentration DF (µg/mL)		95% Confidence interval	99% Confidence interval
	Mean ± SD	% RSD		
14.84	13.64 ± 0.01	0.07	0.039	0.061
42.68	46.16 ± 0.01	0.02	0.075	0.117
94.63	96.11 ± 0.20	0.21	0.218	0.341

Intraday variability for the drug substance at 0.93, 23.27 and 46.55 µg/mL has mean ± standard deviation values of 0.96 ± 0.00, 23.26 ± 0.00 and 46.40 ± 0.03 µg/mL and % relative standard deviations of 0.05, 0.01 and 0.06%. There is also a 95% certainty that the mean detected values fall within 0.95 and 0.96 µg/mL for a 0.93 µg/mL sample, between 23.25 and 23.27 µg/mL for a 23.27 µg/mL sample and 46.33 and 46.47 µg/mL for a 46.55 µg/mL sample. Furthermore, there is a 99% certainty that the mean detected values fall within 0.95 and 0.97 µg/mL for a 0.93 µg/mL sample, between 23.24 and 23.28 µg/mL for a 23.27 µg/mL sample and 46.29 and 46.51 µg/mL for a 46.55 µg/mL sample.

Intraday variability for the commercial drug product with theoretical concentrations of 14.84, 42.68 and 94.63 µg/mL has mean ± standard deviation values of 13.64 ± 0.01, 46.16 ± 0.01 and 96.11 ± 0.20 µg/mL and % relative standard deviations of 0.07, 0.02 and 0.21%.

Furthermore, there is a 95% certainty that the mean detected values will fall within 13.61 and 13.68 µg/mL for a 14.84 µg/mL sample, between 43.08 and 43.23 µg/mL for a 42.68 µg/mL sample and 95.90 and 96.33 µg/mL for a 94.63 µg/mL sample. In addition, there is a 99% certainty that the mean detected values will fall within 13.58 and 13.70 µg/mL for a 14.84 µg/mL sample, between 43.04 and 43.27 µg/mL for a 42.68 µg/mL sample and 95.77 and 96.46 µg/mL for a 94.63 µg/mL sample.

Intraday results confirm that the repeatability requirement has been satisfied for both the drug substance and the commercial drug product.

A.3.1.3 (b) Intermediate precision

Intermediate precision of DNa was established by preparing three different concentrations of the salt in solution, 1, 25 and 50 µg/mL. These contained 0.93, 23.27 and 46.55 µg/mL of DF. Three replicates at each concentration were analysed on different days. The results for each day can be seen in Table A11.

Table A 11 Summary of the daily variability data for DF in DNa (n=3; mean ± SD)

Theoretical concentration DF (µg/mL)	Measured concentration DF (µg/mL)					
	Day 1		Day 2		Day 3	
	Mean ± SD	% RSD	Mean ± SD	% RSD	Mean ± SD	% RSD
0.93	0.95 ± 0.01	0.54	0.96 ± 0.00	0.27	0.97 ± 0.01	1.06
23.27	23.25 ± 0.00	0.01	23.19 ± 0.04	0.18	23.36 ± 0.03	0.11
46.55	46.35 ± 0.04	0.08	46.51 ± 0.06	0.12	46.91 ± 0.07	0.14

The interday variability using three different concentrations, each comprising three replicates per day, can be seen below.

Table A 12 Average interday values for DF in DNa (n=3; mean ± SD). Confidence intervals 95% and 99% were obtained across all samples.

Theoretical concentration DF (µg/mL)	Interday measured concentration DF (µg/mL)		95% Confidence interval	99% Confidence interval
	Mean ± SD	% RSD		
0.93	0.96 ± 0.01	0.62	0.006	0.009
23.27	23.27 ± 0.02	0.10	0.061	0.090
46.55	46.59 ± 0.05	0.11	0.197	0.287

The same analysis was performed measuring DF in a commercial emulgel formulation.

Table A 13 Summary of the daily variability data for DF in a commercial emulgel (n=3; mean ± SD)

Theoretical concentration DF (µg/mL)	Measured concentration DF (µg/mL)					
	Day 1		Day 2		Day 3	
	Mean ± SD*	% RSD	Mean ± SD*	% RSD	Mean ± SD*	% RSD
14.84	13.63 ± 0.02	0.16	13.66 ± 0.02	0.15	13.63 ± 0.00	0.03
42.68	43.16 ± 0.08	0.19	43.15 ± 0.08	0.18	43.03 ± 0.03	0.06
94.63	96.26 ± 0.22	0.23	96.88 ± 0.07	0.07	96.64 ± 0.05	0.05

The interday variability using three different concentrations, each comprising three replicates per day, can be seen below.

Table A 14 Average interday values for DF in a commercial emulgel (n=3; mean ± SD). Confidence intervals 95% and 99% were obtained across all samples.

Theoretical concentration DF (µg/mL)	Interday measured concentration DF (µg/mL)		95% Confidence interval	99% Confidence interval
	Mean ± SD	% RSD		
14.84	13.64 ± 0.02	0.11	0.016	0.023
42.68	43.11 ± 0.06	0.14	0.066	0.097
94.63	96.59 ± 0.11	0.12	0.227	0.331

Interday variability for the drug substance at 0.93, 23.27 and 46.55 µg/mL has mean ± standard deviation values of 0.96 ± 0.01, 23.27 ± 0.02 and 46.59 ± 0.05 µg/mL and % relative standard deviations of 0.62, 0.10 and 0.11 %. There is also a 95% certainty that the mean detected values will fall within 0.95 and 0.97 µg/mL for a 0.93 µg/mL sample, between 23.21 and 23.33 µg/mL for a 23.27 µg/mL sample and 46.39 and 46.80 µg/mL for a 46.55 µg/mL sample. Furthermore, there is a 99% certainty that the mean detected values fall within 0.95 and 0.97 µg/mL for a 0.93 µg/mL sample, between 23.18 and 23.36 µg/mL for a 23.27 µg/mL sample and 46.30 and 46.88 µg/mL for a 46.55 µg/mL sample.

Interday variability for the drug product at 14.84, 42.68 and 94.63 µg/mL has mean ± standard deviation values of 13.64 ± 0.02, 43.11 ± 0.06 and 96.59 ± 0.11 µg/mL and percentage relative standard deviations of 0.11, 0.14 and 0.12%. There is also a 95% certainty that the mean detected values fall within 13.62 and 13.65 µg/mL for a 14.84 µg/mL sample, between 43.05 and 43.18 µg/mL for a 42.68 µg/mL sample and 96.36 and 96.82 µg/mL for a 94.63 µg/mL sample. Furthermore, there is a 99% certainty that the mean detected values fall within 13.62 and 13.66 µg/mL for a 14.84 µg/mL sample, between 43.02 and 43.21 µg/mL for a 42.68 µg/mL sample and 96.26 and 96.92 µg/mL for a 94.63 µg/mL sample.

Interday results confirm that the repeatability requirement has been satisfied in for both the drug substance and the commercial drug product.

A.3.1.4 Robustness

Table A15 below indicates the results of small, but deliberate variations implemented to test the vigour of the original method (method 1, Table A15). The consecutive methods include sequential changes to wavelength, injection volume, solvent ratios,

temperature of column and flow rate. Despite these modifications, the calibration curves under adjusted conditions retained a correlation coefficient (R^2 value) of 1, indicating the robustness of the method.

Table A 15 Robustness tests for method 1. Methods 2 – 6 indicate changes to the HPLC conditions including wavelength, injection volume, solvent ratios, temperature of column and flow rate. The final column refers to the correlation coefficients for the calibration curves obtained using these adjusted methods.

Method	Wavelength (nm)	Injection Volume (µL)	Temperature ° C	Mobile Phase Acetonitrile: 0.1%TFA in H_2O (v/v)	Flow (mL/ min)	R^2
1	277	10	25	70:30	1.00	1
2	267	10	25	70:30	1.00	1
3	277	20	25	70:30	1.00	1
4	277	10	25	80:20	1.00	1
5	277	10	30	70:30	1.00	1
6	277	10	25	70:30	0.8	1

A.3.1.5 Limit of detection (LOD) and limit of quantification (LOQ)

Values for all three potential calibration curves were obtained. The two separate calibration curves provided a lower level of detection than the combined calibration curve, and thus afforded a superior mechanism for the detection and quantification of data as required in this study.

Table A 16 Residual standard deviation, LOD and LOQ for calibration curves

Calibration curve	Concentration values DF (µg/mL)	Residual standard deviation S_{res}	Limit of detection DL (µg/mL)	Limit of quantification LOQ (µg/mL)
Y = 23.052x -2.5264	0.05 - 100	5.74	0.82	2.49
Y = 23.169x -10.435	10 – 100	5.94	0.85	2.56
Y = 22.631x + 0.9929	0.05 - 10	0.55	0.08	0.24

The limit of detection according to this method is 0.08 µg/mL, whilst the limit of quantification is 0.24 µg/mL.

A.3.1.6 System suitability

The ability of the instrument to repeatedly reproduce multiple injections of a homogeneous sample was conducted using 6 homogenous samples.

Table A 17 Comparison of reproducibility of samples based on AUC, retention time and symmetry values (n=6; mean ± SD)

	Mean ± SD	% RSD
Area under the curve	796.08 ± 1.62	0.20
Retention time (min)	6.35 ± 0.00	0.02
Symmetry	0.92 ± 0.00	0.25

The system suitability values are detailed in Table A17 above. The percentage RSD for the area under the curve, retention time and symmetry are 0.2, 0.02 and 0.25 respectively and thus conform with the recommendation of percentage RSD of ≤ 1%.

Appendix B: Method Validation

B.1 Introduction

The validation of *in vitro* permeation testing (IVPT) for diclofenac (DF) was conducted using diclofenac sodium (DNa) in solution over a 24-hour period, consistent with standard IVPT procedures. Recovery of DF was determined by quantifying the amounts in the donor and receptor compartments, as well as in the membrane extracts. Studies were performed both with and without L-histidine monochloride monohydrate (LHSS). In addition, the stability of DNa and a commercial DF product was assessed in the receptor media, namely phosphate-buffered saline (PBS, pH 7.3 ± 0.2) and PBS (pH 7.3 ± 0.2) containing Brij™ O20.

B.2 Materials and methods

B.2.1 Materials

DNa 98% and LHSS 98% were purchased from Acros Organics (VWR, Leceistershire, UK). High vacuum grease was obtained from Dow Corning (Seneffe, Belgium). Oxoid™ Phosphate buffered saline (PBS) tablets were purchased from Thermo Fisher Scientific (Lancashire, UK). Voltarol® 1.16% Emulgel (Voltarol) was purchased from Boots pharmacy (Nottingham, UK). HPLC grade acetonitrile and methanol were purchased from Fisher Scientific (Lancashire, UK). Trifluoroacetic acid was purchased from VWR (Leceistershire, UK). Brij® O20 was obtained from Sigma Aldrich (Dorset, UK). DF was synthesised from DNa as described in Chapter 6.4.2.2.

B.2.2 Methods

B.2.2.1 Stability in the receptor phase was assessed using DF (free acid), DNa, and a commercial DF product (Voltarol®)

To ensure that sink conditions are maintained in the receptor compartment during IVPT, the concentration of the permeant in the receptor solution is kept well below its solubility. The proposed amendment to GN 156 recommends that the solubility of the permeant in the receptor medium should be at least ten times higher than the maximum concentration expected in the receptor solution at the end of the study [91]. To achieve this for lipophilic molecules such as diclofenac, OECD guidelines suggest

the addition of Brij™ O20 [307], which in this study was used at a concentration of 6%.

Stability studies to confirm that the analyte remained stable in the receptor phase were conducted using DF (i.e. the free acid), DNa and a commercial 1% DF product (Voltarol® 1.16%). Experiments were performed both in PBS alone (pH 7.3 ± 0.2) and in PBS containing 6% Brij™ O20, allowing assessment of receptor conditions under both standard and solubility-enhanced media. A minimum of three replicates were included for each experiment. Stock solutions of known analyte concentration were prepared using either PBS or PBS with 6% Brij™ O20 to replicate the receptor phase. These solutions were placed in small glass vials containing stirrer bars, sealed with parafilm™ and incubated in a temperature-controlled water bath at 32 °C ± 1 for the duration of the study. Samples (200 µL) were collected at t0, t24, t48, and t72 h and analysed for detection and quantification using HPLC.

B.2.2.2 Validation of IVPT using mass balance studies

The validation of IVPT for DNa was conducted using DNa alone and in combination with LHSS. The first formulation comprised 107.41 µg/mL of DNa, equivalent to 100 µg/mL of DF, in PBS. The second formulation contained the same concentration of DNa combined with an equimolar amount of LHSS in PBS. Finite doses were applied to the donor compartment, and a 24-hour IVPT was performed. Samples were collected hourly for the first six hours and again at 24 hours. Mass balance studies were carried out as described in Chapter 6.4.2.7.

B.2.3 Results

B.2.3.1 Stability of DF (free acid), DNa, and Voltarol® in the receptor phase

B.2.3.1 (a) Stability of DF in PBS and PBS with Brij™ O20 (6%)

The data presented in Figure B.1 demonstrates that the stability of the active pharmaceutical ingredient remained unaffected over 72 hours in both PBS and PBS containing Brij™ O20 (6%).

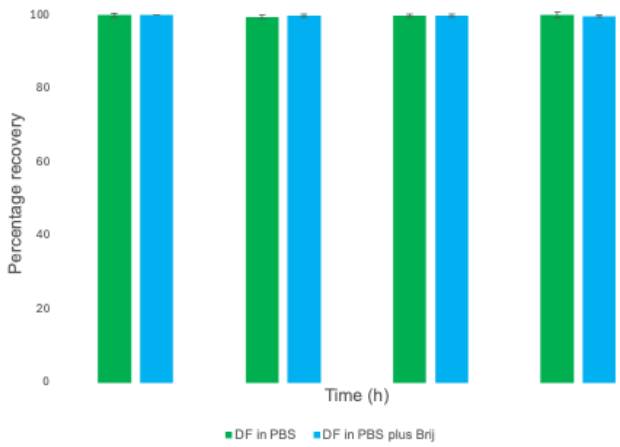

Figure B. 1 Stability of DF in the receptor phase with PBS or PBS plus Brij™ O20 (6%). Results represent the average ± SD for n = 3 experiments at 0, 24, 48 and 72 h

B.2.3.1 (b) Stability of DNa in PBS and PBS with Brij™ O20 (6%)

Over a 72-hour period, the stability of the active pharmaceutical ingredient showed no significant degradation in either PBS or PBS containing 6% Brij™ O20, as shown in Figure B.2.

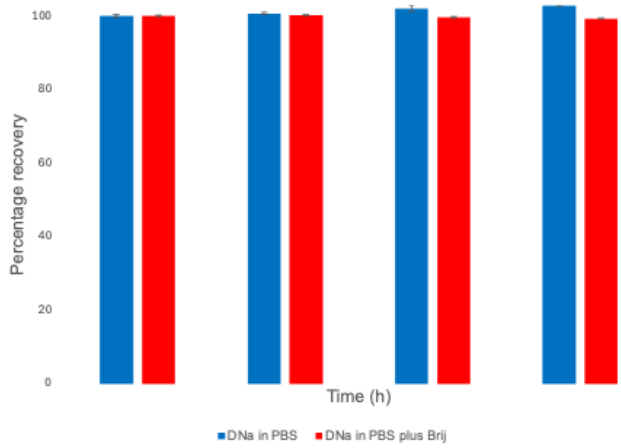

Figure B. 2 Stability of DNa in the receptor phase with PBS or PBS plus Brij™ O20 (6%). Results represent the average ± SD for n = 3 experiments at 0, 24, 48 and 72 h.

B.2.3.1 (c) Stability of Voltarol® in PBS and PBS with Brij™ O20 (6%)

Stability testing demonstrated that the DF component of Voltarol® was maintained without significant change in either PBS or PBS supplemented with Brij™ O20 (6%) throughout the 72-hour study period.

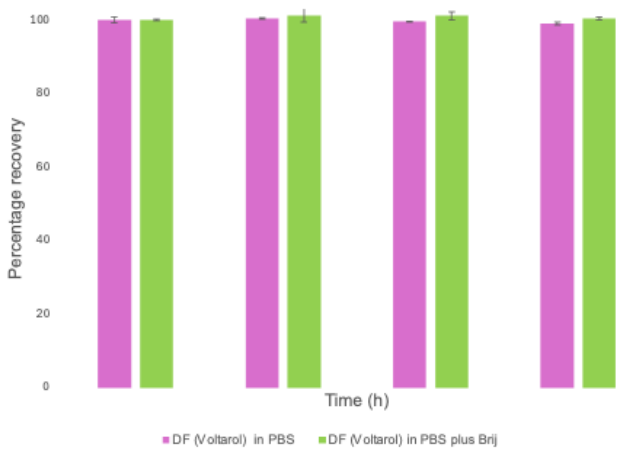

Figure B. 3 Stability of Voltarol® in the receptor phase with PBS or PBS plus brij (6%). Results represent the average ± SD for n = 3 experiments at 0, 24, 48 and 72 h.

B.2.3.2 Validation of IVPT using mass balance studies

The total recovery of DF from aqueous solutions comprising either (i) DNa alone (DNa:LHSS 1:0) or (ii) a combination of DNa and LHSS in equimolar ratios (DNa:LHSS 1:1) was 100.38 ± 4.03% and 101.86 ± 5.14%, respectively. Both values fall within the acceptable recovery range of 90 - 110% outlined in the OECD guidelines (2004c). The mass balance procedure demonstrated that the IVPT system was reliable and that no significant losses of DF occurred, thereby supporting the validity of the method.

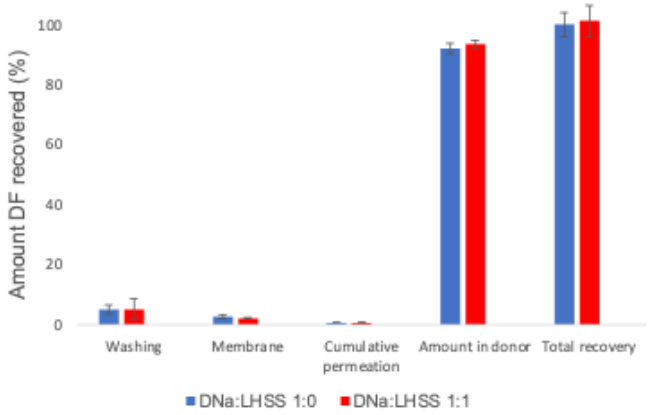

Figure B. 4 IVPT and mass balance results for 24 h finite dose application of DNa: LHSS (1:0) and DNa:LHSS (1:1) on porcine skin

Appendix C: List of publications and presentations

Publications:

Sil, Bruno C., Rebecca G. Belgrave, Miguel P. Alvarez, Lin Luo, Mignon Cristofoli, Matthew R. Penny, David J. Moore, Jonathan Hadgraft, Stephen T. Hilton, and Majella E. Lane. "3D-Printed Franz cells–update on optimization of manufacture and evaluation." *International journal of cosmetic science* 42, no. 4 (2020): 415-419.

Cristofoli, M., Kung, C.-P., Hadgraft, J., Lane, M. E. and Sil, B. C. "Ion pairs for transdermal and dermal drug delivery: A review." *Pharmaceutics* 13 (2021): 909.

Cristofoli, M., Hadgraft, J., Lane, M. E. and Sil, B. C. "A preliminary investigation into the use of amino acids as potential ion pairs for diclofenac transdermal delivery." *International Journal of Pharmaceutics* 623 (2022): 121906-06.

Cristofoli, M., Hadgraft, J., Lane, M. E. and Sil, B. C. "A model binary system for the evaluation of novel ion pair formulations of diclofenac." *RSC Pharmaceutics* 1, no. 2 (2024): 234-244.

Cristofoli, M., Hadgraft, J., Lane, M. E. and Sil, B. C. "Ion pairing as a strategy to enhance the delivery of diclofenac." *RSC Pharmaceutics* 2 (2025): 1163-1174.

Presentations:

Conference poster presentation:

Skin Forum 2022 Malmo, Sweden (21-22 June)

“Investigation into the use of amino acids as potential ion pairs for the transdermal delivery of diclofenac”

Conference podium presentation:

JPAG Pharmaceutical Analysis Research Awards and Careers Fair 2022, London, UK (22 November 2022)
“Next generation ion pairs for the transdermal delivery of diclofenac”

Conference podium presentation:

6th Interdisciplinary Health and Wellbeing Research

The Centre for Primary Health and Social Care and the School of Human Sciences at London Metropolitan University (4-5 May 2023)

“The use of amino acids to increase delivery of diclofenac through the skin”